frontiers | Research Topics

Diabetes augmentation on vascular disease, volume II

Edited by
Godfrey Getz and Catherine A. Reardon

Published in
Frontiers in Cardiovascular Medicine

ISSN 1664-8714
ISBN 978-2-8325-6499-8
DOI 10.3389/978-2-8325-6499-8

Generative AI statement
Any alternative text (Alt text) provided alongside figures in the articles in this ebook has been generated by Frontiers with the support of artificial intelligence and reasonable efforts have been made to ensure accuracy, including review by the authors wherever possible. If you identify any issues, please contact us.

About Frontiers

Frontiers is more than just an open access publisher of scholarly articles: it is a pioneering approach to the world of academia, radically improving the way scholarly research is managed. The grand vision of Frontiers is a world where all people have an equal opportunity to seek, share and generate knowledge. Frontiers provides immediate and permanent online open access to all its publications, but this alone is not enough to realize our grand goals.

Frontiers journal series

The Frontiers journal series is a multi-tier and interdisciplinary set of open-access, online journals, promising a paradigm shift from the current review, selection and dissemination processes in academic publishing. All Frontiers journals are driven by researchers for researchers; therefore, they constitute a service to the scholarly community. At the same time, the *Frontiers journal series* operates on a revolutionary invention, the tiered publishing system, initially addressing specific communities of scholars, and gradually climbing up to broader public understanding, thus serving the interests of the lay society, too.

Dedication to quality

Each Frontiers article is a landmark of the highest quality, thanks to genuinely collaborative interactions between authors and review editors, who include some of the world's best academicians. Research must be certified by peers before entering a stream of knowledge that may eventually reach the public - and shape society; therefore, Frontiers only applies the most rigorous and unbiased reviews. Frontiers revolutionizes research publishing by freely delivering the most outstanding research, evaluated with no bias from both the academic and social point of view. By applying the most advanced information technologies, Frontiers is catapulting scholarly publishing into a new generation.

What are Frontiers Research Topics?

Frontiers Research Topics are very popular trademarks of the *Frontiers journals series*: they are collections of at least ten articles, all centered on a particular subject. With their unique mix of varied contributions from Original Research to Review Articles, Frontiers Research Topics unify the most influential researchers, the latest key findings and historical advances in a hot research area.

Find out more on how to host your own Frontiers Research Topic or contribute to one as an author by contacting the Frontiers editorial office: frontiersin.org/about/contact

Diabetes augmentation on vascular disease, volume II

Topic editors

Godfrey Getz — The University of Chicago, United States

Catherine A. Reardon — The University of Chicago, United States

Citation

Getz, G., Reardon, C. A., eds. (2025). *Diabetes augmentation on vascular disease, volume II*. Lausanne: Frontiers Media SA. doi: 10.3389/978-2-8325-6499-8

Table of contents

frontiers | Frontiers in Cardiovascular Medicine

TYPE Editorial
PUBLISHED 11 June 2025
DOI 10.3389/fcvm.2025.1637222

OPEN ACCESS

EDITED AND REVIEWED BY
Ichiro Manabe,
Chiba University, Japan

*CORRESPONDENCE
Catherine A. Reardon
reardon@uchicago.edu

RECEIVED 29 May 2025
ACCEPTED 02 June 2025
PUBLISHED 11 June 2025

CITATION
Reardon CA and Getz GS (2025) Editorial: Diabetes augmentation on vascular disease, volume II.
Front. Cardiovasc. Med. 12:1637222.
doi: 10.3389/fcvm.2025.1637222

Editorial: Diabetes augmentation on vascular disease, volume II

Catherine A. Reardon[1]* and Godfrey S. Getz[2]

[1]Ben May Department, University of Chicago, Chicago, IL, United States, [2]Department of Pathology, University of Chicago, Chicago, IL, United States

KEYWORDS

diabetes, autonomic neuropathy, triglyceride-glucose index, cardiomyopathy and coronary artery disease, obstructive sleep apnea, SAA, nitric oxide, inflammation

Editorial on the Research Topic
Diabetes augmentation on vascular disease, volume II

In 2021, we summarized eight reports addressing how diabetes augments cardiovascular disease, with a focus primarily on blood sugar and lipid regulation. In this editorial, we review ten more recent studies that expand upon this topic, incorporating systemic variables beyond glycemic and lipid control.

The first report, by Lou et al., investigated heart rate responses to exercise in patients with type 2 diabetes (T2DM), emphasizing autonomic nervous system dynamics. Typically, exercise induces sympathetic activation and parasympathetic withdrawal, which reverses during recovery. In a small Chinese cohort, this autonomic response was blunted both during and after exercise in type 2 diabetics compared to individuals without T2MD. While the authors adjusted for several confounders, the retrospective design limited control over factors such as diabetes duration, glycemic control, and medication use. Though correlative, the findings suggest a potential role for diabetic autonomic neuropathy. Future prospective studies, including larger and more diverse ethnic groups, are warranted.

A second retrospective study by Wang et al. examined the triglyceride-glucose (TyG) index as a predictor of preclinical heart failure with preserved ejection fraction (HFpEF) in a diabetic Chinese population without history of cardiovascular disease. Similar limitations as in the Lou et al. study applied, and the generalizability of the findings must be tested in broader populations.

In a cross-sectional study of 1,973 Chinese patients undergoing coronary angiography, Dong et al. found a positive correlation between glycemia and the presence of multivessel coronary artery disease (CAD), defined as >50% stenosis in at least two major coronary arteries. The association was particularly strong in males over 45 and smokers. For each unit increase in glycemia, the prevalence of multivessel CAD rose by 4%. Although cross-sectional in nature, the study underscores the potential value of glycemic measures as markers of CAD risk in Asian populations, warranting longitudinal validation in other ethnic groups.

Two Mendelian randomization studies in this Research Topic help address confounding factors common in observational research. The first by Liu et al. demonstrated a causal link between obstructive sleep apnea (OSA) and diabetic microvascular complications, including nephropathy and neuropathy in European patients. While OSA also appeared linked to diabetic retinopathy overall, the association was not significant when retinopathy was subclassified into background and

proliferative forms—likely due to limited sample size. Importantly, reverse causality was not supported. Reduced lung function, as measured by forced vital capacity and expiratory volume, was also associated with increased risk of retinopathy and nephropathy.

The second Mendelian randomization study, by Feng et al., used GWAS data from individuals of European descent to explore the role of very low-density lipoprotein (VLDL) in diabetic cardiomyopathy and coronary artery disease (CAD). Type 2 diabetes was associated with a 13% increased risk of CAD and a 2.5% elevation in VLDL levels. Notably, each standard deviation increase in VLDL concentration correlated with a 30% greater likelihood of CAD, implicating VLDL as a potential mediator of diabetic cardiovascular risk.

Wang et al. conducted a bibliometric analysis of diabetic cardiomyopathy publications from 2012 to 2021, revealing a steady increase in research output, with over 250 annual publications by the decade's end. While mechanistic insights were not the focus, hyperglycemia was a recurring theme, alongside oxidative stress, fibrosis, apoptosis, and autophagy. Six institutions—primarily in China, the U.S., Australia, and Hong Kong—accounted for the majority of the contributions. Therapeutic targets were frequently discussed, highlighting the urgency of this underdiagnosed but lethal complication.

den Hartigh et al. provided a comprehensive review of serum amyloid A (SAA) proteins and their role in inflammation-related diseases, including metabolic diseases such as diabetes, obesity, and atherosclerosis. Of the five main SAA subtypes, SAA1 and SAA2 are liver-derived and markedly elevated during acute inflammation. Chronic inflammation elicits a more modest SAA response. SAA's poor solubility leads to its association with high-density lipoprotein. The review raises the question of whether SAA serves as a biomarker or a causal agent in these diseases.

Sharma et al. conducted a preclinical study using ApoE-deficient mice to test modulators of nitric oxide (NO) bioavailability in diabetic atherosclerosis. The soluble guanylate cyclase activator BAY 60 and stimulator BAY 41 were compared. BAY 60 proved more effective in reducing aortic plaque burden and urinary albuminuria, a marker of renal function, over a 10- to 20-week treatment course initiated after streptozotocin-induced diabetes. These findings support NO-pathway targeting as a therapeutic approach in diabetic vascular and renal disease.

Singh et al. explored phosphorylation changes in NF-κB signaling in endothelial cells exposed to high glucose and hypoxia. Using a large panel of phosphorylation-specific antibodies, they identified 65 modulated phosphorylation sites in 35 proteins. Bioinformatic analysis highlighted increased phosphorylation in two B-cell–related proteins BLNK1 and Bruton tyrosine kinase (BTK). Inhibition of BTK led to an attenuation of glucose induced phosphorylation and activation of PKC and increased IκBα levels, suggesting previously underappreciated pathways influenced by diabetic and hypoxic stress.

Finally, Dai et al. used bioinformatic modeling to analyze co-expression of hub genes in male and female patients with T2DM and CAD (defined as >50% stenosis). Among 16 hub genes associated with immune cell infiltration, NPEPPS (a cytosolic aminopeptidase) and ABHD17A (a protein export gene) were co-expressed and upregulated in CD8+ T cells and NK cell, two immune populations more prevalent in healthy controls. This suggests a potential role for immune modulation in the pathogenesis and treatment of both diabetes and CAD.

Together, these ten studies deepen our understanding of the multifactorial pathways linking diabetes and cardiovascular disease and emphasize the value of diverse research methodologies—from molecular biology and bioinformatics to epidemiology and clinical trials—in unraveling this complex relationship.

Author contributions

CR: Writing – review & editing. GG: Writing – original draft, Writing – review & editing.

Conflict of interest

The authors declare that the research was conducted in the absence of any commercial or financial relationships that could be construed as a potential conflict of interest.

Generative AI statement

The author(s) declare that no Generative AI was used in the creation of this manuscript.

Publisher's note

frontiers | Frontiers in Cardiovascular Medicine

TYPE Original Research
PUBLISHED 20 October 2022
DOI 10.3389/fcvm.2022.1018841

OPEN ACCESS

EDITED BY
Catherine A. Reardon,
The University of Chicago,
United States

REVIEWED BY
Mingming Zhang,
Tangdu Hospital, China
Liping Wei,
Nankai University, China

*CORRESPONDENCE
Boxun Zhang
1243876560@qq.com
Linhua Zhao
melonzhao@163.com

†These authors have contributed equally to this work and share first authorship

SPECIALTY SECTION
This article was submitted to Cardiovascular Metabolism, a section of the journal Frontiers in Cardiovascular Medicine

RECEIVED 14 August 2022
ACCEPTED 28 September 2022
PUBLISHED 20 October 2022

CITATION
Wang S, Tian C, Gao Z, Zhang B and Zhao L (2022) Research status and trends of the diabetic cardiomyopathy in the past 10 years (2012–2021): A bibliometric analysis. *Front. Cardiovasc. Med.* 9:1018841. doi: 10.3389/fcvm.2022.1018841

Research status and trends of the diabetic cardiomyopathy in the past 10 years (2012–2021): A bibliometric analysis

Sicheng Wang[1†], Chuanxi Tian[1,2†], Zezheng Gao[1,2†], Boxun Zhang[1*] and Linhua Zhao[1*]

[1]Institute of Metabolic Diseases, Guang'anmen Hospital, China Academy of Chinese Medical Sciences, Beijing, China, [2]Graduate School, Beijing University of Chinese Medicine, Beijing, China

Background: Diabetic cardiomyopathy is one of the most life-threatening diabetic complications. However, the previous studies only discuss a particular aspect or characteristic of DCM, the current state and trends were explored by limited research. We aimed to perform a systemically bibliometric study of DCM research progress status in the past decade, visualize the internal conceptual structure and potential associations, and further explore the prospective study trends.

Methods: Articles related to DCM published from January 2012 to December 2021 were collected in the Web of Science core collection (WoSCC) database on June 24, 2022. We exported all bibliographic records, including titles, abstracts, keywords, authorship, institutions, addresses, publishing sources, references, citation times, and year of publication. In addition, the journal Impact Factor and Hirsch index were obtained from the Journal Citation Report. We conducted the data screening, statistical analysis, and visualization *via* the Bibliometrix R package. VOS viewer software was employed to generate the collaboration network map among countries and institutions for better performance in visualization.

Results: In total, 1,887 original research articles from 2012 to 2021 were identified. The number of annual publications rapidly increased from 107 to 278, and a drastic increase in citation times was observed in 2017–2019. As for global contributions, the United States was the most influential country with the highest international collaboration, while China was the most productive country. Professor Cai Lu was the most prolific author. Shandong University published the most articles. *Cardiovascular Diabetology* journal released the most DCM-related articles. "Metabolic Stress-induced Activation of FoxO1 Triggers Diabetic Cardiomyopathy in Mice" Battiprolu PK et al., J Clin Invest, 2012. was the most top-cited article regarding local citations. The top three keywords in terms of frequency were apoptosis, oxidative stress, and fibrosis. The analysis of future topic trends indicated that "Forkhead box protein O1," "Heart failure with preserved ejection fraction," "Dapagliflozin," "Thioredoxin," "Mitochondria dysfunction," "Glucose," "Pyroptosis," "Cardiac fibroblast" and "Long non-coding RNA" could be promising hotspots.

Conclusion: This study provides meaningful insights into DCM, which is expected to assist cardiologists and endocrinologists in exploring frontiers and future research directions in the domain through a refined and concise summary.

KEYWORDS

diabetic cardiomyopathy, cardiomyopathy, diabetic complications, bibliometric analysis, data visualization

Introduction

Diabetes mellitus (DM) is a prevalent chronic non-communicable disease and one of the most severe and pressing health issues worldwide. Globally, the number of diabetic patients has increased sharply in recent years, it is estimated that 537 million people live with DM worldwide in 2021, which will soar to 784 million in 2045 according to current estimates from International Diabetes Federation (IDF) Diabetes Atlas (1). Cardiovascular disease (CVD) is the leading cause of death in patients with DM, and the association between DM and CVD has been demonstrated for a long time (2, 3). However, several clinical observations including the Framingham Study found that there is a high risk of heart failure (HF) in patients with DM, ranging from 19% to 26% (4–6), and it even occurs independently of traditional CVD risk factors, including coronary heart disease (CAD), hypertension (HTN), etc. In 1972, Rubler and his colleagues observed a unique myocardial injury, and named it the diabetic cardiomyopathy (DCM) (7).

DCM initially has a subclinical period that results from fibrosis, left ventricular hypertrophy (LVH), and myocardial relaxation abnormality manifesting as asymptomatic in early phases (8). Still, with the progress of the disease, the growth of left ventricular mass (LVM) leads to the decline of diastolic left ventricular filling, it gradually becomes symptomatic from diastolic dysfunction to systolic dysfunction, manifesting as cardiac dysfunction eventually characterized by various metabolic and neurohumoral pathway disorders (9–11). Studies have shown that the prevalence of cardiac dysfunction in individuals with type 1 diabetes mellitus (T1DM) and type 2 diabetes mellitus (T2DM) is 14.5% and 35%, respectively (12, 13). Due to the insidious nature of DCM onset, the incidence of DCM has been dramatically underestimated (11, 14), meaning that the number of people with diabetes and cardiac dysfunction is far more significant than expected. DCM research is, therefore, of paramount importance in reducing the global healthcare burden and mortality among patients with DM. Although numerous reviews have previously addressed DCM from pathophysiology, preclinical and clinical perspectives, the previous reviews only discuss a particular aspect or characteristic of DCM through subjectively papers summary, conclusion, and extraction by researchers. Up to now, there is no study to comprehensively present the current status of DCM research including scholars, institutions, countries, journals, and research hotspots. Moreover, the traditional review is difficult to visualize the internal conceptual structure and potential associations of abundant literature objectively.

Bibliometrics analysis, proposed in 1969 by Pritchard, is a quantitative science approach that evaluates the research characteristics and trends in a specific time frame through many published academic literature analyses (15). Compared with traditional systemic reviews, it can be used not only to trace the historical evolution of a particular field, but also to predict the future research directions and collaboration opportunities through visualizing the conceptual, intellectual, and social structures at different scales from macro and micro perspectives. In recent years, with the emergence of an extensive number of medical academic publications, bibliometrics has played a vital role in the health care field. Due to the lack of tools to describe and analyze a massive amount of literature previously, bibliometrics analysis has not yet been used to systematically summarize the literature on DCM. Nowadays, multiple scientometric visualization software are available for bibliometrics analysis. The R programing language is an open-source software with robust analysis and visualization capabilities. As an R-package, *Bibliometrix* is a widely used science mapping application (16), and Java-run software VOS viewer (17) performs better in co-occurrence network visualization, which can help us track frontier dynamics by exploring core items in relevant research fields.

In this study, we retrieved DCM-related publications in the Web of Science^{TM} core collection database over the past decade from 2012 to 2021, conducted an informative systematic and scientific overview, and predicted potential development trends by the following steps: (1) Investigate the output and growth trends of publications and citations; (2) Describe the distribution and characteristic of core countries,

authors, institutions, journals, and top-cited publications; (3) Visualize the collaboration and co-occurrence between core countries, authors, and institutions; (4) Conduct a network of core author's keywords and predict research hotspots and trends by algorithms. Overall, we aim to summarize issues in the literature review on DCM in the past decade and predict future trends. The findings will help academics, including cardiologists and endocrinologists gain a quick understanding of the current state of the DCM knowledge domain in the past decade and help them select journals for publication and collaborators, as well as guide directions and lay solid foundations for future studies.

Materials and methods

Dataset establishment

The online DCM literature data are publications collected from the Science Citation Index Expanded (SCIE) of Clarivate Analytics' Web of Science^{TM}[1] core collection (WoS; WoSCC) database. As a well-known authoritative citation index database of research publications and citations (18), The WoSCC is one of the top sources for bibliometric analysis with a well-established citation network in different research fields, including natural sciences, engineering, biomedicine, etc., (19, 20). To understand the research status in the field of DCM in the past decade, we designed a search strategy to establish our dataset initially: [TS = (diabetic NEAR/0 myocardial) OR TS = (diabetic NEAR/0 cardiomyopathy) OR TS = (diabetic NEAR/0 myocardiopathy) OR TS = (diabetic NEAR/0 cardiomyopathies)] AND PY = (2012.1.1–2021.12.31). We excluded publications in the year of 2022 to obtain a more accurate annual result. All bibliographic records, including titles, abstracts, keywords, authors, institutions, addresses, journals, references, citation times, publication year, etc., were saved as plain TXT files. Our study data were obtained from an open database, so there are no ethical concerns.

Data screening

We integrated all txt files into a zip package and imported them into the analysis software *Biblioshiny* for data screening, which is a partner web interface app version of the Bibliometric R package *Bibliometrix* version 3.2.1 (R version 4.2.0, R studio version 2022.02.2 + 485 "Prairie Trillium" Release) makes the command line function more intuitive and user-friendly (16). To more precisely perform the research status in the field of DCM in the past decade, we used *Biblioshiny* to screen only full-length original articles that meet the requirement of our study, and non-article publications were excluded. The language was restricted to English. Moreover, we conducted a string of codes by *Readxl* R package version 1.4.0 (R version 4.2.0, R studio version 2022.02.2 + 485 "Prairie Trillium" Release) to identify and delete duplicate publications. The detailed search and screen procedure is shown in **Figure 1**. To avoid bias caused by database updates and subjectivity, two authors (WSC and TCX) independently performed data identification and screening on June 24, 2022. The third author (ZBX) made judgments of discrepancies to reach a consensus. Finally, our DCM research status dataset was exported as a CSV file.

Data processing

We imported the CSV file for further data processing in the *Biblioshiny* R package, which can automatically analyze all the selected records and generate relative graphs with a mouse click. In our study, the *Biblioshiny* was employed to analyze all publication characteristics, including publication and citation trends, contributions of authors and journals, collaborations of institutions and countries, and distribution and prediction of hotspots, respectively. To perform more vivid and comprehensible collaboration maps, VOS viewer (version 1.6.18.0, Leiden University, Netherlands), which is one of the most widely used visualization software in bibliometric analysis (17), was employed to visualize collaboration maps among institutions and countries respectively, according to the PageRank score calculated from the *Biblioshiny* of R studio software interface.

It is worth mentioning that we assessed the journal impact factor (IF) and journal citation reports (JCR) ([2]Clarivate Analytics, Philadelphia, United States) category according to the 2021 JCR^{TM}. The Hirsch index (H-index) indicates the academic influence of authors, that is, an author has published at most h papers that have been cited at least h times (21). Local citations (LCS) are used to evaluate the number of times a journal included in this dataset is cited by other journals in the same data set (22). The PageRank algorithm was invented to catalog the Internet web page by Larry Page, the Google company sponsor, becoming a popular and newly emerged bibliometric method for network citation analysis based on the structural characteristics of publications nowadays (23–25). Google used it to embody the relevance and importance of different web pages (26). Now, as an alternative measurement of impact for authors, intuitions, journals, etc., PageRank can sort nodes (Countries and institutions, in our study) by importance (PageRank score) which depends on the number of being cited and the score of each citing items themselves (27).

1 http://isiknowledge.com/

2 http://mjl.clarivate.com/

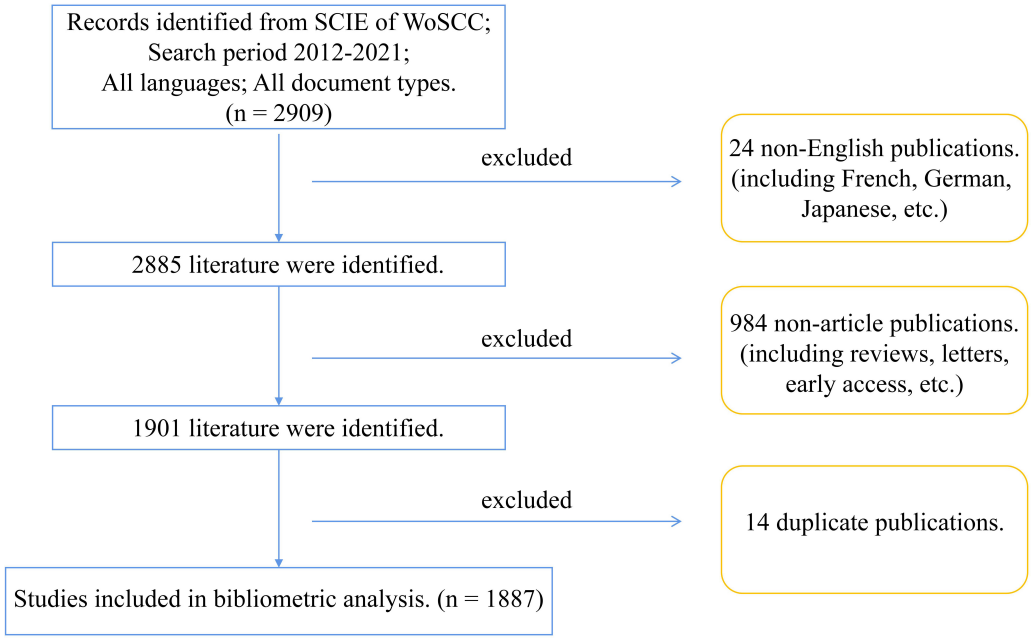

FIGURE 1
Flow chart of the data identification and screening results.

Results

Publication and citation trends in the past decade

As shown in **Figure 2A**. The number of annual publications rapidly increased from 107 to 278 in the past decade, with more than two times the number of publications in 2021 than in 2012, indicating that DCM is an emerging focus of diabetes-related diseases. The total mean citation per year means the yearly average number of times each DCM disease-related publication has been cited. Interestingly, a drastic increase in citation times was observed in 2017–2019, reaching a peak of 6.09 in 2019 (**Figure 2B**).

Analysis of countries and institutions

Table 1 lists the top 10 collaborating countries and institutions in the DCM research field in the past decade ranked by PageRank value and the number of publications—the greater the PageRank value, the more significant its importance, which represents it has more weight in cooperation. The top 50 countries and institutions ranked by PageRank are taken for visual analysis *via* VOS viewer. Circles represent different countries or institutions, the circle size represents the PageRank value, the lines signify the countries' or institutions' collaboration strength, and each color represents a cluster, which is a group of items with comparable attributes within a network. As we expected, related countries and institutions had multi-dimensional cooperation in the field of DCM.

In **Figure 3**, the United States (Publications: 235, RankPage: 0.196) ranks first in the PageRank value, connected to almost all countries in the figure, and China (Publications: 977, RankPage: 0.144) ranks first in the total number of publications and has the most robust connection with the United States. **Figure 4** shows the institutions' cooperation network. The top 5 collaborating institutions in the past decade are Wenzhou Medicine University (Publications: 144, RankPage: 0.068), University of Louisville (Publications: 114, RankPage: 0.061), Jilin University (Publications: 105, RankPage: 0.057), University of Melbourne (Publications: 57, RankPage: 0.057), and University of Hong Kong (Publications: 40, RankPage: 0.346). The network is positioned in 6 clusters, each represented by Wenzhou Medicine University, University of Melbourne, University of Hong Kong, University of Auckland and Monash University, and China Medicine University.

Contribution of authors

A total of 10,443 authors contributed to DCM-related research in the past decade, with an average of 5.53 authors per study. In **Table 2**, we listed the top 20 contributing authors of the DCM field in the past decade while each contributed more than 10 publications. Cai Lu was by far the most prolific

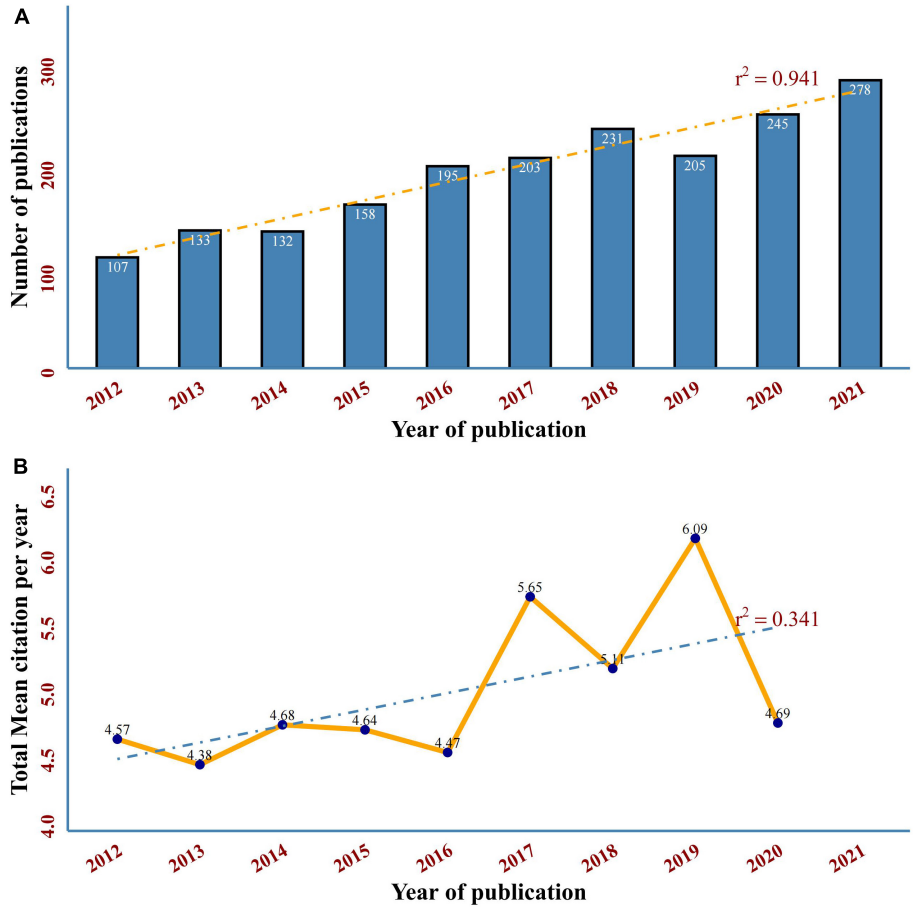

FIGURE 2
(A) Annual trend chart of publications on DCM in 2012–2021. The dotted line represents linear growth with $r^2 = 0.941$. **(B)** Growth of the article cited per year in DCM. The dotted line represents linear growth with $r^2 = 0.341$.

author, with 41 publications and 1,480 citations, followed by Tan Yi (publications: 26, citations: 1,092) and Ritchie Rebecca H. (publications: 21, citations: 1,092), respectively, and the top 3 highest h-index authors are the same. It is noted that many scholars have recognized Lin Jie and Li Yang.

The count of papers and citations per year directly indicates the author's activity in this research field. Suppose an author produces relevant articles every year meanwhile has been cited by many other scholars. In that case, the author has been active in this field with particular influence. The result of the top 20 most prolific authors' annual production and citations from 2012 to 2021 in the field of DCM is shown in **Figure 5**. It is noted that Cai Lu, Tan Yi, Ritchie Rebecca H, and Zhang Wei have been very active in DCM research with higher total citations per year.

The top 3 corresponding author's countries are China, the United States, and Canada, with multiple country publications ratios of 16.3%, 32.3%, and 48.6%, respectively. Most countries' publications with co-authors involved multi-country cooperation. Among the top 20 corresponding author's countries, Germany (18/22) and the United Kingdom (11/15) have more multiple country publications (MCP) than single country publications (SCP), while other countries of corresponding authors lack international cooperation (**Figure 6**).

Outstanding journals

In the past decade, 1,887 articles in the DCM field have been published in 459 different journals. In **Table 3**, the top 20 journals in terms of the count of publications are displayed, *Cardiovascular Diabetology* ($n = 66$) was the leading journal among these and with the highest impact factor (IF = 9.951), followed by *PLoS ONE* ($n = 47$) and *American Journal of Physiology-Heart and Circulatory Physiology* ($n = 47$), accounting for 2.49% and 2.28% of the overall research output respectively. The establishment of *Cardiovascular Diabetology* also indicates that diabetic cardiomyopathy is an increasingly severe diabetic complication that deserves more attention.

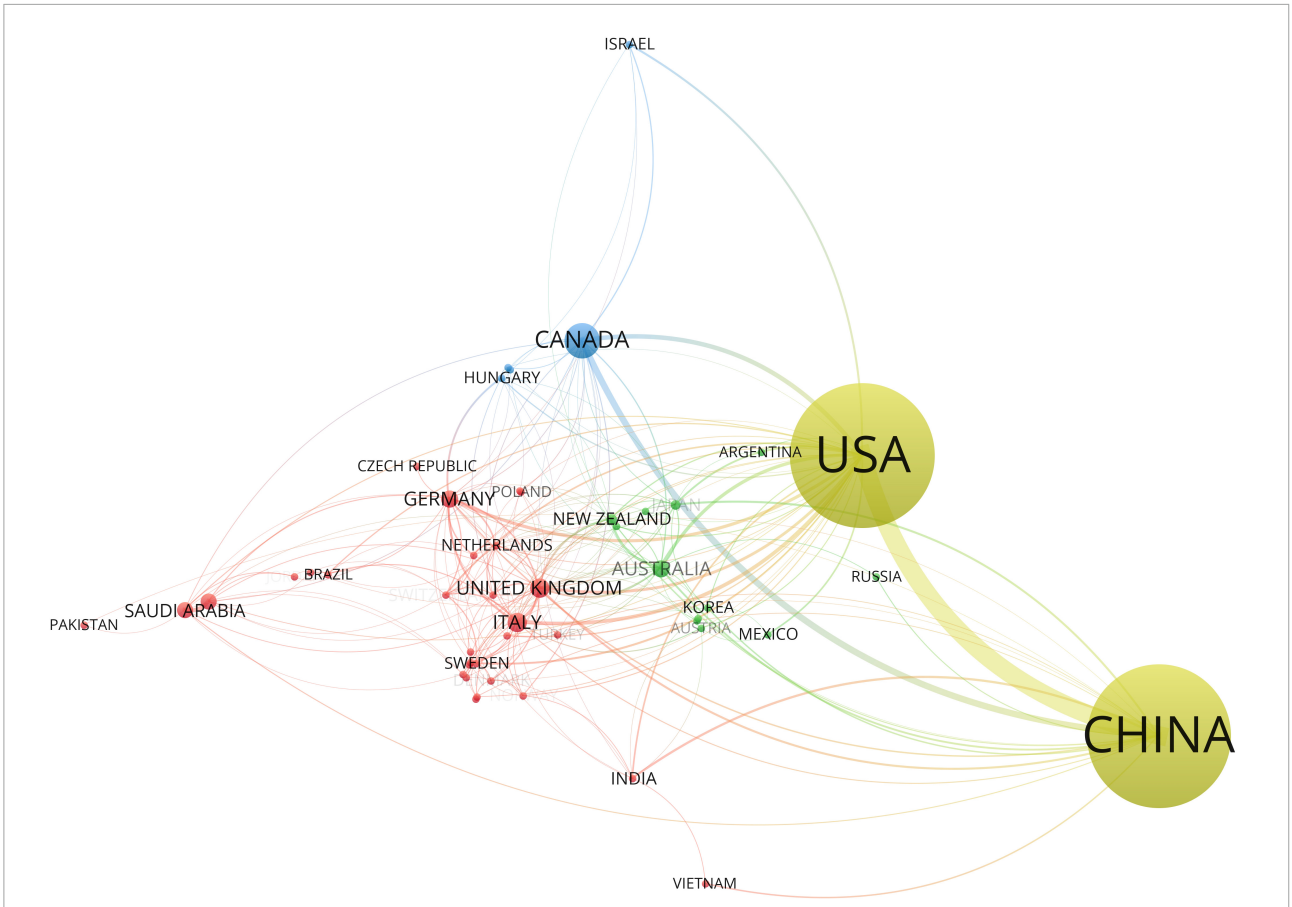

FIGURE 3
Top 50 Countries' collaboration network map in the field of DCM ranked by PageRank.

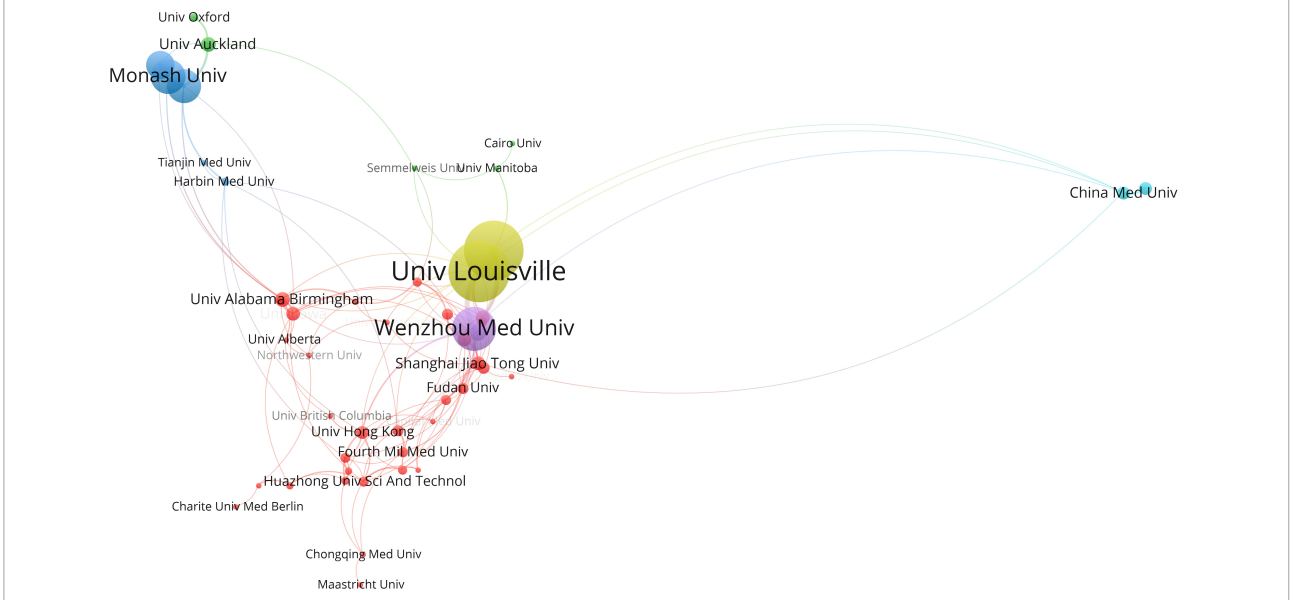

FIGURE 4
Top 50 Institutions' collaboration network map in the field of DCM ranked by PageRank.

TABLE 1 Top 10 countries and institutions in terms of PageRank and publications.

Items	PageRank			Publications		
	Ranking	Name	Value	Ranking	Name	Number
Countries	1	United States	0.196	1	China	977
	2	China	0.144	2	United States	235
	3	United Kingdom	0.056	3	Canada	72
	4	Canada	0.054	4	India	59
	5	Italy	0.053	5	Japan	43
	6	Germany	0.05	6	Australia	42
	7	Australia	0.042	7	Germany	40
	8	Japan	0.027	8	Italy	40
	9	Saudi Arabia	0.025	9	Egypt	36
	10	Egypt	0.025	10	Korea	27
Institutions	1	Wenzhou Med Univ	0.068	1	Shandong Univ	160
	2	Univ Louisville	0.061	2	Wenzhou Med Univ	144
	3	Jilin Univ	0.057	3	Harbin Med Univ	143
	4	Univ Melbourne	0.057	4	Univ Louisville	114
	5	Univ Hong Kong	0.046	5	Jilin Univ	105
	6	Monash Univ	0.044	6	Fourth Mil Med Univ	97
	7	Soochow Univ	0.039	7	China Med Univ	89
	8	Univ Alabama Birmingham	0.035	8	Huazhong Univ Sci And Technol	71
	9	Huazhong Univ Sci And Technol	0.033	9	WUHAN UNIV	69
	10	Baker Heart And Diabet Inst	0.033	10	Univ Melbourne	57

Most of the publishers of these journals are located in the United States and England. It is worth noting that *Diabetes* (LCS = 3,244, IF = 9.461), *PLoS ONE* (LCS = 1,438, IF = 3.240), and *Cardiovascular and Diabetology* (LCS = 1,253, IF = 9.951) are also among the top 20 journals ranked by local citations (**Figure 7**).

Citation analysis

In **Supplementary Table 1** (28–37), we listed the top 10 articles ranked by LCS. The higher the LCS value, the greater the influence of this article in the DCM field. Overall, as branches of the previous research, LCS were not high for articles in the past decade, which most are experimental studies of mechanisms. The top-cited paper is "Metabolic Stress-induced Activation of FoxO1 Triggers Diabetic Cardiomyopathy in Mice" (28) (LCS: 54), published in the *Journal of Clinical Investigation* (IF: 19.386 according to 2021 JCR^{TM}). We further conducted the historiographic analysis, which can provide the year-by-year mapping of the historical directly-cited publications, to better perform the citation connections among influential articles from a period. Each node represents different influential articles while lines represent their connections. Notably, articles without citation connections with others from 2012–2021 will not appear in **Figure 8**.

Keywords analysis and future research direction

We extracted 3,147 Author's keywords from 1,887 articles. Deleting "Diabetic cardiomyopathy" and merging synonyms, a total of 2,774 keywords were obtained, of which 31 keywords appeared more than 20 times. The frequency results are shown in **Supplementary Figure 1**. Then we made a Word Cloud map using the 31 Author's keywords to understand better the current research hotspots (**Figure 9**).

After exploring the frequency of occurrence of each keyword, we further investigated the association between them. Simple correspondence analysis (SCA) is a visual data analysis method that graphically represents the relationship between the categorical data in low dimensional space (38). Multiple correspondence analysis (MCA) is an extension of SCA. Unlike SCA, the main advantage of MCA is that it is a powerful multivariate statistical technique dealing with more than one categorical variable (39). As an unsupervised learning algorithm, this method can explore, summarize and graphically represent the association between multi-dimensional categorical data in large and complex datasets (40). In our case, MCA's output produces points clouds of keywords typically represented by a 2-dimensional graph. The cloud of keywords is constructed on associations between keywords which can synopses the expression of relations between the articles with no underlying

TABLE 2 Top 20 contributing authors of diabetic cardiomyopathy research in the past decade.

Ranking	Author	Count (% of 1887)	h-index	Total citations
1	Cai Lu	41 (2.17%)	22	1480
2	Tan Yi	26 (1.38%)	20	1092
3	Ritchie Rebecca H	21 (1.11%)	13	645
3	Zhang Wei	21 (1.11%)	13	639
4	Liang Guang	17 (0.90%)	13	631
4	Tang Qizhu	17 (0.90%)	13	576
5	Xu Changqing	16 (0.85%)	13	370
6	Li Xiaokun	15 (0.79%)	14	510
6	Zhang Yun	15 (0.79%)	12	652
7	Li Wei	14 (0.74%)	9	566
7	Sun Dongdong	14 (0.74%)	9	537
8	Wang Haichang	13 (0.69%)	10	298
8	Zheng Yang	13 (0.69%)	10	403
9	Chen Chen	12 (0.64%)	8	592
9	Chen Jing	12 (0.64%)	7	491
9	Huang Chihyang	12 (0.64%)	8	455
9	Kiriazis Helen	12 (0.64%)	10	428
9	Kuo Weiwen	12 (0.64%)	9	534
9	Lin Jie	12 (0.64%)	9	296
9	Li Yang	12 (0.64%)	9	324

hypotheses. In a word, in the same quadrant, keywords with the most significant associations were located the closest. Finally, we utilized the hierarchical clustering method to cluster different clouds of keywords into five distinct categories, represented as category 1 (red), category 2 (light blue), category 3 (green), category 4 (purple), and category 5 (orange) respectively (**Figure 10**).

The trend topic analysis is a vital mapping tool that helps to portray the seed of trend integration rooted in the previous stream (41). The topic is an induced and summarized concept, like a bucket filled with keywords with similar meanings or apparent associations. In our case, we identified the author's keywords and examined the keywords that occur at least five times per year, and the word frequency needs to be more than five times. As shown in **Figure 11**, 44 buzz topics of the year were identified as. The circle represents the topic that emerged dramatically in the year, and the blue line denotes the times when the topics frequently occur. Except for the topics like "Diabetic cardiomyopathy," "Cardiomyopathy" and "Diabetes" that we searched for, "Apoptosis," "Oxidative stress" and "Fibrosis" have a higher frequency, "Forkhead box protein O1," "Heart failure with preserved ejection fraction," "Dapagliflozin," "Thioredoxin," "Mitochondria dysfunction," "Glucose," "Pyroptosis," "Cardiac fibroblast" and "Long non-coding RNA" have potential research prospects. "Tissue Doppler imaging," "Arrhythmia" and "Cardiac magnetic resonance imaging" as hot topics in 2013 have become less popular in the future, which may be related to the fact that they have been studied thoroughly.

Discussion

The worldwide surge in individuals suffering from DM brings a dramatic societal burden on substantial healthcare costs and poor health outcomes for affected patients (42). Cardiovascular complications secondary to DM have aroused great concern. As one of the most common complications of DM, DCM, which have a twofold greater risk of HF compared with other complications (43), seriously affects the prognosis of diabetic patients, triggering a high mortality rate (44). Although DCM-related preclinical and clinical research have grown exponentially over the past few decades, the pathogenesis of DCM remains unclear and without consensus on preventive or therapeutic strategies to date (11). So, it is vital to sort out a practical, systematic, and comprehensive review of DCM-related papers in the past few years to enable researchers quickly understand the research status, capture the characteristics and identify the future research direction. Hence, we conducted a bibliometric analysis of 1,887 DCM-related articles from 2012–2021 (a decade) in WoSCC to provide an overview of current knowledge in various categories and potential future hotspots.

We used the *Biblioshiny* to conduct our bibliometric analysis. The chronological trends of publications show that the overall volume of annually published DCM-related original research has increased globally during the study period, which can be divided into two stages (**Figure 2A**). The first stage is 2012–2015, a flat period of the DCM-related original study, the number of articles fluctuated around 150. The year of 2016 is an important milestone toward the second stage when DCM research has entered rapid development and reached its highest level of 278 articles in 2021. In addition, the total mean article cited per year increased from 4.57 to 6.09 in 2019 (**Figure 2B**). The poor performance in 2020 may be related to the fact that the deadline for retrieval was set at the end of 2021. Therefore, the total average citations of articles in 2021 cannot be displayed either, and the mean citations of articles published in 2020 may be underestimated (19). The linear slope of publications and citations growth in the past 10 years is 0.941 and 0.341, respectively, indicating that DCM has become increasingly important as a severe pathological change in the progression of cardiovascular complications with promising research prospects.

As for global contributions, China is the most productive country with 1,232 publications. DM is a global public health problem, especially in developing countries (45, 46). As the

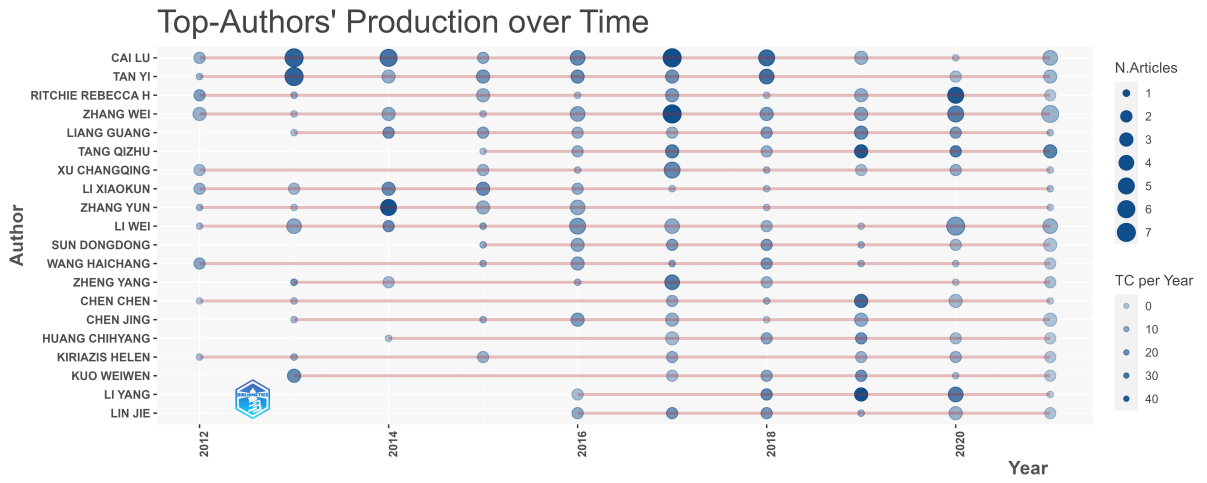

FIGURE 5
Publications and citations per year of the top 20 most prolific authors in the field of DCM research in the past decade.

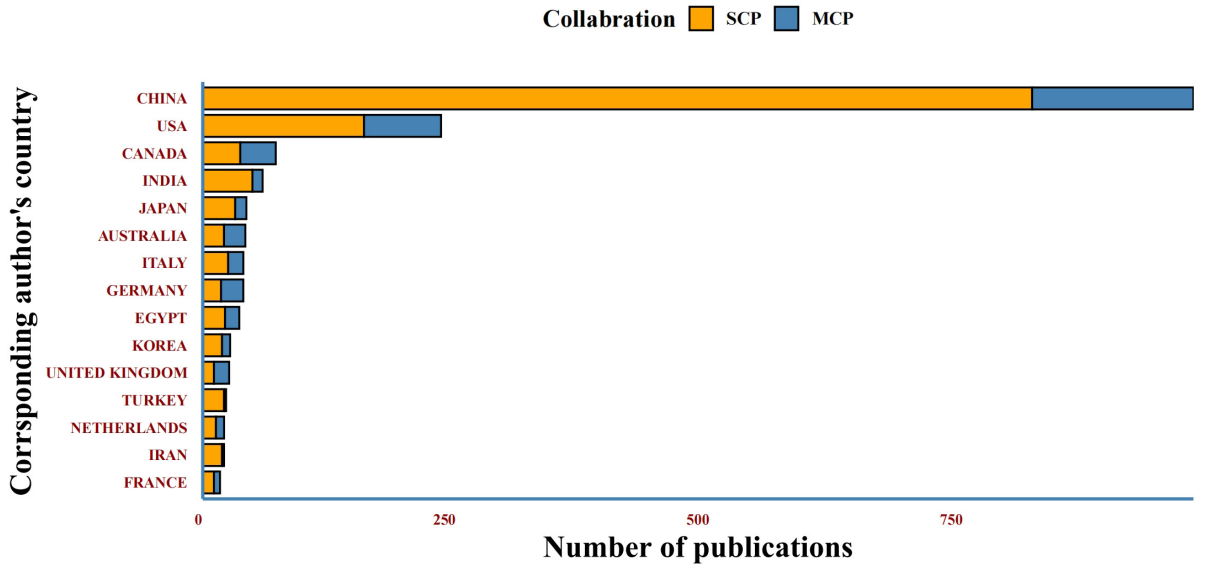

FIGURE 6
Top 20 corresponding author's countries. SCP-Single Country Publications; MCP- Multiple Country Publications.

largest developing country, China has a vast number of individuals with DM, which is still rising and underrated (47, 48). Taken together, China would emphasize more on the study of DM and its complications, including DCM. While the United States had the highest PageRank score, a novel index used to evaluate the importance of items in the collaboration map, implying that it has enormous influence with a high volume of publications as well as cooperation with many countries. Interestingly, the United Kingdom (Publications: 26, RankPage: 0.056) ranks third by PageRank value, but it has only 26 publications, much lower than other countries, which means the United Kingdom does not publish much but has a lot of connections with many other countries. Among institutions, Shandong University ranks first in the number of articles published. In terms of collaboration and influence, Wenzhou medical university, the University of Louisville, Jilin University, and the University of Melbourne have a high clustering density, showing a significant influence in the past decade in the research field of the DCM. Although the University of Hong Kong has 40 publications, it ranks fifth place according to the PageRank value, indicating it has many research partners. Relatively independent research institutions with low PageRank score need to further strengthen cooperation in the future to improve their influence.

TABLE 3 Top 20 journals contributing to publications in diabetic cardiomyopathy in the past decade.

Journal	Count (% of 1887)	Research area	Impact factor	Country/Region
Cardiovascular Diabetology	66 (3.50%)	Endocrinology and Metabolism Cardiac and Cardiovascular Systems	8.941	ENGLAND
PLoS ONE	47 (2.49%)	Multidisciplinary Sciences	3.752	United States
American Journal of Physiology-Heart and Circulatory Physiology	43 (2.28%)	Peripheral Vascular Disease Physiology Cardiac and Cardiovascular Systems	5.125	United States
Scientific Reports	40 (2.12%)	Multidisciplinary Sciences	4.996	ENGLAND
Experimental and Therapeutic Medicine	37 (1.96%)	Medicine, Research and Experimental	2.751	GREECE
Oxidative Medicine and Cellular Longevity	37 (1.96%)	Cell Biology	7.310	United States
Journal Of Cellular and Molecular Medicine	36 (1.91%)	Cell Biology Medicine, Research and Experimental	5.295	ENGLAND
Molecular Medicine Reports	36 (1.91%)	Oncology Medicine, Research and Experimental	3.423	GREECE
Biochemical And Biophysical Research Communications	33 (1.75%)	Biochemistry and Molecular Biology Biophysics	3.332	United States
Diabetes	29 (1.54%)	Endocrinology and Metabolism	9.337	United States
Frontiers In Pharmacology	29 (1.54%)	Pharmacology and Pharmacy	5.988	SWITZERLAND
Biomedicine and Pharmacotherapy	28 (1.48%)	Pharmacology and Pharmacy Medicine, Research and Experimental	7.419	FRANCE
Journal Of Molecular and Cellular Cardiology	28 (1.48%)	Cell Biology Cardiac and Cardiovascular Systems	5.763	ENGLAND
Life Sciences	23 (1.22%)	Pharmacology and Pharmacy Medicine, Research and Experimental	6.780	ENGLAND
Frontiers In Physiology	21 (1.11%)	Physiology	4.755	SWITZERLAND
Molecular And Cellular Biochemistry	21 (1.11%)	Cell Biology	3.842	NETHERLANDS
Biochimica Et Biophysica Acta-Molecular Basis of Disease	19 (1.01%)	Biochemistry and Molecular Biology Biophysics	6.633	NETHERLANDS
Journal Of Cellular Physiology	19 (1.01%)	Cell Biology Physiology	6.513	United States
BMC Cardiovascular Disorders	18 (0.95%)	Cardiac and Cardiovascular Systems	2.174	ENGLAND
European Journal of Pharmacology	18 (0.95%)	Pharmacology and Pharmacy	5.195	NETHERLANDS

Professor Cai Lu, from the University of Louisville in the United States, has the most significant quantity of original full-length articles (41 articles, 1,480 total citations), publishing 2% of all publications, with the greatest h-index. In the 1980s, Metallothionein (MT) was demonstrated as an antioxidant against reactive oxygen and nitrogen species (ROS, RNS) (49, 50). Later, MT was observed it could improve diabetes-induced cardiac deficits by inhibiting ROS/RNS (51). Professor Cai Lu further demonstrated that MT could impede the accumulation of ROS/RNS and prevent cardiac apoptosis by suppressing mitochondrial oxidative stress, which significantly prevents DCM development (52, 53). In general, Cai Lu has made essential contributions to DCM's preclinical pharmacological and pathological mechanism research. **Figure 5** shows that, as one of the high-yielding authors from Monash University and Baker Heart and Diabetes Institution in Australia, Ritchie Rebecca H published many papers and got more citations in the last 3 years. The therapeutic potential of cardiac-targeted gene therapy, especially the adeno-associated viral vector (AAV) gene therapy which could limit pathological remodeling in the diabetic heart and improve cardiac function, are the main research contributions of Ritchie Rebecca H (54–56). In addition, corresponding author countries are primarily domestic. However, a certain amount of international cooperative research is devoted to exploring the possible therapeutic direction of DCM. Researchers from the United Arab Emirates, the United States, Lebanon, Saudi Arabia, and Australia have discussed the progress made in the mechanism of phytochemicals' cardioprotective effect in DM (57), meaning the treatment of DCM is a topic of global interest and consensus, and the research on the treatment of DCM with traditional Chinese medicine may have promising development potential.

Although Asian countries like China lead the area with the most counts of DCM-related articles in the past decade, most of these journals' publishers are located in United States and England. It suggested that Asian countries should strengthen the construction of journals. *Cardiovascular Diabetology* journal released the most DCM-related articles with a high IF, while

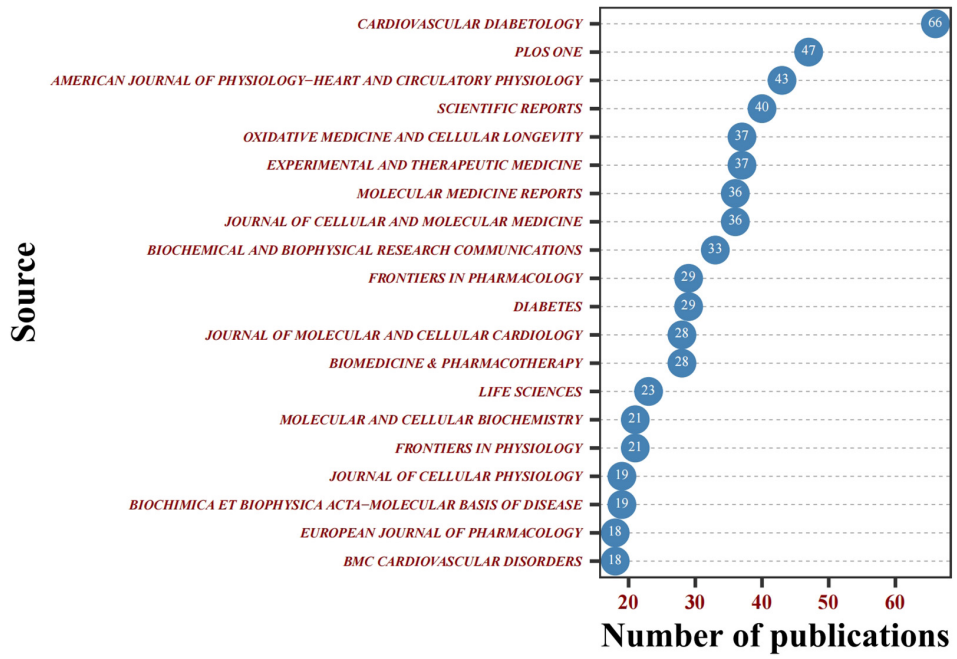

FIGURE 7
Cleveland dot pot of the top 20 journals cited journals.

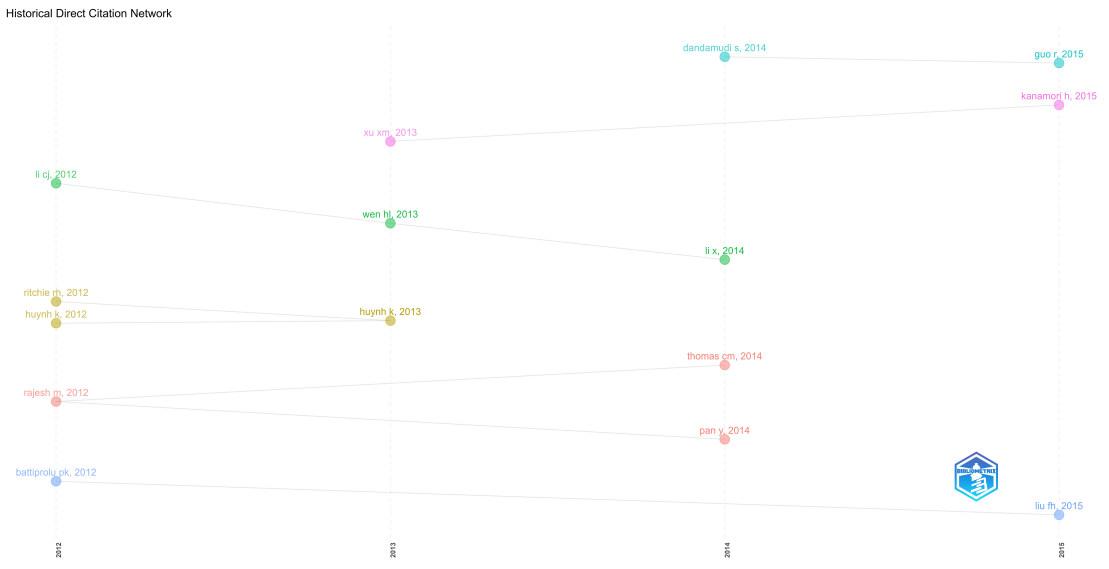

FIGURE 8
Historical analysis of direct citation of top-cited articles in DCM field from 2012–2021 generated from R studio Intellectual Structure menu of *Biblioshiny* package.

the *Diabetes* journal had the highest IF according to the 2021 JCR™. Both journals appeared in the top 20 journals regarding LCS (**Figure 7**), reflecting that these two journals have some authority in the DCM research field.

Despite the fact that the article published in 2012 by Battiprolu PK et al. has not been cited by other high-quality papers. The most significant article with the highest LCS in the past decade has not been cited by the majority of classically-cited articles. A possible explanation is that this article was cited by other newly published papers which have not yet shown their academic impact (high LCS) to date, indicating that it may have a promising research prospect. This study demonstrated

FIGURE 9
Word Cloud map regarding the keywords' frequency of occurrence generated from R studio Documents menu of *Biblioshiny* package.

that the Forkhead box proteins O (FoxO) signaling axis was persistently activated in DCM development for the first time (28). Interestingly, we also found that FoxO1 has enormous developmental potential in our future trend topics analysis (**Figure 11**). Unlike other bibliometric studies (19, 58), our historical analysis does not reflect the inheritance relationship between classically-cited literature, which may be related to the selected research period. **Figure 7** may show the branches of previous studies since DCM research has entered a period of rapid development in the past decade.

We can track the knowledge distribution, association, and future research directions by analyzing the author's keywords which are a scientific article's most concise and accurate generalization. We conducted the analysis from two dimensions. The first dimension is we explored the frequency of keywords and the possible association between them from a cross-sectional perspective. The top three keywords in frequency in the past decade are apoptosis (216 times), oxidative stress (213 times), and fibrosis (192 times), respectively (**Figure 9**). Diabetes is characterized by oxidative stress and low-grade inflammation (59). Under physiological circumstances, a delicate balance between the production and degradation of ROS resulting an average steady-state ROS level. as a predilection site of oxidative stress, the myocardium is vulnerable to a transient or persistent ROS increment due to the DM, which would result in oxidative modification of cellular component and eventually induce cell death *via* apoptosis (60).

It is worth interpreting the significance of the coordinate axes in **Figure 10**. The first coordinate axis (x-axis) emphasizes the characteristics of the DCM study. Higher values (at the right of the conceptual structure map) are concepts related to metabolic, functional, and organ level changes, such as obesity, left ventricle, heart failure, etc. These factors are undoubtedly hot issues in clinical research in the field of DCM because the change in cardiac function and Metabolic problems such as obesity can be observed directly. Conversely, lower values for the x-axis indicate the pathological study in the DCM field. These paramount results say that different characteristics of the DCM study at the bench and clinical courses exist. The second coordinate axis (y-axis) can be interpreted as the studies focusing on some hot issues on the dynamics (61). Overall, the hotspots of increasing interest in DCM research in the last decade mainly focused on pathological mechanisms at the molecular and cellular level.

Considering the findings from MCA results, the interpretation of the Cluster analysis results is that Category 1, Category 2, and Category 3 mainly focus on the DCM study of pathological mechanisms, including autophagy, apoptosis, fibrosis, signaling pathways, etc. Category 4 represents the pathophysiology mechanisms and clinical manifestation of DCM. Interestingly, Category 5 depicts the effects of the hyperglycemic effect on cardiomyocytes with only two items. As endogenous non-coding RNA (ncRNA) molecules, microRNAs (miRNA) can significantly affect different biological processes, primarily through the suppression of mRNA expression. However, the synthesis of those molecules is affected by high glucose levels (62). A recent study found that more than 300 miRNAs are dysregulated in DCM (63), which modulate plenty of cardiomyocyte pathophysiological processes, including apoptosis, inflammation, cell growth, pyroptosis, fibrosis, and response to oxidative stress *via* different pathways (64–67). Although there are many different levels of understanding of the mechanism of DCM, similar to previous studies, hyperglycemia seems to play an essential role in the pathogenesis of diabetic cardiomyopathy, activating a series of pathological changes or processes (68).

The second dimension shows the research trend of DCM in the past 10 years in combination with the evolution of time. Overall, these current and promising future research frontiers reflect that the pathological changes of DCM are diverse. However, the research topics with promising research potential in the future are gradually transitioning to drug-based treatment (**Figure 11**). As discussed above as well as in previous reviews, metabolic disturbance, including hyperglycemia, is a central and essential driver of pathological changes (oxidative stress, cardiac hypertrophy and fibrosis, inflammation, apoptosis, etc.) modulated by a wide range of molecules and cells, affecting the structure and function of the cardiac, particularly the left ventricle (4, 69). Although a few studies have addressed various pathological alterations, the causal relationship between these complex molecular and cellular mechanisms has not been fully elucidated (70). It has ultimately led to the conclusion that there is currently no standard pharmacotherapeutic approach for DCM. Even though diagnostic criteria for pure DCM are demanding, several drugs still showed the treatment potential, inspiring future drug-based therapeutic clinical studies [**Supplementary Table 2** (71–77)].

The new class of antidiabetic drugs Dapagliflozin (DAPA) is a member of sodium-glucose cotransporter-2 (SGLT-2)

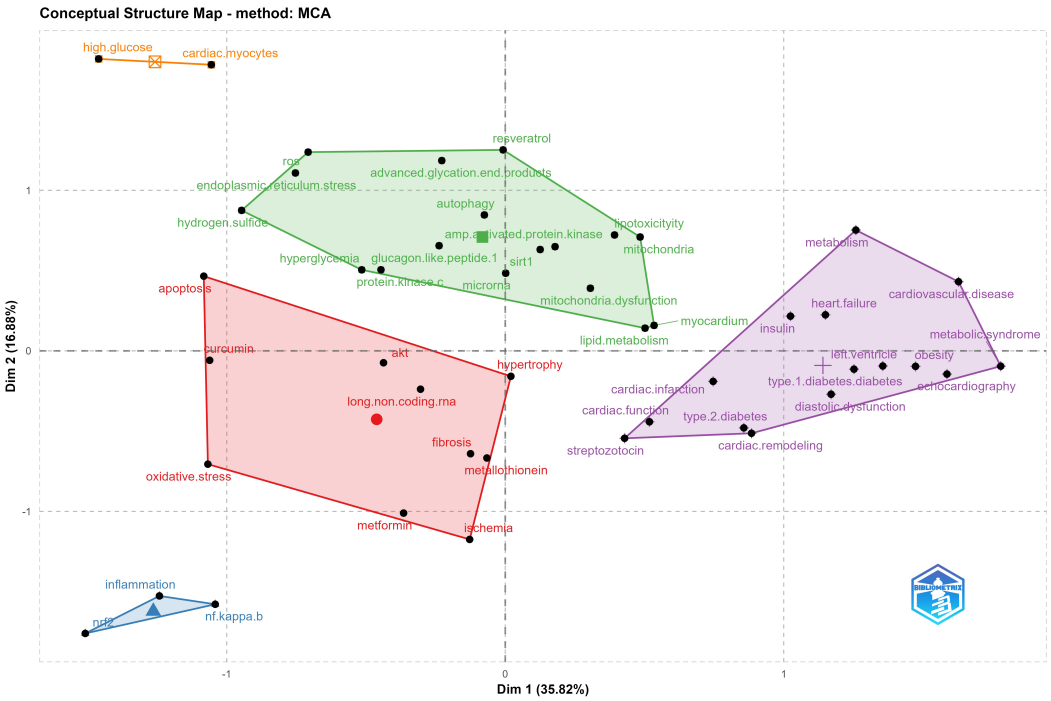

FIGURE 10
Conceptual structure map of author's keywords based on Multiple correspondence analysis with clustering validation (5 categories identified) in DCM field generated from R studio Conceptual Structure menu of *Biblioshiny* package.

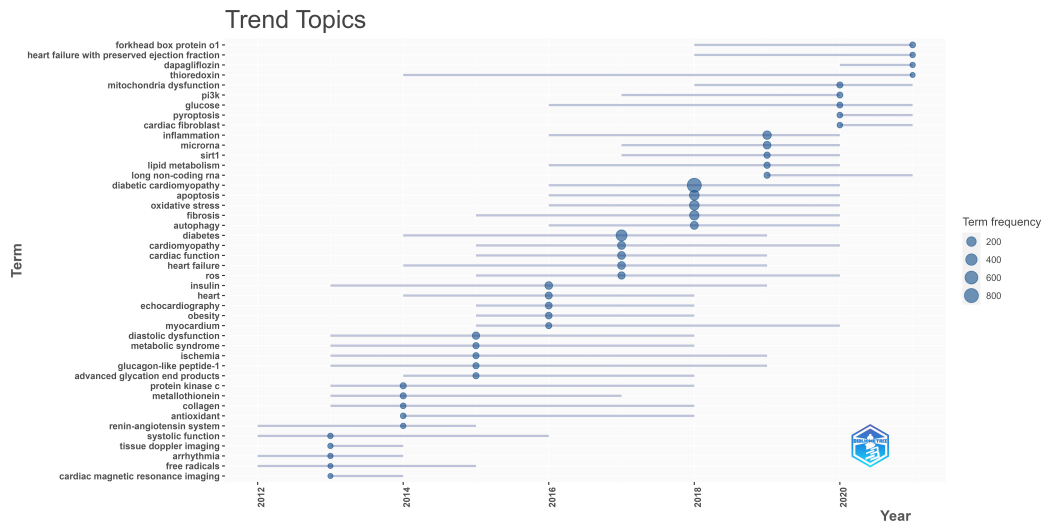

FIGURE 11
Trend topic map of author's keywords in DCM field in the past decade generated from R studio Documents menu of *Biblioshiny* package.

inhibitors showing promising benefits on DM individuals with CVD (78). DAPA has been proved that it could suppress cardiac fibroblast activation and endothelial-to-mesenchymal transition (EndMT) to protect against myocardial fibrosis *via* AMP-activated protein kinaseα (AMPKα)-modulated inhibition of TGF-β/Smad signaling (79). Previous studies have reported that DAPA could also protect cardiomyocytes from inflammation and oxidative stress damage or up-regulating erythropoietin (EPO) levels to decrease apoptosis (80–82). The thioredoxin system is a ubiquitous family of cysteine-dependent antioxidant proteins with a robust ROS scavenging capacity in the cardiomyocyte antioxidant network (83). Overexpression

of thioredoxin has been demonstrated to have a momentous functional implication in mitigating cardiomyocyte dysfunction from DM-induced oxidative stress, which is expected to become a key target for the drug-based treatment of DCM (84, 85).

As the most widely studied subtype of the FoxO family, FoxO1 is commonly involved in the regulation of cell metabolism, apoptosis, and differentiation, especially in pancreatic β-cell (86–88). FoxO1 is a critical transcription factor in insulin cascade affected by different upstream signaling molecules [e.g., phosphatidylinositol 3-kinase (PI3K)/Akt, AMP-activated protein kinase (AMPK), and Sirtuin 1 (SIRT 1)], and it can regulate several downstream proteins, including myocardial pyruvate dehydrogenase (PDH) and peroxisome proliferator-activated receptor α (PPARγ) coactivator-1α (PGC-1α) (89–92). In 2021, several studies proved inhibition of FoxO1 may be an approach to alleviate cardiac fibrosis, diastolic dysfunction, and left ventricular dysfunction and remodeling in the mouse model of DCM (93–95). Thus, FoxO1 could be an attractive target for the pharmacotherapy of DCM.

In addition, ncRNAs have recently played a worthy note regulatory role in human health and disease (96). As one of the most promising topics in the field of DCM, long ncRNAs (LncRNAs) can actively participate in the pathogenesis of CVD, including DCM especially (97). Moreover, like sponges, LncRNAs can block the regulatory function of miRNAs by binding to miRNAs and hindering the interaction with their target (98). Several studies suggested that LncRNAs could mediate cardiomyocyte apoptosis induced by high glucose (99, 100), regulate cardiac remodeling *via* the TGF-β/Smads pathway (101, 102), and mediate cardiomyocyte injury (e.g., ischemia-reperfusion damage, lipotoxic injury) (103, 104).

Regarding clinical significance, our research results indicate that the phenotype of heart failure with preserved ejection fraction (HFpEF) in DCM is attracting more attention, which is discussed above as a precursor stage of heart failure with reduced ejection fraction (HFrEF) phenotype. However, there are also studies indicating that clinical DCM is a two-sided disease composed of HFpEF and HFrEF independently with distinct myocardial effects (10). The occurrence of HFpEF in DCM is primarily due to left ventricular diastolic dysfunction (LVDD) through increased cardiomyocyte stiffness and hypertrophy with high resting tension, which manifests as the left ventricular ejection fraction (LVEF) being greater than or equal to 50% (7, 105). Similar hemodynamic effects were also observed in large clinical studies with a broader range of diabetic patients, to which cardiovascular risk factors including CVD may contribute (106, 107). Thus, the mechanism studies of LVDD in DCM have the potential to provide important insight into DM augmentation on HFpEF. Microcirculation rarefaction and AGES microvascular deposition were observed in HFpEF and HFrEF. However, hyperglycemia, insulin resistance, and lipotoxicity are more closely related to HFpEF, whereas inflammation and autoimmune response are more closely related to HFrEF (108). DCM was proposed and defined over 50 years ago, which characteristics make it challenging to conduct relevant clinical research. However, its enlightening significance was not limited to cardiac dysfunction without CVD and HTN in individuals with DM but expanded to describe the increased vulnerability of the myocardium to metabolism dysfunction of diabetic patients when DM acts like a sole perpetrator (109). In other words, the significance of the study of DCM is to explore the direct effect of glucose-related metabolism disorder on cardiac function independently of other cardiovascular risk factors, which aims to alleviate diabetes augmentation on cardiovascular disease and further improve the symptoms and prognosis of cardiovascular complications of DM.

Our research has two common limitations of bibliometrics (19, 21). One limitation is that only the WoSCC database was selected for publications search due to the R package bibliometrix could not combine other databases to date. However, we are confident that most authority and DCM-related publications were retrieved from the WoSCC database, considered one of the top sources for bibliometric analysis with a well-established citation network (18). The other one is we only included original full-length articles. Non-article publications, including reviews, were excluded from our study, which may have ignored theoretical research hotspots.

Conclusion

We conducted a bibliometric analysis to comprehensively perform the current state of the DCM knowledge domain from 2011 to 2021. Overall, the annual quantity of published articles has increased steadily. China and the United States were found to be influential in this field. Shandong University, professor Cai Lu, and the *Cardiovascular and Diabetology* journal has the highest volume of articles in terms of institutions, authors, and journals. The cooperation between authors, institutions, and countries should be further strengthened in the future. The mainstream DCM research field mainly focused on pathological mechanisms, including apoptosis, oxidative stress, and fibrosis at the molecular and cellular level, and gradually delved into mechanisms studies of DCM drug-based treatment. We believe our bibliometric-based study will benefit academics who focus their work on hotspots reducing outdated research through a comprehensive developed framework.

Data availability statement

The original contributions presented in this study are included in the article/**Supplementary material**, further inquiries can be directed to the corresponding author/s.

Author contributions

SW conceived the study and wrote the first draft of the manuscript. CT helped to draft the manuscript. ZG helped to carry out data analysis and polish the manuscript. BZ and LZ provided the critical revisions. All authors revised the manuscript and approved the submitted version.

Funding

This research was funded by the Scientific and Technological Innovation Project of China Academy of Chinese Medical Sciences (CI2021A01605); the Innovation Team and Talents Cultivation Program of National Administration of Traditional Chinese Medicine (ZYYCXTD-D-202001); the National Key Research and Development Program of China (2019YFC1709904); the National Natural Science Foundation of China (82104835); and the China Postdoctoral Science Foundation (2021M693542).

Acknowledgments

We would like to express our sincere gratitude to all the people who helped with the statistics of our study.

Conflict of interest

The authors declare that the research was conducted in the absence of any commercial or financial relationships that could be construed as a potential conflict of interest.

Publisher's note

All claims expressed in this article are solely those of the authors and do not necessarily represent those of their affiliated organizations, or those of the publisher, the editors and the reviewers. Any product that may be evaluated in this article, or claim that may be made by its manufacturer, is not guaranteed or endorsed by the publisher.

Supplementary material

The Supplementary Material for this article can be found online at: https://www.frontiersin.org/articles/10.3389/fcvm.2022.1018841/full#supplementary-material

References

1. International Diabetes Federation. *IDF Diabetes Atlas*. Brussels: International Diabetes Federation (2021).

2. Benjamin EJ, Virani SS, Callaway CW, Chamberlain AM, Chang AR, Cheng S. Heart Disease and Stroke Statistics-2018 update: a report from the American Heart Association. *Circulation.* (2018) 137:e67–492. doi: 10.1161/CIR.0000000000000558

3. Glovaci D, Fan W, Wong ND. Epidemiology of diabetes mellitus and cardiovascular disease. *Curr Cardiol Rep.* (2019) 21:21. doi: 10.1007/s11886-019-1107-y

4. Jia G, Hill MA, Sowers JR. Diabetic cardiomyopathy: an update of mechanisms contributing to this clinical entity. *Circ Res.* (2018) 122:624–38. doi: 10.1161/CIRCRESAHA.117.311586

5. Thrainsdottir IS, Aspelund T, Thorgeirsson G, Gudnason V, Hardarson T, Malmberg K, et al. The association between glucose abnormalities and heart failure in the population-based Reykjavik study. *Diabetes Care.* (2005) 28:612–6. doi: 10.2337/diacare.28.3.612

6. Kannel WB, Hjortland M, Castelli WP. Role of diabetes in congestive heart failure: the Framingham study. *Am J Cardiol.* (1974) 34:29–34.

7. Rubler S, Dlugash J, Yuceoglu YZ, Kumral T, Branwood AW, Grishman A. New type of cardiomyopathy associated with diabetic glomerulosclerosis. *Am J Cardiol.* (1972) 30:595–602.

8. Aneja A, Tang WH, Bansilal S, Garcia MJ, Farkouh ME. Diabetic cardiomyopathy: insights into pathogenesis, diagnostic challenges, and therapeutic options. *Am J Med.* (2008) 121:748–57. doi: 10.1016/j.amjmed.2008.03.046

9. Shah SJ, Kitzman DW, Borlaug BA, van Heerebeek L, Zile MR, Kass DA, et al. Phenotype-Specific treatment of heart failure with preserved ejection fraction: a multiorgan roadmap. *Circulation.* (2016) 134:73–90. doi: 10.1161/CIRCULATIONAHA.116.021884

10. Seferovic PM, Paulus WJ. Clinical diabetic cardiomyopathy: a two-faced disease with restrictive and dilated phenotypes. *Eur Heart J.* (2015) 36:1718–27. doi: 10.1093/eurheartj/ehv134

11. Tan Y, Zhang Z, Zheng C, Wintergerst KA, Keller BB, Cai L. Mechanisms of diabetic cardiomyopathy and potential therapeutic strategies: preclinical and clinical evidence. *Nat Rev Cardiol.* (2020) 17:585–607. doi: 10.1038/s41569-020-0339-2

12. Konduracka E, Cieslik G, Galicka-Latala D, Rostoff P, Pietrucha A, Latacz P, et al. Myocardial dysfunction and chronic heart failure in patients with long-lasting type 1 diabetes: a 7-year prospective cohort study. *Acta Diabetol.* (2013) 50:597–606. doi: 10.1007/s00592-013-0455-0

13. Bouthoorn S, Valstar GB, Gohar A, den Ruijter HM, Reitsma HB, Hoes AW, et al. The prevalence of left ventricular diastolic dysfunction and heart failure with preserved ejection fraction in men and women with type 2 diabetes: A systematic review and meta-analysis. *Diab Vasc Dis Res.* (2018) 15:477–93. doi: 10.1177/1479164118787415

14. Tarquini R, Pala L, Brancati S, Vannini G, De Cosmo S, Mazzoccoli G, et al. Clinical approach to diabetic cardiomyopathy: a review of human studies. *Curr Med Chem.* (2018) 25:1510–24. doi: 10.2174/0929867324666170705111356

15. Chen C. Science mapping: a systematic review of the literature. *J Inf Sci.* (2017) 2:1–40. doi: 10.1515/jdis-2017-0006

16. Aria M, Cuccurullo C. bibliometrix: An R-Tool for comprehensive science mapping analysis. *J Informetr.* (2018) 11:959–75. doi: 10.1016/j.joi.2017.08.007

17. van Eck NJ, Waltman EL. Software survey: VOSviewer, a computer program for bibliometric mapping. *Scientometrics.* (2010) 84:523–38. doi: 10.1007/s11192-009-0146-3

18. Birkle C, Pendlebury DA, Schnell J, Adams J. Web of Science as a data source for research on scientific and scholarly activity. *Quant Sci Stud.* (2020) 1:363–76. doi: 10.1162/qss_a_00018

19. Ogunsakin RE, Ebenezer O, Ginindza TGA. Bibliometric analysis of the literature on norovirus disease from 1991-2021. *Int J Environ Res Public Health.* (2022) 19:2508. doi: 10.3390/ijerph19052508

20. Sheng RY, Yen Y, Dang HHL. Acupuncture for hot flashes: a literature review of randomized controlled trials conducted in the last 10 years. *World J Trad Chinese Med.* (2021) 7:397–407. doi: 10.4103/wjtcm.wjtcm_27_21

21. Bertoli-Barsotti L, Lando T. A theoretical model of the relationship between the h-index and other simple citation indicators. *Scientometrics.* (2017) 111:1415–48. doi: 10.1007/s11192-017-2351-9

22. Teng B, Xie C, Zhao Y, Wang Z. Studies related to ruptured abdominal aortic aneurysms in the past 10 years (2011-2020): a bibliometric analysis. *Med Sci Monit.* (2022) 28:e935006. doi: 10.12659/MSM.935006

23. Braithwaite J, Herkes J, Churruca K, Long JC, Pomare C, Boyling C, et al. Comprehensive Researcher Achievement Model (CRAM): a framework for measuring researcher achievement, impact and influence derived from a systematic literature review of metrics and models. *BMJ Open.* (2019) 9:e025320. doi: 10.1136/bmjopen-2018-025320

24. Bai X, Xia F, Lee I, Zhang J, Ning Z. Identifying anomalous citations for objective evaluation of scholarly article impact. *PLoS One.* (2016) 11:e0162364. doi: 10.1371/journal.pone.0162364

25. Zeng A, Shen ZS, Zhou JL, Wu JS, Fan Y, Wang YG, et al. The science of science: from the perspective of complex systems. *Phys Rep.* (2017) 714:1–73. doi: 10.1016/j.physrep.2017.10.001

26. Ma N, Guan J, Zhao Y. Bringing PageRank to the citation analysis. *Inf Process Manage.* (2008) 44:800–10. doi: 10.1016/j.ipm.2007.06.006

27. Zhang P, Cheng R. Interdisciplinary influences in headache literature: a network citation analysis of PubMed Central articles. *Headache.* (2021) 61:143–8. doi: 10.1111/head.14022

28. Battiprolu PK, Hojayev B, Jiang N, Wang ZV, Luo X, Iglewski M. Metabolic Stress-Induced activation of FoxO1 triggers diabetic cardiomyopathy in mice. *J Clin Invest.* (2012) 122:1109–18. doi: 10.1172/JCI60329

29. Li CJ, Lv L, Li H, Yu DM. Cardiac fibrosis and dysfunction in experimental diabetic cardiomyopathy are ameliorated by alpha-lipoic acid. *Cardiovasc Diabetol.* (2012) 11:73. doi: 10.1186/1475-2840-11-73

30. Huynh K, Kiriazis H, Du XJ, Love JE, Gray SP, Jandeleit-Dahm KA, et al. Targeting the upregulation of reactive oxygen species subsequent to hyperglycemia prevents type 1 diabetic cardiomyopathy in mice. *Free Radic Biol Med.* (2013) 60:307–17. doi: 10.1016/j.freeradbiomed.2013.02.021

31. Pan Y, Wang Y, Zhao YJ, Peng KS, Li WX, Wang YG, et al. Inhibition of JNK Phosphorylation by a novel curcumin analog prevents high glucose–induced inflammation and apoptosis in cardiomyocytes and the development of diabetic cardiomyopathy. *Diabetes.* (2014) 63:3497–511. doi: 10.2337/db13-1577

32. Bai Y, Cui WP, Xin Y, Miao X, Barati MT, Zhang C, et al. Prevention by sulforaphane of diabetic cardiomyopathy is associated with up-regulation of Nrf2 expression and transcription activation. *J Mol Cell Cardiol.* (2013) 57:82–95. doi: 10.1016/j.yjmcc.2013.01.008

33. Rajesh M, Batkai S, Kechrid M, Mukhopadhyay P, Lee WS, Horvath B, et al. Cannabinoid 1 receptor promotes cardiac dysfunction, oxidative stress, inflammation, and fibrosis in diabetic cardiomyopathy. *Diabetes.* (2012) 61:716–27. doi: 10.2337/db11-0477

34. Kanamori H, Takemura G, Goto K, Tsujimoto A, Mikami A, Ogino A, et al. Autophagic adaptations in diabetic cardiomyopathy differ between type 1 and type 2 diabetes. *Autophagy.* (2015) 11:1146–60. doi: 10.1080/15548627.2015.1051295

35. Li X, Du N, Zhang Q, Li J, Chen X, Liu X, et al. MicroRNA-30d regulates cardiomyocyte pyroptosis by directly targeting Foxo3a in diabetic cardiomyopathy. *Cell Death Dis.* (2014) 5:e1479. doi: 10.1038/cddis.2014.430

36. Xu XM, Kobayashi S, Chen K, Timm D, Volden P, Huang Y, et al. Diminished autophagy limits cardiac injury in mouse models of type 1 diabetes. *J Biol Chem.* (2013) 288:18077–92. doi: 10.1074/jbc.M113.474650

37. Dandamudi S, Slusser J, Mahoney DW, Redfield MM, Rodeheffer RJ, Chen HH. The prevalence of diabetic cardiomyopathy: a population-based study in olmsted county. *Minnesota. J Card Fail.* (2014) 20:304–9. doi: 10.1016/j.cardfail.2014.02.007

38. Alhuzali T, Beh EJ, Stojanovski E. Multiple correspondence analysis as a tool for examining Nobel Prize data from 1901 to 2018. *PLoS One.* (2022) 17:e0265929. doi: 10.1371/journal.pone.0265929

39. Florensa D, Godoy P, Mateo J, Solsona F, Pedrol T, Mesas M, et al. The use of multiple correspondence analysis to explore associations between categories of qualitative variables and cancer incidence. *IEEE J Biomed Health Inform.* (2021) 25:3659–67. doi: 10.1109/JBHI.2021.3073605

40. Murtagh F. Multiple correspondence analysis and related methods. *Psychometrika.* (2007) 72:275–7. doi: 10.1007/s11336-006-1579-x

41. Dai Z, Xu S, Wu X, Hu R, Li H, He H, et al. Knowledge mapping of multicriteria decision analysis in healthcare: a bibliometric analysis. *Front Public Health.* (2022) 10:895552. doi: 10.3389/fpubh.2022.895552

42. Cho NH, Shaw JE, Karuranga S, Huang Y, da Rocha Fernandes JD, Ohlrogge AW. IDF Diabetes Atlas: global estimates of diabetes prevalence for 2017 and projections for 2045. *Diabetes Res Clin Pract.* (2018) 138:271–81. doi: 10.1016/j.diabres.2018.02.023

43. Kim AH, Jang JE, Han J. Current status on the therapeutic strategies for heart failure and diabetic cardiomyopathy. *Biomed Pharm.* (2022) 145:112463. doi: 10.1016/j.biopha.2021.112463

44. Eldesoqui M, Eldken ZH, Mostafa SA, Al-Serwi RH, El-Sherbiny M, Elsherbiny N, et al. Exercise augments the effect of SGLT2 inhibitor dapagliflozin on experimentally induced diabetic cardiomyopathy, possible underlying mechanisms. *Metabolites.* (2022) 12:635. doi: 10.3390/metabo12070635

45. Li MZ, Su L, Liang BY, Tan JJ, Chen Q, Long JX, et al. Trends in prevalence, awareness, treatment, and control of diabetes mellitus in mainland china from 1979 to 2012. *Int J Endocrinol.* (2013) 2013:753150. doi: 10.1155/2013/753150

46. Rahman MS, Akter S, Abe SK, Islam MR, Mondal MN, Rahman JA, et al. Awareness, treatment, and control of diabetes in Bangladesh: a nationwide population-based study. *PLoS One.* (2015) 10:e0118365. doi: 10.1371/journal.pone.0118365

47. Ma RCW. Epidemiology of diabetes and diabetic complications in China. *Diabetologia.* (2018) 61:1249–60. doi: 10.1007/s00125-018-4557-7

48. Yan Y, Wu T, Zhang M, Li C, Liu Q, Li F. Prevalence, awareness and control of type 2 diabetes mellitus and risk factors in Chinese elderly population. *BMC Public Health.* (2022) 22:1382. doi: 10.1186/s12889-022-13759-9

49. Thornalley PJ, Vasak M. Possible role for metallothionein in protection against radiation-induced oxidative stress: Kinetics and mechanism of its reaction with superoxide and hydroxyl radicals. *Biochim Biophys Acta.* (1985) 827:36–44. doi: 10.1016/0167-4838(85)90098-6

50. Thomas JP, Bachowski GJ, Girotti AW. Inhibition of cell membrane lipid peroxidation by cadmium- and zinc-metallothioneins. *Biochim Biophys Acta.* (1986) 884:448–61. doi: 10.1016/0304-4165(86)90195-9

51. Ye G, Metreveli NS, Ren J, Epstein PN. Metallothionein prevents diabetes-induced deficits in cardiomyocytes by inhibiting reactive oxygen species production. *Diabetes.* (2003) 52:777–83. doi: 10.2337/diabetes.52.3.777

52. Cai L, Wang JX, Li Y, Sun XH, Wang LP, Zhou ZX, et al. Inhibition of superoxide generation and associated nitrosative damage is involved in metallothionein prevention of diabetic cardiomyopathy. *Diabetes.* (2005) 54:1829–37. doi: 10.2337/diabetes.54.6.1829

53. Cai L, Wang Y, Zhou G, Chen T, Song Y, Li X, et al. Attenuation by metallothionein of early cardiac cell death via suppression of mitochondrial oxidative stress results in a prevention of diabetic cardiomyopathy. *J Am Coll Cardiol.* (2006) 48:1688–97. doi: 10.1016/j.jacc.2006.07.022

54. Prakoso D, De Blasio MJ, Tate M, Kiriazis H, Donner DG, Qian H, et al. Gene therapy targeting cardiac phosphoinositide 3-kinase (p110alpha) attenuates cardiac remodeling in type 2 diabetes. *Am J Physiol Heart Circ Physiol.* (2020) 318:H840–52. doi: 10.1152/ajpheart.00632.2019

55. Prakoso D, Tate M, Blasio MJ, Ritchie RH. Adeno-associated viral (AAV) vector-mediated therapeutics for diabetic cardiomyopathy – current and future perspectives. *Clin Sci.* (2021) 135:1369–87. doi: 10.1042/CS20210052

56. Tate M, Perera N, Prakoso D, Willis AM, Deo M, Oseghale O, et al. Bone morphogenetic protein 7 gene delivery improves cardiac structure and function in a murine model of diabetic cardiomyopathy. *Front Pharmacol.* (2021) 12:719290. doi: 10.3389/fphar.2021.719290

57. Ojha S, Kurdi A, Sadek B, Kaleem M, Cai L, Kamal MA, et al. Phytochemicals as prototypes for pharmaceutical leads towards drug development against diabetic cardiomyopathy. *Curr Pharm Des.* (2016) 22:3058–70. doi: 10.2174/1381612822666160322145255

58. Mao YQ, Zhang F, Song HB, Li YF, Tang JF, Yang P, et al. CiteSpace-based metrical and visualization analysis of tai chi chuan analgesia. *World J Trad Chinese Med.* (2021) 7:477–82. doi: 10.4103/2311-8571.317994

59. De Geest B, Mishra M. Role of oxidative stress in heart failure: insights from gene transfer studies. *Biomedicines.* (2021) 9:1645. doi: 10.3390/biomedicines9111645

60. Santos, CXC, Anilkumar N, Zhang M, Brewer AC, Shah AM. Redox signaling in cardiac myocytes. *Free Radic Biol Med.* (2011) 50:777–93. doi: 10.1016/j.freeradbiomed.2011.01.003

61. Gatto A, Drago C, Ruggeri M. On the Frontline-A bibliometric Study on Sustainability, Development, Coronaviruses, and COVID-19. *Environ Sci Pollut Res Int.* (2022) [Epub ahead of print]. doi: 10.1007/s11356-021-18396-0

62. Hu X, Bai T, Xu Z, Liu Q, Zheng Y, Cai L. Pathophysiological fundamentals of diabetic cardiomyopathy. *Compr Physiol.* (2017) 7:693–711. doi: 10.1002/cphy.c160021

63. Jakubik D, Fitas A, Eyileten C, Jarosz-Popek J, Nowak A, Czajka P, et al. MicroRNAs and long non-coding RNAs in the pathophysiological processes of diabetic cardiomyopathy: emerging biomarkers and potential therapeutics. *Cardiovasc Diabetol.* (2021) 20:55. doi: 10.1186/s12933-021-01245-2

64. Feng B, Chen S, George B, Feng Q, Chakrabarti S. MiR133a regulates cardiomyocyte hypertrophy in diabetes. *Diabetes Metab Res Rev.* (2010) 26:40–9. doi: 10.1002/dmrr.1054

65. Yang X, Li X, Lin Q, Xu Q. Up-regulation of microRNA-203 inhibits myocardial fibrosis and oxidative stress in mice with diabetic cardiomyopathy through the inhibition of PI3K/Akt signaling pathway via PIK3CA. *Gene.* (2019) 715:143995. doi: 10.1016/j.gene.2019.143995

66. Chavali V, Tyagi SC, Mishra PK. Differential expression of dicer, miRNAs, and inflammatory markers in diabetic Ins2 ± Akita hearts. *Cell Biochem Biophys.* (2014) 68:25–35. doi: 10.1007/s12013-013-9679-4

67. Yin Z, Zhao Y, He M, Li H, Fan J, Nie X, et al. MiR-30c/PGC-1 beta protects against diabetic cardiomyopathy via PPAR alpha. *Cardiovasc Diabetol.* (2019) 18:7. doi: 10.1186/s12933-019-0811-7

68. Teupe C, Rosak C. Diabetic cardiomyopathy and diastolic heart failure - Difficulties with relaxation. *Diabetes Res Clin Pract.* (2012) 97:185–94. doi: 10.1016/j.diabres.2012.03.008

69. Salvatore T, Pafundi PC, Galiero R, Albanese G, Di Martino A, Caturano A, et al. The diabetic cardiomyopathy: the contributing pathophysiological mechanisms. *Front Med.* (2021) 8:695792. doi: 10.3389/fmed.2021.695792

70. Kaludercic N, Di Lisa F. Mitochondrial ROS formation in the pathogenesis of diabetic cardiomyopathy. *Front Cardiovasc Med.* (2020) 7:12. doi: 10.3389/fcvm.2020.00012

71. Bizino MB, Jazet IM, Westenberg JJM, van Eyk HJ, Paiman EHM, Smit JWA, et al. Effect of liraglutide on cardiac function in patients with type 2 diabetes mellitus: randomized placebo-controlled trial. *Cardiovasc Diabetol.* (2019) 18:55. doi: 10.1186/s12933-019-0857-6

72. Cooper GJS, Young AA, Gamble GD, Occleshaw CJ, Dissanayake AM, Cowan BR, et al. A copper (II)-selective chelator ameliorates left-ventricular hypertrophy in type 2 diabetic patients: a randomised placebo-controlled study. *Diabetologia.* (2009) 52:715–22. doi: 10.1007/s00125-009-1265-3

73. Pala S, Esen O, Akcakoyun M, Kahveci G, Kargin R, Tigen K, et al. Rosiglitazone, but not pioglitazone, improves myocardial systolic function in type 2 diabetic patients: a tissue doppler study. *Echocardiography.* (2010) 27:512–8. doi: 10.1111/j.1540-8175.2009.01083.x

74. van der Meer RW, Rijzewijk LJ, de Jong HWAM, Lamb HJ, Lubberink M, Romijn JA, et al. Pioglitazone improves cardiac function and alters myocardial substrate metabolism without affecting cardiac triglyceride accumulation and high-energy phosphate metabolism in patients with well-controlled type 2 diabetes mellitus. *Circulation.* (2009) 119:2068–u87. doi: 10.1161/CIRCULATIONAHA.108.803916

75. Lee TM, Lin MS, Lin S, Tsai CH, Huang CL. Effects of sulfonylureas on left ventricular mass in type 2 diabetic patients. *Am J Physiol-Heart Circul Physiol.* (2007) 292:H608–13. doi: 10.1152/ajpheart.00516.2006

76. Giannetta E, Isidori AM, Galea N, Carbone I, Mandosi E, Vizza CD, et al. Chronic inhibition of cGMP phosphodiesterase 5A improves diabetic cardiomyopathy a randomized, controlled clinical trial using magnetic resonance imaging with myocardial tagging. *Circulation.* (2012) 125:2323. doi: 10.1161/CIRCULATIONAHA.111.063412

77. Nogueira KC, Furtado M, Fukui RT, Correia MRS, dos Santos RF, Andrade JL, et al. Left ventricular diastolic function in patients with type 2 diabetes treated with a dipeptidyl peptidase-4 inhibitor- a pilot study. *Diabetol Metab Syndr.* (2014) 6:103. doi: 10.1186/1758-5996-6-103

78. Udell JA, Cavender MA, Bhatt DL, Chatterjee S, Farkouh ME, Scirica BM. Glucose-lowering drugs or strategies and cardiovascular outcomes in patients with or at risk for type 2 diabetes: a meta-analysis of randomised controlled trials. *Lancet Diabetes Endocrinol.* (2015) 3:356–66.

79. Tian J, Zhang M, Suo M, Liu D, Wang X, Liu M. Dapagliflozin alleviates cardiac fibrosis through suppressing EndMT and fibroblast activation via AMPKalpha/TGF-beta/Smad signalling in type 2 diabetic rats. *J Cell Mol Med.* (2021) 25:7642–59. doi: 10.1111/jcmm.16601

80. Ye YM, Bajaj M, Yang HC, Perez-Polo JR, Birnbaum Y. SGLT-2 inhibition with Dapagliflozin reduces the activation of the Nlrp3/ASC inflammasome and attenuates the development of diabetic cardiomyopathy in mice with type 2 diabetes. Further augmentation of the effects with saxagliptin, a DPP4 inhibitor. *Cardiovasc Drugs Ther.* (2017) 31:119–32. doi: 10.1007/s10557-017-6725-2

81. Arow M, Waldman M, Yadin D, Nudelman V, Shainberg A, Abraham NG, et al. Sodium-glucose cotransporter 2 inhibitor Dapagliflozin attenuates diabetic cardiomyopathy. *Cardiovasc Diabetol.* (2020) 19:7. doi: 10.1186/s12933-019-0980-4

82. El-Sayed N, Mostafa YM, AboGresha NM, Ahmed AAM, Mahmoud IZ, El-Sayed NM. Dapagliflozin attenuates diabetic cardiomyopathy through erythropoietin up-regulation of AKT/JAK/MAPK pathways in streptozotocin-induced diabetic rats. *Chem Biol Interact.* (2021) 347:109617. doi: 10.1016/j.cbi.2021.109617

83. Yoshioka J. Thioredoxin superfamily and its effects on cardiac physiology and pathology. *Compr Physiol.* (2015) 5:513–30. doi: 10.1002/cphy.c140042

84. Mukai N, Nakayama Y, Abdali SA, Yoshioka J. Cardiomyocyte-specific Txnip C247S mutation improves left ventricular functional reserve in streptozotocin-induced diabetic mice. *Am J Physiol Heart Circ Physiol.* (2021) 321:H259–74. doi: 10.1152/ajpheart.00174.2021

85. Matsuzaki S, Eyster C, Newhardt MF, Giorgione JR, Kinter C, Young ZT, et al. Insulin signaling alters antioxidant capacity in the diabetic heart. *Redox Biol.* (2021) 47:102140. doi: 10.1016/j.redox.2021.102140

86. Xing YQ, Li A, Yang Y, Li XX, Zhang LN, Guo HC. The regulation of FOXO1 and its role in disease progression. *Life Sci.* (2018) 193:124–31. doi: 10.1016/j.lfs.2017.11.030

87. Chen ZF, Li YB, Han JY, Wang J, Yin JJ, Li JB, et al. The double-edged effect of autophagy in pancreatic beta cells and diabetes. *Autophagy.* (2021) 7:12–6. doi: 10.4161/auto.7.1.13607

88. Li XD, Wan TT, Li YB. Role of FoxO1 in regulating autophagy in type 2 diabetes mellitus. *Exp Ther Med.* (2021) 22:707. doi: 10.3892/etm.2021.10139

89. Li Q, Jia S, Xu L, Li B, Chen N. Metformin-induced autophagy and irisin improves INS-1 cell function and survival in high-glucose environment via AMPK/SIRT1/PGC-1α signal pathway. *Food Sci Nutr.* (2019) 7:1695–703. doi: 10.1002/fsn3.1006

90. Martins R, Lithgow GJ, Link W. Long live FoxO: unraveling the role of FoxO proteins in aging and longevity. *Aging Cell.* (2016) 15:196–207. doi: 10.1111/acel.12427

91. Yu W, Chen CJ, Cheng JD. The role and molecular mechanism of FoxO1 in mediating cardiac hypertrophy. *ESC Heart Fail.* (2020) 7:3497–504. doi: 10.1002/ehf2.13065

92. Gopal K, Saleme B, Al Batran R, Aburasayn H, Eshreif A, Ho KL, et al. FoxO1 regulates myocardial glucose oxidation rates via transcriptional control of pyruvate dehydrogenase kinase 4 expression. *Am J Physiol Heart Circ Physiol.* (2017) 313:H479–90. doi: 10.1152/ajpheart.00191.2017

93. Vivar R, Anfossi R, Humeres C, Catalan M, Reyes C, Cardenas S, et al. FoxO1 is required for high glucose-dependent cardiac fibroblasts into myofibroblast phenoconversion. *Cell Signal.* (2021) 83:109978. doi: 10.1016/j.cellsig.2021.109978

94. Gopal K, Al Batran R, Altamimi TR, Greenwell AA, Saed CT, Dakhili SAT, et al. FoxO1 inhibition alleviates type 2 diabetes-related diastolic dysfunction by increasing myocardial pyruvate dehydrogenase activity. *Cell Reports.* (2021) 35:108935. doi: 10.1016/j.celrep.2021.108935

95. Zhang M, Sui WH, Xing YQ, Cheng J, Cheng C, Xue F, et al. Angiotensin IV attenuates diabetic cardiomyopathy via suppressing FoxO1-induced excessive autophagy, apoptosis and fibrosis. *Theranostics.* (2021) 11:8624–39. doi: 10.7150/thno.48561

96. Esteller M. Non-coding RNAs in human disease. *Nat Rev Genet.* (2011) 12:861–74. doi: 10.1038/nrg3074

97. Uchida S, Dimmeler S. Long noncoding RNAs in cardiovascular diseases. *Circ Res.* (2015) 116:737–50. doi: 10.1161/CIRCRESAHA.116.302521

98. López-Urrutia E, Montes LPB, Cervantes DLD, Pérez-Plasencia C, Campos-Parra AD. Crosstalk between long non-coding RNAs, Micro-RNAs and mRNAs: deciphering molecular mechanisms of master regulators in cancer. *Front Oncol.* (2019) 9:669. doi: 10.3389/fonc.2019.00669

99. Li X, Wang H, Yao B, Xu W, Chen J, Zhou X. lncRNA H19/miR-675 axis regulates cardiomyocyte apoptosis by targeting VDAC1 in diabetic cardiomyopathy. *Sci Rep.* (2016) 6:36340. doi: 10.1038/srep36340

100. Yu M, Shan X, Liu Y, Zhu J, Cao Q, Yang F, et al. RNA-Seq analysis and functional characterization revealed lncRNA NONRATT007560.2 regulated cardiomyocytes oxidative stress and apoptosis induced by high glucose. *J Cell Biochem.* (2019) 120:18278–87. doi: 10.1002/jcb.29134

101. Yang F, Qin Y, Lv J, Wang Y, Che H, Chen X, et al. Silencing long non-coding RNA Kcnq1ot1 alleviates pyroptosis and fibrosis in diabetic cardiomyopathy. *Cell Death Dis.* (2018) 9:1000. doi: 10.1038/s41419-018-1029-4

102. Yang F, Qin Y, Wang Y, Li A, Lv J, Sun X, et al. LncRNA KCNQ1OT1 mediates pyroptosis in diabetic cardiomyopathy. *Cell Physiol Biochem.* (2018) 50:1230–44. doi: 10.1159/000494576

103. Zlobine I, Gopal K, Ussher JR. Lipotoxicity in obesity and diabetes-related cardiac dysfunction. *Biochim Biophys Acta.* (2016) 1861:1555–68. doi: 10.1016/j.bbalip.2016.02.011

104. Zhao ZH, Hao W, Meng QT, Du XB, Lei SQ, Xia ZY. Long non-coding RNA MALAT1 functions as a mediator in cardioprotective effects of fentanyl in myocardial ischemia-reperfusion injury. *Cell Biol Int.* (2017) 41:62–70. doi: 10.1002/cbin.10701

105. Groenewegen A, Rutten FH, Mosterd A, Hoes AW. Epidemiology of heart failure. *Eur J Heart Fail.* (2020) 22:1342–56. doi: 10.1002/ejhf.1858

106. Lindman BR, Davila-Roman VG, Mann DL, McNulty S, Semigran MJ, Lewis GD, et al. Cardiovascular phenotype in HFpEF patients with or without diabetes A RELAX trial ancillary Study. *J Am Coll Cardiol.* (2014) 64:541–9. doi: 10.1016/j.jacc.2014.05.030

107. Kristensen SL, Mogensen UM, Jhund PS, Petrie MC, Preiss D, Win S, et al. Clinical and echocardiographic characteristics and cardiovascular outcomes according to diabetes status in patients with heart failure and preserved ejection fraction a report from the I-preserve trial (Irbesartan in Heart Failure With Preserved Ejection Fraction). *Circulation.* (2017) 135:724–35. doi: 10.1161/CIRCULATIONAHA.116.024593

108. Quinaglia T, Oliveira DC, Matos-Souza JR, Sposito AC. Diabetic cardiomyopathy: factual or factoid? *Rev Assoc Med Bras.* (2019) 65:61–9. doi: 10.1590/1806-9282.65.1.69

109. Kenny HC, Abel ED. Heart failure in type 2 diabetes mellitus impact of glucose-lowering agents, heart failure therapies, and novel therapeutic strategies. *Circ Res.* (2019) 124:121–41. doi: 10.1161/CIRCRESAHA.118.311371

frontiers | Frontiers in Cardiovascular Medicine

TYPE Original Research
PUBLISHED 30 January 2023
DOI 10.3389/fcvm.2023.1086978

OPEN ACCESS

EDITED BY
Catherine A. Reardon,
The University of Chicago,
United States

REVIEWED BY
Alfredo Caturano,
University of Campania Luigi Vanvitelli,
Italy
Byoungjin Park,
Yonsei University Health System,
Republic of Korea

*CORRESPONDENCE
Lichan Tao
✉ sherry0019@126.com
Xiaolin Huang
✉ hxl4038@czfph.com

†These authors have contributed equally to this work

SPECIALTY SECTION
This article was submitted to Cardiovascular Metabolism, a section of the journal Frontiers in Cardiovascular Medicine

RECEIVED 01 November 2022
ACCEPTED 11 January 2023
PUBLISHED 30 January 2023

CITATION
Wang T, Xu J, Zhang H, Tao L and Huang X (2023) Triglyceride-glucose index for the detection of subclinical heart failure with preserved ejection fraction in patients with type 2 diabetes.
Front. Cardiovasc. Med. 10:1086978.
doi: 10.3389/fcvm.2023.1086978

Triglyceride-glucose index for the detection of subclinical heart failure with preserved ejection fraction in patients with type 2 diabetes

Tingting Wang[1†], Jiani Xu[2†], Hong Zhang[2†], Lichan Tao[1*] and Xiaolin Huang[2*]

[1]Department of Cardiology, The Third Affiliated Hospital of Soochow University, Changzhou, China,
[2]Department of Endocrinology, The Third Affiliated Hospital of Soochow University, Changzhou, China

Objectives: The triglyceride-glucose (TyG) index has been identified as a reliable and simple surrogate of insulin resistance. In this study, we sought to determine the association between TyG index and cardiac function among asymptomatic individuals with type 2 diabetes (T2DM) without history of any cardiovascular disease.

Materials and methods: The cross-sectional study enrolled 180 T2DM patients without cardiac symptoms. Heart failure with preserved ejection fraction (HFpEF) was defined as Heart Failure Association (HFA)-PEFF score≥5 points.

Results: A total of 38 (21.1%) diabetic patients were identified with HFpEF. Compared with the low-TyG group (TyG index <9.47), patients in high-TyG group (TyG index ≥9.47) showed increased risk of metabolic syndrome and diastolic dysfunction (p<0.05 for each). Furthermore, after adjustment of confounding variables, the TyG index showed positive correlation with risk factors of metabolic syndrome (including BMI, waist circumference, blood pressure, HbA1c, TG, TC, non-HDL-C, and fasting blood glucose, p<0.05 for each) and parameters of diastolic dysfunction (E/e' ratio, p<0.0001) in patients with T2DM. Moreover, Receiver Operating Characteristic *curve* analysis showed that the TyG index could be better to predict the risk of suspected HFpEF than other indicators (AUC: 0.706, 95% CI: 0.612–0.801). According, on multiple regression analysis, TyG index was independently correlated with the incidence of HFpEF (odds ratio: 0.786, p=0.0019), indicating that TyG index could be a reliable biomarker to predict the risk of HFpEF.

Conclusion: The TyG index showed a positive correlation with the risk of subclinical HFpEF in patients with T2DM, providing a new marker to predict and treat HFpEF in diabetes.

KEYWORDS

triglyceride-glucose index, heart failure with preserved ejection fraction, type II diabetes, insulin resistance, HbA1c - hemoglobin A1c

Introduction

Diabetes mellitus (DM) can contribute to cardiac abnormalities both structurally and functionally, predisposing individuals to a heightened risk of cardiovascular disease (CVD) (1, 2). Diabetic cardiomyopathy (DCM) was initially described as a human pathological condition in which heart failure occurred independent of coronary artery disease (CAD), hypertension, and valvular heart disease (3, 4). DCM in early stage is characterized by asymptomatic cardiac dysfunction or described as heart failure (HF)

at stage B (subclinical HF). Cardiac disorders include left atrial (LA) dilatation, concentric left ventricular (LV) remodeling, LV diastolic dysfunction, and reduced global longitudinal strain (5). Regardless of concomitant LV systolic dysfunction, mounting evidence from epidemiological studies imply that comparing to healthy individuals, patients with diastolic dysfunction impart poor prognostic implications, with an increased 3-fold risk of death in diabetic patients (6). Thus, in view of the large number of diabetic patients and related cardiac complications, it will be of great importance to identify high risk individuals prone to cardiac dysfunction through effective and simple diagnostic strategy at early stage.

Clinical evidence establishes that glycemic control correlates with elevated risk of DCM (7, 8). Moreover, higher glycosylated hemoglobin, type A1c (HbA1c) variability is identified to be correlated with heightened risk of all-cause and cardiovascular mortality in diabetic patients (9). However, the severity and progression of HF vary in diabetic patients with poor glycemic control, and HF may also occur in patients with well-controlled blood glucose levels. Therefore, in addition to hyperglycemia, other risk factors may also participate in the development of clinical manifestation of DCM.

Chronic hyperglycemia and insulin resistance (IR) are the major mechanisms involved in the pathology of diabetic complications (10). During diabetic and IR states, metabolic, structural, and functional alterations in the myocardium and vascular beds or vascular tissues lead to coronary artery disease (CAD), myocardial ischemia, and HF (5). Previous clinical studies demonstrated that homeostasis model of IR (HOMA-IR) was independently correlated with LV diastolic dysfunction (11). However, it is not clear whether IR predicts subclinical cardiac diastolic dysfunction in patients with diabetes.

At present, no specific methods are available for the accurate detection of IR. HOMA-IR is a validated and widely used surrogate by incorporating insulin concentrations and serum glucose level, but the clinical practice is limited due to atypical assessment of serum insulin levels (12). The triglyceride glucose (TyG) index, a product derived from fasting triglycerides (TG) and fasting blood pressure (FBG), has been proven to be superior to HOMA-IR in evaluating IR in individuals with or without diabetes (13). Therefore, the aim of this study was to investigate the association between TyG index and the risk of cardiac diastolic dysfunction in patients with type 2 diabetes (T2DM) and the predictive value of TyG index to provide novel clues for the early recognition and prevention of HF in diabetic patients.

Abbreviations: TyG, triglyceride-glucose; T2DM, type 2 diabetes; HFpEF, Heart failure with preserved ejection fraction; HFA, Heart Failure Association; ROC, receive operating characteristic; OR, odds ratio; CI, confidence interval; DM, Diabetes mellitus; CVD, cardiovascular disease; HF, heart failure; LA, left atrial; LV, left ventricular; HbA1c, Hemoglobin type A1c. IR, insulin resistance; CAD, coronary artery disease; HOMA-IR, homeostasis model of insulin resistance; MAP, mean arterial pressure; SBP, systolic blood pressure; DBP, diastolic blood pressure; TG, triglycerides; ALT, glutamic oxaloacetic transaminase; AST, alanine aminotransferase; Cr, creatinine; BUN, blood urea nitrogen; TC, total cholesterol; LDL-C, low-density lipoprotein cholesterol; HDL-C, high-density lipoprotein cholesterol; FBG, fasting blood glucose; eGFR, estimated glomerular filtration rate; LAD, left atrial diameter; LVESD, left ventricular end-systolic diameter; LVEDD, left ventricular end-diastolic diameter; IVSD, interventricular septal diameter; LVPWT, left ventricular posterior wall thickness; LVEF, left ventricular ejection fraction; MFV A, peak late diastolic trans-mitral flow velocity; MFV E, peak early diastolic trans-mitral flow velocity; LVMI, Left ventricular mass index; RWT, Relative ventricular wall thickness; SD, standard deviation; AUC, area under curve; CAS, coronary artery stenoses; ABI, ankle-branchial index.

Methods

Subject design and recruitment

A retrospective consecutive case series of T2DM patients hospitalized in the Department of Endocrinology at the Changzhou First People's Hospital (Changzhou, Jiangsu, China) were recruited from April 2018 to May 2022. The Inclusion criteria were: (1) diagnosed T2DM according to the criteria of World Health Organization (14) and Chinese Diabetes Society (15) without cardiac symptoms; (2) aged from 18 to 70 years old independent of T2DM duration. The exclusion criteria were: (1) subjects with hypertension (Hypertension was diagnosed according to the following Chinese hypertension guidelines: a mean systolic blood pressure $\geq$ 140 mmHg and/or a mean diastolic blood pressure $\geq$ 90 mmHg and/or self-reported use of antihypertensive medication in the past 2 weeks) (16, 17), CAD, atrial fibrillation, structural heart disease or history of any cardiovascular-related disease; (2) subjects with diabetic complications including macro and microvascular diseases such as neuropathy, retinopathy, kidney disease, stroke and peripheral vascular disease; (3) pregnancy; (4) other serious comorbidities, including thyroid disturbances, malignant tumors, liver and renal insufficiency, rheumatic diseases or major mental illness. All the subjects signed written informed consent forms before the start of this study. The study was approved by the Institutional Review Committee and the Ethics Committee of the Third Affiliated Hospital of Soochow University.

Clinical and biochemical measurements

Baseline characteristics including age, sex, weight, height, body mass index (BMI), waist circumference, diabetic duration and other complete medical history were recorded in detail on the day of admission. After fasting for at least 8 h, peripheral venous blood was collected before administration of hypoglycemic drugs on the morning after admission. Briefly, the concentration of HbA1c was evaluated through high performance liquid chromatography. Glutamic oxaloacetic transaminase (AST), alanine aminotransferase (ALT), creatinine (Cr), blood urea nitrogen (BUN), homocysteine, total cholesterol (TC), TG, low-density lipoprotein cholesterol (LDL-C), high-density lipoprotein cholesterol (HDL-C), FBG, and C peptide (0 min, 30 min, 60 min, 120 min, and 180 min) were analyzed by an automatic analyzer. Blood pressure including systolic (SBP) and diastolic blood pressure (DBP) were measured three times at 2-min intervals following at least 5 min of rest on the morning after admission.

Echocardiographic measurements

The following parameters were measured and analyzed by echocardiography: the left atrial diameter (LAD), left ventricular end-systolic diameter (LVESD), left ventricular end-diastolic diameter (LVEDD), interventricular septal diameter (IVSD), left ventricular posterior wall thickness (LVPWT), left ventricular ejection fraction% (LVEF%), peak late diastolic trans-mitral flow velocity (MFV A), peak early diastolic trans-mitral flow velocity (MFV E), mitral valve septal velocity e, mitral valve lateral velocity e, and LA volume. e' was defined as: (ventricular septal velocity e + mitral valve velocity e)/2. Left atrial volume index (LAVI) was defined as: LA volume/body surface area, where the body surface area was equal to 0.0128*weight (kg) + 0.006*height (cm) - 0.1529. Left ventricular mass index (LVMI)

was defined as: 0.8*10.4 (IVSD+LVPWT+LVEDD). Relative ventricular wall thickness (RWT) was defined as: (LVPWT/LVEDD) *2.

TyG index and HFA-PEFF score definition

The TyG index was calculated as: In [fasting TG (mg/dl) x fasting glucose (mg/dl)/2]. The Heart Failure Association (HFA)-PEFF score was originated from HFA-PEFF diagnostic algorithm, including functional, morphological, and biomarker domains (18). Data of the peak tricuspid velocity and global longitudinal strain were not available in this study. In the HFA-PEFF diagnostic algorithm, a total score ≥ 5 points was identified to be diagnostic of heart failure with preserved ejection fraction (HFpEF), while a score ≤ 1 was considered to be very unlikely of HFpEF. Patients with an intermediate PEFF score (2–4 points) required further functional and etiology assessment (18).

Statistical analysis

All data in this study were analyzed using SPSS statistical software 26.0. p value <0.05 was defined to be of statistical significance. The specific statistical analysis in this study were outlined as follows.

Baseline and echocardiographic data of subjects

The baseline and echocardiographic data of diabetic patients were stratified based on binary TyG index. The differences between two groups were evaluated, continuous normal distribution variables were expressed as mean ± standard deviation (SD) by independent sample t-test, nonnormal distribution variables were expressed as median P50 (P25, P75) by Mann–Whitney U test, and the categorical variables were presented as number (percentage) and analyzed by χ^2 test.

Correlation analysis

Pearson correlation analysis was used to analysis independent variables with the TyG index. Partial correlation analysis was used to correct suspicious confounding factors (make it/them a constant).

Logistic regression

A logistic multivariable regression analysis with cardiac diastolic dysfunction categorized as HFA-PEFF score (≤1, 2–4, and ≥ 5 points) was used to determine the associations between the TyG index and HFpEF. The goodness of fit of the regression model was assessed by Hosmer-Lemeshow test ($p > 0.05$). In the logistic regression analysis, three models were set up, Model 1: adjusted by age and sex; Model 2: adjusted by BMI, waist circumference, and diabetic duration based on model 1; Model 3: adjusted by estimated glomerular filtration rate (eGFR), mean arterial pressure (MAP), TC and HbA1c based on model 2.

Receiver operating characteristic curve analysis

Receiver operating characteristic curve (ROC) analysis was constructed to evaluate the predictive value of TyG index, FBG, postprandial blood glucose (PBG), TG, TC, LDL-C, TG/HDL-C, and HbA1c for the subclinical HFpEF presence according to the value of the area under the ROC curve (AUC).

Subgroup analysis

A stratified analysis was conducted based on sex, age, HbA1c and T2DM duration to eliminate the interference of confounding factors. Among them, means of age and HbA1c were defined as stratification criteria while the median of duration was used for the cut-off point since the latter does not conform to the normal distribution.

Results

Clinical characteristics of T2DM patients stratified by binary TyG index

A total of 180 subjects with T2DM (102 men and 78 women), aged 53.82 ± 9.20 years old, with a median diabetic duration of 6 years (interquartile range 0.75–10 years) were included in this study. According to the mean value of TyG index, diabetic patients were separated into two groups as low-TyG group (TyG index <9.47, $N = 88$) and high-TyG group (TyG index ≥9.47, $N = 92$). Compared with the low-TyG group, patients in high-TyG group showed higher levels of metabolic syndrome-related risk factors, as indicated by elevated BMI, waist circumference, SBP, DBP, HbA1c, TG, TC, non-HDL-C, and FBG, and reduced HDL-C ($p < 0.05$ for each; Table 1). Accordingly, the TyG index was positively associated with these metabolic parameters (including BMI, waist circumference, MAP, SBP, DBP, TG, TC, non-HDL, LDL-C, and FBG; $p < 0.05$ for each) and negatively associated with HDL-C and eGFR ($p < 0.05$; Supplementary Table S1) after adjusting for age, sex, and duration of diabetes. In addition, Patients in high-TyG group were more likely to use biguanides, glucagon-like peptide 1 (GLP-1) receptor agonists, and statins ($p < 0.05$ for each; Table 1).

Echocardiographic characteristics of T2DM patients stratified by binary TyG index

Compared with patients in low-TyG group, patients in high-TyG group showed cardiac diastolic disorder, as exhibited by elevated E/e' ratio and LA volume ($p < 0.05$ for each; Table 2). Additionally, correlation analysis showed that the TyG index was positively associated with E/e' ratio ($r = 0.273$, $p = 0.0002$) and negatively associated with septal e' velocity ($r = -0.245$, $p = 0.0010$) and lateral e' velocity ($r = -0.339$, $p < 0.0001$; Supplementary Table S2) after adjusting for age, sex, and duration of diabetes. However, no differences were detected in the systolic function and ventricular remodeling between two groups.

ROC analysis for the identification of diabetic patients with risk of HFpEF

To confirm that TyG index is particularly well related to IR in patients with diabetes, we evaluated the association between other simultaneously measured IR or insulin sensitivity indices and TyG index. Previous studies have revealed that the lipid profile in T2DM patients with IR often manifested as a TG/HDL-C axis disorder, with elevations of TG and reductions of HDL-C. TG/HDL-C ratio was thus identified as one of the major risk factors for IR and CVD (19). Additionally, C-peptide is secreted from pancreatic β cells at an equimolar ratio to insulin, reflecting endogenous insulin secretion (20). In this study, patients with a higher TyG index had a higher TG/HDL-C ratio and C-peptide values at 0 min and 30 min (Table 3; $p < 0.05$ for each), suggesting that TyG index could be a reliable marker for IR in T2DM patients.

TABLE 1 Clinical and metabolic characteristics in T2DM patients stratified by binary TyG index.

Variables	TyG index <9.47 (*N*=88)	TyG index ≥9.47(*N*=92)	*p*-value
Age (years)	54.06 ± 9.62	53.80 ± 8.63	0.9854
Male (*n*, %)	52 (59.1%)	50 (54.3%)	0.5209
Diabetes duration(years)	6.00 (0.50–10.00)	6.00 (1.00–10.00)	0.5549
BMI (kg/m^2)	23.62 ± 3.36	25.22 ± 3.41	0.0013
Waist circumference (cm)	86.95 ± 8.70	90.64 ± 9.94	0.0133
MAP (mmHg)	91.14 ± 9.86	94.57 ± 10.09	0.0224
SBP (mmHg)	122.81 ± 12.70	125.63 ± 12.82	0.0491
DBP (mmHg)	75.79 ± 9.65	78.87 ± 10.08	0.0308
HbA1c (%)	9.00 (7.30–10.70)	10.15 (8.53–11.75)	0.0094
ALT (U/L)	18.00 (12.30–25.70)	22.00 (14.03–32.18)	0.0839
AST (U/L)	18.00 (15.30–23.00)	20.00 (16.00–25.60)	0.1884
TG (mmol/L)	1.29 ± 0.47	3.41 ± 2.65	<0.0001
TC (mmol/L)	4.60 ± 0.98	5.16 ± 1.15	0.0005
HDL-C (mmol/L)	1.18 ± 0.30	0.91 ± 0.19	<0.0001
Non-HDL (mmol/L)	3.41 ± 0.90	4.25 ± 1.15	<0.0001
LDL-C (mmol/L)	2.66 ± 0.79	2.89 ± 0.82	0.0593
Serum creatinine (μmol/L)	59.26 ± 14.06	62.21 ± 16.13	0.1937
eGFR [mL/(min*1.73m^2)]	114.28 (99.21–145.34)	112.18 (92.61–135.29)	0.2787
FBG (mmol/L)	6.80 (5.79–8.79)	10.02 (7.83–12.82)	<0.0001
Postprandial glucose (mmol/L)	13.67 (10.20–16.86)	14.65 (11.85–17.45)	0.0770
Homocysteine (umol/L)	10.04 (8.63–10.68)	9.98 (9.70–10.80)	0.4915
BNP (pg/mL)	29.00 (18.88–43.33)	28.75 (15.25–49.98)	0.9282
cTnI (ng/mL)	0.0021 (0.0015–0.0037)	0.0019 (0.0010–0.0035)	0.1226
CK-MB (U/L)	1.56 (1.00–1.71)	1.30 (0.80–1.71)	0.0885
Myo (ng/mL)	20.17 (13.73–23.50)	18.75 (12.45–25.80)	0.7053
Medication			
Insulin (n, %)	62 (70.5%)	72 (78.3%)	0.2300
Biguanides (n, %)	61 (69.3%)	79 (85.9%)	0.0076
Sulfonylureas (n, %)	13 (14.8%)	12 (13.0%)	0.7374
α-glucosidase inhibitors (n, %)	62 (70.5%)	68 (73.9%)	0.6046
Thiazolidinediones (n, %)	2 (2.3%)	3 (3.3%)	1.0000
SGLT2 inhibitors (n, %)	23 (26.1%)	24 (26.1%)	0.9940
GLP-1 receptor agonists (n, %)	11 (12.5%)	4 (4.3%)	0.0479
DPP4 inhibitors (n, %)	18 (20.5%)	24 (26.1%)	0.3718
Statins (n, %)	43 (48.9%)	59 (64.1%)	0.0388

BMI, body mass index; MAP, mean arterial pressure; SBP, Systolic blood pressure; DBP, Diastolic blood pressure; HbA1c, glycosylated hemoglobin, type A1c; Glutamic oxaloacetic transaminase (AST), alanine aminotransferase (ALT); TG, triglycerides; TC, total cholesterol; HDL-C, high-density lipoprotein cholesterol; LDL-C, low-density lipoprotein cholesterol; eGFR, estimated glomerular filtration rate; FBG, fasting blood glucose; BNP, brain natriuretic peptide; cTnI, cardiac tropin I; CK-MB, creatine Kinase-MB; Myo, myoglobin; SGLT2 inhibitors, sodium-glucose cotransporter 2 inhibitors; GLP-1 receptor agonists, glucagon-like peptide 1 receptor agonists; dipeptidyl peptidase-4 (DPP4) inhibitors, dipeptidyl peptidase 4 inhibitors.

Next, we compared the significance of TyG index, TG/HDL-C ratio, FBG, and HbA1c to identify diabetic patients with subclinical cardiac dysfunction. First, previous studies have demonstrated that DM-related HF shifted from an asymptomatic stage to HFpEF, which was manifested by LV shrinkage but not LV dilatation, and finally developed to LV dilatation with reduced EF (HFrEF) (21). The HFA-PEFF score was a scoring system for suspected HFpEF assessing brain natriuretic peptide (BNP) and echocardiographic parameters (18). In this study, among 180 asymptomatic T2DM patients, 38 (21.1%) patients were identified with HFpEF as calculated by HFA-PEFF score ≥ 5 points, 33 (18,3%) patients were identified negative (HFA-PEFF score ≤ 1), and 109 (60.6%) patients were suspected to be positive (2 ≤ HFA-PEFF score ≤ 4). Compared to the negative group, the TyG index were higher in suspicious positive and positive HFpEF group (Figure 1). Furthermore, ROC analysis for detecting suspicious or positive HFpEF showed that AUC of TyG index was 0.706 (95% confidence interval (CI): 0.612–0.801), significantly higher than that of FBG, PBG, TG, TC, LDL-C,

TABLE 2 Echocardiographic data of in T2DM patients stratified by binary TyG index.

Variables	TyG index <9.47 (*N*=88)	TyG index ≥9.47 (*N*=92)	*p*-value
LVEF (%)	64.44 ± 2.80	63.99 ± 2.95	0.0905
LVEDD (mm)	46.53 ± 3.98	47.30 ± 3.40	0.1636
LVESD (mm)	30.15 ± 2.78	30.74 ± 2.43	0.1295
IVSD (mm)	9.00 (8.00–9.00)	9.00 (8.00–9.00)	0.1583
LVPWT (mm)	9.00 (8.00–9.00)	9.00 (8.00–9.00)	0.1751
septal e (cm/s)	7.30 (6.00–8.40)	7.00 (5.63–8.00)	0.0609
lateral e (cm/s)	10.00 (8.60–11.08)	8.55 (7.53–10.10)	0.0031
E/A	0.85 (0.74–1.08)	0.87 (0.75–1.11)	0.6075
E/e'	8.23 (6.92–10.37)	9.83 (8.22–11.05)	0.0015
LA (mm)	34.40 ± 3.63	34.93 ± 4.15	0.3578
LA volume (mm)	43.67 ± 11.31	47.84 ± 12.72	0.0215
LAVI (mL/m^2)	26.57 ± 6.65	28.00 ± 7.89	0.1899

LVEF (%), left ventricular ejection fraction%; LVEDD, left ventricular end-diastolic diameter; LVESD, left ventricular end-systolic diameter; IVSD, interventricular septal diameter; LVPWT, left ventricular posterior wall thickness; LA, left atrial; LAVI, left atrial volume index.

TABLE 3 Data of insulin resistance indices in T2DM patients stratified by binary TyG index.

Variables	TyG index <9.47 (*N*=88)	TyG index ≥9.47 (*N*=92)	*p*-value
TG/HDL-C	1.04 ± 0.49	3.75 ± 4.42	<0.0001
C peptide 0 min (pmol/L)	452.26 ± 256.93	637.63 ± 285.30	<0.0001
C peptide 30 min (pmol/L)	636.67 ± 351.08	798.57 ± 350.84	0.0019
C peptide 60 min (pmol/L)	861.46 ± 494.17	989.97 ± 457.90	0.0545
C peptide 120 min (pmol/L)	1121.06 ± 705.74	1302.37 ± 727.72	0.0762
C peptide 180 min (pmol/L)	1041.36 ± 588.20	1151.46 ± 633.69	0.2480

TG, triglycerides; HDL-C, high-density lipoprotein cholesterol.

TG/HDL-C, and HbA1c (AUC < 0.5 not shown in the Figure 2). When the Youden Index reached the maximum, the optimal cut-off point of the TyG index was 9.0067. The corresponding sensitivity and specificity were 72.8 and 60.6%, respectively.

Multivariate analysis of the correlation between TyG index and HFA-PEFF score in diabetic patients

To further explore the relationship between TyG index and HFpEF in diabetic patients, multivariate logistic stepwise regression analysis was performed. Data showed that the TyG index was independently correlated with the risk of HFpEF (HFA-PEFF score ≥ 5) after adjusting for age, sex, BMI, waist circumference, MAP, diabetes duration, TC, eGFR, and HbA1c (Odds Ratio (OR): 0.786, 95% CI: 0.290–1.282, $p = 0.0019$; Table 4). Then we performed subgroup analyzes to evaluate the impact of other risk factors based on the following stratification variables: sex, age, HbA1c, and duration of diabetes (Table 5). An increased TyG index remained significantly correlated with the risk of HFpEF in the subgroups of age, sex, HbA1c, and duration of diabetes ($p < 0.05$ for each). Stronger correlations were found in the subgroups of male (OR: 0.877, $p = 0.0174$), age < 54 years (OR: 1.055, $p = 0.0078$), HbA1c ≥ 9.75% (OR: 1.084, $p = 0.0032$) and duration of diabetes after multivariable adjustment. However, no significant association was detected in female patients, patients aged ≥54, and patients with HbA1c < 9.75%. Clinical and metabolic characteristics stratified by HbA1c, and duration of DM were presented in Supplementary Tables S3 and S4, respectively.

Discussion

This retrospective study demonstrated that among 180 asymptomatic patients with T2DM, 38 (21.1%) patients were identified with HFpEF as calculated by HFA-PEFF score ≥ 5 points. Elevated TyG index was positively corrected with metabolic syndrome-related risk factors (BMI, waist circumference, blood pressure, HbA1c, TG, TC, non-HDL-C, and FBG, $p < 0.05$ for each) and parameters of diastolic dysfunction (E/e' ratio, $p < 0.0001$) after adjustment of confounding factors. Importantly, TyG index was independently correlated with greater risk of developing HFpEF as evaluated by HFA-PEFF. Our results suggested that in diabetic patients, TyG index might be considered as a reliable biomarker to identify asymptomatic patients with high HFpEF risk.

The TyG index, derived from FBG and TG, was proven to be a reliable and simple surrogate for metabolic syndrome and IR (22). Mounting evidence has proved the crucial value of TyG index in predicting diabetic complications in patients with T2DM (23–25). Study by Liu et al. showed a significant association between TyG index and the risk of diabetic nephropathy in 682 adult patients

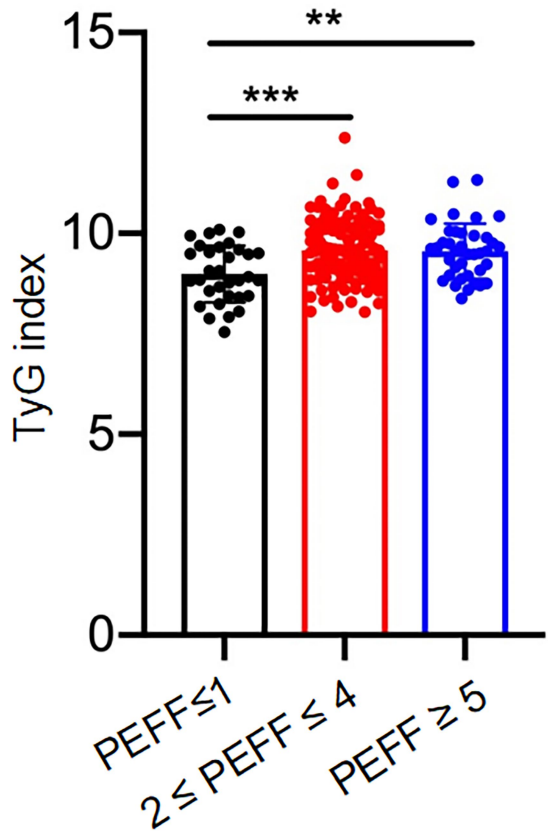

FIGURE 1
TyG index in diabetic patients stratified by HFA-PEFF score. **p<0.05. ***p<0.001.

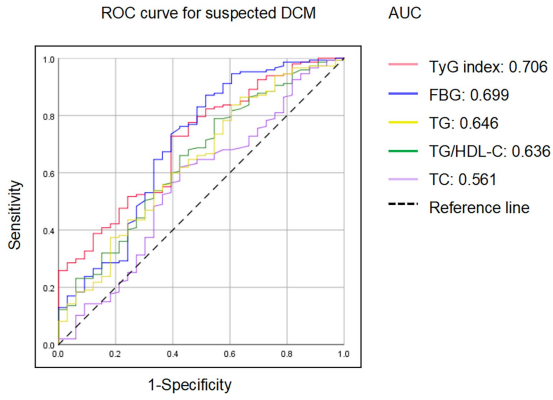

FIGURE 2
ROC analysis for the identification of diabetic patients with risk of HFpEF. TyG, triglyceride-glucose; FBG, fasting blood glucose; TG, triglycerides; HDL-C, high-density lipoprotein cholesterol; TC, total cholesterol.

with T2DM (26). Pan et al. confirmed the predictive value of TyG index in distinguishing diabetic patients at an increased risk of lower limb vascular stenosis and nephric microvascular disorder (18). Furthermore, recent studies suggested that TyG index could be recognized as a risk factor for CVD even in asymptomatic

TABLE 4 Logistic regression analysis of the association between the TyG index and HFA-PEFF score.

	EXP (95%CI)	p-value
Model 1	0.626 (0.226–1.025)	0.0021
Model 2	0.640 (0.219–1.062)	0.0029
Model 3	0.786 (0.290–1.282)	0.0019

Model 1, Adjusted for age, sex; Model 2, Model 1+ BMI, Waist circumference, DM duration; Model 3, Model 2+ eGFR, MAP, TC, HbA1c. BMI, body mass index; eGFR, estimated glomerular filtration rate; MAP, mean arterial pressure; TC, total cholesterol; HbA1c, glycosylated hemoglobin, type A1c.

patients. Lee et al. showed that higher level of TyG index was correlated with increased risk of coronary artery stenoses (CAS) in asymptomatic diabetic patients (27). Thai et al. confirmed this hypothesis and proposed that TyG index was positively associated with the number and severity of artery stenoses (28). However, the predictive value of TyG index in subclinical HF in diabetic patients has not been well evaluated. In accordance with prior studies, our findings showed that the TyG index had a strong association with metabolic syndrome and HFpEF in subjects with T2DM, including BMI, waist circumference, blood pressure, HbA1c, TG, TC, HDL-C, non-HDL-C, LDL-C and FBG.

As an indicator of IR, the relationship between TyG index and the occurrence of CVD in different groups, including non-diabetic and diabetic individuals, has been widely explored (22). However, few studies have investigated the association between TyG index and cardiac structure and hemodynamics evaluated by echocardiography, which may predict the risk of CVD. An observational study enrolled 823 general subjects found that high TyG index was correlated with elevated LA diameter and decreased LVEF (%) and ankle-branchial index (ABI) (29). These results were partly consistent with the data by Wang et al., in which TyG index was positively associated with cardiac hemodynamics such as LVESD, LVEDV, LVPW, IVS, and LV mass and negatively associated with LVEF. The latter study was conducted in 201 healthy controls and 446 asymptomatic patients with T2DM (30). Nevertheless, our results demonstrated that TyG index was positively correlated with E/e' ratio and negatively correlated with septal e' and lateral e', but not correlated with parameters of cardiac systolic function. Of note, high TyG index was significantly positively correlated with increased risk of HFA-PEFF score ≥ 5 points, indicating a strong association between the TyG index and cardiac diastolic function. This inconsistence may be attributed to different recruited subjects, diverse diseases of enrolled population, and the potential impacts of drugs. Our study focused on exploring the diagnostic value of the TyG index to early detection of cardiac structural changes in diabetic patients, which may be of special significance for clinical cardiovascular risk assessment and secondary prevention.

Moreover, previous studies showed that myocardial dilatation defects are reported to be abnormal in patients with hyperglycemia and IR. Thus, the factors that determine TyG levels (high TG and high glucose at the baseline condition) related to the following conditions (1) hypo-insulinemia with hyperglycemia and (2) hyperinsulinemia and hyperglycemia with insulin resistance. To clarify the relationship between these conditions, we evaluated the association between TyG index and IR, or insulin deficiency. Our results showed that TyG index was positively related to HG/HDL-C

TABLE 5 Subgroup analysis of odds ratios of the TyG index with HFA-PEFF score in T2DM.

	N	Model 1		Model 2		Model 3	
		OR (95%CI)	*p*-value	OR (95%CI)	*p*-value	OR (95%CI)	*p*-value
Sex							
Female	78	0.574 (−0.016–1.164)	0.0565	0.730 (0.094–1.366)	0.0246	0.542 (−0.216–1.300)	0.1608
Male	102	0.684 (0.131–1.238)	0.0154	0.521 (−0.085–1.128)	0.0918	0.877 (0.154–1.599)	0.0174
Age (year)							
<54	78	0.696 (0.118–1.274)	0.0182	0.742 (0.124–1.361)	0.0187	1.055 (0.277–1.832)	0.0078
≥54	102	0.564 (−0.014–1.142)	0.0558	0.566 (−0.047–1.178)	0.0701	0.628 (−0.060–1.316)	0.0736
HbA1c (%)							
<9.75%	88	0.573 (−0.041–1.189)	0.0677	0.447 (−0.211–1.104)	0.1827	0.322 (−0.470–1.135)	0.4167
≥9.75%	92	0.674 (0.139–1.208)	0.0135	0.781 (0.203–1.359)	0.0081	1.084 (0.363–1.805)	0.0032
Duration (year)							
<6	85	0.647 (0.079–1.216)	0.0255	0.584 (−0.056–1.225)	0.0738	1.008 (0.215–1.802)	0.0127
≥6	95	0.580 (0.005–1.155)	0.0481	0.634 (0.041–1.226)	0.0360	0.752 (0.002–1.502)	0.0494

Model 1, Adjusted for age, sex; Model 2, Model 1+ BMI, Waist circumference, DM duration; Model 3, Model 2+ eGFR, MAP, TC, HbA1c.

value (IR biomarker) and C-peptide at 0 min and 30 min (insulin secretion marker). Additionally, subgroup analysis demonstrated that there was stronger association between TyG index and increased risk of HFpEF in patients with insufficient glycemic control (HbA1c ≥ 9.75%), suggesting that TyG index was mainly dependent on the second condition. Importantly, ROC analysis revealed that compared to sustained hyperglycemia status, TyG index preserved a higher predictive value for HFpEF in patients with T2DM, confirming the crucial role of IR in diabetic related cardiac dysfunction.

There are some limitations need to be emphasized in this study. Firstly, parameters evaluating cardiac diastolic function and HFA-PEFF score were incomplete, including tricuspid valve velocity and global longitudinal strain data. These missing data in the HFA-PEFF score may reduce statistical power and cause selection bias. More complete echocardiographic data in the future may improve the reliability and stability of TyG index in predicting diabetic patients with high HF risk. Secondly, HF is a series of dynamic and progressive disorders, the calculation of the baseline TyG index alone does not represent the longitudinal correlation between the TyG index and risk of diabetes-induced HF over time. Cumulative TyG index (the summation of average TyG index for each pair of consecutive assessments multiplied by the time between these two-consecutive inclusion in years) may be better than single TyG index at baseline in predicting HF or even other CVDs (31). Finally, the number of eligible patients was relatively limited, which may be due to the very specific population in this study. DM is often accompanied by different subtypes of CVDs involving multiple risk factors. Nevertheless, clinical studies of diabetic status itself (hyperglycemia with or without IR) on CVDs, especially on subclinical CVDs are limited. Thus, to simply the impact of diabetes on cardiac structure and function, we screened diabetic patients without any other risk factors to confirm the predictive value of TyG index in subclinical HF. Therefore, more sample size and multi-center studies are warranted to explore the crucial role of hyperglycemia and IR in diabetic complications. The diagnostic criteria for subclinical diabetic cardiac dysfunction also needs to be further refined.

Conclusion

In conclusion, we explored a significant correlation between TyG index and an increased risk of HFpEF in asymptomatic patients with T2DM. IR plays a crucial role in the pathophysiology of HFpEF and may be identified as a novel target for its prevention and treatment. Further studies are warranted to explore the correlation between the IR parameters, especially TyG index, and the risk of HF in patients with T2DM at different stages.

Data availability statement

The raw data supporting the conclusions of this article will be made available by the authors, without undue reservation.

Ethics statement

The studies involving human participants were reviewed and approved by The Third Affiliated Hospital of Soochow University. The patients/participants provided their written informed consent to participate in this study.

Author contributions

LT and XH designed the work. TW wrote the original version of this manuscript and analyzed the clinical data. LT performed the manuscript reviewing and editing. JX and HZ collected the clinical data. All authors read and approved the final manuscript.

Funding

This research was funded by the National Natural Science Foundation of China (NSFC) grants 82170356 and Changzhou Sci&Tech Program grant CJ20210091.

Conflict of interest

The authors declare that the research was conducted in the absence of any commercial or financial relationships that could be construed as a potential conflict of interest.

Publisher's note

All claims expressed in this article are solely those of the authors and do not necessarily represent those of their affiliated organizations, or those of the publisher, the editors and the reviewers. Any product that may be evaluated in this article, or claim that may be made by its manufacturer, is not guaranteed or endorsed by the publisher.

Supplementary material

The Supplementary material for this article can be found online at: https://www.frontiersin.org/articles/10.3389/fcvm.2023.1086978/full#supplementary-material

References

1. Wang, Y, Yang, H, Huynh, Q, Nolan, M, Negishi, K, and Marwick, TH. Diagnosis of nonischemic stage B heart failure in type 2 diabetes mellitus: optimal parameters for prediction of heart failure. *J Am Coll Cardiol Img*. (2018) 11:1390–400. doi: 10.1016/j.jcmg.2018.03.015
2. Yancy, CW, Jessup, M, Bozkurt, B, Butler, J, Casey, DE Jr, Colvin, MM, et al. 2017 ACC/AHA/HFSA focused update of the 2013 ACCF/AHA guideline for the Management of Heart Failure: a report of the American College of Cardiology/American Heart Association task force on clinical practice guidelines and the Heart Failure Society of America. *J Am Coll Cardiol*. (2017) 70:776–803. doi: 10.1016/j.jacc.2017.04.025
3. Dillmann, WH. Diabetic cardiomyopathy. *Circ Res*. (2019) 124:1160–2. doi: 10.1161/CIRCRESAHA.118.314665
4. Ritchie, RH, and Abel, ED. Basic mechanisms of diabetic heart disease. *Circ Res*. (2020) 126:1501–25. doi: 10.1161/CIRCRESAHA.120.315913
5. Jia, G, Whaley-Connell, A, and Sowers, JR. Diabetic cardiomyopathy: a hyperglycaemia- and insulin-resistance-induced heart disease. *Diabetologia*. (2018) 61:21–8. doi: 10.1007/s00125-017-4390-4
6. Galderisi, M. Diastolic dysfunction and diastolic heart failure: diagnostic, prognostic and therapeutic aspects. *Cardiovasc Ultrasound*. (2005) 3:9. doi: 10.1186/1476-7120-3-9
7. Mozaffarian, D, Benjamin, EJ, Go, AS, Arnett, DK, Blaha, MJ, Cushman, M, et al. Heart disease and stroke Statistics-2016 update: a report from the American Heart Association. *Circulation*. (2016) 133:e38–e360. doi: 10.1161/CIR.0000000000000350
8. Iribarren, C, Karter, AJ, Go, AS, Ferrara, A, Liu, JY, Sidney, S, et al. Glycemic control and heart failure among adult patients with diabetes. *Circulation*. (2001) 103:2668–73. doi: 10.1161/01.cir.103.22.2668
9. Lee, S, Liu, T, Zhou, J, Zhang, Q, Wong, WT, and Tse, G. Predictions of diabetes complications and mortality using hba 1c variability: a 10-year observational cohort study. *Acta Diabetol*. (2021) 58:171–80. doi: 10.1007/s00592-020-01605-6
10. Paolillo, S, Marsico, F, Prastaro, M, Renga, F, Esposito, L, De Martino, F, et al. Diabetic cardiomyopathy: definition, diagnosis, and therapeutic implications. *Heart Fail Clin*. (2019) 15:341–7. doi: 10.1016/j.hfc.2019.02.003
11. Peterson, V, Norton, GR, Raymond, A, Libhaber, CD, Millen, AM, Majane, OH, et al. Insulin resistance-associated decreases in left ventricular diastolic function are strongly modified by the extent of concentric remodeling in a community sample. *Int J Cardiol*. (2016) 220:349–55. doi: 10.1016/j.ijcard.2016.06.206
12. Minh, HV, Tien, HA, Sinh, CT, Thang, DC, Chen, CH, Tay, JC, et al. Assessment of preferred methods to measure insulin resistance in Asian patients with hypertension. *J Clin Hypertens (Greenwich)*. (2021) 23:529–37. doi: 10.1111/jch.14155
13. Simental-Mendía, LE, Rodríguez-Morán, M, and Guerrero-Romero, F. The product of fasting glucose and triglycerides as surrogate for identifying insulin resistance in apparently healthy subjects. *Metab Syndr Relat Disord*. (2008) 6:299–304. doi: 10.1089/met.2008.0034
14. Alberti, KG, and Zimmet, PZ. Definition, diagnosis and classification of diabetes mellitus and its complications. Part 1: diagnosis and classification of diabetes mellitus provisional report of a WHO consultation. *Diabetic Med*. (1998) 15:539–53. doi: 10.1002/(SICI)1096-9136(199807)15:7<539::AID-DIA668>3.0.CO;2-S
15. Chinese Diabetes Society; National Office for Primary Diabetes Care. National guidelines for the prevention and control of diabetes in primary care (2022). *Zhonghua Nei Ke Za Zhi*. (2022) 61:249–62. doi: 10.3760/cma.j.cn112138-20220120-000063
16. Joint Committee for Guideline Revision. 2018 Chinese guidelines for prevention and treatment of hypertension-a report of the revision Committee of Chinese Guidelines for prevention and treatment of hypertension. *J Geriatr Cardiol*. (2019) 16:182–241. doi: 10.11909/j.issn.1671-5411.2019.03.014
17. Liu, LS. 2010 Chinese guidelines for the management of hypertension. *Zhonghua Xin Xue Guan Bing Za Zhi*. (2011) 39:579–615. doi: 10.3760/cma.j.cn501113-20220824-00436
18. Pieske, B, Tschöpe, C, de Boer, RA, Fraser, AG, Anker, SD, Donal, E, et al. How to diagnose heart failure with preserved ejection fraction: the HFA-PEFF diagnostic algorithm: a consensus recommendation from the heart failure association (HFA) of the European Society of Cardiology (ESC). *Eur Heart J*. (2019) 40:3297–317. doi: 10.1093/eurheartj/ehz641
19. Szapary, PO, and Rader, DJ. The triglyceride-high-density lipoprotein axis: an important target of therapy? *Am Heart J*. (2004) 148:211–21. doi: 10.1016/j.ahj.2004.03.037
20. Saisho, Y. Postprandial C-peptide to glucose ratio as a marker of β cell function: implication for the Management of Type 2 diabetes. *Int J Mol Sci*. (2016) 17:744. doi: 10.3390/ijms17050744
21. Seferović, PM, and Paulus, WJ. Clinical diabetic cardiomyopathy: a two-faced disease with restrictive and dilated phenotypes. *Eur Heart J*. (2015) 36:1718–27. doi: 10.1093/eurheartj/ehv134
22. Tao, LC, Xu, JN, Wang, TT, Hua, F, and Li, JJ. Triglyceride-glucose index as a marker in cardiovascular diseases: landscape and limitations. *Cardiovasc Diabetol*. (2022) 21:68. doi: 10.1186/s12933-022-01511-x
23. Wang, L, Cong, HL, Zhang, JX, Hu, YC, Wei, A, Zhang, YY, et al. Triglyceride-glucose index predicts adverse cardiovascular events in patients with diabetes and acute coronary syndrome. *Cardiovasc Diabetol*. (2020) 19:80. doi: 10.1186/s12933-020-01054-z
24. Pan, Y, Zhong, S, Zhou, K, Tian, Z, Chen, F, Liu, Z, et al. Association between diabetes complications and the triglyceride-glucose index in hospitalized patients with type 2 diabetes. *J Diabetes Res*. (2021) 2021:8757996. doi: 10.1155/2021/8757996
25. Srinivasan, S, Singh, P, Kulothungan, V, Sharma, T, and Raman, R. Relationship between triglyceride glucose index, retinopathy and nephropathy in type 2 diabetes. *Endocrinol Diabetes Metab*. (2021) 4:e00151. doi: 10.1002/edm2.151
26. Liu, L, Xia, R, Song, X, Zhang, B, He, W, Zhou, X, et al. Association between the triglyceride-glucose index and diabetic nephropathy in patients with type 2 diabetes: a cross-sectional study. *J Diabetes Investig*. (2021) 12:557–65. doi: 10.1111/jdi.13371
27. Lee, EY, Yang, HK, Lee, J, Kang, B, Yang, Y, Lee, SH, et al. Triglyceride glucose index, a marker of insulin resistance, is associated with coronary artery stenosis in asymptomatic subjects with type 2 diabetes. *Lipids Health Dis*. (2016) 15:155. doi: 10.1186/s12944-016-0324-2
28. Thai, PV, Tien, HA, Van Minh, H, and Valensi, P. Triglyceride glucose index for the detection of asymptomatic coronary artery stenosis in patients with type 2 diabetes. *Cardiovasc Diabetol*. (2020) 19:137. doi: 10.1186/s12933-020-01108-2
29. Chiu, TH, Tsai, HJ, Chiou, HC, Wu, PY, Huang, JC, and Chen, SC. A high triglyceride-glucose index is associated with left ventricular dysfunction and atherosclerosis. *Int J Med Sci*. (2021) 18:1051–7. doi: 10.7150/ijms.53920
30. Wang, C, Zhao, Z, Deng, X, Cai, Z, Gu, T, Li, L, et al. Association of triglyceride-glucose with cardiac hemodynamics in type 2 diabetes. *Diab Vasc Dis Res*. (2022) 19:14791641221083396. doi: 10.1177/14791641221083396
31. Cui, H, Liu, Q, Wu, Y, and Cao, L. Cumulative triglyceride-glucose index is a risk for CVD: a prospective cohort study. *Cardiovasc Diabetol*. (2022) 21:22. doi: 10.1186/s12933-022-01456-1

frontiers | Frontiers in Cardiovascular Medicine

TYPE Review
PUBLISHED 15 June 2023
DOI 10.3389/fcvm.2023.1197432

OPEN ACCESS

EDITED BY
Catherine A. Reardon,
The University of Chicago, United States

REVIEWED BY
George Sack,
Johns Hopkins Medicine, United States
Xuchu Que,
University of California, San Diego,
United States

*CORRESPONDENCE
Laura J. den Hartigh
✉ lauradh@u.washington.edu

RECEIVED 31 March 2023
ACCEPTED 15 May 2023
PUBLISHED 15 June 2023

CITATION
den Hartigh LJ, May KS, Zhang XS, Chait A and Blaser MJ (2023) Serum amyloid A and metabolic disease: evidence for a critical role in chronic inflammatory conditions.
Front. Cardiovasc. Med. 10:1197432.
doi: 10.3389/fcvm.2023.1197432

Serum amyloid A and metabolic disease: evidence for a critical role in chronic inflammatory conditions

Laura J. den Hartigh[1,2]*, Karolline S. May[1,2], Xue-Song Zhang[3], Alan Chait[1,2] and Martin J. Blaser[3]

[1]Department of Medicine, Division of Metabolism, Endocrinology, and Nutrition, University of Washington, Seattle, WA, United States, [2]Diabetes Institute, University of Washington, Seattle, WA, United States, [3]Center for Advanced Biotechnology and Medicine, Rutgers University, Piscataway, NJ, United States

Serum amyloid A (SAA) subtypes 1–3 are well-described acute phase reactants that are elevated in acute inflammatory conditions such as infection, tissue injury, and trauma, while SAA4 is constitutively expressed. SAA subtypes also have been implicated as playing roles in chronic metabolic diseases including obesity, diabetes, and cardiovascular disease, and possibly in autoimmune diseases such as systemic lupus erythematosis, rheumatoid arthritis, and inflammatory bowel disease. Distinctions between the expression kinetics of SAA in acute inflammatory responses and chronic disease states suggest the potential for differentiating SAA functions. Although circulating SAA levels can rise up to 1,000-fold during an acute inflammatory event, elevations are more

Abbreviations

ABCA1, ATP binding cassette subfamily A member 1; AGE, advanced glycation end products; $AgNO_3$, silver nitrate; AKT, protein kinase B; ALT, alanine aminotransferase; apoA1, apolipoprotein-1; apoB, apolipoprotein B; BMDM, bone marrow-derived macrophages; BMI, body mass index; C/EBPβ, CCAAT enhancer binding protein beta; CD, Chron's disease; CD36, class B scavenger receptor; CDAI, Crohn's disease activity index; CHO, Chinese Ovary Cells; COVID-19, Coronavirus disease 19; CML, carboxy methyl lysine; CRP, C-reactive protein; CVD, cardiovascular disease; DSS, dextran sodium sulfate; ECM, extracellular matrix; ERK, extracellular signal-regulated kinase; EVs, extracellular vesicles; FMT, fecal microbial transplant' FPR1, formyl peptide receptor like-1; FPR2, formyl peptide receptor like-2; GD, gestational diabetes; GLUT4, glucose transporter 4; GM-CSF, granulocyte-macrophage colony stimulating factor; HbA1c, hemoglobin A1c; HDL, high density lipoprotein; HFD, high fat diet; HMGB1, high mobility group box 1; HNF, hepatocyte nuclear factor; HO-1, heme oxygenase type-1; HOMA-IR, homeostatic model assessment for insulin resistance; hSAA, human serum amyloid A; HUVEC, human umbilical vein endothelial cells; IBD, inflammatory bowel disease; IBS, irritable bowel syndrome; IκBα, nuclear factor of kappa light polypeptide gene enhancer in B cells inhibitor alpha; IL-1, interleukin-1; IL-1α, interleukin-1 alpha; IL-1β, interleukin-1 beta; IL-6, interleukin-6; IL-8, interleukin-8; IL-10, interleukin-10; IL-12, interleukin 12; IL-17, interleukin-17; IL-22, interleukin-22; IL-23, interleukin-23; iNOS, inducible nitric oxide synthase; IP-10, interferon γ-induced protein 10; JNK, c-Jun N-terminal kinase; LDL, low-density lipoprotein; LDLR, low-density protein receptor; LFD, low fat diet; LOX-1, oxidized low-density lipoprotein; LPS, lipopolysaccharide; Mϕ, macrophage; MAPK, mitogen-activated protein kinase; MCP-1, monocyte chemotactic protein-1; M-CSF, monocyte colony stimulating factor; MDMs, monocyte-derived macrophages; MIP1α, macrophage inflammatory protein-1 alpha; NAFLD, non-alcoholic fatty liver disease; NFκB, nuclear factor kappa B; NO, nitric oxide; PAT, pulsed therapeutic-level antibiotic; PBMCs, peripheral blood mononuclear cells; PCOS, polycystic ovary syndrome; PKA, protein kinase A; PKR, protein kinase R; PLIN, perilipin; PPARγ, peroxisome proliferator-activated receptor gamma; RA, rheumatoid arthritis; RAGE, receptor for advanced glycation end-products; RANTES, regulated on activation, normal T cell expressed and secreted; RBP4, retinol-binding protein 4; rSAA, recombinant serum amyloid A; SAA, serum amyloid A, SAA1, serum amyloid A1; SAA2, serum amyloid A2; SAA3, serum amyloid A3; SAA4, serum amyloid A4; SAF-1, serum amyloid A-activating factor 1; SELS, selenoprotein S; SES-CD, simplified endoscopy score for Crohn's disease; SLE, Systemic lupus erythematosus; SPF, specific pathogen-free; SRB1, scavenger receptor class B type 1; STZ, streptozotocin; T1D, type 1 diabetes; T2D, type 2 diabetes; TGFβ, transforming growth factor β; Th17, T-helper 17 cells; THP-1, human leukemia monocytic cell line; TLR-2, toll-like receptor 2; TLR-4, toll-like receptor 4; TNBS, trinitrobenzone sulfonic acid; TNFα, tumor necrosis factor alpha; UC, ulcerative colitis; VCAM-1, vascular cell adhesion molecule 1; VLCD, very low carbohydrate diet; VLDL, very low-density lipoprotein; WAT, white adipose tissue.

modest (~5-fold) in chronic metabolic conditions. The majority of acute-phase SAA derives from the liver, while in chronic inflammatory conditions SAA also derives from adipose tissue, the intestine, and elsewhere. In this review, roles for SAA subtypes in chronic metabolic disease states are contrasted to current knowledge about acute phase SAA. Investigations show distinct differences between SAA expression and function in human and animal models of metabolic disease, as well as sexual dimorphism of SAA subtype responses.

KEYWORDS

obesity, diabetes, cardiovascular disease, SAA, intestine, liver, adipocytes, macrophages

1. Introduction

Members of the serum amyloid A (SAA) family are acute phase reactants and chemokines that are elevated in acute inflammatory conditions such as infection (1, 2), as well as chronic inflammatory conditions including autoimmune disorders (3–8), obesity (9–13), type 2 diabetes (T2D) (14, 15), and cardiovascular disease (CVD) (16–19) (reviewed extensively in 20, 21). Several SAA subtypes are present across diverse animal species (22), including invertebrates (23), suggesting important conserved functions. Since SAA is poorly soluble in aqueous solutions, it circulates associated with lipoproteins, in particular high density lipoprotein (HDL), and is considered an apolipoprotein (24, 25). Functions of particular SAA subtypes include roles in host defense (26–30), chemoattraction (31–34), lipid metabolism (35–37), and inflammation (38). We now review the emerging knowledge about distinctive functions of the different SAA subtypes.

1.1. SAA subtypes and receptors

Of the 4 known SAA subtypes, SAA1 and SAA2 are highly expressed in the liver in mammals including humans in response to inflammatory stimuli, and can circulate at high concentrations, usually bound to HDL (39). SAA1 and SAA2 are highly homologous, differing in only a few amino acids. In contrast, SAA3 is more highly expressed in extrahepatic tissues in particular animal species (40, 41). SAA3 is not known to circulate under most conditions, with the exception of high dose lipopolysaccharide (LPS) injection (42). SAA3 is considered to be a pseudogene in humans due to a premature stop codon (43), leading to a frame shift in codon 31, thereby deleting the last ten amino acids (44). SAA3 is only ~40% homologous to SAA1/2. Since in humans SAA1 and SAA2 are expressed from both liver and extrahepatic tissues, it has been difficult to conclusively distinguish hepatic from extrahepatic SAA functions in humans. However, phenotypic distinctions between hepatic and extra-hepatic SAA subtypes in mice, due to the predominance of extrahepatic Saa3, allow sharper definition (18, 38, 44). SAA3 protein has been detected in human mammary gland epithelial cell lines (45), although its expression is more commonly found in non-human mammals. SAA4 is constitutively expressed by most cell types and responds only minimally to inflammatory stimuli (46, 47). In many prior studies, distinctions between specific SAA subtypes were not reported, perhaps due to the lack of available antibodies capable of distinguishing them. This is unfortunate, as it is possible that different SAA subtypes exert different functions in the context of metabolic disease. In this review, we use the term "SAA" to refer to SAA1/2, or to reflect that the authors of work described did not specify particular SAA subtypes. In addition, in accordance with scientific nomenclature standards, "SAA" will refer to humans, while "Saa" corresponds to mouse.

The major identified SAA receptors are listed in **Table 1**. SAA binds to formyl peptide like receptors 1 and 2 (FPLR1 and FPLR2) in human monocytes, neutrophils, human embryonic kidney (HEK293) cells, and human umbilical vein endothelial cells (HUVECs), thus promoting chemotaxis and increased calcium flux. In response to varied stimuli (**Table 1**), mitogen-activated protein kinases (MAPKs) and nuclear factor kappa B (NFκB) pathways are further activated, which leads to secretion of tumor necrosis factor alpha (TNFα), interleukin-8 (IL-8), and monocyte chemotactic protein-1 (MCP-1) (32, 33, 48–51, 69, 70). The receptor for advanced glycation end products (RAGE) is another known SAA receptor present on several tissues and cell types. SAA mediates the activation of the AGE/RAGE axis and NFκB pathways, with subsequent transcription of interleukin-6 (IL-6), heme oxygenase type-1 (HO-1) and monocyte colony stimulating factor (M-CSF) (52–55). Moreover, SAA induces signal transducer and activator of transcription 1 (STAT1)-mediated high mobility group box 1 (HMGB1) expression and protein kinase R (PKR) activation, potentially through RAGE and toll-like receptors (TLRs) (52). SAA has affinity for TLR2 and TLR4 (56–61, 71, 72), and to the oxidized low-density lipoprotein receptor (LOX-1) (62) and scavenger receptor class B type 1 (SRB1), thus mainly signaling via the MAPK pathway in both immune and epithelial cells. A recently described SAA receptor is Selenoprotein S/Tanis [SELS in humans (63, 65, 67, 68), Tanis in animal models (68)]. Tanis/SELS is highly expressed in liver, skeletal muscle, and adipose tissue (68), which may distinguish SAA effects mediated by this receptor from those found primarily on immune cells. SELS expression on adipose tissue is highly correlated to circulating SAA levels, suggesting a potential feed-forward mechanism (68, 73). Importantly, most of these potential SAA receptors respond to multiple ligands, with SELS having the highest degree of SAA-specificity. Collectively, varied SAA receptor expression patterns on different cell and tissue types could indicate different SAA functions.

TABLE 1 SAA receptors and downstream signaling pathways.

SAA receptors	SAA	Host specificity		Ligand(s)/stimuli	Target tissue/ cell	Signaling pathways	Outcomes
		Human	Rodent				
FPRL1/ FPRL2	SAA1, SAA2	(32, 33, 48–51)	(32)	SAA (0.01–2 μM) rhSAA1 (20 μg) LPS (100 ng/ml) GM-CSF (100 ng/ml)	Neutrophils Monocytes Cell lines: HEK 293, HUVEC	Calcium signaling Cell migration NFκB MAPK (ERK/ p38/JNK) AKT	↑ intracellular Ca^{2+} (32, 33, 51) ↑ chemotaxis (32, 33) ↑ IL-8, CCL2 (Cell media/ plasma) (50, 51) ↑ IL-8, TNFα mRNA/protein (48) ↑ p-ERK, p-p38, p-JNK (48, 50) ↑ p-AKT (48)
RAGE	SAA1, SAA2	(52, 53)	(52–55)	rSAA1 (0.1–10 μg/ml) LPS (5 mg/kg) $AgNO_3$ (0.5 ml of a 2% solution) AEF (100 μg) Azocasein (7%) sRAGE VC1 (100 μg) peptide 5 (100 μg)	Kidney, Liver, Spleen Primary macrophages Cell lines: RAW264.7, THP-1, U937, BV-2	AGE-RAGE NFκB STAT1 PKR	↑ SAA (Tissue distribution) (55) ↑ NO (52) ↑ AGE, CML (plasma) (53) ↑ IL-6, IL-12, HGMB1, MCP-1, RANTES (Cell media/plasma) (52) ↑ RAGE, IL-6, HO-1, M-CSF mRNA (53, 54) ↑ p-STAT1, p-PKR (52)
TLR2	SAA1, SAA2	(56)	(56, 57)	rhSAA (1 μM) Concavalin (10 mg/kg)	Liver, Spleen Cell line: HeLa	TLR NFκB MAPK (ERK/ p38/JNK)	↑ ALT, AST (57) ↑ SAA, SAF-1, IL-6, IFN_Y, TNF-α (plasma) (56) ↑ SAA1, MCP-1, MIP1α/β, IL-1R, IL-10, IL-8, IL-18, IL-23, IP-10, eotaxin mRNA (56, 57) ↑ CD4+, Th17, T-reg, F4/80 + CD11b+ (57) ↓ p-IκBα (57) ↑ p-ERK1/2, p38, JNK (57)
TLR4	SAA1, SAA2, SAA3	_	(58–61)	SAA3 (0.3–1 μg/ml) LPS (0.01–1 μg/ml) Concavalin (10 μg) S100A8, S100A9 (70–100 μg)	Kidney, Liver, Lungs Primary macrophage Myeloid cells (Mac1 +) Cell lines: MCF7, RAW264.7	NFκB MAPK (ERK/ p38/JNK) AKT Rho GTPase	↑ Chemotaxis (58, 60) ↑ NO, iNOS (59) ↑ SAA3, IL-6, TNFα mRNA (58, 60) ↓ TLR4 mRNA (61) ↑p-IkB (58) ↑ p-ERK, p-p38, p-JNK (59, 60) ↑ p-AKT (59)
LOX-1	SAA1, SAA2, SAA3	_	(62)	hSAA3 (2 μg/ml) LPS (1 μg/ml)	Cell lines: LU65, LU99, MCF7, HUVEC H292, T47D	MAPK (ERK)	↔ hSAA2, hSAA3 mRNA (62) ↑ p-ERK (62) ↑ IL-6, IL-1β (plasma) (62)
SR-B1/CLA-1	SAA1, SAA2	(66, 67)	(63, 66)	SAA (0–10 μg/ml) Recombinant adenovirus SAA1/2 LPS (25 μg)	Cell lines: HeLa, HepG2, THP-1, CHO	Cholesterol efflux MAPK (ERK/ p38)	↑ ABCA1- and SR-B1 dependent cholesterol efflux (64, 65) ↓ Cholesteryl ester uptake (63) ↑ p-ERK1/2, p-38 (63)
SELS/Tanis	SAA1, SAA2	(65, 68, 73)	(68)	Insulin (6–100 nM) Glucose (12–35 mM) Euglycemic-hyperinsulinemic clamp (40 $mU{\cdot}m^{-2}{\cdot}min^{-1}$)	Adipose tissue, skeletal muscle, liver Cell lines: HepG2, C2C12, 3T3-L1	MAPK (ERK/ p38) Inflammatory pathways	↑ SAA (plasma) (68) ↑ IL-8 (Cell media) (66) ↑↓ Tanis/Sels mRNA (67, 68) ↑ p-ERK1/2, p-p38 (66) ↑ cardiometabolic risk factors (67, 68)

ABCA1, ATP-binding cassette A1; AEF, amyloid-enhancing factor; AGE, Advanced glycation end-products; AKT, protein kinase B; AEF, Amyloid-enhancing factor; ApoA1, apolipoprotein A1; CCL2, C-C Motif Chemokine Ligand 2; CHO, Chinese hamster ovary cells; CML, Carboxy methyl lysine; ERK, extracellular signal-regulated kinase; FPRL1, formyl peptide receptor-like 1; FPRL2, formyl peptide receptor-like 2; FPRL1, formyl peptide receptor-like 1; GM-CSF1, Granulocyte-macrophage colony-stimulating factor; HMGB1, high mobility group box 1 protein; HO-1, heme oxygenase 1; hSAA, human serum amyloid A; HUVEC, human umbilical vein endothelial cells; IκBα, nuclear factor of kappa light polypeptide gene enhancer in B-cells inhibitor alpha; IL-1β, interleukin 1 beta; IL-6, interleukin 6; IL-8, interleukin-8; IL-10, interleukin 10; IL12, interleukin 12; IP-10, Interferon gamma-induced protein 10; JNK, c-Jun N-terminal kinase; LOX-1, oxidized low-density lipoprotein receptor 1; MCP-1, monocyte chemotactic protein 1; M-CSF, macrophage colony-stimulating factor; MIP-1α, macrophage inflammatory protein 1 alpha; NFκB, nuclear factor kappa-light-chain-enhancer of activated B cells; NO, nitric oxide; PKR, protein kinase R; RAGE, receptor for advanced glycation end-products; RANTES, Regulated upon Activation, Normal T Cell Expressed and Presumably Secreted; rhSAA, recombinant human serum amyloid A; SAA1, serum amyloid A1; SAA2, serum amyloid A2; SAA3, serum amyloid A3; SAF-1, Serum amyloid A-activating factor-1; SELS, selenoprotein S; sRAGE, Soluble for advanced glycation end-products; SR-B1, scavenger receptor B1; TLR2, toll-like receptor 2; TLR4, toll-like receptor 4; TNFα, tumor necrosis factor-alpha.
↑, increased; ↓, decreased; ↔, non-affected.

1.2. SAA regulation in the acute phase response

Considerable research has been focused on the kinetics of hepatic SAA expression and secretion during an acute inflammatory response [reviewed in (20, 74)]. The mechanics of SAA expression and secretion vary with the stimulus type. Systemic levels of SAA can be 1,000-fold higher than baseline during an acute inflammatory response to sepsis (75, 76), viral infections including COVID-19 (1, 77, 78), vaccinations (79), or

tissue trauma (80). The immediate systemic levels of SAA are primarily hepatic in origin during infection (44), with contributions from extra-hepatic sources following tissue trauma (81). Hepatic SAA production is triggered by bacterial products such as endotoxin or inflammatory cytokines interleukin-1 beta (IL-1β), interleukin-6 (IL-6), and TNFα that reach the liver (74). While much prior work has focused on the hepatic acute-phase SAA1 and SAA2 subtypes, important roles for extra-hepatic SAA in the chronic inflammatory processes associated with metabolic diseases are now emerging (82, 83).

1.3. SAA vs. CRP

Since its discovery nearly 100 years ago, C-reactive protein (CRP) has been used in clinical practice as a marker of acute inflammation (84). CRP is known to rapidly increase in response to infection or trauma, and has a short half-life that enables a rapid decrease when the stimulus ceases (85). However, SAA rises in parallel with CRP in the same acute inflammatory conditions, and may be a more sensitive marker for acute events (19, 86–88). Similar to CRP, hepatic SAA is regulated by the above inflammatory cytokines (IL-1β, IL-6, and TNFα 89, 90), although CRP can be induced by pathways related to interleukin-17 (IL-17) and hepatocyte nuclear factor (HNF), in contrast to SAA (91). In addition to inflammatory cytokines, hormones including glucocorticoids, leptin, and thyroid hormone also regulate SAA expression (92, 93). Indeed, SAA levels may be better predictors of coronary artery disease (CAD), cancer, and of related poor outcomes than CRP (19, 94). However, CRP levels more accurately predict poor outcome in elderly populations (95). SAA as a biomarker of acute infection or traumatic injury remains less widely used clinically due to a lack of robust calibration reagents and routine assays. There would be great value to developing reliable, robust, and cost-effective SAA clinical assays.

2. SAA in chronic metabolic diseases

Chronic inflammatory conditions tend to promote much lower elevations in systemic SAA (~3 to 10-fold) than acute inflammatory conditions and may be sustained, deriving from diverse tissues such as the liver, adipose tissue, lung, small and large intestines, and hematopoietic cells such as macrophages (9, 11, 18, 96–100). The markedly different systemic SAA levels observed in acute vs. chronic inflammatory conditions suggests the potential for different mechanisms (91), prompting speculation that SAA is an important concentration-dependent effector of innate and adaptive immune responses (44). Aging has been associated with increased SAA levels (83, 101, 102), as have aging-related metabolic conditions. Evidence for potential roles of SAA in several metabolic diseases are discussed in the sections that follow, with an emphasis on obesity, diabetes, non-alcoholic fatty liver disease (NAFLD), CVD, autoimmune conditions such as systemic lupus erythematosus (SLE) and rheumatoid arthritis (RA), and inflammatory bowel diseases (IBD) ulcerative colitis (UC) and Crohn's disease (CD) (**Figure 1**).

2.1. Obesity and metabolic syndrome

The increased circulating SAA levels observed in individuals with obesity are highly correlated with body mass index (BMI), body weight, adiposity, and SAA1 and SAA2 mRNA expression in white adipose tissue (WAT) (11, 96), and are not related to hepatic SAA1 or SAA2 expression (9, 97, 98, 103). Circulating SAA levels have been positively associated with visceral adiposity (104), suggesting visceral fat as a potential source. However, the relative contributions of subcutaneous and visceral WAT to SAA production are not known, nor has it been determined that WAT-derived SAA contributes to the circulating SAA pool in obesity (105), or whether WAT-derived SAA induces local cytokine production that stimulates hepatic SAA expression. SELS, a major SAA receptor, is expressed in adipose tissue and directly associates with adiposity and BMI (65), suggesting a potential feed-forward mechanism that contributes to the sustained adipose tissue inflammatory state in obesity (71). Whether increased SAA expression in WAT plays a local or systemic role in obesity pathogenesis, or whether it is merely a biomarker of disease severity, is unknown. The extent to which WAT, liver, or both contribute to systemic SAA levels has not been resolved.

An initial study of 34 subjects with obesity showed a 6-fold increase in SAA expression in subcutaneous WAT compared with 27 lean controls; this was associated with 20-fold higher expression from adipocytes than the WAT stromal vascular fraction (96), which contains pre-adipocytes, immune cells, and vasculature. A meta-analysis confirmed a strong positive association between BMI and circulating SAA levels (13), and showed that SAA1 and SAA2 expression was higher in subcutaneous WAT in people with overweight and/or obesity (97, 106). In addition, serum SAA levels are positively associated with adipocyte diameter (106, 107). Distinctions between SAA1 and SAA2 were generally not made in these early studies due to the lack of distinguishing primers and subtype-specific antibodies that persists.

Conversely, weight loss can reduce circulating and adipose tissue-derived SAA levels in humans. A meta-analysis of 10 studies showed that weight loss significantly reduced circulating SAA levels (13). Weight loss following a low-fat (LFD) ($n = 19$) or very low carbohydrate diet (VLCD) ($n = 22$) led to reduced circulating SAA levels proportional to the amount of weight lost and also associated with insulin resistance (88). Several independent studies showed that weight loss due to a VLCD in women ($n = 33$–48) was strongly associated with reduced plasma SAA and adipocyte-derived SAA (9, 10, 96, 108), while insulin sensitivity was not consistently affected (9, 108). These divergent phenotypes could reflect different subject characteristics, with postmenopausal women showing a metabolic benefit from SAA reduction (9, 10) while premenopausal women did not (108). Another study in 439 women reported similar reductions in

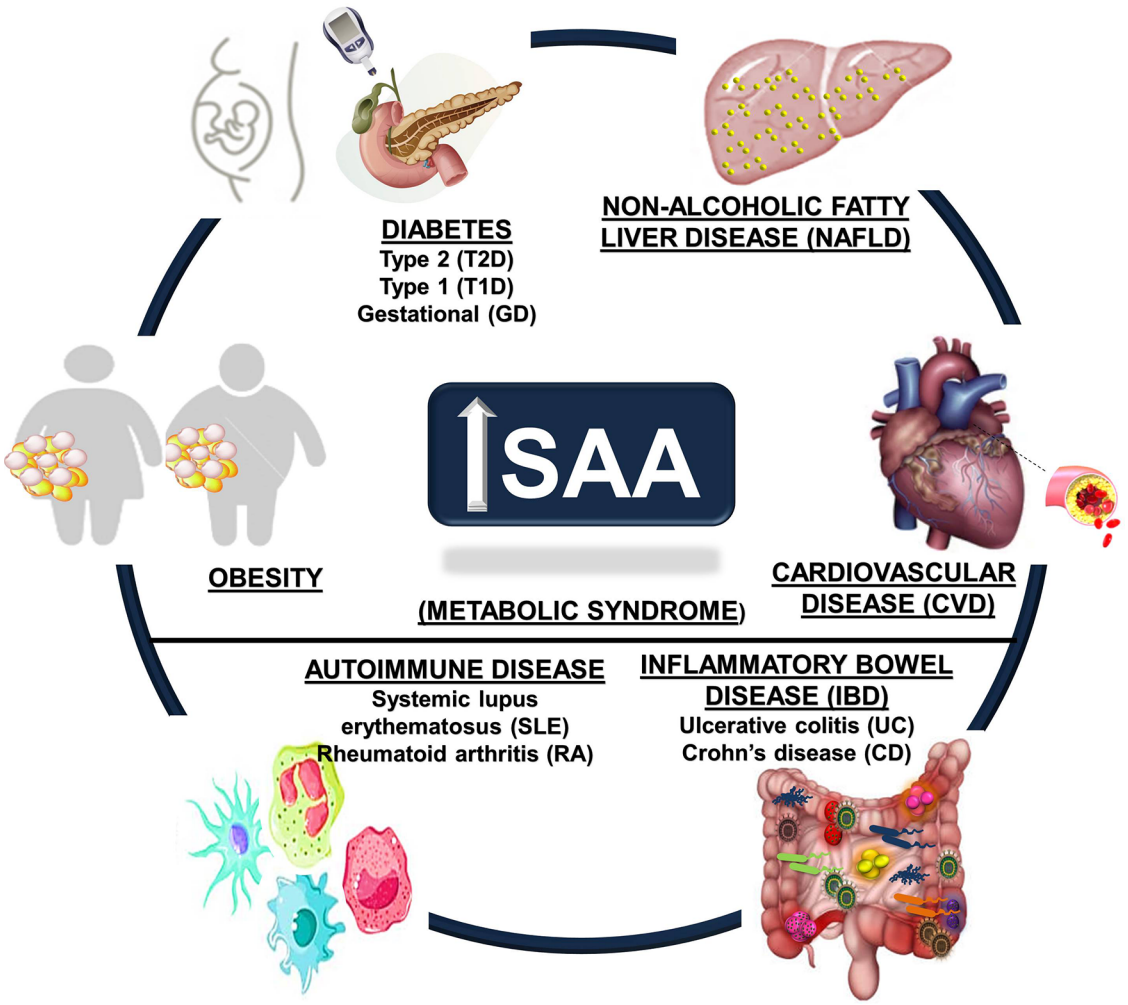

FIGURE 1
Metabolic disease states associated with increased circulating SAA. Obesity, cardiovascular disease (CVD), autoimmune diseases (including systemic lupus erythematosus (SLE) and rheumatoid arthritis (RA)), diabetes (Type 1, Type 2, and gestational), inflammatory bowel disease (IBD, including Crohn's disease (CD) and ulcerative colitis (UC)), and non-alcoholic fatty liver disease (NAFLD) are chronic metabolic conditions that are all associated with increased circulating SAA levels.

plasma SAA with weight loss due to dietary intervention, but not exercise (109). Importantly, other inflammatory markers including MCP1 and CRP also decreased during weight loss (109). Roux-en-Y gastric bypass significantly reduced circulating SAA levels in women with obesity ($n = 20$) (110). Additional studies are required to determine whether specifically reducing SAA in the context of weight loss is beneficial.

Mouse studies parallel the observation that SAA levels are increased in humans with obesity, and that adipose tissue mRNA expression of Saa is similarly increased in the obese state. Initial studies identified Saa3 as the specific subtype expressed in murine adipocytes (111) and macrophages (112, 113), both essential for development of obesity. Ob/ob mice, which spontaneously develop obesity due to increased food consumption subsequent to leptin deficiency, have elevated circulating and adipose tissue Saa levels (114, 115). Further, diet-induced obese mice consistently have elevated Saa3 mRNA levels in adipose tissue (82, 116–121). However, obesity-associated adipose-derived Saa3 does not contribute to circulating Saa levels in mice (105). Mice engineered to express luciferase via the Saa3 promotor only show luciferase activity in adipose tissue following long-term high fat diet (HFD)-fed conditions, with no detectable luciferase in any tissue examined after one week of HFD or after acute injection with LPS, providing temporal data about Saa3 expression kinetics (121). However, using more sensitive mass spectrometry, we have shown that a single high dose LPS injection is sufficient to induce Saa3 expression in adipose tissue, associated with increases circulating Saa (42), an effect supported by identifying Saa3 in LPS-stimulated plasma using isoelectric focusing gels and ELISA (122).

Sleep deprivation has been associated with sharp increases in SAA. Circulating SAA levels increased by more than 4-fold in mice experiencing paradoxical sleep deprivation for 72 h, an effect coincident with increased adipose tissue Saa3 mRNA expression, but not Saa1/2 (123). Circulating Saa and Saa3 mRNA returned to basal levels when sleep was restored.

Importantly, increased circulating SAA also has been observed in humans deprived of sleep for either 24 or 48 h (123). In another study, SAA levels were 2-fold elevated in 17 adults who regularly experienced obstructive sleep apnea, which disrupts sleep, compared to weight-matched controls (124). Obstructive sleep apnea is strongly associated with the metabolic syndrome (125), also associated with SAA levels, which may confound interpretation of these studies. Because sleep deprivation and disrupted sleep schedules increase risk for obesity and its complications, disrupted sleep-induced SAA could be considered a novel risk factor for metabolic disease.

Studies in which mouse Saa is perturbed genetically have yielded ambiguous results. Mice engineered to express human SAA1 from WAT had elevated circulating human SAA1 mirroring obesity levels even without an obesogenic stimulus (126), providing evidence that WAT-derived SAA circulates. However, overexpressing SAA1 from WAT had no observed effects on body weight, WAT inflammation, or glucose or insulin tolerance (127). Loss of extrahepatic Saa3 in obese mice led to improved local WAT inflammation and systemic lipoprotein profiles and to resistance to high fat diet (HFD)-induced obesity, particularly in female mice (82). By contrast, subsequent Saa3 knock out mice were more prone to HFD-induced obesity with increased adiposity (128). Further, triple knock-out mice (Saa1, Saa2, and Saa3-deficient) showed no effect of a HFD on body weight or adiposity, but had worsened glucose and insulin tolerance (129). These divergent results suggest that the distinct metabolic characteristics of the models used, such as the inclusion of dietary sucrose/cholesterol, which particular Saa subtypes are perturbed, or gut microbiota composition and function, could have major impacts on observed phenotypes related to Saa.

Despite such phenotypic differences in obesity when SAA subtypes were perturbed, several studies point towards SAA promoting adipose tissue expansion. Silencing Saa3 in cultured pre-adipocytes reduced their adipogenic potential, leading to smaller adipose tissue depots when injected into NUDE mice (130). Similarly, targeting Saa using anti-sense oligonucleotides reduced adipose tissue expansion and inflammation as well as circulating endotoxin levels in male Swiss Webster mice (131), suggesting that disrupting Saa signaling also improved intestinal barrier integrity. Increased Saa3 expression in visceral adipose tissue from obese mice is highly correlated with macrophage number and inflammatory expression profile (121), suggesting that interaction with macrophages may drive adipocyte Saa3 expression. Thus, the crosstalk between adipocytes and macrophages that promotes adipose tissue inflammation and subsequent insulin resistance in obesity may require SAA (121).

2.2. Type 2 diabetes and gestational diabetes

Excess visceral adiposity and increased systemic inflammation are associated with insulin resistance (132, 133), which is the reduced capacity for insulin-stimulated glucose uptake in metabolically active tissues such as adipose tissue and skeletal muscle. Pancreatic insulin secretion subsequently increases to compensate for reduced insulin sensitivity to maintain euglycemia. If the pancreatic beta cells are unable to secrete sufficient insulin to compensate for the reduced insulin sensitivity (termed beta cell dysfunction), hyperglycemia ensues, leading to glucose intolerance and eventually T2D (134). Cross-sectional studies in men of European, Asian Indian, and American descent have shown that total, visceral, and subcutaneous adiposity, BMI, and waist circumference are all negatively associated with insulin sensitivity (135, 136). In addition to its association with obesity, with a key contribution from adipose tissue, SAA is similarly associated with T2D in humans and in animal models. In 134 patients with T2D, circulating SAA levels strongly correlated with hemoglobin A1c (HbA1c) and homeostatic model assessment for insulin resistance (HOMA-IR) after controlling for age, sex, and BMI status (14), suggesting a relationship between SAA and insulin resistance.

In humans, diabetes and circulating SAA levels are strongly related (11, 107, 137–140), and a prospective association between SAA and incident T2D has been reported (15). In a study of 765 older men (mean age 77), 112 with T2D, serum SAA strongly correlated with diabetes status, an association lost when adjusted for BMI, waist circumference, or fasting insulin levels (141). In a small study, omental adipose tissue from subjects with diabetes ($n = 6$) had a 3-fold increase in SAA mRNA expression compared with non-diabetic controls ($n = 10$), and omental SAA expression strongly correlated with fasting glucose levels and total body fat mass (142). In 134 subjects with T2D, HbA1c and HOMA-IR strongly correlated with circulating SAA levels after controlling for age, sex, and BMI (14); the effect was reduced with adjustment for parameters related to glucose metabolism (15), suggesting linkage between SAA and insulin resistance. In subjects with both obesity and T2D, SAA is bound to apoB-containing lipoproteins including very low-density lipoproteins (VLDL) and low-density lipoproteins (LDL), in addition to HDL [its usual transport partner in plasma (37)], similar to observations in mice (143). The mechanism for SAA binding to these lipoproteins in people with diabetes is unknown. Evidence exists that a truncated form of SAA1, which is missing an N-terminal arginine, is reduced in subjects with T2D and is negatively associated with glycemic control (144). Adipose tissue SELS was positively associated with measures of glycemic control in both lean and obese subjects (65, 73), as well as in age- and weight-matched subjects with diabetes (145). Moreover, insulin increases SELS expression in cultured adipocytes (65), suggesting a potential feed-forward mechanism for increased SAA expression in insulin resistance. SAA disrupts insulin signaling in cultured adipocytes (120, 146), suggesting a potential mechanism for its association with T2D. Most T2D subjects also have abdominal obesity, making it difficult to tease apart obesity-specific and T2D-specific contributions of SAA.

However, a strong association exists between diabetes and SAA that is independent of obesity. One study of 182 T2D subjects showed elevated serum SAA levels compared to healthy

weight-matched controls ($n = 180$), with mean BMI of 24 in both groups (147). A small study similarly showed that SAA levels were elevated in age- and weight-matched subjects with T2D compared with normoglycemic controls (73). Controlling for age, sex, and BMI revealed a sustained correlation between indices of glucose dysregulation (i.e., HbA1c, HOMA-IR) and SAA, suggesting an effect specific to the diabetic state (14). However, another study found no differences in SAA levels between weight-matched subjects with obesity or T2D (110). To our knowledge, only a single study has reported no differences in SAA between healthy insulin-sensitive subjects and those with T2D (148). Emerging evidence suggests that improving insulin sensitivity drives the reduction in SAA levels following weight loss. In a small study in which subjects with overweight or obesity were given rosiglitazone for 12 weeks, circulating SAA levels were reduced by 37% despite the absence of weight loss, and WAT explants from these subjects showed lower SAA secretion post-treatment (9). Pharmacotherapy for T2D (i.e., metformin, glipizide, rosiglitazone, insulin, or acarbose) reduces serum SAA levels in T2D subjects (9, 139, 149). Thus, while the diabetic state and SAA levels are directly associated, whether SAA plays a distinct role in T2D pathology independent of a role in obesity remains to be determined.

SAA levels are further elevated in subjects with T2D and nephropathy (147, 150) and retinopathy (151). SAA may be an important predictor for end-stage renal disease and death in patients with diabetic kidney disease, with elevated intra-renal SAA expression (152). SAA is elevated in T2D patients with proteinuria, with serum SAA levels positively associated with albumin excretion rate and glomerular membrane thickening (140, 153), consistent with a potential causal role.

Similar links between Saa and T2D have been observed in animal models. In mice, a HFD promotes early increases in Saa3 expression in white adipose tissue, with subsequently elevated hepatic levels of Saa1 and Saa2 (120). In these models, insulin resistance is highly correlated with circulating Saa levels (120). In hepatocytes, overexpression of the Saa receptor, Tanis, led to decreased insulin-stimulated glucose uptake and glycogen synthesis, indicating increased insulin resistance (73). Db/db mice, which lack the leptin receptor and spontaneously develop features resembling obesity and T2D, express high levels of Saa3 from adipocytes, but not the liver (114). In a common rodent model of T2D in which obesity is initiated by consumption of a HFD and hyperglycemia is triggered by the administration of low-dose streptozotocin (STZ), a beta cell toxin that promotes hyperglycemia, renal Saa3 is increased (154).

Systemic SAA levels are elevated in pregnancy, especially in women with gestational diabetes (GD) (101). Serum SAA levels were 14% higher in 39 pregnant women with GD than in 25 healthy controls, and SAA was positively associated with BMI, age, oral glucose tolerance test, and HbA1c levels (155). It is unknown whether GD itself increases systemic SAA levels, or whether increased SAA simply reflects gestational weight gain (156). While one study did not observe increased SAA levels in GD patients, decreased variability in SAA levels was observed (157). Further studies are required to conclusively determine if SAA plays a detrimental role in GD. Indeed, a prospective clinical trial (NCT04238936) aims to compare SAA levels between women diagnosed with GD and healthy controls.

2.3. Polycystic ovary syndrome (PCOS)

PCOS is a chronic inflammatory condition that impacts ~5%–10% of women of reproductive age in industrialized countries and is associated with an increased incidence of obesity, diabetes, and atherosclerosis (158, 159). In a study of 83 subjects with PCOS, serum SAA levels were double those of 39 age-matched controls (160). Omental and subcutaneous WAT biopsies showed increased SAA mRNA and protein expression, suggesting that the circulating SAA derived at least in part from adipose tissue. Incubation of adipose tissue explants with glucose increased SAA production, providing evidence that SAA secretion may be regulated by hyperglycemia. PCOS subjects were insulin-resistant, and a 6-month treatment regimen with metformin reduced circulating SAA levels, suggesting a possible link between SAA and adipose tissue insulin sensitivity (160). Because PCOS is associated with enhanced WAT lipolysis (161), and WAT-derived SAA also augments lipolysis (9), we speculate that WAT-derived SAA may play a causal role in PCOS-mediated metabolic dysfunction.

2.4. Non-alcoholic fatty liver disease (NAFLD)

NAFLD is commonly present as part of the metabolic syndrome (162), a constellation of disorders that increase the risk for CVD and diabetes, including abdominal obesity, hyperglycemia/insulin resistance, hypertension, and dyslipidemia (163). NAFLD is characterized by triglyceride accumulation in hepatocytes (steatosis), which can progress to steatohepatitis, characterized by the accumulation of inflammatory cells. SAA levels often are elevated in patients with the metabolic syndrome (164, 165). SAA was found to be 2–3-fold higher in patients with non-alcoholic steatohepatitis relative to age-matched healthy controls (166). Because liver biopsy, the gold standard diagnostic test for the presence of NAFLD, is an invasive procedure, non-invasive biomarkers for this condition would be highly desirable. However, although SAA could potentially be a useful biomarker for NAFLD, it is too non-specific to justify its use for this purpose.

Mechanisms linking SAA and NAFLD remain speculative. In the Cohort on Diabetes and Atherosclerosis Maastricht (CODAM) study, in which alanine amino transferase (ALT) was used as a surrogate measure of NAFLD, multiple linear regression analysis was used to investigate the association between ALT and several metabolic syndrome components as potential mediators of the liver disease. Their findings suggest that insulin resistance is the key pathophysiological mechanism to explain the association between the metabolic syndrome and NAFLD, with adipose tissue inflammation, endothelial dysfunction and free fatty acid levels likely playing lesser roles (167). However, ALT is an

imperfect biomarker for NAFLD. Cytokines produced by liver-resident and infiltrating inflammatory cells may play important roles in liver inflammation and NAFLD. SAA may exacerbate hepatic steatosis via the TLR4-mediated NFκB signaling pathway (168). Hepatocyte-derived SAA1 promotes intrahepatic platelet aggregation and aggravates liver inflammation in NAFLD (169). Studies using hypercholesterolemic mice deficient in IL-1α or IL-1β showed the importance of these two cytokines in transforming steatosis to steatohepatitis and liver fibrosis (170). Given the well-documented link between SAA and IL-1β, SAA may also be important for liver disease progression. However, this requires additional study.

2.5. Cardiovascular disease (CVD)

Inflammation is a hallmark of atherosclerosis (171), and a recent clinical trial, The Canakinumab Anti-Inflammatory Thrombosis Outcomes Study (CANTOS), for the first time showed in a proof-of-concept trial that inhibiting inflammation using an antibody against Il-1β decreased cardiovascular events (172). The relationship between inflammation and CVD has been extensively studied by measurement of the inflammatory marker, CRP, which consistently has been shown to be modestly and chronically elevated in CVD patients and to predict the risk of cardiovascular events in a similar manner to SAA (19, 173, 174), although SAA has not been studied as extensively as CRP. As noted earlier, acute phase SAA is a good predictor of coronary artery disease outcomes (19, 94).

SAA could simply be a biomarker of the chronic inflammatory state that is present in CVD, similar to CRP; alternatively, it may play pathogenic roles. As described below, considerable evidence points to its role as a mediator rather than simply being a marker of atherosclerotic CVD. In considering its possible mediating role, potential differences between effects of lipoprotein-bound SAA and free SAA derived from extrahepatic cells in the artery wall must be distinguished.

SAA mRNA is present in macrophages, smooth muscle cells and endothelial cells in human atherosclerotic lesions (18), findings that suggest an immune response within the atherosclerotic artery wall, in which locally generated SAA is unlikely to be associated with lipoproteins. However, other studies showed immunohistochemical colocalization of Saa with apolipoproteins, including apoA1, the major apolipoprotein of HDL, in murine atherosclerotic lesions (175), consistent with SAA being transported to the artery wall by plasma lipoproteins.

Several studies in mice provide evidence for Saa being an atherosclerosis mediator. LDL receptor (Ldlr)-deficient mice fed a pro-inflammatory diet with or without added cholesterol showed marked increases in plasma Saa levels, which correlated with atherosclerosis extent (116). Mice in which Saa was either overexpressed or silenced suggest Saa roles in atherosclerosis pathogenesis, although the data are not uniform. Chow-fed Apoe-deficient mice in whom Saa was overexpressed using a lentiviral vector had increased *en face* and aortic root lesions compared to control-fed mice, although differences were not observed with an atherogenic diet (176). Plasma levels of IL-6 and TNFα and expression of vascular cell adhesion molecule 1 (VCAM-1) and monocyte chemotactic protein-1 (MCP-1), and lesion macrophage content all increased with Saa overexpression (176). In another experimental approach, a single injection of a human Saa-containing adenovirus in Apoe-deficient mice increased plasma Saa levels for ∼10 days, leading to increased atherosclerosis (177). When repeated injections of the human SAA-containing adenovirus were administered to immune-deficient mice to prevent an antibody response to the human protein, brachiocephalic lesions and aortic lesion area were markedly increased (177). The authors postulated that the increase in atherosclerosis was due to SAA-mediated induction of transforming growth factor-β (TGFβ), which increased vascular biglycan expression and led to increased LDL retention (see later). Deficiency of Saa in Ldlr-deficient mice led to reduced atherosclerosis in the ascending aortic arch but not in the aortic root or innominate artery at 6 weeks, although this difference was lost by 12 weeks (178). Parallel findings were observed in male Ldlr-deficient mice also deficient in FPLR2, one of the major Saa receptors, although the effect was more prolonged than in the Saa/Ldlr double knockout mice (179). In both studies, transplantation of Saa-deficient bone marrow-derived cells replicated the findings, suggesting that the reduced atherosclerosis may have resulted from the absence of free Saa in lesions rather than in the circulation. However, in Apoe/Saa double knockout mice, no difference in lesion area was observed at ∼50 weeks (180), although no early time points were examined. A subsequent study in Apoe-deficient male mice also lacking Saa1 and Saa2 using Saa3 suppression with an anti-sense oligonucleotide showed significantly reduced atherosclerosis (181). These results imply that all acute phase Saa isoforms have pro-atherogenic properties, and that deficiency/suppression of all 3 acute phase isoforms is required for atheroprotection in mice. Saa3 effects on atherosclerosis were not reported in female mice, despite sexually dimorphic Saa3 expression (182) (see below). Saa transgenic rabbits failed to show an increase in atherosclerotic lesions (183). Therefore, in summary, while most mouse studies suggest that Saa contributes to the development of early atherosclerotic lesions, results in Saa-deficient models are not consistent, possibly related to the nature of the model and the timing of observations. Nevertheless, such studies raise the question of how Saa might affect the atherogenic process. Several potential mechanisms are plausible.

Since SAA can be expressed by several cells of the artery wall (18), including perivascular adipocytes (184) and macrophages (18, 112, 113, 182–187), the locally produced SAA in lesions unattached to lipoproteins could have signaling functions that might be atherogenic. These include activation of the NFkB and MAPK signaling pathways via interaction with receptors such as class B scavenger receptor CD36, TLR4, TLR2, FPLR2 and RAGE (176, 188, 189). Activation of monocytes/macrophages and perivascular adipocytes can generate chemoattractant molecules such as MCP-1, which could lead to the recruitment of additional inflammatory cells and vascular smooth muscle

cells. SAA also can be a direct chemoattractant (190). Moreover, direct activation of the chemoattractant receptor, FPLR2, by free SAA could further attract inflammatory cells into developing vascular lesions. Free SAA also has been shown to induce a phenotypic switch in vascular smooth muscle cells towards a more proliferative type of cell that synthesizes more matrix molecules (188). However, *in vitro* studies using free SAA should be interpreted cautiously, since minor contamination with endotoxin could lead to similar effects.

HDL-bound SAA also may play a role in atherogenesis. When SAA is secreted by the liver as part of the acute or chronic inflammatory response, it circulates in plasma bound to HDL, although it can associate with less dense lipoproteins under certain circumstances (24, 25, 37, 143). HDL particles that carry SAA, so-called "inflammatory HDL", is less atheroprotective than normal HDL, with reduced inhibition of inflammation in cells due to its being trapped by cell surface proteoglycans (191), versican in the case of adipocytes and biglycan produced by macrophages (118). Trapping of SAA-containing HDL at the cell surface prevents it from adequately promoting reverse cholesterol transport (192). HDL derived from inflamed mice devoid of Saa1 and Saa2 functioned normally, as it did when the proteoglycans were removed from the cell surface either chemically or by genetic manipulation (118). Humans treated with low levels of endotoxin also had impaired cholesterol efflux capacity from macrophages, despite no change in circulating HDL-cholesterol levels. Proteomic analyses showed that the cholesterol efflux capacity of HDL correlated inversely with Saa1 and Saa2 content (193). Binding of SAA-containing HDL by extracellular proteoglycans such as biglycan in humans (194) and perlecan in mice (174) may lead to HDL retention in the vascular intima, increasing susceptibility to oxidative and enzymatic damage similarly to trapped LDL (195). Retained HDL could thus be pro-atherogenic, compared to its more widely accepted anti-atherogenic properties. The products of oxidative and enzymatic damage to retained lipoproteins may play important roles in atherogenesis (196).

Finally, SAA might stimulate thrombosis, which often precipitates clinical events. SAA can induce tissue factor production by monocyte/macrophages (197) and platelet activation (198). Thus, SAA could play multiple roles in the atherosclerotic process from monocyte adhesion, inflammatory and smooth muscle cell chemotaxis, cellular inflammation, HDL function, retention of atherogenic lipoproteins in the artery wall, and thrombogenesis. The net effect is that SAA is likely to play a causative role in atherogenesis, although the extensive data are not fully consistent.

2.6. Type 1 diabetes

In contrast to T2D, type 1 diabetes (T1D) develops as a result of autoimmune destruction of pancreatic beta cells, reducing insulin production capacity; subjects with T1D thus require exogenous insulin to maintain euglycemia. Little is known regarding SAA and T1D. One study has shown that SAA levels were elevated in 1,139 subjects with T1D compared with 848 healthy controls (199); however, these plasma donors were not age-matched, and the T1D subjects tended to be older. However, SAA increased specifically in HDL in subjects with T1D compared to age-, sex-, and BMI-matched controls, an effect much stronger when subjects were stratified by HbA1c and was not observed for CRP (200). A common T1D model can be generated in mice by injecting them with the pancreatic beta cell toxin STZ, leading to beta cell apoptosis (201, 202). In such STZ-treated mice, circulating SAA levels increased (203), with increased Saa3 expression specifically from adipocytes (114). Whether hyperglycemia or STZ itself stimulated adipose Saa3 was not determined. However, treating cultured 3T3-L1 adipocytes with 12–25 mM glucose induces Saa3 mRNA expression (114, 190, 204), an effect replicated by hyperglycemic clamps in mice (114), suggesting that hyperglycemia is the critical factor. Whether glucose-stimulated SAA expression changes systemic SAA levels or performs local functions is not known. As with studies related to T2M, mechanistic studies are needed in mice to determine whether SAA is sufficient or required for the pathology of T1D.

2.7. Autoimmune diseases: systemic lupus erythematosus (SLE) and rheumatoid arthritis (RA)

SLE and RA are chronic diseases in which a person's immune system attacks its own tissues, resulting in inflammation and tissue damage in affected organs. While RA can be physically debilitating but typically is not life-threatening, SLE can lead to severe complications such as kidney failure, seizures, and increased risk of thrombosis. SAA may be a biomarker for both conditions (3, 6, 205–207). SAA promotes T-helper 17 (Th17) differentiation (208, 209), which plays important immunologic roles. However, excessive Th17 responses also can promote autoimmune conditions including SLE and RA (210). In patients with RA, their joints contain elevated SAA (6, 205), with levels correlating with plasma SAA levels and disease progression (211, 212). Rather than simply diffusing into joints from the bloodstream, SAA itself may be expressed in synoviocytes, macrophages, and endothelial cells within synovial tissues in RA patients (6, 213). Computational modeling identified Saa3 as the gene most strongly correlated with the severity of collagen-induced arthritis (214). Moreover, synovial fibroblasts isolated and cultured from patients with RA produced 2–4 times more SAA than those from healthy subjects (213). Whether SAA directly contributes to these autoimmune diseases remains to be elucidated. A potential mechanism is that in RA patients, SAA and associated cytokines potently induce matrix degrading enzymes in synovial fibroblasts (213, 215, 216), which if left unchecked could contribute to disease pathogenesis and joint destruction. Treatment with the TNF antagonist etanercept reduces RA disease severity while simultaneously reducing circulating SAA levels (217), providing one linkage between SAA and RA, but the causal direction is unknown.

2.8. Inflammatory bowel disease (IBD)

The two major types of IBD include ulcerative colitis (UC) and Crohn's disease (CD). Both are complex conditions that result from chronic dysregulated immune function in the gastrointestinal tract (218). UC is limited to the colon; however, CD can involve any part of the gastrointestinal tract, but usually affects the distal small intestine and/or the colon (219). Previous work suggests that SAA may be a more sensitive biomarker for IBD than CRP (8, 220, 221), as SAA levels remain elevated while CRP disappears in patients who are in clinical remission (222).

Patients presenting with either UC or CD consistently show elevated serum SAA levels (220, 223). In humans, intestinal biopsies from CD patients showed significantly increased colonic SAA1/2 expression levels (224). From an extensive panel of inflammatory markers, including CRP, IL-22, and IL-6, SAA had among the highest positive associations with a Simplified Endoscopy Score for CD (SES-CD, $r = 0.4$), fecal calprotectin ($r = 0.39$), Crohn's Disease Activity Index (CDAI, $r = 0.14$), and stool frequency ($r = 0.18$) (223). Such studies link intestinal SAA to potential roles in disease development or protection. Subjects with CD without mucosal healing had higher SAA levels than subjects in clinical remission (225), suggesting SAA as a marker for CD severity. In patients with UC who were in remission, consumption of a low-fat, high-fiber diet improved quality of life, in conjunction with reduced circulating SAA levels (226). In one clinical trial, SAA was a highly significant predictor of CD severity, and treatment with filgotinib, a selective JAK1/STAT inhibitor, improved CD symptoms while simultaneously reducing circulating SAA levels (223).

Mouse models of IBD similarly display elevated circulating SAA levels. Systemic SAA as well as local Saa3 expression levels become elevated within days of administration of dextran sodium sulfate (DSS) in drinking water in a mouse model of colitis (227–229), an effect that may function to protect colonic epithelium from acute injury by recruiting IL-22-producing neutrophils (228). This does not appear to be specific to that model, as mice given trinitrobenzone sulfonic acid (TNBS) via colonic catheter, in another well-studied colitis model, also responded with increased systemic SAA (230, 231). Pharmacological treatments including 6-thioguanine and cyclosporine A, utilized to improve colitis outcomes in mice, effectively reduced circulating SAA levels (229), as did administration of *Bacillus subtilis* spores as a probiotic (230). To date, only a few studies have indirectly examined IBD phenotypes with concurrent SAA genetic perturbation. One study showed that mice concurrently deficient in Saa1, Saa2, and Saa3 had attenuated colitis as assessed by histology (209). However, in the proximal colon of the mouse, Saa1 and Saa2 expression is confined to the epithelium, while Saa3 expression is found in immune cells including monocytes, macrophages, and dendritic cells (209). These data suggest that Saa1/2 exert system-wide functions of mucosal sensing and defense, while Saa3 drives local function, due in part to the differential potentiation of Th17 responses by these subtypes (209). Similarly, mice that were deficient in Saa1 and Saa2 that had colitis-associated colon cancer showed attenuated weight loss, gut histological damage, and gut inflammation (232), findings that suggest that Saa1/2 may augment colitis severity. Saa1/2 deficiency resulted in reduced Saa3 colonic expression (232). Conversely, specific deletion of only Saa3 rendered mice more susceptible to dextran sulfate sodium (DSS)-induced colitis (228), implying that Saa3 may be protective against IBD. Collectively, the precise roles for different SAA subtypes in IBD remain unknown, but emerging evidence suggests that Saa1/2 and Saa3 have different triggers and functions.

3. Tissue- and stimulus-specific SAA effects

Expression kinetics for each SAA subtype varies greatly by tissue source and stimulus type. While SAA1 and SAA2 are primary players in the acute phase response, in mice Saa3 may play a more prominent role in local inflammation. Mice express Saa3 in many extra-hepatic tissues including adipose tissue, lung, macrophages, and small/large intestine, with the liver predominantly producing Saa1 and Saa2 (40). This distinct division in murine subtype expression patterns enables the study of extra-hepatic Saa in metabolic disease. Extra-hepatic Saa expression appears predominant in chronic inflammatory conditions, while Saa derives largely from the liver in more acute inflammation (9, 18, 20, 91, 96, 98, 100). In humans, it is much more difficult to separate the contribution of extra-hepatic SAA to metabolic disease phenotypes in humans, because SAA1 and SAA2 are expressed both from liver and extra-hepatic tissues. Thus, much of our knowledge of extra-hepatic SAA originates from mouse models. In this section, the various SAA subtypes and their expression patterns in response to particular stimuli from various tissue and cell types will be discussed (**Table 2**).

3.1. Liver

The liver is perhaps the most frequently studied SAA-expressing tissue, wherein hepatic resident macrophages (i.e., Kupffer cells) produce Saa3 (in mice) and hepatocytes make SAA1/2 (233, 239). As such, an influx of immune cells could specifically increase Saa3 expression in the liver in mice. In cultured hepatocytes, particular combinations of cytokines predictably increase SAA1 and SAA2 gene and protein expression (234). Hepatocytes secrete high levels of SAA during an acute inflammatory insult in mice and humans (22). HepG2 cells, a human hepatocyte cell line, can express SAA1 and SAA2 in response to IL-1β and IL-6 in a dose-dependent manner, an effect augmented by pre-treatment with dexamethasone or TNFα (89, 248, 250). Primary human Kupffer cells co-cultured with hepatocytes secrete high levels of SAA2 following treatment with IL-1β and IL-6 (237), suggesting a potential paracrine signaling mechanism.

TABLE 2 Tissue- and stimulus-specific SAA effects in humans and rodents.

Tissue/cell type	Model	Stimulus	SAA subtypes[a]
Liver			
Human	HepG2 cells (234)	IL-1β, IL-6	↑↑ SAA1, SAA2 (15–25-fold)
		TNFα (10 ng/ml)	↔ SAA1, SAA2
	HepG2 cells (89, 248)	IL-6	↑↑ SAA1, SAA2 (5-fold)
		TNFα, DEX	↔ SAA1, SAA2
	HepG2 cells (252)	IL-1 β	↑ SAA1
	Primary hepatocytes (251)	LPS (20–500 ng/ml)	↑↑ SAA1, SAA2
	Liver tissue (98)	Obesity	↔ SAA1
Rodent	BALB/c mice (40, 238)	LPS (50 μg)	↑↑ Saa1, Saa2, Saa3 (100-fold)
		Casein (0.5 ml 10%)	↔ Saa1, Saa2
	Swiss mice (236)	LPS (100 μg)	↑↑ Saa1
	C57Bl6/J mice (122, 233)	LPS (100 μg)	↑↑ Saa1, Saa2, Saa3 (2,000–5,000-fold)
	Primary hepatocytes (122)	LPS (25 μg)	↑↑ Saa1, Saa2, Saa3
	Mouse fibrosis model (239)	Ccl4 (0.5 μl/g)	↑ Saa1, Saa3 (10–40-fold)
	Mouse HSCs (239)	Ccl4 (0.5 μl/g)	↔ Saa1, ↑ Saa3 (40-fold)
	C57Bl6/J mice (42)	LPS (25 μg)	↑↑ Saa1–4 (200, 2,000, 1,000-fold)
		$AgNO_3$ (0.5 ml 1%)	↑↑ Saa1, Saa2 (400, 10,000-fold)
		Casein (0.5 ml 5%)	↔ Saa4, ↑ Saa1–3 (60, 1,000, 8-fold)
	Ldlr-/-.Leiden mice (244)	DIO (50 weeks HFD)	↔ Saa1
	FVB mice (114)	STZ- hyperglycemia	↔ Saa3
	db/db mice (114)	Genetic T2D	↔ Saa3
	C57Bl6/J (121)	DIO (16 weeks)	↔ Saa3
	Mouse liver (113)	Amyloidosis	↓ Saa1, Saa2
	Mink liver (269)	LPS (3 mg/kg)	↑ Saa1
	C57Bl6/J (209)	MOG- autoimmune encephalomyelitis	↑↑ Saa1–2, ↔ Saa3 (10, 20-fold)
Adipocytes/WAT			
Human	Omental and SQ adipose tissue (9)	Obesity	↑↑ SAA1
		DEX, insulin	↑ SAA1 (6-fold secretion)
		Rosiglitazone	↓ SAA1 (70% reduction in secretion)
	SQ adipose tissue (96, 98)	Obesity	↑ SAA1–2, SAA4 (6-fold)
		Obesity → weight loss	↓ SAA1, SAA2 (1.6–2.2-fold)
	MADS (253)	rSAA (1–30 μg/ml)	↑ SAA1 (7-fold)
	Primary breast adipocytes (254)	DHA (50–100 μM)	↑ SAA1
Rodent	C57Bl6/J mice (42)	LPS (25 μg/mouse)	↑↑ Saa1, Saa2, Saa3 (60, 30, 750-fold)
		$AgNO_3$ (0.5 ml 1%)	↔ Saa1–3
		Casein (0.5 ml 5%)	↔ Saa1–3
	C57Bl6/J mice (122)	LPS (100 μg)	↑ Saa1 (100-fold), ↑↑ Saa3 (400-fold)
	Ldlr-/-.Leiden mice (44)	DIO (50 weeks HFD)	↓ Saa1
	3T3-L1 adipocytes (114)	TNFα, LPS	↑↑ Saa3
		Insulin, Rosi, IL-6	↔ Saa3
		Hyperglycemia (25 mM)	↑ Saa3
	FVB mice (114)	LPS (100 ng/g)	↑↑ Saa3 (200-fold)
		STZ- hyperglycemia	↑ Saa3
	ob/ob mice (114, 121)	Obesity	↑↑ Saa3
	db/db mice (114, 121)	Genetic T2D	↑ Saa3 (8-fold)
	3T3-L1 adipocytes (190)	SFA (12:0, 14:0, 16:0)	↑ Saa3 (2-fold)
		Hyperglycemia (25 mM)	↑ Saa3 (5-fold)
		PUFA (20:4, 20:5, 22:6)	↓ Saa3
	3T3-L1 adipocytes (245)	IL-1β	↑ Saa3 (10,000-fold)
	C57Bl6/J (121)	DIO (16 weeks)	↑ Saa3 (11-fold)
	3T3-L1 adipocytes (246)	LPS	↑ Saa1 (2-fold)
		LPS + RAW264.7 cells	↑ Saa1 (2-fold)
	3T3-L1 adipocytes (242)	rSAA (5 μg/ml)	↑ Saa3 (3-fold)
	Swiss Webster mice (271)	Presense of microbes	↑ Saa3 (10-fold), ↔ Saa1, Saa2
Monocytes			
Human	PBMC (250)	IL-1β, IL-6, TNFα	↑ SAA2 (7-fold)
	THP-1 cells (187)	LPS + DEX, or DEX	↑ SAA1
	U-937 cells (187)	LPS, DEX, IL-1, IL-6	↔ SAA1
	HL-60 cells (187)	LPS, DEX, IL-1, IL-6	↔ SAA1
Macrophages			
Human	Coronary artery sections (18)	Atherosclerosis	↑ SAA1
	THP-1 macrophages (187)	LPS	↔ SAA1
		DEX	↑ SAA1
	U-937 macrophages (187)	DEX	↑ SAA1
	HL-60 macrophages (187)	LPS, DEX, IL-1, IL-6	↔ SAA1

(*continued*)

TABLE 2 Continued

Tissue/cell type	Model	Stimulus	SAA subtypes[a]
Rodent	BALB/c mice (40)	LPS (50 μg)	↑↑ Saa3 (100-fold)
	RAW264.7 cells (246)	LPS	↔ Saa1
	RAW264.7 cells (271)	LPS	↑ Saa3
	Kupffer cells (233)	LPS	↑ Saa1
	Peritoneal macrophages (233)	LPS	↑ Saa1
	Peritoneal macrophages (113)	Amyloidosis	↑↑ Saa3
	Microglia, MDM (209)	MOG- autoimmune encephalomyelitis	↑ Saa3
Intestine			
Rodent	BALB/c mice (40)	LPS (50 μg)	↑↑ Saa1 (1–4-fold), Saa3 (3–25-fold)
		Casein (0.5 ml 10%)	↔ Saa1, Saa3
	C57Bl6/J (121)	DIO (16 weeks)	↔ Saa3
	CONV-R vs. GF mice (271)	Presence of microbes	↔ Saa1, Saa2, ↑ Saa3
	CONV-R vs. GF mice (278)	Presence of microbes	↑↑ Saa1, Saa2, Saa3 (4-fold)
	CMT-93 colonic epithelial cells (224, 271)	LPS	↑↑ Saa3 (7-fold), ↔ Saa1–2
	Mink intestine (269)	LPS (3 mg/kg)	↑↑ Saa1

12:0, lauric acid; 14:0, myristic acid; 16:0, palmitic acid; 20:4, arachidonic acid; 20:5, eicosapentaenoic acid; 22:6, docosahexaenoic acid; $AgNO_3$, silver nitrate; Ccl4, tetrachloride; CLA, conjugated linoleic acid; CONV-R, conventionally-reared; DEXv dexamethasone; db/db mice: DIO, diet-induced obesity; leptin receptor-deficient mice; DEX, dexamethasone; DHA, docohexaenoic acid; GF, germ-free; HepG2, human hepatoma cells; HSC, hepatic stellate cells; IL-1β, interleukin 1 beta; IL-6, interleukin 6; LPS, lipopolysaccharide; MDM, monocyte-derived macrophage; MOG, myelin oligodendrocyte glycoprotein; ob/ob mice, leptin-deficient mice; PBMCs, peripheral blood mononuclear cells; PUFA, polyunsaturated fatty acids; rSAA, recombinant SAA; SFA, short chain fatty acids; SQ, subcutaneous; STZ, streptozotocin; T2D, type 2 diabetes; TNFα, tumor necrosis factor alpha; WAT, white adipose tissue; ↑, modest increase; ↑↑, robust increase; ↔, no change.
[a]Fold-mRNA expression, unless otherwise indicated.

As discussed above, potent inflammatory stimuli initiate robust, rapid, but short-lived (~24 h) SAA1 and SAA2 expression from the liver. LPS at dosages ranging from 0.25 to 100 μg/mouse increases murine hepatic mRNA expression of Saa1 (up to 2,000-fold), Saa2 (up to 200-fold), and to a lesser extent Saa3 (up to 40-fold) in an NFκB-dependent manner, with circulating SAA levels subsequently increasing to 3,000 μg/ml (42, 236, 238). All three SAA subtypes reach peak hepatic mRNA expression 12 h after LPS administration (238). Only high-dose LPS (25 μg) increases circulating Saa3 in mice (42, 122). Similarly, LPS activates SAA1 and SAA2 mRNA expression and secretion in human primary hepatocytes (251). Patients with sepsis have elevated SAA levels (235), which are stronger predictive markers of sepsis severity (76). SAA was a more sensitive and earlier predictor of neonatal sepsis than the more traditional CRP (75).

Other models of sterile inflammation in mice also have been shown to increase hepatic Saa levels. Silver nitrate ($AgNO_3$), administered by subcutaneous injection of 0.5 ml of a 1% solution, increases hepatic Saa1 (40-fold), Saa2 (1,000-fold), and Saa3 (200-fold), and leads to circulating Saa levels equivalent to that observed with high doses of LPS (42). However, in contrast to findings after LPS, we did not find evidence of Saa3 in plasma following $AgNO_3$ injection (42). Injection with casein (administered by subcutaneous injection of 0.5 ml of a 5% solution) modestly increased hepatic Saa1 (6-fold), Saa2 (100-fold), and Saa3 (5-fold) mRNA expression, resulting in much smaller increases in plasma Saa levels (42). Collectively, acute inflammatory stimuli differ in the resulting hepatic expression levels of SAA1–3, leading to varied systemic SAA concentrations, suggesting differential regulation.

In metabolic disease states such as obesity and T2D, hepatic SAA expression likely results from cytokine signaling from extra-hepatic tissues such as WAT (240, 252). A recent study identified SAA1 protein from both WAT and liver as a candidate biomarker associated with low-grade inflammation. There was a much stronger correlation of SAA1 with inflammation in the liver than with WAT inflammation (244), suggesting a more dominant hepatic role of SAA1. However, this particular study mined gene ontology datasets using general inflammatory search terms, so the particular metabolic conditions (i.e., obesity) of the original study subjects were not indicated.

3.2. Adipocytes

The acute inflammatory studies cited above showed effects on SAA subtypes expressed in the liver, but there also were strong SAA responses in adipose tissue. While reported hepatic SAA responses to LPS in mice are largely due to Saa1 and Saa2, adipose tissue responds to LPS with massive (~500-fold) increases in Saa3 mRNA compared with 40-fold Saa3 increases in the liver (42). This effect appears to be LPS-specific, as neither $AgNO_3$ or casein altered Saa1, Saa2, or Saa3 mRNA levels in adipose tissue (42). Thus, we speculate that LPS can induce expression of all three Saa subtypes in both liver and adipose tissue that all contribute to circulating levels, while $AgNO_3$ and casein primarily target hepatic Saa. In this section, we present evidence for differential SAA subtype expression in response to several inflammatory mediators and metabolic factors.

Many stimuli have been shown to increase Saa3 mRNA and protein expression in cultured adipocytes. These include high levels of glucose (114, 190, 204), saturated fatty acids (190, 204), conjugated linoleic acids (204), pro-inflammatory cytokines including TNFα and IL-1β (114, 190, 245), and LPS (114). Conversely, anti-inflammatory stimuli such as polyunsaturated fatty acids (190) and rosiglitazone (114) reduce adipocyte Saa3 expression. In addition to chemical activation, 3T3-L1 adipocytes

also express Saa3 in response to macrophage-derived components (121, 246), suggesting an important role in cell-cell communication, with similar effects observed in cultured human adipocytes and in mice. Human SGBS cells treated with saturated fatty acids display increased Saa1 expression, while polyunsaturated fatty acids decreased glucose-induced Saa1 (190), suggesting that the major adipose SAA subtype in humans is SAA1. Mice injected with LPS robustly increased Saa3 expression in visceral WAT comparable to hepatic Saa1/2 expression levels in the same mice (42); using mass spectrometry methods, Saa3 was identified in their plasma (42), suggesting that Saa3 can circulate under particular inflammatory conditions.

Recombinant (i.e., exogenous) SAA can directly impact adipocyte metabolism. In cultured 3T3-L1 adipocytes, recombinant SAA (rSAA, 5 μg/ml) reduced adipogenesis, accompanied by reduced adipogenic transcription factors and proteins including peroxisome proliferator-activated receptor gamma (PPARγ), CCAAT enhancer binding protein beta (C/EBPβ), and GLUT4 (242). rSAA also reduced lipid accumulation, increased lipolysis, prevented glucose uptake, triggered secretion of inflammatory cytokines IL6 and TNFα and increased mRNA expression of Saa3. In multipotent adipose-derived stem (MADS) cells isolated from human subcutaneous adipose tissue induced to differentiate into primary adipocytes *in vitro*, free- and HDL-associated rSAA increased MCP-1, IL-6, and IL-8 secretion in a dose-dependent manner (253). This pro-inflammatory phenotype was dependent on NFkB, not due to endotoxin contamination (243, 253). Moreover, rSAA treatment reduced mRNA expression of adiponectin, fatty acid synthase (FAS), C/EBPα, PPARγ, and GLUT4 (253, 254), suggesting impaired adipogenesis capacity. A propensity for rSAA to increase lipolysis also has been reported in human adipose tissue (9). The pro-inflammatory, pro-lipolytic, and anti-adipogenic effects of SAA also have been shown in primary porcine adipocytes (243).

Recent technical advances have enabled the study of adipose tissue down to the single-cell level (255, 256). Spatial transcriptomics on human subcutaneous abdominal adipose tissue sections has revealed 3 distinct subsets of adipocytes, including those rich in genes for leptin (Adipo^{LEP}), the lipid droplet-associated proteins perilipin1 and −4 (Adipo^{PLIN}), and SAA1/2 (Adipo^{SAA}) (257). Adipo^{LEP} was enriched in genes encoding matrix metabolism, Adipo^{PLIN} in genes associated with lipid and glucose metabolism, and Adipo^{SAA} in multiple retinol-binding adipokines (i.e., RBP4) (257). These have been linked with obesity co-morbidities including T2D, hepatic steatosis, inflammation, and metabolic syndrome (258, 259). Approximately 8% of the adipocytes examined were Adipo^{SAA}, with similar proportions in donors with or without obesity, but there was high variability among donors (from 2%–18% of all adipocyte populations) (257). Whether or not the proportion of Adipo^{SAA} cells differs in omental WAT, or is related to sex, is of interest.

In addition to secreting adipokines and nutrients into the circulation, adipocytes also secrete extracellular vesicles (EVs), including microvesicles, exosomes, and apoptotic bodies (260). EVs are heterogeneous membrane vesicles secreted by many cell types, including adipocytes, and function to facilitate intercellular communication within and between tissues via protein signaling, immune responses, and nutrient transport (261). EVs contain diverse cargo including proteins, lipids, and miRNAs. Adipocyte-derived exosomes can be identified by their adipocyte-specific protein cargo, chiefly adiponectin and perilipin (262). EVs differing in cellular origins possess unique biological properties, enabling cell- or tissue-specific effects. EV production derived from WAT is increased during obesity (263–266), and is correlated with insulin resistance in both humans and in animal models. SAA1 and SAA2 have been identified in EVs isolated from human adipose tissue (262), and Saa3 observed within vesicle-like structures within murine adipose tissue (121). These findings raise the possibility that adipose tissue-derived SAA communicates systemically with other target tissues, in addition to its local effects.

3.3. Macrophages

Macrophages are present in all peripheral tissues and contribute to systemic metabolism. Macrophage classification schema are emerging, but largely revolve around their functional potential, including the capacity to elicit an inflammatory response and ability to phagocytose pathogens and cellular debris (267). As such, macrophages can either contribute to or resolve inflammation. Moreover, macrophages that only reside within particular tissues often receive their own classification, such as hepatic Kupffer cells or central microglia. All tissues from which Saa3 expression can be detected have a dynamic macrophage population, suggesting a potential common source of Saa3.

In obesity, adipose tissue exhibits both increased SAA expression (SAA1 and SAA2 in humans and Saa3 in mice), as well as increased macrophage infiltration. Importantly, all SAA subtypes are expressed from macrophages (187). Initial studies showed that acute inflammatory stimuli, including LPS and casein, induced only Saa3 mRNA in murine macrophages (40, 113). Saa3 mRNA also increases in activated RAW264.7 macrophages (121), murine bone marrow-derived macrophages (121), murine J774.1 macrophages (18, 112), and murine foam cells within atherosclerotic lesions (18), but not in the human THP-1 cell line (187). Saa3 protein co-localizes with F4/80^{+} macrophages in obese adipose tissue (121).

That macrophages express SAA subtypes as well as SAA receptors, including TLR2, TLR4, RAGE, and SRB1, suggests autocrine activities that likely contribute to local effects (20, 268). Deletion of putative SAA receptors yields a blunted macrophage response to SAA. BMDMs from mice deficient in TLR2 exhibit a blunted inflammatory response to SAA (1 μM) (56), and neutralizing antibodies to TLR2 blunted SAA-mediated activation of THP-1 macrophages (20). Similar effects have been observed in peritoneal macrophages from TLR4-deficient mice (59). SAAs may bind to macrophage-produced extracellular matrix (ECM) components, including proteoglycans and glycoproteins (195). Collectively, an increasing body of work connects SAA and macrophages.

Monocytes freshly isolated from humans or monocytic cell lines consistently respond to SAA with potent pro-inflammatory responses. Within an hour of treating with rSAA, peripheral human blood mononuclear cells (PBMCs), THP-1 monocytic cells, and monocyte-derived macrophages (MDMs) all exhibit rapid expression of IL-1β, MCP1, IL-6, IL-8, TNFα, and macrophage inflammatory protein 1 alpha (MIP-1α), an effect that is sustained for 8–24 h and is similar to LPS (241). Similar effects were observed in RAW264 monocytes treated with rSAA, which yielded a pro-inflammatory phenotype characterized by increased MCP-1, IL-6, IL-8, and TNFα secretion (9). While a potent inflammatory stimulus (i.e., LPS or casein) initiates a robust, rapid, but short-lived (~24 h) hepatic Saa response, and from macrophages directly treated in culture, a similarly rapid but more prolonged Saa3 response (72 h) has been observed in isolated peripheral macrophages, indicating markedly different hepatic expression kinetics (40, 113). Whether such different expression kinetics reflect a more prolonged response that is cell-type specific or is an effect secondary to the acute phase response remains to be determined.

3.4. Intestine

Intestinal SAA can be induced by several mechanisms, which are complicated by the potential for differing SAA subtype expression from varying intestinal cells. SAA1/2 are highly expressed in intestinal epithelium and in the endothelium lining the intestinal submucosal blood vessels in rabbits, rodents, and humans (224, 269, 270). Conversely, Saa3 has been detected at low levels in mouse colonic epithelium (224), but is more prevalent in intestinal immune cells (209). Moreover, in mice, Saa3 expression is more strongly induced by LPS and microbes in colonic epithelium than Saa1/2 (224, 247, 271). Induction of SAA1 and SAA2 in small intestinal epithelial cells by commensal microbes requires both IL-23 and IL-22 in a STAT3-dependent manner (272). Male Syrian hamsters injected with LPS (100 μg/g body weight) also expressed high Saa levels (unknown subtypes) in the duodenum, jejunum, and ileum (273). Mouse intestinal Saa3 is most closely related to human SAA1 with 70% amino acid homology (271), and may serve local gut functions (247).

SAA expression differs markedly throughout the intestinal tract, with SAA2 having the most variable expression between the ileum and rectum in subjects with IBD (274). Germ-free mice have very low ileal levels of Saa1 and Saa2, but higher expression in the colon than in conventional mice (275). These findings are consistent with an anti-bacterial SAA role in relation to an omnipresent colonic microbiota, and a much more variable ileal microbiota. As conventional mice mature, intestinal Saa rises in the ileum, reflecting the increasing bacterial load, but do not change in the colon. Perturbing early-in-life gut microbiome affected intestinal Saa expression. With pulsed therapeutic-level antibiotic (PAT) exposures at early ages after weaning, non-obese diabetic (NOD) mice have consistently decreased Saa1/2 and Saa3 expression in the ileum but not in the colon (249, 276, 277). Younger mice (P12) had significantly increased Saa1/2 and Saa3 expression in both ileum and colon two days after antibiotic exposure ended, indicating that intestinal Saa can biphasically respond to gut microbiome changes in patterns that are both age- and microbiome context-dependent during this critical period for host immune development. The early-life antibiotic-exposed mice showed significantly increased Saa1/2 and Saa3 expression in the ileum but not in the colon at P17 days (277). These studies further confirmed that early-life intestinal SAA expression is subject to regulation linked to gut microbiota composition, potentially reflecting an ancient evolutionary strategy to regulate the establishment of immune responses or tolerance in the developing animal.

Mono-colonization of germ-free mice with segmented filamentous bacteria (SFB) rapidly induces expression of Saa1, Saa2, and Saa3 in the terminal ileum, consistent with the unique spatial expression patterns of SAA in the gut. Induction of ileal Saa is further increased by conventionalization using fecal microbial transplant (FMT) from specific pathogen-free (SPF) mice (278). Induction of ileal Saa1 and Saa2 by SFB is mediated through the IL-23/IL-22 circuit in ileal epithelial cells (272). The SFB-induced ileal Saa proteins promote Th17 cell differentiation from ileal lamina propria dendritic cells and contribute to protective immune responses in the ileal mucosa (278).

Conversely, as anti-bacterial molecules, SAA may modulate gut bacterial growth and composition either directly or through downstream intestinal immune responses. Consistent with observations in mice, *in vitro* studies showed that overexpression of Saa1/2 in intestinal epithelial cell lines reduces growth of co-cultured bacterial cells (224). Similarly, in zebrafish SAA in intestinal epithelial cells derived via transgene expression constrains the bactericidal activity of neutrophils, and promotes neutrophil recruitment to the intestine that is functionally distinct from hepatic SAA expression (279). In a mouse model of DSS-induced colitis, Saa induction in the large intestine was required to dampen local inflammation, while SAA1/2 overexpression in cultured epithelial cells reduced the viability of co-cultured *E.coli* (224), suggesting a potential bactericidal function of SAA that may contribute to barrier integrity. Transgenic mice engineered to overexpress Saa1 are partially protected against inflammatory responses to cecal ligation and puncture (280), suggesting an inverse relationship between gut-derived SAA and inflammation.

The anti-inflammatory properties of intestinal Saa1 are most specific to LPS-induced inflammation, an effect that could be dosage-dependent. Saa1 has the ability to bind LPS and form a complex, which then facilitates the clearance of LPS by macrophages (280). The transition of Saa1 from exerting pro-inflammatory effects to anti-inflammatory effects may reflect the proteolysis of the Saa1 protein. The N-terminal and C-terminal domains of Saa1 are crucial for its pro-inflammatory activity, and their removal via proteolysis can transform Saa1 into an anti-inflammatory agent (280, 281). Whether other SAA proteins also are capable of switching from pro-inflammatory to anti-inflammatory functions is unknown. The precise functions of intestinal SAAs deserve further investigation.

4. Sexual dimorphism of SAA

Circulating SAA is positively associated with BMI and adiposity, with a propensity to also associate with fasting glucose, insulin, HbA1C, and HOMA-IR. An emerging literature describes unique sexual dimorphic relationships between SAA and several metabolic disease states. Fully characterizing sex differences in SAA expression kinetics and functional potential is thus of great importance.

Large-scale RNA-sequencing studies of healthy humans showed that adipose tissue contains ~3,000 sexually differentiated genes, one of the highest levels of all tissues examined (282). There was higher expression in women of all known SAA subtypes (SAA1, SAA2, and SAA3(p) (the SAA3 pseudogene)), which were among the most highly sex-differential genes (283). In contrast, with the exception of breast and skin, no other SAA-expressing tissues (i.e., liver, lung, blood) show SAA subtypes in their lists of sex-biased genes (283). These findings have been replicated in several large-scale sequencing studies spanning dozens of tissues in healthy men and women (284, 285), and in mice (286). SELS, a major SAA receptor, is elevated in the adipose tissue of subjects with T2DM and correlated with measures of glycemic control (73), but sex was not investigated in these studies. Collectively, many studies indicate that adipose tissue from female mice and humans expresses higher SAA than tissue from males, but the involvement of sex differences in the pathophysiology of obesity or associated metabolic disorders is not known.

Healthy women (with BMI < 25) have higher circulating SAA than age-matched men, despite the men having a slightly higher average BMI (287). SAA positively correlates with BMI, waist circumference, waist-to-hip ratio, insulin, and HOMA-IR in both sexes. After adjusting for BMI, only the correlations with insulin and HOMA-IR remained significant for men, but not women.

One of the first studies to address potential sex differences in SAA kinetics characterized the association between adipocyte size and circulating SAA levels in men and women over a large range in BMIs, with the additional aim to examine potential associations with measures of glycemic control (107). Women generally had higher circulating SAA levels than men, and stronger correlations with BMI, adiposity, subcutaneous adipocyte diameter, fasting insulin, HOMA-IR, and leptin (107). This could relate to the higher proportion of subcutaneous WAT in women than men.

By contrast, the liver, the source of most acute-phase SAA, has rarely been implicated in sex differential SAA expression. In contrast to several studies that have not found SAA to be differentially expressed by sex in the liver (282, 283), one study has shown that males tend to express slightly higher levels of SAA subtypes than female mice. Male CD-1 mice have modestly higher hepatic mRNA expression levels of Saa1, Saa2, and Saa3 than females (288). Adipose tissue-derived SAA may be impacted by sex steroids, as WAT is highly enriched in these molecules (289), with levels widely varying in metabolic disease. In experiments using cultured murine peritoneal macrophages and BMDMs, testosterone and 17β-estradiol directly impacted Saa3 gene expression (182). Saa3-deleted macrophages show sexually dimorphic responses to sex steroids. After estradiol exposure, Saa3-deficient BMDMs harvested from male mice showed a massive increase in inflammatory gene expression compared to wild-type macrophages, with concurrent elevation of the estrogen receptor (182). Thus, a relationship between macrophages, sex steroid signaling, SAA, and metabolic disease is present but needs further definition.

Our prior studies have supported a potential sexual dimorphic role of Saa3 in a mouse model with global Saa3 deficiency (82). When given a high fat high sucrose (HFHS) diet, female mice, but not male mice, were protected from body weight gain and associated insulin resistance. To determine whether there was similar sexually dimorphic protection against atherosclerosis in female mice, we crossed our global Saa3-KO mice with mice deficient in LDLR, which promotes hypercholesterolemia and is a common model for studying atherosclerosis. In that study, male $Saa3^{-/-}$ $Ldlr^{-/-}$ mice were protected from atherosclerosis, while female $Saa3^{-/-}$ $Ldlr^{-/-}$ mice were not (182). We speculate that in these models, Saa3 modulates effects via pathways that could be tissue-specific. In the obese state, Saa3 is expressed primarily from hypertrophic adipocytes, and also expressed from adipose tissue macrophages (96). Conversely, in the setting of hypercholesterolemic atherosclerosis, Saa3 expression likely originates from aortic and/or hepatic macrophages in addition to adipose tissue. Thus, in these different models, Saa3 deficiency leads to divergent phenotypes in males and females.

Other studies also suggest a potential interaction between sex hormones and SAA. Women with RA had higher SAA levels than men with RA (211, 212, 290). In a linear regression model involving the ratio of estradiol to testosterone (E2:T), sex and the E2:T ratio were highly significant and independent predictors of circulating SAA (290). Women with BMI < 25 have also been reported to have higher SAA levels than men (287), and SAA correlates more strongly with BMI and adiposity in women than in men (11). These observations suggest that sex hormones play roles in regulating SAA expression. Circulating SAA is higher in women taking oral estrogen-containing contraceptives (291, 292) and in women undergoing estrogen replacement therapy (287, 293). The apparent estradiol-mediated increase in SAA observed in these studies was secondary to elevations in CRP. More work is required to determine the mechanisms linking sex hormones and SAA.

Phenotypic responses to pro-inflammatory stimuli have differed in macrophages harvested from male or female mice (182). Compared to male mice, bone marrow-derived macrophages (BMDMs) isolated from female mice and treated with pro-inflammatory fatty acids or LPS showed lower levels of inflammatory cytokine expression (294). This effect appears to be cell-autonomous, since sex hormones were not present. Transplanting male bone marrow into donor female mice led to a phenotypically male pattern of obesity-associated adipose tissue inflammation (294). However, the absence of Saa3 in BMDMs negated this inherent sex-specific effect (182). The specific interactions between Saa3 and sex hormones remains to be

characterized, but could explain the sexually dimorphic observations related to SAA expression in metabolic disease.

5. SAA-targeting therapies

Targeting SAA may be a potential therapeutic avenue for dampening inflammation. One approach is to target pathways that will reduce SAA expression. Tocilizumab, a monoclonal antibody that targets IL-6 and reduces SAA levels (295), has been effective in treating a small number of patients with amyloidosis involving the gastrointestinal tract (296) and kidneys associated with Familial Mediterranean Fever (297, 298), and amyloidosis associated with rheumatoid arthritis (299), but this approach could potentially also be developed for use in other chronic inflammatory conditions. Anakinra and canakinumab, monoclonal antibodies that target IL-1β, have been used to reduce SAA levels in inflammatory conditions such as Familial Mediterranean Fever (300) and gouty arthritis (301). Moreover, the CANTOS trial, for the first time, showed that inhibition of inflammation using an antibody against Il-1β decreased cardiovascular events (172), providing further evidence for the importance of inflammation in atherosclerosis. Since SAA appears to play a role in the pathogenesis of atherosclerosis (see previous sections), it is possible an approach that inhibits Il-1β could be more widely adapted for preventing atherosclerosis, as well as rheumatic diseases and even in hyperinflammatory states associated with COVID-19 (302).

SAA contains binding sites that are specific for heparin and heparin sulfate, which have been postulated to be useful for preventing amyloidogenic conformation of SAA (303). SAA also inhibits acyl coenzyme A cholesterol acyltransferase and enhances cholesterol esterase activities shifting stored intracellular cholesteryl esters to free cholesterol, which can be transported from cells. Liposomal preparations of small synthetic peptides of SAA can bind and neutralize SAA, facilitating reverse cholesterol transport and preventing and reversing aortic lesions in mouse models of atherosclerosis (304). Eprodisate, which binds to the glycosaminoglycan binding site on amyloid fibrils, thus preventing polymerization and tissue deposition, may slow the progression of AA amyloidosis-related renal disease (64, 305), and also may be applicable to other amyloid related conditions.

All these approaches are still in experimental phases, but demonstrate potential proof-of-concept mechanisms for future SAA-targeted therapies.

6. Concluding remarks and perspectives

Elevations of SAA subtypes have been consistently associated with metabolic diseases such as obesity, diabetes, CVD, and autoimmune conditions in humans and in animal models. After 40 years of investigation, evidence is not yet sufficient to determine whether SAA plays causal roles in metabolic disease development and progression, or is merely a biomarker of broader phenomena akin to CRP. In this review, we have presented evidence that associations with several metabolic disease states differ in expression kinetics and dominant SAA subtypes, as well as tissue, cellular, and spatial expression patterns, implicating the tissue microenvironment as crucial to SAA function. In particular, while evidence suggests that WAT SAA expression increases in obesity, whether such increases contribute to the circulating SAA pool is not known. Due to distinct subtype expression patterns in mice vs. humans, it could be possible for WAT-SAA to circulate in humans, but not in mice. As such, we propose that the SAA functions associated with metabolic disease are physiologically distinct from those in acute-phase reactions. Moreover, accumulating evidence suggests that different SAA subtypes, long considered to be pro-inflammatory molecules, may play beneficial roles in conditions like IBD, highlighting the importance of the microenvironment for particular SAA-mediated phenotypes. Finally, we speculate that SAA could play important roles in the differential progression of sexually dimorphic metabolic conditions.

Author contributions

LJD, KSM, XSZ, AC, and MJB reviewed the literature and contributed to the preparation of this manuscript. LJdH and KSM prepared the figures and tables. All authors contributed to the article and approved the submitted version.

Funding

The authors are thankful for research support from the United States Department of Agriculture (USDA) National Institute of Food and Agriculture (NIFA) award #2020-67001-30716. This work was also supported by the National Institutes of Health training program in Diabetes, Obesity, and Metabolism (T32 DK007247) and the training program in Nutrition, Obesity, and Atherosclerosis (T32 HL007028), both at the University of Washington; and U01 AI22285 from NIH, Transatlantic Program of the Fondation Leducq, and the Emch Foundation, at Rutgers.

Conflict of interest

The authors declare that the research was conducted in the absence of any commercial or financial relationships that could be construed as a potential conflict of interest.

Publisher's note

References

1. Miwata H, Yamada T, Okada M, Kudo T, Kimura H, Morishima T. Serum amyloid A protein in acute viral infections. *Arch Dis Child*. (1993) 68:210–4. doi: 10.1136/adc.68.2.210

2. Pizzini C, Mussap M, Plebani M, Fanos V. C-reactive protein and serum amyloid A protein in neonatal infections. *Scand J Infect Dis*. (2000) 32:229–35. doi: 10.1080/00365540050165848

3. Cunnane G, Grehan S, Geoghegan S, McCormack C, Shields D, Whitehead AS, et al. Serum amyloid A in the assessment of early inflammatory arthritis. *J Rheumatol*. (2000) 27:58–63.

4. Lange U, Boss B, Teichmann J, Klör HU, Neeck G. Serum amyloid A–an indicator of inflammation in ankylosing spondylitis. *Rheumatol Int*. (2000) 19:119–22. doi: 10.1007/s002960050114

5. Gang N, Drenth JP, Langevitz P, Zemer D, Brezniak N, Pras M, et al. Activation of the cytokine network in familial Mediterranean fever. *J Rheumatol*. (1999) 26:890–7.

6. O'Hara R, Murphy EP, Whitehead AS, FitzGerald O, Bresnihan B. Acute-phase serum amyloid A production by rheumatoid arthritis synovial tissue. *Arthritis Res*. (2000) 2:142–4. doi: 10.1186/ar78

7. Vallon R, Freuler F, Desta-Tsedu N, Robeva A, Dawson J, Wenner P, et al. Serum amyloid A (apoSAA) expression is up-regulated in rheumatoid arthritis and induces transcription of matrix metalloproteinases. *J Immunol*. (2001) 166:2801–7. doi: 10.4049/jimmunol.166.4.2801

8. Niederau C, Backmerhoff F, Schumacher B. Inflammatory mediators and acute phase proteins in patients with Crohn's disease and ulcerative colitis. *Hepatogastroenterology*. (1997) 44:90–107.

9. Yang RZ, Lee MJ, Hu H, Pollin TI, Ryan AS, Nicklas BJ, et al. Acute-phase serum amyloid A: an inflammatory adipokine and potential link between obesity and its metabolic complications. *PLoS Med*. (2006) 3:e287. doi: 10.1371/journal.pmed.0030287

10. Yang RZ, Blumenthal JB, Glynn NM, Lee MJ, Goldberg AP, Gong DW, et al. Decrease of circulating SAA is correlated with reduction of abdominal SAA secretion during weight loss. *Obesity (Silver Spring)*. (2014) 22:1085–90. doi: 10.1002/oby.20657

11. Lappalainen T, Kolehmainen M, Schwab U, Pulkkinen L, Laaksonen DE, Rauramaa R, et al. Serum concentrations and expressions of serum amyloid A and leptin in adipose tissue are interrelated: the Genobin study. *Eur J Endocrinol*. (2008) 158:333–41. doi: 10.1530/EJE-07-0598

12. Santana AB, Gurgel MS, de Oliveira Montanari JF, Bonini FM, de Barros-Mazon S. Serum amyloid a is associated with obesity and estrogen receptor-negative tumors in postmenopausal women with breast cancer. *Cancer Epidemiol Biomarkers Prev*. (2013) 22:270–4. doi: 10.1158/1055-9965.EPI-12-1020

13. Zhao Y, He X, Shi X, Huang C, Liu J, Zhou S, et al. Association between serum amyloid A and obesity: a meta-analysis and systematic review. *Inflamm Res*. (2010) 59:323–34. doi: 10.1007/s00011-010-0163-y

14. Leinonen E, Hurt-Camejo E, Wiklund O, Hultén LM, Hiukka A, Taskinen MR. Insulin resistance and adiposity correlate with acute-phase reaction and soluble cell adhesion molecules in type 2 diabetes. *Atherosclerosis*. (2003) 166:387–94. doi: 10.1016/s0021-9150(02)00371-4

15. Marzi C, Huth C, Herder C, Baumert J, Thorand B, Rathmann W, et al. Acute-phase serum amyloid A protein and its implication in the development of type 2 diabetes in the KORA S4/F4 study. *Diabetes Care*. (2013) 36:1321–6. doi: 10.2337/dc12-1514

16. Fyfe AI, Rothenberg LS, DeBeer FC, Cantor RM, Rotter JI, Lusis AJ. Association between serum amyloid A proteins and coronary artery disease: evidence from two distinct arteriosclerotic processes. *Circulation*. (1997) 96:2914–9. doi: 10.1161/01.CIR.96.9.2914

17. Kosuge M, Ebina T, Ishikawa T, Hibi K, Tsukahara K, Okuda J, et al. Serum amyloid A is a better predictor of clinical outcomes than C-reactive protein in non-ST-segment elevation acute coronary syndromes. *Circ J*. (2007) 71:186–90. doi: 10.1253/circj.71.186

18. Meek RL, Urieli-Shoval S, Benditt EP. Expression of apolipoprotein serum amyloid A mRNA in human atherosclerotic lesions and cultured vascular cells: implications for serum amyloid A function. *Proc Natl Acad Sci U S A*. (1994) 91:3186–90. doi: 10.1073/pnas.91.8.3186

19. Johnson BD, Kip KE, Marroquin OC, Ridker PM, Kelsey SF, Shaw LJ, et al. Serum amyloid A as a predictor of coronary artery disease and cardiovascular outcome in women: the national heart, lung, and blood institute-sponsored women's ischemia syndrome evaluation (WISE). *Circulation*. (2004) 109:726–32. doi: 10.1161/01.CIR.0000115516.54550.B1

20. Sack GH. Serum amyloid A—a review. *Mol Med*. (2018) 24:46. doi: 10.1186/s10020-018-0047-0

21. Getz GS, Krishack PA, Reardon CA. Serum amyloid A and atherosclerosis. *Curr Opin Lipidol*. (2016) 27:531–5. doi: 10.1097/MOL.0000000000000331

22. Uhlar CM, Burgess CJ, Sharp PM, Whitehead AS. Evolution of the serum amyloid A (SAA) protein superfamily. *Genomics*. (1994) 19:228–35. doi: 10.1006/geno.1994.1052

23. Wang J, Yang Y, Zhang A, Zeng L, Xiao S, Ma H, et al. Serum amyloid protein (SAA) as a healthy marker for immune function in Tridacna crocea. *Fish Shellfish Immunol*. (2022) 122:495–500. doi: 10.1016/j.fsi.2022.02.038

24. Benditt EP, Eriksen N. Amyloid protein SAA is associated with high density lipoprotein from human serum. *Proc Natl Acad Sci U S A*. (1977) 74:4025–8. doi: 10.1073/pnas.74.9.4025

25. Benditt EP, Eriksen N, Hanson RH. Amyloid protein SAA is an apoprotein of mouse plasma high density lipoprotein. *Proc Natl Acad Sci U S A*. (1979) 76:4092–6. doi: 10.1073/pnas.76.8.4092

26. Badolato R, Johnston JA, Wang JM, McVicar D, Xu LL, Oppenheim JJ, et al. Serum amyloid A induces calcium mobilization and chemotaxis of human monocytes by activating a pertussis toxin-sensitive signaling pathway. *J Immunol*. (1995) 155:4004–10. doi: 10.4049/jimmunol.155.8.4004

27. Zheng H, Li H, Zhang J, Fan H, Jia L, Ma W, et al. Serum amyloid A exhibits pH dependent antibacterial action and contributes to host defense against. *J Biol Chem*. (2020) 295:2570–81. doi: 10.1074/jbc.RA119.010626

28. Cai Z, Cai L, Jiang J, Chang KS, van der Westhuyzen DR, Luo G. Human serum amyloid A protein inhibits hepatitis C virus entry into cells. *J Virol*. (2007) 81:6128–33. doi: 10.1128/JVI.02627-06

29. Hirakura Y, Carreras I, Sipe JD, Kagan BL. Channel formation by serum amyloid A: a potential mechanism for amyloid pathogenesis and host defense. *Amyloid*. (2002) 9:13–23. doi: 10.3109/13506120209072440

30. Badolato R, Wang JM, Stornello SL, Ponzi AN, Duse M, Musso T. Serum amyloid A is an activator of PMN antimicrobial functions: induction of degranulation, phagocytosis, and enhancement of anti-Candida activity. *J Leukoc Biol*. (2000) 67:381–6. doi: 10.1002/jlb.67.3.381

31. Badolato R, Wang JM, Murphy WJ, Lloyd AR, Michiel DF, Bausserman LL, et al. Serum amyloid A is a chemoattractant: induction of migration, adhesion, and tissue infiltration of monocytes and polymorphonuclear leukocytes. *J Exp Med*. (1994) 180:203–9. doi: 10.1084/jem.180.1.203

32. Liang TS, Wang JM, Murphy PM, Gao JL. Serum amyloid A is a chemotactic agonist at FPR2, a low-affinity N-formylpeptide receptor on mouse neutrophils. *Biochem Biophys Res Commun*. (2000) 270:331–5. doi: 10.1006/bbrc.2000.2416

33. Su SB, Gong W, Gao JL, Shen W, Murphy PM, Oppenheim JJ, et al. A seven-transmembrane, G protein-coupled receptor, FPRL1, mediates the chemotactic activity of serum amyloid A for human phagocytic cells. *J Exp Med*. (1999) 189:395–402. doi: 10.1084/jem.189.2.395

34. Olsson N, Siegbahn A, Nilsson G. Serum amyloid A induces chemotaxis of human mast cells by activating a pertussis toxin-sensitive signal transduction pathway. *Biochem Biophys Res Commun*. (1999) 254:143–6. doi: 10.1006/bbrc.1998.9911

35. Coetzee GA, Strachan AF, van der Westhuyzen DR, Hoppe HC, Jeenah MS, de Beer FC. Serum amyloid A-containing human high density lipoprotein 3. Density, size, and apolipoprotein composition. *J Biol Chem*. (1986) 261:9644–51. doi: 10.1016/S0021-9258(18)67562-3

36. Benditt EP, Hoffman JS, Eriksen N, Parmelee DC, Walsh KA. SAA, an apoprotein of HDL: its structure and function. *Ann N Y Acad Sci*. (1982) 389:183–9. doi: 10.1111/j.1749-6632.1982.tb22136.x

37. Jahangiri A, Wilson PG, Hou T, Brown A, King VL, Tannock LR. Serum amyloid A is found on ApoB-containing lipoproteins in obese humans with diabetes. *Obesity (Silver Spring)*. (2013) 21:993–6. doi: 10.1002/oby.20126

38. Ye RD, Sun L. Emerging functions of serum amyloid A in inflammation. *J Leukoc Biol*. (2015) 98:923–9. doi: 10.1189/jlb.3VMR0315-080R

39. Webb NR. High-density lipoproteins and serum amyloid A (SAA). *Curr Atheroscler Rep*. (2021) 23:7. doi: 10.1007/s11883-020-00901-4

40. Meek RL, Benditt EP. Amyloid A gene family expression in different mouse tissues. *J Exp Med*. (1986) 164:2006–17. doi: 10.1084/jem.164.6.2006

41. Upragarin N, Landman WJ, Gaastra W, Gruys E. Extrahepatic production of acute phase serum amyloid A. *Histol Histopathol*. (2005) 20:1295–307. doi: 10.14670/HH-20.1295

42. Chait A, den Hartigh LJ, Wang S, Goodspeed L, Babenko I, Altemeier WA, et al. Presence of serum amyloid A3 in mouse plasma is dependent on the nature and extent of the inflammatory stimulus. *Sci Rep*. (2020) 10:10397. doi: 10.1038/s41598-020-66898-7

43. Kluve-Beckerman B, Drumm ML, Benson MD. Nonexpression of the human serum amyloid A three (SAA3) gene. *DNA Cell Biol*. (1991) 10:651–61. doi: 10.1089/dna.1991.10.651

44. De Buck M, Gouwy M, Wang JM, Van Snick J, Opdenakker G, Struyf S, et al. Structure and expression of different Serum amyloid A (SAA) variants and their

concentration-dependent functions during host insults. *Curr Med Chem*. (2016) 23:1725–55. doi: 10.2174/0929867323666160418114600

45. Larson MA, Wei SH, Weber A, Weber AT, McDonald TL. Induction of human mammary-associated serum amyloid A3 expression by prolactin or lipopolysaccharide. *Biochem Biophys Res Commun*. (2003) 301:1030–7. doi: 10.1016/S0006-291X(03)00045-7

46. Uhlar CM, Whitehead AS. Serum amyloid A, the major vertebrate acute-phase reactant. *Eur J Biochem*. (1999) 265:501–23. doi: 10.1046/j.1432-1327.1999.00657.x

47. de Beer MC, de Beer FC, Gerardot CJ, Cecil DR, Webb NR, Goodson ML, et al. Structure of the mouse Saa4 gene and its linkage to the serum amyloid A gene family. *Genomics*. (1996) 34:139–42. doi: 10.1006/geno.1996.0253

48. Lee HY, Kim MK, Park KS, Shin EH, Jo SH, Kim SD, et al. Serum amyloid A induces contrary immune responses via formyl peptide receptor-like 1 in human monocytes. *Mol Pharmacol*. (2006) 70:241–8. doi: 10.1124/mol.105.022103

49. He R, Sang H, Ye RD. Serum amyloid A induces IL-8 secretion through a G protein-coupled receptor, FPRL1/LXA4R. *Blood*. (2003) 101:1572–81. doi: 10.1182/blood-2002-05-1431

50. Lee HY, Kim SD, Shim JW, Kim HJ, Yun J, Baek SH, et al. A pertussis toxin sensitive G-protein-independent pathway is involved in serum amyloid A-induced formyl peptide receptor 2-mediated CCL2 production. *Exp Mol Med*. (2010) 42:302–9. doi: 10.3858/emm.2010.42.4.029

51. Christenson K, Björkman L, Tängemo C, Bylund J. Serum amyloid A inhibits apoptosis of human neutrophils via a P2X7-sensitive pathway independent of formyl peptide receptor-like 1. *J Leukoc Biol*. (2008) 83:139–48. doi: 10.1189/jlb.0507276

52. Li W, Zhu S, Li J, D'Amore J, D'Angelo J, Yang H, et al. Serum amyloid A stimulates PKR expression and HMGB1 release possibly through TLR4/RAGE receptors. *Mol Med*. (2015) 21:515–25. doi: 10.2119/molmed.2015.00109

53. Röcken C, Kientsch-Engel R, Mansfeld S, Stix B, Stubenrauch K, Weigle B, et al. Advanced glycation end products and receptor for advanced glycation end products in AA amyloidosis. *Am J Pathol*. (2003) 162:1213–20. doi: 10.1016/S0002-9440(10)63917-X

54. Yan SD, Zhu H, Zhu A, Golabek A, Du H, Roher A, et al. Receptor-dependent cell stress and amyloid accumulation in systemic amyloidosis. *Nat Med*. (2000) 6:643–51. doi: 10.1038/76216

55. Kennel SJ, Williams A, Stuckey A, Richey T, Wooliver C, Chazin W, et al. The pattern recognition reagents RAGE VC1 and peptide p5 share common binding sites and exhibit specific reactivity with AA amyloid in mice. *Amyloid*. (2016) 23:8–16. doi: 10.3109/13506129.2015.1112782

56. Cheng N, He R, Tian J, Ye PP, Ye RD. Cutting edge: TLR2 is a functional receptor for acute-phase serum amyloid A. *J Immunol*. (2008) 181:22–6. doi: 10.4049/jimmunol.181.1.22

57. Ji YR, Kim HJ, Bae KB, Lee S, Kim MO, Ryoo ZY. Hepatic serum amyloid A1 aggravates T cell-mediated hepatitis by inducing chemokines via Toll-like receptor 2 in mice. *J Biol Chem*. (2015) 290:12804–11. doi: 10.1074/jbc.M114.635763

58. Hiratsuka S, Watanabe A, Sakurai Y, Akashi-Takamura S, Ishibashi S, Miyake K, et al. The S100A8-serum amyloid A3-TLR4 paracrine cascade establishes a pre-metastatic phase. *Nat Cell Biol*. (2008) 10:1349–55. doi: 10.1038/ncb1794

59. Sandri S, Rodriguez D, Gomes E, Monteiro HP, Russo M, Campa A. Is serum amyloid A an endogenous TLR4 agonist? *J Leukoc Biol*. (2008) 83:1174–80. doi: 10.1189/jlb.0407203

60. Deguchi A, Tomita T, Omori T, Komatsu A, Ohto U, Takahashi S, et al. Serum amyloid A3 binds MD-2 to activate p38 and NF-κB pathways in a MyD88-dependent manner. *J Immunol*. (2013) 191:1856–64. doi: 10.4049/jimmunol.1201996

61. Poltorak A, He X, Smirnova I, Liu MY, Van Huffel C, Du X, et al. Defective LPS signaling in C3H/HeJ and C57BL/10ScCr mice: mutations in Tlr4 gene. *Science*. (1998) 282:2085–8. doi: 10.1126/science.282.5396.2085

62. Tomita T, Ieguchi K, Sawamura T, Maru Y. Human serum amyloid A3 (SAA3) protein, expressed as a fusion protein with SAA2, binds the oxidized low density lipoprotein receptor. *PLoS One*. (2015) 10:e0118835. doi: 10.1371/journal.pone.0118835

63. Cai L, de Beer MC, de Beer FC, van der Westhuyzen DR. Serum amyloid A is a ligand for scavenger receptor class B type I and inhibits high density lipoprotein binding and selective lipid uptake. *J Biol Chem*. (2005) 280:2954–61. doi: 10.1074/jbc.M411555200

64. Dember LM, Hawkins PN, Hazenberg BP, Gorevic PD, Merlini G, Butrimiene I, et al. Eprodisate for the treatment of renal disease in AA amyloidosis. *N Engl J Med*. (2007) 356:2349–60. doi: 10.1056/NEJMoa065644

65. Olsson M, Olsson B, Jacobson P, Thelle DS, Björkegren J, Walley A, et al. Expression of the selenoprotein S (SELS) gene in subcutaneous adipose tissue and SELS genotype are associated with metabolic risk factors. *Metab Clin Exp*. (2011) 60:114–20. doi: 10.1016/j.metabol.2010.05.011

66. van der Westhuyzen DR, Cai L, de Beer MC, de Beer FC. Serum amyloid A promotes cholesterol efflux mediated by scavenger receptor B-I. *J Biol Chem*. (2005) 280:35890–5. doi: 10.1074/jbc.M505685200

67. Baranova IN, Vishnyakova TG, Bocharov AV, Kurlander R, Chen Z, Kimelman ML, et al. Serum amyloid A binding to CLA-1 (CD36 and LIMPII analogous-1) mediates serum amyloid A protein-induced activation of ERK1/2 and p38 mitogen-activated protein kinases. *J Biol Chem*. (2005) 280:8031–40. doi: 10.1074/jbc.M405009200

68. Walder K, Kantham L, McMillan JS, Trevaskis J, Kerr L, De Silva A, et al. Tanis: a link between type 2 diabetes and inflammation? *Diabetes*. (2002) 51:1859–66. doi: 10.2337/diabetes.51.6.1859

69. Gao JL, Murphy PM. Species and subtype variants of the N-formyl peptide chemotactic receptor reveal multiple important functional domains. *J Biol Chem*. (1993) 268:25395–401. doi: 10.1016/S0021-9258(19)74405-6

70. Abouelasrar Salama S, Gouwy M, Van Damme J, Struyf S. Acute-serum amyloid A and A-SAA-derived peptides as formyl peptide receptor (FPR) 2 ligands. *Front Endocrinol (Lausanne)*. (2023) 14:1119227. doi: 10.3389/fendo.2023.1119227

71. De Buck M, Gouwy M, Wang JM, Van Snick J, Proost P, Struyf S, et al. The cytokine-serum amyloid A-chemokine network. *Cytokine Growth Factor Rev*. (2016) 30:55–69. doi: 10.1016/j.cytogfr.2015.12.010

72. Ray A, Shakya A, Kumar D, Benson MD, Ray BK. Inflammation-responsive transcription factor SAF-1 activity is linked to the development of amyloid A amyloidosis. *J Immunol*. (2006) 177:2601–9. doi: 10.4049/jimmunol.177.4.2601

73. Karlsson HK, Tsuchida H, Lake S, Koistinen HA, Krook A. Relationship between serum amyloid A level and Tanis/SelS mRNA expression in skeletal muscle and adipose tissue from healthy and type 2 diabetic subjects. *Diabetes*. (2004) 53:1424–8. doi: 10.2337/diabetes.53.6.1424

74. Jensen LE, Whitehead AS. Regulation of serum amyloid A protein expression during the acute-phase response. *Biochem J*. (1998) 334(Pt 3):489–503. doi: 10.1042/bj3340489

75. Arnon S, Litmanovitz I, Regev RH, Bauer S, Shainkin-Kestenbaum R, Dolfin T. Serum amyloid A: an early and accurate marker of neonatal early-onset sepsis. *J Perinatol*. (2007) 27:297–302. doi: 10.1038/sj.jp.7211682

76. Yu MH, Chen MH, Han F, Li Q, Sun RH, Tu YX. Prognostic value of the biomarkers serum amyloid A and nitric oxide in patients with sepsis. *Int Immunopharmacol*. (2018) 62:287–92. doi: 10.1016/j.intimp.2018.07.024

77. Li Y, Xiaojing H, Zhuanyun L, Li D, Yang J. Prognostic value of serum amyloid A in COVID-19: a meta-analysis. *Medicine (Baltimore)*. (2022) 101:e28880. doi: 10.1097/MD.0000000000028880

78. Nakayama T, Sonoda S, Urano T, Yamada T, Okada M. Monitoring both serum amyloid protein A and C-reactive protein as inflammatory markers in infectious diseases. *Clin Chem*. (1993) 39:293–7. doi: 10.1093/clinchem/39.2.293

79. Perez L. Acute phase protein response to viral infection and vaccination. *Arch Biochem Biophys*. (2019) 671:196–202. doi: 10.1016/j.abb.2019.07.013

80. Villapol S, Kryndushkin D, Balarezo MG, Campbell AM, Saavedra JM, Shewmaker FP, et al. Hepatic expression of serum amyloid A1 is induced by traumatic brain injury and modulated by telmisartan. *Am J Pathol*. (2015) 185:2641–52. doi: 10.1016/j.ajpath.2015.06.016

81. Soriano S, Moffet B, Wicker E, Villapol S. Serum amyloid A is expressed in the brain after traumatic brain injury in a sex-dependent manner. *Cell Mol Neurobiol*. (2020) 40:1199–211. doi: 10.1007/s10571-020-00808-3

82. den Hartigh LJ, Wang S, Goodspeed L, Ding Y, Averill M, Subramanian S, et al. Deletion of serum amyloid A3 improves high fat high sucrose diet-induced adipose tissue inflammation and hyperlipidemia in female mice. *PLoS One*. (2014) 9:e108564. doi: 10.1371/journal.pone.0108564

83. Anuurad E, Enkhmaa B, Gungor Z, Zhang W, Tracy RP, Pearson TA, et al. Age as a modulator of inflammatory cardiovascular risk factors. *Arterioscler Thromb Vasc Biol*. (2011) 31:2151–6. doi: 10.1161/ATVBAHA.111.232348

84. Sproston NR, Ashworth JJ. Role of C-reactive protein at sites of inflammation and infection. *Front Immunol*. (2018) 9:754. doi: 10.3389/fimmu.2018.00754

85. Pepys MB, Baltz ML. Acute phase proteins with special reference to C-reactive protein and related proteins (pentaxins) and serum amyloid A protein. *Adv Immunol*. (1983) 34:141–212. doi: 10.1016/s0065-2776(08)60379-x

86. Maury CP. Comparative study of serum amyloid A protein and C-reactive protein in disease. *Clin Sci (Lond)*. (1985) 68:233–8. doi: 10.1042/cs0680233

87. Chambers RE, Hutton CW, Dieppe PA, Whicher JT. Comparative study of C reactive protein and serum amyloid A protein in experimental inflammation. *Ann Rheum Dis*. (1991) 50:677–9. doi: 10.1136/ard.50.10.677

88. O'Brien KD, Brehm BJ, Seeley RJ, Bean J, Wener MH, Daniels S, et al. Diet-induced weight loss is associated with decreases in plasma serum amyloid a and C-reactive protein independent of dietary macronutrient composition in obese subjects. *J Clin Endocrinol Metab*. (2005) 90:2244–9. doi: 10.1210/jc.2004-1011

89. Thorn CF, Lu ZY, Whitehead AS. Regulation of the human acute phase serum amyloid A genes by tumour necrosis factor-alpha, interleukin-6 and glucocorticoids in hepatic and epithelial cell lines. *Scand J Immunol*. (2004) 59:152–8. doi: 10.1111/j.0300-9475.2004.01369.x

90. Speelman T, Dale L, Louw A, Verhoog NJD. The association of acute phase proteins in stress and inflammation-induced T2D. *Cells*. (2022) 11(14):2163. doi: 10.3390/cells11142163

91. Ehlting C, Wolf SD, Bode JG. Acute-phase protein synthesis: a key feature of innate immune functions of the liver. *Biol Chem*. (2021) 402:1129–45. doi: 10.1515/hsz-2021-0209

92. Moura Neto A, Parisi MC, Tambascia MA, Pavin EJ, Alegre SM, Zantut-Wittmann DE. Relationship of thyroid hormone levels and cardiovascular events in patients with type 2 diabetes. *Endocrine*. (2014) 45:84–91. doi: 10.1007/s12020-013-9938-6

93. Moura Neto A, Parisi MC, Alegre SM, Pavin EJ, Tambascia MA, Zantut-Wittmann DE. Relation of thyroid hormone abnormalities with subclinical inflammatory activity in patients with type 1 and type 2 diabetes mellitus. *Endocrine*. (2016) 51:63–71. doi: 10.1007/s12020-015-0651-5

94. Raynes JG, Cooper EH. Comparison of serum amyloid A protein and C-reactive protein concentrations in cancer and non-malignant disease. *J Clin Pathol*. (1983) 36:798–803. doi: 10.1136/jcp.36.7.798

95. Hogarth MB, Gallimore R, Savage P, Palmer AJ, Starr JM, Bulpitt CJ, et al. Acute phase proteins, C-reactive protein and serum amyloid A protein, as prognostic markers in the elderly inpatient. *Age Ageing*. (1997) 26:153–8. doi: 10.1093/ageing/26.2.153

96. Poitou C, Viguerie N, Cancello R, De Matteis R, Cinti S, Stich V, et al. Serum amyloid A: production by human white adipocyte and regulation by obesity and nutrition. *Diabetologia*. (2005) 48:519–28. doi: 10.1007/s00125-004-1654-6

97. Sjöholm K, Palming J, Olofsson LE, Gummesson A, Svensson PA, Lystig TC, et al. A microarray search for genes predominantly expressed in human omental adipocytes: adipose tissue as a major production site of serum amyloid A. *J Clin Endocrinol Metab*. (2005) 90:2233–9. doi: 10.1210/jc.2004-1830

98. Poitou C, Coussieu C, Rouault C, Coupaye M, Cancello R, Bedel JF, et al. Serum amyloid A: a marker of adiposity-induced low-grade inflammation but not of metabolic status. *Obesity (Silver Spring)*. (2006) 14:309–18. doi: 10.1038/oby.2006.40

99. Maier W, Altwegg LA, Corti R, Gay S, Hersberger M, Maly FE, et al. Inflammatory markers at the site of ruptured plaque in acute myocardial infarction: locally increased interleukin-6 and serum amyloid A but decreased C-reactive protein. *Circulation*. (2005) 111:1355–61. doi: 10.1161/01.CIR.0000158479.58589.0A

100. Yamada T, Kakihara T, Kamishima T, Fukuda T, Kawai T. Both acute phase and constitutive serum amyloid A are present in atherosclerotic lesions. *Pathol Int*. (1996) 46:797–800. doi: 10.1111/j.1440-1827.1996.tb03552.x

101. Rosenthal CJ, Franklin EC. Variation with age and disease of an amyloid A protein-related serum component. *J Clin Invest*. (1975) 55:746–53. doi: 10.1172/JCI107985

102. Holzer M, Trieb M, Konya V, Wadsack C, Heinemann A, Marsche G. Aging affects high-density lipoprotein composition and function. *Biochim Biophys Acta*. (2013) 1831:1442–8. doi: 10.1016/j.bbalip.2013.06.004

103. Danesh J, Muir J, Wong YK, Ward M, Gallimore JR, Pepys MB. Risk factors for coronary heart disease and acute-phase proteins. A population-based study. *Eur Heart J*. (1999) 20:954–9. doi: 10.1053/euhj.1998.1309

104. Lee CG, Carr MC, Murdoch SJ, Mitchell E, Woods NF, Wener MH, et al. Adipokines, inflammation, and visceral adiposity across the menopausal transition: a prospective study. *J Clin Endocrinol Metab*. (2009) 94:1104–10. doi: 10.1210/jc.2008-0701

105. Chiba T, Han CY, Vaisar T, Shimokado K, Kargi A, Chen MH, et al. Serum amyloid A3 does not contribute to circulating SAA levels. *J Lipid Res*. (2009) 50:1353–62. doi: 10.1194/jlr.M900089-JLR200

106. Jernås M, Palming J, Sjöholm K, Jennische E, Svensson PA, Gabrielsson BG, et al. Separation of human adipocytes by size: hypertrophic fat cells display distinct gene expression. *FASEB J*. (2006) 20:1540–2. doi: 10.1096/fj.05-5678fje

107. Sjöholm K, Lundgren M, Olsson M, Eriksson JW. Association of serum amyloid A levels with adipocyte size and serum levels of adipokines: differences between men and women. *Cytokine*. (2009) 48:260–6. doi: 10.1016/j.cyto.2009.08.005

108. Siklova-Vitkova M, Klimcakova E, Polak J, Kovacova Z, Tencerova M, Rossmeislova L, et al. Adipose tissue secretion and expression of adipocyte-produced and stromavascular fraction-produced adipokines vary during multiple phases of weight-reducing dietary intervention in obese women. *J Clin Endocrinol Metab*. (2012) 97:E1176–81. doi: 10.1210/jc.2011-2380

109. Imayama I, Ulrich CM, Alfano CM, Wang C, Xiao L, Wener MH, et al. Effects of a caloric restriction weight loss diet and exercise on inflammatory biomarkers in overweight/obese postmenopausal women: a randomized controlled trial. *Cancer Res*. (2012) 72:2314–26. doi: 10.1158/0008-5472.CAN-11-3092

110. Catalán V, Gómez-Ambrosi J, Ramirez B, Rotellar F, Pastor C, Silva C, et al. Proinflammatory cytokines in obesity: impact of type 2 diabetes mellitus and gastric bypass. *Obes Surg*. (2007) 17:1464–74. doi: 10.1007/s11695-008-9424-z

111. Benditt EP, Meek RL. Expression of the third member of the serum amyloid A gene family in mouse adipocytes. *J Exp Med*. (1989) 169:1841–6. doi: 10.1084/jem.169.5.1841

112. Meek RL, Eriksen N, Benditt EP. Murine serum amyloid A3 is a high density apolipoprotein and is secreted by macrophages. *Proc Natl Acad Sci U S A*. (1992) 89:7949–52. doi: 10.1073/pnas.89.17.7949

113. Rokita H, Shirahama T, Cohen AS, Meek RL, Benditt EP, Sipe JD. Differential expression of the amyloid SAA 3 gene in liver and peritoneal macrophages of mice undergoing dissimilar inflammatory episodes. *J Immunol*. (1987) 139:3849–53. doi: 10.4049/jimmunol.139.11.3849

114. Lin Y, Rajala MW, Berger JP, Moller DE, Barzilai N, Scherer PE. Hyperglycemia-induced production of acute phase reactants in adipose tissue. *J Biol Chem*. (2001) 276:42077–83. doi: 10.1074/jbc.M107101200

115. Soukas A, Cohen P, Socci ND, Friedman JM. Leptin-specific patterns of gene expression in white adipose tissue. *Genes Dev*. (2000) 14:963–80. doi: 10.1101/gad.14.8.963

116. Subramanian S, Han C, Chiba T, McMillen T, Wang S, Haw AR, et al. Dietary cholesterol worsens adipose tissue macrophage accumulation and atherosclerosis in obese LDL receptor-deficient mice. *Arterioscler Thromb Vasc Biol*. (2008) 28:685–91. doi: 10.1161/ATVBAHA.107.157685

117. Subramanian S, Goodspeed L, Wang S, Kim J, Zeng L, Ioannou GN, et al. Dietary cholesterol exacerbates hepatic steatosis and inflammation in obese LDL receptor-deficient mice. *J Lipid Res*. (2011) 52:1626–35. doi: 10.1194/jlr.M016246

118. Han CY, Kang I, Harten IA, Gebe JA, Chan CK, Omer M, et al. Adipocyte-derived versican and macrophage-derived biglycan control adipose tissue inflammation in obesity. *Cell Rep*. (2020) 31:107818. doi: 10.1016/j.celrep.2020.107818

119. Den Hartigh LJ, Omer M, Goodspeed L, Wang S, Wietecha T, O'Brien KD, et al. Adipocyte-specific deficiency of NADPH oxidase 4 delays the onset of insulin resistance and attenuates adipose tissue inflammation in obesity. *Arterioscler Thromb Vasc Biol*. (2017) 37:466–75. doi: 10.1161/ATVBAHA.116.308749

120. Scheja L, Heese B, Zitzer H, Michael MD, Siesky AM, Pospisil H, et al. Acute-phase serum amyloid A as a marker of insulin resistance in mice. *Exp Diabetes Res*. (2008) 2008:230837. doi: 10.1155/2008/230837

121. Sanada Y, Yamamoto T, Satake R, Yamashita A, Kanai S, Kato N, et al. Serum amyloid A3 gene expression in adipocytes is an indicator of the interaction with macrophages. *Sci Rep*. (2016) 6:38697. doi: 10.1038/srep38697

122. Tannock LR, De Beer MC, Ji A, Shridas P, Noffsinger VP, den Hartigh L, et al. Serum amyloid A3 is a high density lipoprotein-associated acute-phase protein. *J Lipid Res*. (2018) 59:339–47. doi: 10.1194/jlr.M080887

123. de Oliveira EM, Visniauskas B, Tufik S, Andersen ML, Chagas JR, Campa A. Serum amyloid A production is triggered by sleep deprivation in mice and humans: is that the link between sleep loss and associated comorbidities? *Nutrients*. (2017) 9(3):311. doi: 10.3390/nu9030311

124. Svatikova A, Wolk R, Shamsuzzaman AS, Kara T, Olson EJ, Somers VK. Serum amyloid a in obstructive sleep apnea. *Circulation*. (2003) 108:1451–4. doi: 10.1161/01.CIR.0000089091.09527.B8

125. Parish JM, Adam T, Facchiano L. Relationship of metabolic syndrome and obstructive sleep apnea. *J Clin Sleep Med*. (2007) 3:467–72. doi: 10.5664/jcsm.26910

126. Olsson M, Ahlin S, Olsson B, Svensson PA, Ståhlman M, Borén J, et al. Establishment of a transgenic mouse model specifically expressing human serum amyloid A in adipose tissue. *PLoS One*. (2011) 6:e19609. doi: 10.1371/journal.pone.0019609

127. Ahlin S, Olsson M, Olsson B, Svensson PA, Sjöholm K. No evidence for a role of adipose tissue-derived Serum amyloid A in the development of insulin resistance or obesity-related inflammation in hSAA1(+/-) transgenic mice. *PLoS One*. (2013) 8:e72204. doi: 10.1371/journal.pone.0072204

128. Ather JL, Poynter ME. Serum amyloid A3 is required for normal weight and immunometabolic function in mice. *PLoS One*. (2018) 13:e0192352. doi: 10.1371/journal.pone.0192352

129. Ji A, Trumbauer AC, Noffsinger VP, Jeon H, Patrick AC, De Beer FC, et al. Serum amyloid A is not obligatory for high-fat, high-sucrose, cholesterol-fed diet-induced obesity and its metabolic and inflammatory complications. *PLoS One*. (2022) 17:e0266688. doi: 10.1371/journal.pone.0266688

130. Vercalsteren E, Vranckx C, Vermeire I, Gooijen M, Lijnen R, Scroyen I. Serum amyloid A3 deficiency impairs in vitro and in vivo adipocyte differentiation. *Adipocyte*. (2021) 10:242–50. doi: 10.1080/21623945.2021.1916220

131. de Oliveira EM, Ascar TP, Silva JC, Sandri S, Migliorini S, Fock RA, et al. Serum amyloid A links endotoxaemia to weight gain and insulin resistance in mice. *Diabetologia*. (2016) 59:1760–8. doi: 10.1007/s00125-016-3970-z

132. Qatanani M, Lazar MA. Mechanisms of obesity-associated insulin resistance: many choices on the menu. *Genes Dev*. (2007) 21:1443–55. doi: 10.1101/gad.1550907

133. Burhans MS, Hagman DK, Kuzma JN, Schmidt KA, Kratz M. Contribution of adipose tissue inflammation to the development of type 2 diabetes Mellitus. *Compr Physiol*. (2018) 9:1–58. doi: 10.1002/cphy.c170040

134. Kahn SE, Hull RL, Utzschneider KM. Mechanisms linking obesity to insulin resistance and type 2 diabetes. *Nature*. (2006) 444:840–6. doi: 10.1038/nature05482

135. Raji A, Seely EW, Arky RA, Simonson DC. Body fat distribution and insulin resistance in healthy Asian Indians and Caucasians. *J Clin Endocrinol Metab*. (2001) 86:5366–71. doi: 10.1210/jcem.86.11.7992

136. Paradisi G, Smith L, Burtner C, Leaming R, Garvey WT, Hook G, et al. Dual energy x-ray absorptiometry assessment of fat mass distribution and its association with the insulin resistance syndrome. *Diabetes Care*. (1999) 22:1310–7. doi: 10.2337/diacare.22.8.1310

137. Griffiths K, Pazderska A, Ahmed M, McGowan A, Maxwell AP, McEneny J, et al. Type 2 diabetes in young females results in increased Serum amyloid A and changes to features of high density lipoproteins in both HDL2 and HDL3. *J Diabetes Res*. (2017) 2017:1314864. doi: 10.1155/2017/1314864

138. Tsun JG, Shiu SW, Wong Y, Yung S, Chan TM, Tan KC. Impact of serum amyloid A on cellular cholesterol efflux to serum in type 2 diabetes mellitus. *Atherosclerosis*. (2013) 231:405–10. doi: 10.1016/j.atherosclerosis.2013.10.008

139. Du JL, Liu JF, Men LL, Yao JJ, Sun LP, Sun GH, et al. Effects of five-year intensive multifactorial intervention on the serum amyloid A and macroangiopathy in patients with short-duration type 2 diabetes mellitus. *Chin Med J (Engl)*. (2009) 122:2560–6. doi: 10.3760/cma.j.issn.0366-6999.2009.21.007

140. Kumon Y, Suehiro T, Itahara T, Ikeda Y, Hashimoto K. Serum amyloid A protein in patients with non-insulin-dependent diabetes mellitus. *Clin Biochem*. (1994) 27:469–73. doi: 10.1016/0009-9120(94)00044-v

141. Helmersson J, Vessby B, Larsson A, Basu S. Association of type 2 diabetes with cyclooxygenase-mediated inflammation and oxidative stress in an elderly population. *Circulation*. (2004) 109:1729–34. doi: 10.1161/01.CIR.0000124718.99562.91

142. Samaras K, Botelho NK, Chisholm DJ, Lord RV. Subcutaneous and visceral adipose tissue gene expression of serum adipokines that predict type 2 diabetes. *Obesity (Silver Spring)*. (2010) 18:884–9. doi: 10.1038/oby.2009.443

143. Lewis KE, Kirk EA, McDonald TO, Wang S, Wight TN, O'Brien KD, et al. Increase in serum amyloid a evoked by dietary cholesterol is associated with increased atherosclerosis in mice. *Circulation*. (2004) 110:540–5. doi: 10.1161/01.CIR.0000136819.93989.E1

144. Yassine HN, Trenchevska O, He H, Borges CR, Nedelkov D, Mack W, et al. Serum amyloid a truncations in type 2 diabetes mellitus. *PLoS One*. (2015) 10: e0115320. doi: 10.1371/journal.pone.0115320

145. Du JL, Sun CK, Lü B, Men LL, Yao JJ, An LJ, et al. Association of SelS mRNA expression in omental adipose tissue with Homa-IR and serum amyloid A in patients with type 2 diabetes mellitus. *Chin Med J (Engl)*. (2008) 121:1165–8. doi: 10.1097/00029330-200807010-00003

146. Ye XY, Xue YM, Sha JP, Li CZ, Zhen ZJ. Serum amyloid A attenuates cellular insulin sensitivity by increasing JNK activity in 3T3-L1 adipocytes. *J Endocrinol Invest*. (2009) 32:568–75. doi: 10.1007/BF03346510

147. Liu Q, Sun J, Xu T, Bian G, Yang F. Associations of serum amyloid A and 25-hydroxyvitamin D with diabetic nephropathy: a cross-sectional study. *J Clin Lab Anal*. (2022) 36:e24283. doi: 10.1002/jcla.24283

148. Pitsavos C, Tampourlou M, Panagiotakos DB, Skoumas Y, Chrysohoou C, Nomikos T, et al. Association between low-grade systemic inflammation and type 2 diabetes mellitus among men and women from the ATTICA study. *Rev Diabet Stud*. (2007) 4:98–104. doi: 10.1900/RDS.2007.4.98

149. Ebeling P, Teppo AM, Koistinen HA, Viikari J, Rönnemaa T, Nissén M, et al. Troglitazone reduces hyperglycaemia and selectively acute-phase serum proteins in patients with type II diabetes. *Diabetologia*. (1999) 42:1433–8. doi: 10.1007/s001250051315

150. Azabdaftari A, van der Giet M, Schuchardt M, Hennermann JB, Plöckinger U, Querfeld U. The cardiovascular phenotype of adult patients with phenylketonuria. *Orphanet J Rare Dis*. (2019) 14:213. doi: 10.1186/s13023-019-1188-0

151. Loporchio DF, Tam EK, Cho J, Chung J, Jun GR, Xia W, et al. Cytokine levels in human vitreous in proliferative diabetic retinopathy. *Cells*. (2021) 10(5):1069. doi: 10.3390/cells10051069

152. Dieter BP, McPherson SM, Afkarian M, de Boer IH, Mehrotra R, Short R, et al. Serum amyloid a and risk of death and end-stage renal disease in diabetic kidney disease. *J Diabetes Complications*. (2016) 30:1467–72. doi: 10.1016/j.jdiacomp.2016.07.018

153. Dalla Vestra M, Mussap M, Gallina P, Bruseghin M, Cernigoi AM, Saller A, et al. Acute-phase markers of inflammation and glomerular structure in patients with type 2 diabetes. *J Am Soc Nephrol*. (2005) 16(Suppl 1):S78–82. doi: 10.1681/asn.2004110961

154. Saliu TP, Yazawa N, Hashimoto K, Miyata K, Kudo A, Horii M, et al. Serum amyloid A3 promoter-driven luciferase activity enables visualization of diabetic kidney disease. *Int J Mol Sci*. (2022) 23(2):899. doi: 10.3390/ijms23020899

155. Eren MA, Vural M, Cece H, Camuzcuoglu H, Yildiz S, Toy H, et al. Association of serum amyloid A with subclinical atherosclerosis in women with gestational diabetes. *Gynecol Endocrinol*. (2012) 28:1010–3. doi: 10.3109/09513590.2012.705371

156. Hrolfsdottir L, Schalkwijk CG, Birgisdottir BE, Gunnarsdottir I, Maslova E, Granström C, et al. Maternal diet, gestational weight gain, and inflammatory markers during pregnancy. *Obesity (Silver Spring)*. (2016) 24:2133–9. doi: 10.1002/oby.21617

157. Pöyhönen-Alho M, Ebeling P, Saarinen A, Kaaja R. Decreased variation of inflammatory markers in gestational diabetes. *Diabetes Metab Res Rev*. (2011) 27:269–76. doi: 10.1002/dmrr.1170

158. Dunaif A. Insulin resistance and the polycystic ovary syndrome: mechanism and implications for pathogenesis. *Endocr Rev*. (1997) 18:774–800. doi: 10.1210/edrv.18.6.0318

159. Diamanti-Kandarakis E. Insulin resistance in PCOS. *Endocrine*. (2006) 30:13–7. doi: 10.1385/ENDO:30:1:13

160. Tan BK, Adya R, Shan X, Aghilla M, Lehnert H, Keay SD, et al. The anti-atherogenic aspect of metformin treatment in insulin resistant women with the polycystic ovary syndrome: role of the newly established pro-inflammatory adipokine acute-phase serum amyloid A; evidence of an adipose tissue-monocyte axis. *Atherosclerosis*. (2011) 216:402–8. doi: 10.1016/j.atherosclerosis.2010.08.069

161. Arner P. Effects of testosterone on fat cell lipolysis. Species differences and possible role in polycystic ovarian syndrome. *Biochimie*. (2005) 87:39–43. doi: 10.1016/j.biochi.2004.11.012

162. Yki-Järvinen H. Non-alcoholic fatty liver disease as a cause and a consequence of metabolic syndrome. *Lancet Diabetes Endocrinol*. (2014) 2:901–10. doi: 10.1016/S2213-8587(14)70032-4

163. Grundy SM, Brewer HB, Cleeman JI, Smith SC, Lenfant C, Association AH, et al. Definition of metabolic syndrome: report of the national heart, lung, and blood institute/American heart association conference on scientific issues related to definition. *Circulation*. (2004) 109:433–8. doi: 10.1161/01.CIR.0000111245.75752.C6

164. Reddy P, Lent-Schochet D, Ramakrishnan N, McLaughlin M, Jialal I. Metabolic syndrome is an inflammatory disorder: a conspiracy between adipose tissue and phagocytes. *Clin Chim Acta*. (2019) 496:35–44. doi: 10.1016/j.cca.2019.06.019

165. Kappelle PJ, Bijzet J, Hazenberg BP, Dullaart RP. Lower serum paraoxonase-1 activity is related to higher serum amyloid a levels in metabolic syndrome. *Arch Med Res*. (2011) 42:219–25. doi: 10.1016/j.arcmed.2011.05.002

166. Yuan ZY, Zhang XX, Wu YJ, Zeng ZP, She WM, Chen SY, et al. Serum amyloid A levels in patients with liver diseases. *World J Gastroenterol*. (2019) 25:6440–50. doi: 10.3748/wjg.v25.i43.6440

167. Jacobs M, van Greevenbroek MM, van der Kallen CJ, Ferreira I, Feskens EJ, Jansen EH, et al. The association between the metabolic syndrome and alanine amino transferase is mediated by insulin resistance via related metabolic intermediates (the cohort on diabetes and atherosclerosis Maastricht [CODAM] study). *Metab Clin Exp*. (2011) 60:969–75. doi: 10.1016/j.metabol.2010.09.006

168. Jiang B, Wang D, Hu Y, Li W, Liu F, Zhu X, et al. Serum amyloid A1 exacerbates hepatic steatosis via TLR4-mediated NF-κB signaling pathway. *Mol Metab*. (2022) 59:101462. doi: 10.1016/j.molmet.2022.101462

169. Li D, Xie P, Zhao S, Zhao J, Yao Y, Zhao Y, et al. Hepatocytes derived increased SAA1 promotes intrahepatic platelet aggregation and aggravates liver inflammation in NAFLD. *Biochem Biophys Res Commun*. (2021) 555:54–60. doi: 10.1016/j.bbrc.2021.02.124

170. Sultan M, Ben-Ari Z, Masoud R, Pappo O, Harats D, Kamari Y, et al. Interleukin-1α and interleukin-1β play a central role in the pathogenesis of fulminant hepatic failure in mice. *PLoS One*. (2017) 12:e0184084. doi: 10.1371/journal.pone.0184084

171. Ross R. The pathogenesis of atherosclerosis–an update. *N Engl J Med*. (1986) 314:488–500. doi: 10.1056/NEJM198602203140806

172. Ridker PM, Everett BM, Thuren T, MacFadyen JG, Chang WH, Ballantyne C, et al. Antiinflammatory therapy with canakinumab for atherosclerotic disease. *N Engl J Med*. (2017) 377:1119–31. doi: 10.1056/NEJMoa1707914

173. Ridker PM, Hennekens CH, Buring JE, Rifai N. C-reactive protein and other markers of inflammation in the prediction of cardiovascular disease in women. *N Engl J Med*. (2000) 342:836–43. doi: 10.1056/NEJM200003233421202

174. Jousilahti P, Salomaa V, Rasi V, Vahtera E, Palosuo T. The association of c-reactive protein, serum amyloid a and fibrinogen with prevalent coronary heart disease–baseline findings of the PAIS project. *Atherosclerosis*. (2001) 156:451–6. doi: 10.1016/s0021-9150(00)00681-x

175. O'Brien KD, McDonald TO, Kunjathoor V, Eng K, Knopp EA, Lewis K, et al. Serum amyloid A and lipoprotein retention in murine models of atherosclerosis. *Arterioscler Thromb Vasc Biol*. (2005) 25:785–90. doi: 10.1161/01.ATV.0000158383.65277.2b

176. Dong Z, Wu T, Qin W, An C, Wang Z, Zhang M, et al. Serum amyloid A directly accelerates the progression of atherosclerosis in apolipoprotein E-deficient mice. *Mol Med*. (2011) 17:1357–64. doi: 10.2119/molmed.2011.00186

177. Thompson JC, Jayne C, Thompson J, Wilson PG, Yoder MH, Webb N, et al. A brief elevation of serum amyloid A is sufficient to increase atherosclerosis. *J Lipid Res*. (2015) 56:286–93. doi: 10.1194/jlr.M054015

178. Krishack PA, Bhanvadia CV, Lukens J, Sontag TJ, De Beer MC, Getz GS, et al. Serum amyloid A facilitates early lesion development in ldlr-/- mice. *J Am Heart Assoc*. (2015) 4(7):e001858. doi: 10.1161/JAHA.115.001858

179. Petri MH, Laguna-Fernández A, Gonzalez-Diez M, Paulsson-Berne G, Hansson GK, Bäck M. The role of the FPR2/ALX receptor in atherosclerosis development and plaque stability. *Cardiovasc Res*. (2015) 105:65–74. doi: 10.1093/cvr/cvu224

180. Webb NR, De Beer MC, Wroblewski JM, Ji A, Bailey W, Shridas P, et al. Deficiency of endogenous acute-phase Serum amyloid A protects apoE-/- mice from angiotensin II-induced abdominal aortic aneurysm formation. *Arterioscler Thromb Vasc Biol*. (2015) 35:1156–65. doi: 10.1161/ATVBAHA.114.304776

181. Thompson JC, Wilson PG, Shridas P, Ji A, de Beer M, de Beer FC, et al. Serum amyloid A3 is pro-atherogenic. *Atherosclerosis*. (2017) 268:32–5. doi: 10.1016/j.atherosclerosis.2017.11.011

182. Chait A, Wang S, Goodspeed L, Gomes D, Turk KE, Wietecha T, et al. Sexually dimorphic relationships among Saa3 (Serum amyloid A3) inflammation, and

cholesterol metabolism modulate atherosclerosis in mice. *Arterioscler Thromb Vasc Biol*. (2021):ATVBAHA121316066. doi: 10.1161/ATVBAHA.121.316066

183. Koike T, Kitajima S, Yu Y, Nishijima K, Zhang J, Ozaki Y, et al. Human C-reactive protein does not promote atherosclerosis in transgenic rabbits. *Circulation*. (2009) 120:2088–94. doi: 10.1161/CIRCULATIONAHA.109.872796

184. Shridas P, Ji A, Trumbauer AC, Noffsinger VP, Leung SW, Dugan AJ, et al. Adipocyte-Derived Serum amyloid A promotes angiotensin II-induced abdominal aortic aneurysms in obese C57BL/6J mice. *Arterioscler Thromb Vasc Biol*. (2022) 42:632–43. doi: 10.1161/ATVBAHA.121.317225

185. Yamada T, Wada A, Itoh K, Igari J. Serum amyloid A secretion from monocytic leukaemia cell line THP-1 and cultured human peripheral monocytes. *Scand J Immunol*. (2000) 52:7–12. doi: 10.1046/j.1365-3083.2000.00734.x

186. Ray BK, Ray A. Involvement of an SAF-like transcription factor in the activation of serum amyloid A gene in monocyte/macrophage cells by lipopolysaccharide. *Biochemistry*. (1997) 36:4662–8. doi: 10.1021/bi9624595

187. Urieli-Shoval S, Meek RL, Hanson RH, Eriksen N, Benditt EP. Human serum amyloid A genes are expressed in monocyte/macrophage cell lines. *Am J Pathol*. (1994) 145:650–60.

188. Zhang X, Chen J, Wang S. Serum amyloid A induces a vascular smooth muscle cell phenotype switch through the p38 MAPK signaling pathway. *Biomed Res Int*. (2017) 2017:4941379. doi: 10.1155/2017/4941379

189. Lv M, Xia YF, Li B, Liu H, Pan JY, Li BB, et al. Serum amyloid A stimulates vascular endothelial growth factor receptor 2 expression and angiogenesis. *J Physiol Biochem*. (2016) 72:71–81. doi: 10.1007/s13105-015-0462-4

190. Yeop Han C, Kargi A, Omer M, Chan C, Wabitsch M, O'Brien K, et al. Differential effect of saturated and unsaturated free fatty acids on the generation of monocyte adhesion and chemotactic factors by adipocytes: dissociation of adipocyte hypertrophy from inflammation. *Diabetes*. (2010) 59:386–96. doi: 10.2337/db09-0925

191. Han CY, Tang C, Guevara ME, Wei H, Wietecha T, Shao B, et al. Serum amyloid A impairs the antiinflammatory properties of HDL. *J Clin Invest*. (2016) 126:266–81. doi: 10.1172/JCI83475

192. Han CY, Kang I, Omer M, Wang S, Wietecha T, Wight TN, et al. Serum amyloid A-containing HDL binds adipocyte-derived versican and macrophage-derived biglycan, reducing its antiinflammatory properties. *JCI Insight*. (2020) 5(20): e142635. doi: 10.1172/jci.insight.142635

193. Vaisar T, Tang C, Babenko I, Hutchins P, Wimberger J, Suffredini AF, et al. Inflammatory remodeling of the HDL proteome impairs cholesterol efflux capacity. *J Lipid Res*. (2015) 56:1519–30. doi: 10.1194/jlr.M059089

194. O'Brien KD, Olin KL, Alpers CE, Chiu W, Ferguson M, Hudkins K, et al. Comparison of apolipoprotein and proteoglycan deposits in human coronary atherosclerotic plaques: colocalization of biglycan with apolipoproteins. *Circulation*. (1998) 98:519–27. doi: 10.1161/01.cir.98.6.519

195. Chiba T, Chang MY, Wang S, Wight TN, McMillen TS, Oram JF, et al. Serum amyloid A facilitates the binding of high-density lipoprotein from mice injected with lipopolysaccharide to vascular proteoglycans. *Arterioscler Thromb Vasc Biol*. (2011) 31:1326–32. doi: 10.1161/ATVBAHA.111.226159

196. Williams KJ, Tabas I. The response-to-retention hypothesis of atherogenesis reinforced. *Curr Opin Lipidol*. (1998) 9:471–4. doi: 10.1097/00041433-199810000-00012

197. Song C, Shen Y, Yamen E, Hsu K, Yan W, Witting PK, et al. Serum amyloid A may potentiate prothrombotic and proinflammatory events in acute coronary syndromes. *Atherosclerosis*. (2009) 202:596–604. doi: 10.1016/j.atherosclerosis.2008.04.049

198. Page MJ, Thomson GJA, Nunes JM, Engelbrecht AM, Nell TA, de Villiers WJS, et al. Serum amyloid A binds to fibrin(ogen), promoting fibrin amyloid formation. *Sci Rep*. (2019) 9:3102. doi: 10.1038/s41598-019-39056-x

199. Zhi W, Sharma A, Purohit S, Miller E, Bode B, Anderson SW, et al. Discovery and validation of serum protein changes in type 1 diabetes patients using high throughput two dimensional liquid chromatography-mass spectrometry and immunoassays. *Mol Cell Proteomics*. (2011) 10:M111.012203. doi: 10.1074/mcp.M111.012203

200. McEneny J, Daniels JA, McGowan A, Gunness A, Moore K, Stevenson M, et al. A cross-sectional study demonstrating increased Serum amyloid A related inflammation in high-density lipoproteins from subjects with type 1 diabetes Mellitus and how this association was augmented by poor glycaemic control. *J Diabetes Res*. (2015) 2015:351601. doi: 10.1155/2015/351601

201. Lenzen S. The mechanisms of alloxan- and streptozotocin-induced diabetes. *Diabetologia*. (2008) 51:216–26. doi: 10.1007/s00125-007-0886-7

202. Rakieten N, Rakieten ML, Nadkarni MR. Studies on the diabetogenic action of streptozotocin (NSC-37917). *Cancer Chemother Rep*. (1963) 29:91–8.

203. Pahwa R, Balderas M, Jialal I, Chen X, Luna RA, Devaraj S. Gut microbiome and inflammation: a study of diabetic inflammasome-knockout mice. *J Diabetes Res*. (2017) 2017:6519785. doi: 10.1155/2017/6519785

204. den Hartigh LJ, Han CY, Wang S, Omer M, Chait A. 10E,12Z-conjugated Linoleic acid impairs adipocyte triglyceride storage by enhancing fatty acid oxidation, lipolysis, and mitochondrial reactive oxygen species. *J Lipid Res*. (2013) 54:2964–78. doi: 10.1194/jlr.M035188

205. Shen C, Sun XG, Liu N, Mu Y, Hong CC, Wei W, et al. Increased serum amyloid A and its association with autoantibodies, acute phase reactants and disease activity in patients with rheumatoid arthritis. *Mol Med Rep*. (2015) 11:1528–34. doi: 10.3892/mmr.2014.2804

206. Hilliquin P. Biological markers in inflammatory rheumatic diseases. *Cell Mol Biol (Noisy-le-Grand)*. (1995) 41:993–1006.

207. Maury CP, Teppo AM, Wegelius O. Relationship between urinary sialylated saccharides, serum amyloid A protein, and C-reactive protein in rheumatoid arthritis and systemic lupus erythematosus. *Ann Rheum Dis*. (1982) 41:268–71. doi: 10.1136/ard.41.3.268

208. Kasahara K, Tanoue T, Yamashita T, Yodoi K, Matsumoto T, Emoto T, et al. Commensal bacteria at the crossroad between cholesterol homeostasis and chronic inflammation in atherosclerosis. *J Lipid Res*. (2017) 58:519–28. doi: 10.1194/jlr.M072165

209. Lee JY, Hall JA, Kroehling L, Wu L, Najar T, Nguyen HH, et al. Serum amyloid A proteins induce pathogenic Th17 cells and promote inflammatory disease. *Cell*. (2020) 180:79–91.e16. doi: 10.1016/j.cell.2019.11.026

210. Furuzawa-Carballeda J, Vargas-Rojas MI, Cabral AR. Autoimmune inflammation from the Th17 perspective. *Autoimmun Rev*. (2007) 6:169–75. doi: 10.1016/j.autrev.2006.10.002

211. Chambers RE, MacFarlane DG, Whicher JT, Dieppe PA. Serum amyloid-A protein concentration in rheumatoid arthritis and its role in monitoring disease activity. *Ann Rheum Dis*. (1983) 42:665–7. doi: 10.1136/ard.42.6.665

212. de Seny D, Cobraiville G, Charlier E, Neuville S, Esser N, Malaise D, et al. Acute-phase serum amyloid a in osteoarthritis: regulatory mechanism and proinflammatory properties. *PLoS One*. (2013) 8:e66769. doi: 10.1371/journal.pone.0066769

213. O'Hara R, Murphy EP, Whitehead AS, FitzGerald O, Bresnihan B. Local expression of the serum amyloid A and formyl peptide receptor-like 1 genes in synovial tissue is associated with matrix metalloproteinase production in patients with inflammatory arthritis. *Arthritis Rheum*. (2004) 50:1788–99. doi: 10.1002/art.20301

214. Geurts J, Joosten LA, Takahashi N, Arntz OJ, Glück A, Bennink MB, et al. Computational design and application of endogenous promoters for transcriptionally targeted gene therapy for rheumatoid arthritis. *Mol Ther*. (2009) 17:1877–87. doi: 10.1038/mt.2009.182

215. Connolly M, Mullan RH, McCormick J, Matthews C, Sullivan O, Kennedy A, et al. Acute-phase serum amyloid A regulates tumor necrosis factor α and matrix turnover and predicts disease progression in patients with inflammatory arthritis before and after biologic therapy. *Arthritis Rheum*. (2012) 64:1035–45. doi: 10.1002/art.33455

216. Migita K, Kawabe Y, Tominaga M, Origuchi T, Aoyagi T, Eguchi K. Serum amyloid A protein induces production of matrix metalloproteinases by human synovial fibroblasts. *Lab Invest*. (1998) 78:535–9.

217. Hwang YG, Balasubramani GK, Metes ID, Levesque MC, Bridges SL, Moreland LW. Differential response of serum amyloid A to different therapies in early rheumatoid arthritis and its potential value as a disease activity biomarker. *Arthritis Res Ther*. (2016) 18:108. doi: 10.1186/s13075-016-1009-y

218. Eichele DD, Kharbanda KK. Dextran sodium sulfate colitis murine model: an indispensable tool for advancing our understanding of inflammatory bowel diseases pathogenesis. *World J Gastroenterol*. (2017) 23:6016–29. doi: 10.3748/wjg.v23.i33.6016

219. Roda G, Chien Ng S, Kotze PG, Argollo M, Panaccione R, Spinelli A, et al. Crohn's disease. *Nat Rev Dis Primers*. (2020) 6:22. doi: 10.1038/s41572-020-0156-2

220. Bourgonje AR, von Martels JZH, Gabriëls RY, Blokzijl T, Buist-Homan M, Heegsma J, et al. A combined set of four serum inflammatory biomarkers reliably predicts endoscopic disease activity in inflammatory bowel disease. *Front Med (Lausanne)*. (2019) 6:251. doi: 10.3389/fmed.2019.00251

221. Chambers RE, Stross P, Barry RE, Whicher JT. Serum amyloid A protein compared with C-reactive protein, alpha 1-antichymotrypsin and alpha 1-acid glycoprotein as a monitor of inflammatory bowel disease. *Eur J Clin Invest*. (1987) 17:460–7. doi: 10.1111/j.1365-2362.1987.tb01143.x

222. Wakai M, Hayashi R, Tanaka S, Naito T, Kumada J, Nomura M, et al. Serum amyloid A is a better predictive biomarker of mucosal healing than C-reactive protein in ulcerative colitis in clinical remission. *BMC Gastroenterol*. (2020) 20:85. doi: 10.1186/s12876-020-01229-8

223. Roblin X, Serone A, Yoon OK, Zhuo L, Grant E, Woo J, et al. Effects of JAK1-preferential inhibitor filgotinib on circulating biomarkers and whole blood genes/pathways of patients with moderately to severely active Crohn's disease. *Inflamm Bowel Dis*. (2022) 28:1207–18. doi: 10.1093/ibd/izab253

224. Eckhardt ER, Witta J, Zhong J, Arsenescu R, Arsenescu V, Wang Y, et al. Intestinal epithelial serum amyloid A modulates bacterial growth in vitro and pro-inflammatory responses in mouse experimental colitis. *BMC Gastroenterol*. (2010) 10:133. doi: 10.1186/1471-230X-10-133

225. Yarur AJ, Quintero MA, Jain A, Czul F, Barkin JS, Abreu MT. Serum amyloid A as a surrogate marker for mucosal and histologic inflammation in patients with Crohn's disease. *Inflamm Bowel Dis*. (2017) 23:158–64. doi: 10.1097/MIB.0000000000000991

226. Fritsch J, Garces L, Quintero MA, Pignac-Kobinger J, Santander AM, Fernández I, et al. Low-Fat, high-fiber diet reduces markers of inflammation and dysbiosis and improves quality of life in patients with ulcerative colitis. *Clin Gastroenterol Hepatol*. (2021) 19:1189–99.e30. doi: 10.1016/j.cgh.2020.05.026

227. Vidal-Lletjós S, Andriamihaja M, Blais A, Grauso M, Lepage P, Davila AM, et al. Mucosal healing progression after acute colitis in mice. *World J Gastroenterol*. (2019) 25:3572–89. doi: 10.3748/wjg.v25.i27.3572

228. Zhang G, Liu J, Wu L, Fan Y, Sun L, Qian F, et al. Elevated expression of serum amyloid A 3 protects colon epithelium against acute injury through TLR2-dependent induction of neutrophil IL-22 expression in a mouse model of colitis. *Front Immunol*. (2018) 9:1503. doi: 10.3389/fimmu.2018.01503

229. Sann H, Erichsen J, Hessmann M, Pahl A, Hoffmeyer A. Efficacy of drugs used in the treatment of IBD and combinations thereof in acute DSS-induced colitis in mice. *Life Sci*. (2013) 92:708–18. doi: 10.1016/j.lfs.2013.01.028

230. Foligné B, Peys E, Vandenkerckhove J, Van Hemel J, Dewulf J, Breton J, et al. Spores from two distinct colony types of the strain Bacillus subtilis PB6 substantiate anti-inflammatory probiotic effects in mice. *Clin Nutr*. (2012) 31:987–94. doi: 10.1016/j.clnu.2012.05.016

231. Kono T, Kaneko A, Hira Y, Suzuki T, Chisato N, Ohtake N, et al. Anti-colitis and -adhesion effects of daikenchuto via endogenous adrenomedullin enhancement in Crohn's disease mouse model. *J Crohns Colitis*. (2010) 4:161–70. doi: 10.1016/j.crohns.2009.09.006

232. Davis TA, Conradie D, Shridas P, de Beer FC, Engelbrecht AM, de Villiers WJS. Serum amyloid A promotes inflammation-associated damage and tumorigenesis in a mouse model of colitis-associated cancer. *Cell Mol Gastroenterol Hepatol*. (2021) 12:1329–41. doi: 10.1016/j.jcmgh.2021.06.016

233. Ramadori G, Rieder H, Sipe J, Shirahama T, Meyer zum Büschenfelde KH. Murine tissue macrophages synthesize and secrete amyloid proteins different to amyloid A (AA). *Eur J Clin Invest*. (1989) 19:316–22. doi: 10.1111/j.1365-2362.1989.tb00236.x

234. Hagihara K, Nishikawa T, Isobe T, Song J, Sugamata Y, Yoshizaki K. IL-6 plays a critical role in the synergistic induction of human serum amyloid A (SAA) gene when stimulated with proinflammatory cytokines as analyzed with an SAA isoform real-time quantitative RT-PCR assay system. *Biochem Biophys Res Commun*. (2004) 314:363–9. doi: 10.1016/j.bbrc.2003.12.096

235. Cicarelli DD, Vieira JE, Benseñor FE. Comparison of C-reactive protein and serum amyloid a protein in septic shock patients. *Mediators Inflamm*. (2008) 2008:631414. doi: 10.1155/2008/631414

236. Morrow JF, Stearman RS, Peltzman CG, Potter DA. Induction of hepatic synthesis of serum amyloid A protein and actin. *Proc Natl Acad Sci U S A*. (1981) 78:4718–22. doi: 10.1073/pnas.78.8.4718

237. Nguyen TV, Ukairo O, Khetani SR, McVay M, Kanchagar C, Seghezzi W, et al. Establishment of a hepatocyte-kupffer cell coculture model for assessment of proinflammatory cytokine effects on metabolizing enzymes and drug transporters. *Drug Metab Dispos*. (2015) 43:774–85. doi: 10.1124/dmd.114.061317

238. Lowell CA, Stearman RS, Morrow JF. Transcriptional regulation of serum amyloid A gene expression. *J Biol Chem*. (1986) 261:8453–61. doi: 10.1016/S0021-9258(19)83933-9

239. Siegmund SV, Schlosser M, Schildberg FA, Seki E, De Minicis S, Uchinami H, et al. Serum amyloid A induces inflammation, proliferation and cell death in activated hepatic stellate cells. *PLoS One*. (2016) 11:e0150893. doi: 10.1371/journal.pone.0150893

240. Betts JC, Cheshire JK, Akira S, Kishimoto T, Woo P. The role of NF-kappa B and NF-IL6 transactivating factors in the synergistic activation of human serum amyloid A gene expression by interleukin-1 and interleukin-6. *J Biol Chem*. (1993) 268:25624–31. doi: 10.1016/S0021-9258(19)74435-4

241. Song C, Hsu K, Yamen E, Yan W, Fock J, Witting PK, et al. Serum amyloid A induction of cytokines in monocytes/macrophages and lymphocytes. *Atherosclerosis*. (2009) 207:374–83. doi: 10.1016/j.atherosclerosis.2009.05.007

242. Filippin-Monteiro FB, de Oliveira EM, Sandri S, Knebel FH, Albuquerque RC, Campa A. Serum amyloid A is a growth factor for 3T3-L1 adipocytes, inhibits differentiation and promotes insulin resistance. *Int J Obes (Lond)*. (2012) 36:1032–9. doi: 10.1038/ijo.2011.193

243. Liu LR, Lin SP, Chen CC, Chen YJ, Tai CC, Chang SC, et al. Serum amyloid A induces lipolysis by downregulating perilipin through ERK1/2 and PKA signaling pathways. *Obesity (Silver Spring)*. (2011) 19:2301–9. doi: 10.1038/oby.2011.176

244. van Bilsen JHM, van den Brink W, van den Hoek AM, Dulos R, Caspers MPM, Kleemann R, et al. Mechanism-based biomarker prediction for low-grade inflammation in liver and adipose tissue. *Front Physiol*. (2021) 12:703370. doi: 10.3389/fphys.2021.703370

245. Sommer G, Weise S, Kralisch S, Scherer PE, Lössner U, Blüher M, et al. The adipokine SAA3 is induced by interleukin-1beta in mouse adipocytes. *J Cell Biochem*. (2008) 104:2241–7. doi: 10.1002/jcb.21782

246. Nakarai H, Yamashita A, Nagayasu S, Iwashita M, Kumamoto S, Ohyama H, et al. Adipocyte-macrophage interaction may mediate LPS-induced low-grade inflammation: potential link with metabolic complications. *Innate Immun*. (2012) 18:164–70. doi: 10.1177/1753425910393370

247. Reigstad CS, Bäckhed F. Microbial regulation of SAA3 expression in mouse colon and adipose tissue. *Gut Microbes*. (2010) 1:55–7. doi: 10.4161/gmic.1.1.10514

248. Thorn CF, Whitehead AS. Differential glucocorticoid enhancement of the cytokine-driven transcriptional activation of the human acute phase serum amyloid A genes, SAA1 and SAA2. *J Immunol*. (2002) 169:399–406. doi: 10.4049/jimmunol.169.1.399

249. Zhang XS, Yin YS, Wang J, Battaglia T, Krautkramer K, Li WV, et al. Maternal cecal microbiota transfer rescues early-life antibiotic-induced enhancement of type 1 diabetes in mice. *Cell Host Microbe*. (2021) 29:1249–65.9. doi: 10.1016/j.chom.2021.06.014

250. Uhlar CM, Grehan S, Steel DM, Steinkasserer A, Whitehead AS. Use of the acute phase serum amyloid A2 (SAA2) gene promoter in the analysis of pro- and anti-inflammatory mediators: differential kinetics of SAA2 promoter induction by IL-1 beta and TNF-alpha compared to IL-6. *J Immunol Methods*. (1997) 203:123–30. doi: 10.1016/s0022-1759(96)00220-7

251. Migita K, Abiru S, Nakamura M, Komori A, Yoshida Y, Yokoyama T, et al. Lipopolysaccharide signaling induces serum amyloid A (SAA) synthesis in human hepatocytes in vitro. *FEBS Lett*. (2004) 569:235–9. doi: 10.1016/j.febslet.2004.05.072

252. Edbrooke MR, Foldi J, Cheshire JK, Li F, Faulkes DJ, Woo P. Constitutive and NF-kappa B-like proteins in the regulation of the serum amyloid A gene by interleukin 1. *Cytokine*. (1991) 3:380–8. doi: 10.1016/1043-4666(91)90041-b

253. Faty A, Ferré P, Commans S. The acute phase protein Serum amyloid A induces lipolysis and inflammation in human adipocytes through distinct pathways. *PLoS One*. (2012) 7:e34031. doi: 10.1371/journal.pone.0034031

254. Wang YC, Kuo WH, Chen CY, Lin HY, Wu HT, Liu BH, et al. Docosahexaenoic acid regulates serum amyloid A protein to promote lipolysis through down regulation of perilipin. *J Nutr Biochem*. (2010) 21:317–24. doi: 10.1016/j.jnutbio.2009.01.004

255. Sun W. Analysis of single-cell/nucleus transcriptome data in adipose tissue. *Methods Mol Biol*. (2022) 2448:291–306. doi: 10.1007/978-1-0716-2087-8_19

256. Deutsch A, Feng D, Pessin JE, Shinoda K. The impact of single-cell genomics on adipose tissue research. *Int J Mol Sci*. (2020) 21(13):4773. doi: 10.3390/ijms21134773

257. Bäckdahl J, Franzén L, Massier L, Li Q, Jalkanen J, Gao H, et al. Spatial mapping reveals human adipocyte subpopulations with distinct sensitivities to insulin. *Cell Metab*. (2021) 33:2301. doi: 10.1016/j.cmet.2021.10.012

258. Kotnik P, Fischer-Posovszky P, Wabitsch M. RBP4: a controversial adipokine. *Eur J Endocrinol*. (2011) 165:703–11. doi: 10.1530/EJE-11-0431

259. Funcke JB, Scherer PE. Beyond adiponectin and leptin: adipose tissue-derived mediators of inter-organ communication. *J Lipid Res*. (2019) 60:1648–84. doi: 10.1194/jlr.R094060

260. Doyle LM, Wang MZ. Overview of extracellular vesicles, their origin, composition, purpose, and methods for exosome isolation and analysis. *Cells*. (2019) 8(7):727. doi: 10.3390/cells8070727

261. Zhao R, Zhao T, He Z, Cai R, Pang W. Composition, isolation, identification and function of adipose tissue-derived exosomes. *Adipocyte*. (2021) 10:587–604. doi: 10.1080/21623945.2021.1983242

262. Hartwig S, De Filippo E, Göddeke S, Knebel B, Kotzka J, Al-Hasani H, et al. Exosomal proteins constitute an essential part of the human adipose tissue secretome. *Biochim Biophys Acta Proteins Proteom*. (2019) 1867:140172. doi: 10.1016/j.bbapap.2018.11.009

263. Lazar I, Clement E, Dauvillier S, Milhas D, Ducoux-Petit M, LeGonidec S, et al. Adipocyte exosomes promote melanoma aggressiveness through fatty acid oxidation: a novel mechanism linking obesity and cancer. *Cancer Res*. (2016) 76:4051–7. doi: 10.1158/0008-5472.CAN-16-0651

264. Eguchi A, Lazic M, Armando AM, Phillips SA, Katebian R, Maraka S, et al. Circulating adipocyte-derived extracellular vesicles are novel markers of metabolic stress. *J Mol Med (Berl)*. (2016) 94:1241–53. doi: 10.1007/s00109-016-1446-8

265. Dang SY, Leng Y, Wang ZX, Xiao X, Zhang X, Wen T, et al. Exosomal transfer of obesity adipose tissue for decreased miR-141-3p mediate insulin resistance of hepatocytes. *Int J Biol Sci*. (2019) 15:351–68. doi: 10.7150/ijbs.28522

266. Pardo F, Villalobos-Labra R, Sobrevia B, Toledo F, Sobrevia L. Extracellular vesicles in obesity and diabetes mellitus. *Mol Aspects Med*. (2018) 60:81–91. doi: 10.1016/j.mam.2017.11.010

267. Kanter JE, Hsu CC, Bornfeldt KE. Monocytes and macrophages as protagonists in vascular complications of diabetes. *Front Cardiovasc Med*. (2020) 7:10. doi: 10.3389/fcvm.2020.00010

268. Kisilevsky R, Subrahmanyan L. Serum amyloid A changes high density lipoprotein's cellular affinity. A clue to serum amyloid A's principal function. *Lab Invest*. (1992) 66:778–85.

269. Marhaug G, Hackett B, Dowton SB. Serum amyloid A gene expression in rabbit, mink and mouse. *Clin Exp Immunol*. (1997) 107:425–34. doi: 10.1111/j.1365-2249.1997.287-c31178.x

270. Gutfeld O, Prus D, Ackerman Z, Dishon S, Linke RP, Levin M, et al. Expression of serum amyloid A, in normal, dysplastic, and neoplastic human colonic mucosa:

implication for a role in colonic tumorigenesis. *J Histochem Cytochem*. (2006) 54:63–73. doi: 10.1369/jhc.5A6645.2005

271. Reigstad CS, Lundén GO, Felin J, Bäckhed F. Regulation of serum amyloid A3 (SAA3) in mouse colonic epithelium and adipose tissue by the intestinal microbiota. *PLoS One*. (2009) 4:e5842. doi: 10.1371/journal.pone.0005842

272. Sano T, Huang W, Hall JA, Yang Y, Chen A, Gavzy SJ, et al. An IL-23R/IL-22 circuit regulates epithelial Serum amyloid A to promote local effector Th17 responses. *Cell*. (2015) 163:381–93. doi: 10.1016/j.cell.2015.08.061

273. Hardardóttir I, Sipe J, Moser AH, Fielding CJ, Feingold KR, Grünfeld C. LPS And cytokines regulate extra hepatic mRNA levels of apolipoproteins during the acute phase response in Syrian hamsters. *Biochim Biophys Acta*. (1997) 1344:210–20. doi: 10.1016/s0005-2760(96)00143-9

274. Lloyd-Price J, Arze C, Ananthakrishnan AN, Schirmer M, Avila-Pacheco J, Poon TW, et al. Multi-omics of the gut microbial ecosystem in inflammatory bowel diseases. *Nature*. (2019) 569:655–62. doi: 10.1038/s41586-019-1237-9

275. Larsson E, Tremaroli V, Lee YS, Koren O, Nookaew I, Fricker A, et al. Analysis of gut microbial regulation of host gene expression along the length of the gut and regulation of gut microbial ecology through MyD88. *Gut*. (2012) 61:1124–31. doi: 10.1136/gutjnl-2011-301104

276. Livanos AE, Greiner TU, Vangay P, Pathmasiri W, Stewart D, McRitchie S, et al. Antibiotic-mediated gut microbiome perturbation accelerates development of type 1 diabetes in mice. *Nat Microbiol*. (2016) 1:16140. doi: 10.1038/nmicrobiol.2016.140

277. Zhang XS, Li J, Krautkramer KA, Badri M, Battaglia T, Borbet TC, et al. Antibiotic-induced acceleration of type 1 diabetes alters maturation of innate intestinal immunity. *Elife*. (2018) 7:e37816. doi: 10.7554/eLife.37816

278. Ivanov II, Atarashi K, Manel N, Brodie EL, Shima T, Karaoz U, et al. Induction of intestinal Th17 cells by segmented filamentous bacteria. *Cell*. (2009) 139:485–98. doi: 10.1016/j.cell.2009.09.033

279. Murdoch CC, Espenschied ST, Matty MA, Mueller O, Tobin DM, Rawls JF. Intestinal Serum amyloid A suppresses systemic neutrophil activation and bactericidal activity in response to microbiota colonization. *PLoS Pathog*. (2019) 15: e1007381. doi: 10.1371/journal.ppat.1007381

280. Cheng N, Liang Y, Du X, Ye RD. Serum amyloid A promotes LPS clearance and suppresses LPS-induced inflammation and tissue injury. *EMBO Rep*. (2018) 19(10): e45517. doi: 10.15252/embr.201745517

281. Zhou H, Chen M, Zhang G, Ye RD. Suppression of lipopolysaccharide-induced inflammatory response by fragments from Serum amyloid A. *J Immunol*. (2017) 199:1105–12. doi: 10.4049/jimmunol.1700470

282. Gershoni M, Pietrokovski S. The landscape of sex-differential transcriptome and its consequent selection in human adults. *BMC Biol*. (2017) 15:7. doi: 10.1186/s12915-017-0352-z

283. Oliva M, Muñoz-Aguirre M, Kim-Hellmuth S, Wucher V, Gewirtz ADH, Cotter DJ, et al. The impact of sex on gene expression across human tissues. *Science*. (2020) 369(6509):eaba3066. doi: 10.1126/science.aba3066

284. Lopes-Ramos CM, Chen CY, Kuijjer ML, Paulson JN, Sonawane AR, Fagny M, et al. Sex differences in gene expression and regulatory networks across 29 human tissues. *Cell Rep*. (2020) 31:107795. doi: 10.1016/j.celrep.2020.107795

285. Hartman RJG, Mokry M, Pasterkamp G, den Ruijter HM. Sex-dependent gene co-expression in the human body. *Sci Rep*. (2021) 11:18758. doi: 10.1038/s41598-021-98059-9

286. Lamason R, Zhao P, Rawat R, Davis A, Hall JC, Chae JJ, et al. Sexual dimorphism in immune response genes as a function of puberty. *BMC Immunol*. (2006) 7:2. doi: 10.1186/1471-2172-7-2

287. Jylhävä J, Haarala A, Eklund C, Pertovaara M, Kähönen M, Hutri-Kähönen N, et al. Serum amyloid A is independently associated with metabolic risk factors but not with early atherosclerosis: the cardiovascular risk in young finns study. *J Intern Med*. (2009) 266:286–95. doi: 10.1111/j.1365-2796.2009.02120.x

288. Lau-Corona D, Suvorov A, Waxman DJ. Feminization of male mouse liver by persistent growth hormone stimulation: activation of sex-biased transcriptional networks and dynamic changes in chromatin states. *Mol Cell Biol*. (2017) 37(19): e00301–17. doi: 10.1128/MCB.00301-17

289. Bélanger C, Luu-The V, Dupont P, Tchernof A. Adipose tissue intracrinology: potential importance of local androgen/estrogen metabolism in the regulation of adiposity. *Horm Metab Res*. (2002) 34:737–45. doi: 10.1055/s-2002-38265

290. Masi AT, Rehman AA, Jorgenson LC, Smith JM, Aldag JC. Sexual dimorphisms of adrenal steroids, sex hormones, and immunological biomarkers and possible risk factors for developing rheumatoid arthritis. *Int J Endocrinol*. (2015) 2015:929246. doi: 10.1155/2015/929246

291. Abbas A, Fadel PJ, Wang Z, Arbique D, Jialal I, Vongpatanasin W. Contrasting effects of oral versus transdermal estrogen on serum amyloid A (SAA) and high-density lipoprotein-SAA in postmenopausal women. *Arterioscler Thromb Vasc Biol*. (2004) 24:e164–167. doi: 10.1161/01.ATV.0000140198.16664.8e

292. van Rooijen M, Hansson LO, Frostegård J, Silveira A, Hamsten A, Bremme K. Treatment with combined oral contraceptives induces a rise in serum C-reactive protein in the absence of a general inflammatory response. *J Thromb Haemost*. (2006) 4:77–82. doi: 10.1111/j.1538-7836.2005.01690.x

293. Wakatsuki A, Okatani Y, Ikenoue N, Fukaya T. Effect of medroxyprogesterone acetate on vascular inflammatory markers in postmenopausal women receiving estrogen. *Circulation*. (2002) 105:1436–9. doi: 10.1161/hc1202.105945

294. Singer K, Maley N, Mergian T, DelProposto J, Cho KW, Zamarron BF, et al. Differences in hematopoietic stem cells contribute to sexually dimorphic inflammatory responses to high fat diet-induced obesity. *J Biol Chem*. (2015) 290:13250–62. doi: 10.1074/jbc.M114.634568

295. Henes JC, Saur S, Kofler DM, Kedor C, Meisner C, Schuett M, et al. Tocilizumab for the treatment of familial Mediterranean fever-A randomized, double-blind, placebo-controlled phase II study. *J Clin Med*. (2022) 11(18):5360. doi: 10.3390/jcm11185360

296. Hamanoue S, Suwabe T, Hoshino J, Sumida K, Mise K, Hayami N, et al. Successful treatment with humanized anti-interleukin-6 receptor antibody (tocilizumab) in a case of AA amyloidosis complicated by familial Mediterranean fever. *Mod Rheumatol*. (2016) 26:610–3. doi: 10.3109/14397595.2014.908810

297. Inui K, Sawa N, Suwabe T, Mizuno H, Yamanouchi M, Hiramatsu R, et al. Long term administration of tocilizumab improves renal amyloid A (AA) amyloidosis deposition in Familial Mediterranean fever. *Mod Rheumatol Case Rep*. (2020) 4:310–1. doi: 10.1080/24725625.2020.1739193

298. Yamada Y, Ueno T, Irifuku T, Nakashima A, Doi S, Ichinohe T, et al. Tocilizumab histologically improved AA renal amyloidosis in a patient with multicentric castleman disease: a case report. *Clin Nephrol*. (2018) 90:232–6. doi: 10.5414/CN109273

299. Okuda Y, Takasugi K. Successful use of a humanized anti-interleukin-6 receptor antibody, tocilizumab, to treat amyloid A amyloidosis complicating juvenile idiopathic arthritis. *Arthritis Rheum*. (2006) 54:2997–3000. doi: 10.1002/art.22118

300. Siligato R, Gembillo G, Calabrese V, Conti G, Santoro D. Amyloidosis and glomerular diseases in familial Mediterranean fever. *Medicina (Kaunas)*. (2021) 57 (10):1049. doi: 10.3390/medicina57101049

301. Jena M, Tripathy A, Mishra A, Maiti R. Effect of canakinumab on clinical and biochemical parameters in acute gouty arthritis: a meta-analysis. *Inflammopharmacology*. (2021) 29:35–47. doi: 10.1007/s10787-020-00753-z

302. Almusalami EM, Lockett A, Ferro A, Posner J. Serum amyloid A-A potential therapeutic target for hyper-inflammatory syndrome associated with COVID-19. *Front Med (Lausanne)*. (2023) 10:1135695. doi: 10.3389/fmed.2023.1135695

303. Ancsin JB, Kisilevsky R. The heparin/heparan sulfate-binding site on apo-serum amyloid A. Implications for the therapeutic intervention of amyloidosis. *J Biol Chem*. (1999) 274:7172–81. doi: 10.1074/jbc.274.11.7172

304. Tam SP, Ancsin JB, Tan R, Kisilevsky R. Peptides derived from serum amyloid A prevent, and reverse, aortic lipid lesions in apoE-/- mice. *J Lipid Res*. (2005) 46:2091–101. doi: 10.1194/jlr.M500191-JLR200

305. Manenti L, Tansinda P, Vaglio A. Eprodisate in amyloid A amyloidosis: a novel therapeutic approach? *Expert Opin Pharmacother*. (2008) 9:2175–80. doi: 10.1517/14656566.9.12.2175

frontiers | Frontiers in Cardiovascular Medicine

TYPE Original Research
PUBLISHED 12 July 2023
DOI 10.3389/fcvm.2023.1220095

OPEN ACCESS

EDITED BY
Isabella Russo,
University of Turin, Italy

REVIEWED BY
Shuai Yuan,
University of Pittsburgh, United States
Murugesan Velayutham,
West Virginia University, United States

*CORRESPONDENCE
Arpeeta Sharma
arpeeta.sharma@baker.edu.au

RECEIVED 10 May 2023
ACCEPTED 28 June 2023
PUBLISHED 12 July 2023

CITATION
Sharma A, Choi J, Sim L, Dey A, Mohan M, Kantharidis P, Dietz L, Sandner P and de Haan JB (2023) Ameliorating diabetes-associated atherosclerosis and diabetic nephropathy through modulation of soluble guanylate cyclase.
Front. Cardiovasc. Med. 10:1220095.
doi: 10.3389/fcvm.2023.1220095

Ameliorating diabetes-associated atherosclerosis and diabetic nephropathy through modulation of soluble guanylate cyclase

Arpeeta Sharma[1,2]*, Judy Choi[1], Lachlan Sim[1], Abhiroop Dey[1], Muthukumar Mohan[2], Phillip Kantharidis[2], Lisa Dietz[3], Peter Sandner[3,4] and Judy B. de Haan[1,5,6,7,8]

[1]Cardiovascular Inflammation and Redox Biology Laboratory, Baker Heart and Diabetes Institute, Melbourne, VIC, Australia, [2]Department of Diabetes, Monash University, Central Clinical School, Melbourne, VIC, Australia, [3]Pharmaceuticals Research and Development, Bayer AG, Wuppertal, Germany, [4]Institute of Pharmacology, Hannover Medical School, Hanover, Germany, [5]Baker Department of Cardiometabolic Health, University of Melbourne, Parkville, VIC, Australia, [6]Department Immunology and Pathology, Central Clinical School, Monash University, Melbourne, VIC, Australia, [7]Baker Department Cardiovascular Research, Translation and Implementation, La Trobe University, Melbourne, VIC, Australia, [8]Faculty of Science, Engineering and Technology, Swinburne University, Melbourne, VIC, Australia

Diabetes mellitus (DM) is an independent risk factor for micro- and macrovascular complications such as nephropathy and atherosclerosis respectively, which are the major causes of premature morbidity and mortality in Type 1 and Type 2 diabetic patients. Endothelial dysfunction is the critical first step of vascular disease and is characterized by reduced bioavailability of the essential endothelial vasodilator, nitric oxide (NO), coupled with an elevation in inflammation and oxidative stress. A novel pathway to bolster NO activity is to upregulate soluble guanylate cyclase (sGC), an enzyme responsible for mediating the protective actions of NO. Two classes of sGC modulators exist, activators and stimulators, with differing sensitivity to oxidative stress. In this study, we investigated the therapeutic effects of the sGC stimulator BAY 41-2272 (Bay 41) and the sGC activator BAY 60-2770 (Bay 60) on endpoints of atherosclerosis and renal disease as well as inflammation and oxidative stress in diabetic Apolipoprotein E knockout (ApoE-/-) mice. We hypothesized that under oxidative conditions known to accompany diabetes, sGC activation might be more efficacious than sGC stimulation in limiting diabetic vascular complications. We demonstrate that Bay 60 not only significantly decreased nitrotyrosine staining ($P < 0.01$) and F4/80 positive cells by 75% ($P < 0.05$), but it also significantly reduced total plaque area ($P < 0.05$) and improved endothelial function ($P < 0.01$). Our data suggest an important anti-atherogenic role for Bay 60 accompanied by reduced oxidative stress and inflammation under diabetic settings. Treatment with the stimulator Bay 41, on the other hand, had minimal effects or caused no changes with respect to cardiovascular or renal pathology. In the kidneys, treatment with Bay 60 significantly lessened urinary albuminuria, mesangial expansion and nitrotyrosine staining under diabetic conditions. In summary, our head-to-head comparator is the first preclinical study to show that a sGC activator is more efficacious than a sGC stimulator for the treatment of diabetes-associated vascular and renal complications.

KEYWORDS

soluble guanylate cyclase, type 2 diabetes, atherosclerosis, endothelial dysfunction, nitric oxide, inflammation, oxidative stress

Abbreviations

DM, Diabetes mellitus; Bay 41, Bay 41-2272; Bay 60, Bay 60-2770; IL-1β, Interleukin-1β; NO, Nitric oxide; VCAM-1, Vascular cell adhesion molecule 1; ICAM-1, Intercellular cell adhesion molecule 1; MCP-1, Monocyte chemoattractant protein 1; TNF-α, Tumour necrosis factor-α; $ApoE^{-/-}$, Apolipoprotein E KO; STZ, Streptozotocin; ACh, Acetylcholine; PE, Phenylephrine; HAoSMCs, Human aortic smooth muscle cells.

1. Introduction

Diabetes mellitus (DM) is a highly prevalent chronic metabolic disorder, characterized by elevated blood glucose, and considered a major health burden on western societies. Diabetes affects around 537 million people worldwide, and is predicted to reach 643 million by 2030 (1). Diabetic patients are highly susceptible to developing vascular complications, including atherosclerosis and chronic kidney disease leading to kidney failure. Often these occur as co-morbidities (2, 3) suggesting an underlying pathogenic etiology. These vascular complications are the major cause of morbidity and mortality in both Type 1 and Type 2 diabetic patients (4). There is currently no cure, despite standard treatments which include glucose and lipid lowering and blood pressure control.

A critical first step in the progression of vascular complications is the development of endothelial dysfunction, which is characterized by the reduced bioavailability of nitric oxide (NO) coupled with an elevation in oxidative stress (5). NO is a potent endogenous vasodilator that regulates vascular tone by increasing cGMP. NO is produced by endothelial nitric oxide synthase (eNOS) from L-arginine in the presence of co-factors HSP90, tetrahydrobiopterin (BH_4) and the calcium-calmodulin complex. Once formed, NO diffuses to the vascular smooth muscle cells where it binds to soluble guanylate cyclase (sGC) which generates cyclic guanosine 3′,5′-monophosphate (cGMP). This NO-sGC-cGMP signalling pathway regulates numerous physiological downstream processes including vasodilation (6). NO-cGMP signalling is also anti-atherogenic via its ability to inhibit platelet aggregation, inflammatory cell adhesion and smooth muscle cell migration, all of which contribute to the pathogenesis of atherosclerosis (7, 8). Enhanced NO signalling is also associated with a higher glomerular filtration rate (GFR) as determined via measures of cystatin C and creatinine (9). Thus, increasing NO bioavailability is seen as an attractive therapeutic strategy to improve endothelial dysfunction, limit atherosclerosis and improve kidney function (10, 11).

Strategies to increase NO bioavailability particularly for diabetes-associated vascular complications, have faced major clinical limitations. For example, treatment with L-arginine has not shown improvements in endothelial function in diabetic patients (12), while nitrate administration has shown lack of sustainability due to the development of tolerance in humans (13). BH_4 is easily oxidized and is temperature and light sensitive, limiting its use as a chronic drug treatment. In contrast, direct targeting of the sGC enzyme with small molecules has become the focus of a new treatment strategy to overcome the loss of NO bioavailability (14).

sGC is a heterodimeric enzyme, consisting of an alpha-subunit and a smaller heme-binding beta-subunit. Upon NO binding to the heme moiety, the enzyme becomes catalytically active. Under conditions of oxidative stress, ferrous (Fe^{2+}) heme is oxidised to ferric (Fe^{3+}) heme, leading to the loss of the heme group, which lessens or completely inhibits the response of sGC to NO by losing the NO-binding site (15). This is particularly prevalent under hyperglycemic conditions where the accumulation of oxidized heme-sGC results in a state of NO resistance, decreased NO-dependent cGMP accumulation and impaired vasodilation (16). Additionally, dyslipidemia, a common feature of diabetes leads to the dysregulation of sGC expression and activity, leading to vascular dysfunction and neointimal formation (16), both of which are key events in atherosclerotic progression.

Pharmacological compounds that directly target the sGC-cGMP pathway overcome limitations of NO tolerance. Two classes of compounds exist that increase the catalytic activity of the enzyme, namely sGC stimulators and sGC activators. Both sGC stimulators and sGC activators have a unique mode of action and can bind to sGC and trigger cGMP production independent of NO. In addition, sGC stimulators act by sensitizing sGC to low levels of NO by stabilizing the nitrosyl-heme complex. Thus, sGC stimulators also work synergistically with NO and upregulate sGC activity at reduced levels of NO (16, 17). In phase III clinical trials, Riociguat (BAY 63-2521), a sGC stimulator, has shown positive improvements in pulmonary arterial hypertension (18). In contrast to sGC stimulators, sGC activators modulate sGC when the enzyme is in an oxidized or a heme-free state (16, 17). Therefore, it is expected that sGC activators are advantageous under settings of oxidative stress such as diabetes, due to their ability to target heme-free sGC. However, in a comparative study by Costell et al. (19), both the sGC stimulator BAY 60-4552 and the sGC activator GSK2181236A demonstrated differential beneficial effects in spontaneous hypertensive stroke-prone rats, a model that is associated with high levels of oxidative stress.

Several studies have documented the protective effects of sGC modulation against atherosclerosis. For example, the sGC stimulator Riocuguat attenuated atherosclerosis in Western diet fed Apolipoprotein E knockout (ApoE-/-) mice (20). More recently it was shown that the sGC stimulator BAY-747 reduced atherosclerotic plaque formation in atherosclerosis-prone Ldlr−/− mice (21). In addition, sGC activation reduced cholesterol accumulation in macrophages by upregulating cholesterol efflux (22). Furthermore, both sGC stimulators and activators exhibit anti-fibrotic and anti-proliferative effects, which is of particular relevance to atherosclerotic plaque development (23–26). Several studies have also shown the renoprotective effects of sGC stimulators and activators in chronic kidney disease models (27, 28). However, little is known about the role of sGC modulation in diabetes-associated vascular complications.

Based on current knowledge, we aimed to show that sGC modulation will protect against diabetes-induced vascular dysfunction, atherosclerosis and nephropathy. Our preclinical studies directly compared the sGC stimulator, Bay 41-2272 (Bay 41), with the sGC activator, Bay 60-2770 (Bay 60) (17, 29). In particular, we hypothesized that under oxidative conditions known to accompany diabetes, sGC activation might be more efficacious than sGC stimulation in limiting diabetic vascular complications. Specifically, we aimed to investigate the effects of sGC stimulation or activation on cell types pertinent to the development of atherosclerosis (human aortic smooth muscle cells) under diabetic conditions. We also directly compared the effects of sGC stimulation or activation on vasodilation, atherosclerotic plaque development and renal function and injury in a mouse model of Type 1 diabetes.

2. Methods

2.1. Cell culture

Non-diabetic and diabetic human aortic smooth muscle cells (HAoSMC) from a single donor were purchased from Lonza Clonetics and cultured in smooth muscle cell media (SmBM-2, Lonza) in a humidified incubator at 37°C and 5% CO_2. Cells were supplemented with 2% FBS at 37°C in 5% CO_2.

2.1.1. Proliferation assays of HAoSMCs treated with sGC activators and stimulators

To quantitate HAoSMC proliferation, diabetic and non-diabetic HAoSMC were seeded in 24-well tissue culture plates. After 24 h, cells were synchronised for an additional 24 h in serum-free media. Next, cells were stimulated with serum and TNF-α, with and without the addition of the sGC stimulator Bay 41 or the activator Bay 60, and analysed after a 48-hour period. Cells were counted using the TALI cytometer (Thermofischer). Additionally, a colorimetric water-soluble tetrazolium (WST)-1 assay (Roche Diagnostics) was used to measure cell proliferation.

2.1.2. Gene expression of HAoSMCs treated with sGC activators and stimulators

Non-diabetic and diabetic HAoSMC were treated with TNF-α for 4 h in the presence or absence of the sGC stimulator Bay 41 or the activator Bay 60. Cells were harvested and RNA extraction, cDNA synthesis and qRT-PCR were performed as described previously (30). Gene expression analysis was performed to assess pro-inflammatory markers.

2.2. Animal groups and experimental design

To induce a model of Type 1 diabetes, eight-week old male $ApoE^{-/-}$ mice were made diabetic with intraperitoneal injections of streptozotocin (STZ; 100 mg/kg on 2 consecutive days), dissolved in 25 mM citrate buffer at pH4.5. At 10 weeks of age, non-diabetic and diabetic (>25 mM blood glucose) mice were randomised to receive either the sGC stimulator Bay 41 (1 mg/kg and 10 mg/kg), the sGC activator Bay 60 (0.3 mg/kg and 3 mg/kg) or vehicle control (carboxy methylcellulose suspension) for a period of 10 or 20 weeks, via oral gavage, twice a day. For quantification of the exposure, blood (Lithium Heparin Plasma) was collected 1 h and 4 h after oral gavage and Bay 60 and Bay 41 were analyzed in plasma using an LC-system (Kinetex, 2.6 µm, C18 100 A LC Column 150 × 4.6 mm) coupled to a 4,500 Triple Quad Sciex mass analyzer (MS/MS), which was used in positive mode. The injection volume was 5 µl. An acetonitrile and ammonium acetate buffer (10 mM pH 6.8) gradient at a flow rate of 1 ml/min was used for mass separation. The generic internal standard was added to the samples before LCMS analysis and quality control samples were used to monitor the LCMS/MS quality. The 11-point calibration curve of Bay 60 and Bay 41 together with the internal standard was used for quantification.

After 10-weeks of treatment, mice were killed using lethabarb (100 mg/kg), and the aortas were dissected out for vascular function and gene expression analysis. After the 20 week end-point, mouse hearts and kidneys were weighed, and tibia length was determined. Blood was collected into heparinised tubes. 20 ul of blood was removed and white blood cells, neutrophils and monocytes were calculated using a Hemavet system (Drew Scientific). The remaining blood was centrifuged at 4,000 × g for 10 min at room temperature to separate plasma. Lipid composition was then analysed using a HPLC system (31). Aortae were dissected and assessed for the presence of atherosclerotic plaque by an *en face* method that included the pinning flat of the arch, thoracic and abdominal segments after Sudan IV staining to assess regional lesions (10). Additionally markers of renal damage were assessed by ELISA and immunohistochemistry.

2.3. Assessment of vascular function

Vascular function was assessed by myography as previously published by our group (32, 33). Briefly, the aorta was dissected out and cleaned of peripheral fat. Thereafter, two 4 mm segments of the thoracic aortae were mounted on two L-shaped metal prongs. Aortae were equilibrated for 30 min at a resting tension of 5 mN. All aortae were then exposed to high-potassium physiological salt solution (HPPSS) to determine viability. Next, cumulative concentration responses to acetylcholine (ACh; 1 nmol/L–100 µmol/L) were recorded in aortae preconstricted to −50% HPPSS with phenylephrine (PE). All vasorelaxation responses are presented as percentage relaxation of the preconstriction response. Additionally, a concentration-response curve to PE (1 nmol/L–100 µmol/L) was performed to assess vascular contractility. The variable slope sigmoidal concentration-response curves to all agonists for each mouse were calculated and plotted using GraphPad Prism (version 8.0).

2.4. Gene expression analysis

Total RNA was extracted from tissue after homogenization of snap frozen aortae and kidney. Gene expression of vascular cell adhesion molecule-1 (VCAM-1), intracellular adhesion molecule (ICAM-1), nuclear factor-κB subunit p65 (p65 NF-κB), monocyte chemoattractant protein-1 (MCP-1), interleukin-1β (IL-1β), and tumor necrosis factor-α (TNF-α) was analyzed by quantitative RT-PCR (qRT-PCR) as described previously (10).

2.5. Immunohistochemistry

Aortic and kidney nitrotyrosine as well as aortic F4/80 localization and expression were determined by immunohistochemistry. In brief, 4-µm paraffin sections mounted on Superfrost slides were dewaxed, and endogenous peroxidases were inactivated with 3% H_2O_2 in Tris-buffered saline. Antigen retrieval was performed for kidney

sections. Thereafter, sections were incubated with a serum blocking agent and a biotin-avidin blocking kit (Vector Laboratories). Primary antibodies were added to sections and incubated overnight at 4°C. The next day, secondary antibody, biotinylated anti-rabbit Ig, or the biotinylated anti-rat secondary antibody was added for 30 min followed by horseradish peroxidase–conjugated streptavidin (1:500), incubated for 3 min in 3,3′-diaminobenzidine tetrahydrochloride, and counterstained with hematoxylin. All sections were examined under an Olympus BX-50 light microscope (Olympus Optical) and digital quantitation (Image-Pro Plus software version 6.0) and assessments were performed in a blinded manner. Nitrotyrosine staining was expressed as postively stained area over total area of the section while F4/80 positive cells were counted and averaged over sections.

2.6. Renal injury

Renal injury was assessed by measuring urinary albumin at midpoint (10 weeks of diabetes) and endpoint (20-weeks of diabetes) and PAS staining to quantify mesangial expansion. Urinary albumin was measured using a mouse albumin ELISA kit (Bethyl Laboratories) as per the manufacturer's instructions. PAS staining was performed and counterstained with hematoxylin. All sections were examined under an Olympus BX-50 light microscope (Olympus Optical) with digital quantitation (Image-Pro Plus software version 6.0) and assessments performed in a blinded manner.

2.7 Statistical analysis

Data are expressed as mean ± standard error of mean (SEM). A Shapiro-Wilk normality test was performed in GraphPad Prism to check for normality of data. If data is distributed normally, a one-way ANOVA with Tukey's multiple comparison *post hoc* tests was performed for comparisons between groups. If data was not normally distributed, a Kruskal-Wallis test was performed. All statistical analyses were performed using GraphPad Prism version 8.0. A P value < 0.05 was considered statistically significant.

3. Results

3.1. The sGC activator BAY60 and the stimulator BAY41 limit cell proliferation of human aortic smooth muscle cells in culture

Diabetic HAoSMC exhibited a significantly greater hyperproliferative profile in response to serum and TNF-α treatment as compared to non-diabetic HAoSMC (comparison of the black bars), as examined by both cell counting (**Figure 1A**, $P < 0.01$) and the WST-1 colorimetric assay (**Figure 1B**; $P < 0.001$).

In non-diabetic cells, Bay 60 caused a small yet significant reduction in cell number at 0.1 μM (**Figure 1A**, $P < 0.05$). Importantly, treatment with Bay 41 and Bay 60 reduced proliferation in a dose-dependent manner in diabetic HAoSMC

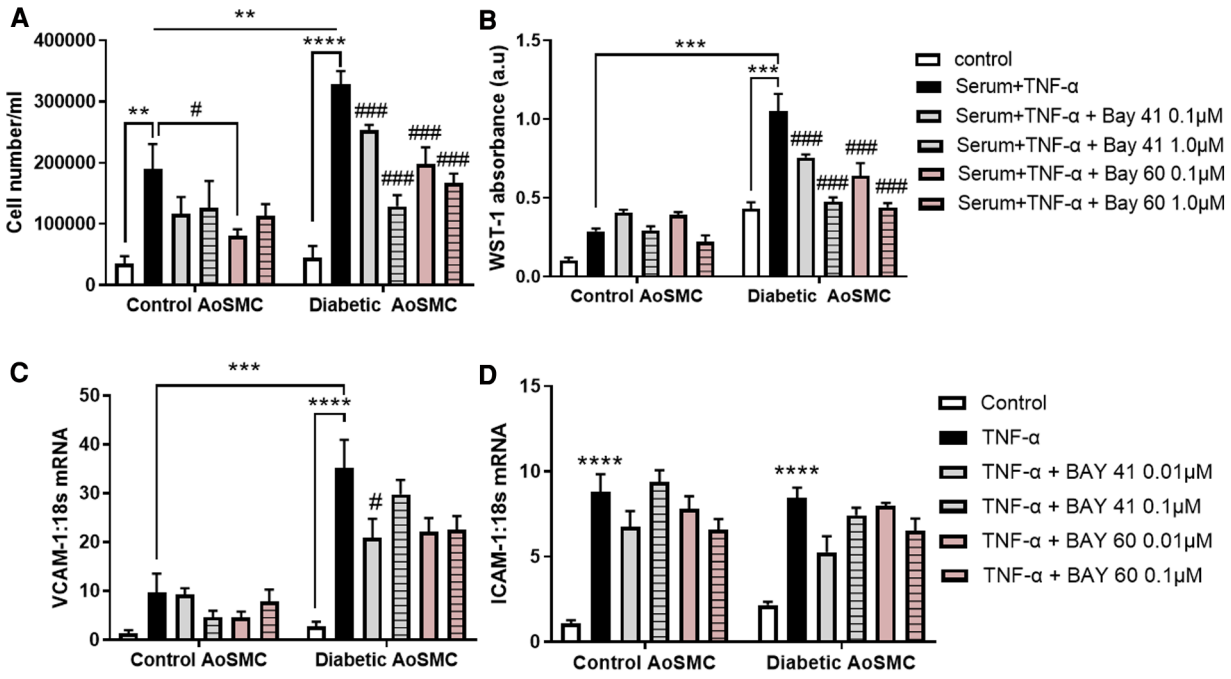

FIGURE 1
Treatment with Bay 41 and Bay 60 lessens cell proliferation in two independent assays. (**A**) Cell number and (**B**) a WST-1 proliferation assay of non-diabetic and diabetic HAoSMC treated with TNF-α and two doses of Bay 41 or Bay 60 as indicated. (**C**,**D**) Inflammatory gene expression analysis of (**C**) VCAM-1 and (**D**) ICAM-1 in non-diabetic and diabetic HAoSMC treated with TNF-α ± Bay 41 or Bay 60. Data is presented as mean ± SEM. $n = 8$/group with 2-3 independent experiments performed. #$P < 0.05$, **$P < 0.01$, ***$P < 0.001$ and ****$P < 0.0001$ as indicated. #$P < 0.05$, ##$P < 0.01$ and ###$P < 0.001$ vs. Diabetic HAoSMC + TNF-α.

(Figures 1A,B; $P < 0.001$) when assessed by both cell counting and the WST-1 absorbance assay. Collectively, both Bay 41 and Bay 60 inhibited cellular proliferation of diabetic human aortic smooth muscle cells in a dose-dependent manner with the higher concentration of 1μM being more effective.

3.2. sGC activator Bay 60 and stimulator Bay 41 lessen inflammation

Diabetic HAoSMC showed increased expression of the pro-inflammatory marker, VCAM-1 (Figure 1C; $P < 0.001$) compared with non-diabetic HAoSMC. Bay 41 (0.01 µM) significantly lessened VCAM-1 gene expression in diabetic HAoSMC (Figure 1C). There was a tendency to lessen VCAM-1 gene expression by Bay 60 at both concentrations in treated diabetic HAoSMCs compared with untreated diabetic HAoSMCs although significance was not reached (P value = 0.1).

ICAM-1 was significantly increased in both non-diabetic and diabetic HAoSMC, however Bay 41 and Bay 60 treatment had no significant effect on ICAM-1 expression (Figure 1D). A trend towards decrease expression after BAY41 (0.01 µM) treatment in both control and diabetic cells ($P = 0.06$) was observed. A dose-dependent trend was also observed after Bay 60 treatment in diabetic HAoSMCs.

Taken together, these *in vitro* experiments in diabetic HAoSMCs suggest that soluble guanylate cyclase activators and stimulators limit HAoSMC growth and the diabetes-mediated pro-inflammatory phenotype.

3.3 Plasma exposure of Bay 60 and Bay 41 after oral dosing in ApoE -/-mice

After oral dosing, plasma exposure of the sGC activator Bay 60 and the sGC stimulator BAY41 was determined 1, 2 and 4 h post treatment in ApoE -/- mice. Overall, plasma concentrations of Bay 41 were dose linear between 1 and 10 mg/kg oral doses over time (Supplementary Figure S1A). Plasma concentrations of Bay 60 showed no dose-linear increase in exposure after 3 mg/kg compared to 0.3 mg/kg (see Supplementary Figure S1A).

3.4. sGC activation improves vascular function and lessens oxidative stress

After 10-weeks of treatment with either Bay 41 or Bay 60, non-diabetic and diabetic vessels were assessed for improvements in vascular function. Diabetic vessels (black circles) exhibited a significantly greater contraction in response to increasing concentrations of phenylephrine (PE) compared with non-diabetic vessels (open circles) (Figures 2A,C, $P < 0.01$), suggesting significant diabetes-induced vascular dysfunction. Treatment with Bay41 did not significantly affect PE contractility at both doses although a small reduction was observed at 10 mg/kg (Figures 2A, C). Treatment with Bay 60 reduced PE contractility both at 0.3 mg/kg and 3 mg/kg (Figures 2B,C, $P < 0.01$), suggesting that both doses, which showed similar plasma exposure of the sGC activator, protected against diabetes-mediated vascular dysfunction. In non-diabetic vessels, both Bay 41 and Bay 60 showed a small but not significant reduction in PE contractility (Figures 2A,B). Interestingly, there was no effect of sGC treatment on the responses to acetylcholine (Ach) in diabetic or non-diabetic vessels (Supplementary Figure S3), suggesting that improvement in vascular function by the sGC activator is driven mainly via positive effects on vascular smooth muscle cells.

Vascular oxidative stress was evaluated via immunohistochemical staining for nitrotyrosine, a marker of peroxynitrite induced oxidative damage (Figures 2D,E). Nitrotyrosine staining showed a trend towards increased expression in diabetic aortae compared with non-diabetic aortae ($P = 0.1$). Treatment with Bay 60 (0.3 mg/kg) significantly attenuated the extent of nitrotyrosine staining ($P < 0.05$) (Figures 2D,E) while a trend towards decreased expression was noted after Bay 41 (10 mg/kg) treatment, suggesting that sGC activation and stimulation lessens oxidative stress.

3.5 End-point metabolic parameters

End-point parameters were assessed after 20-weeks of Bay 41 and Bay 60 treatment. There was no significant difference in body weight between non-diabetic and diabetic mice (Table 1). Non-diabetic mice (vehicle treated) had a mean body weight of 25.1 g ± 0.6 and diabetic mice had a mean body weight of 26.4 g ± 0.7. Treatment with the sGC activators and stimulators at either dose had no effect on the body weights of the mice.

Blood pressure was measured before termination using a tail cuff method (Table 1). There was no observed change in blood pressure between non-diabetic and diabetic mice. Furthermore, treatment with the sGC stimulator Bay 41 or the activator Bay 60 had no effect on blood pressure as observed by tail cuff measurements.

The ratio of heart weight to tibia length remained unaltered with the induction of diabetes and treatment with sGC modulators (Table 1), suggesting that there was no hypertrophy of the heart in this study, and that treatment with the stimulators and activators had no effect on heart size. There was a slight trend towards increased right kidney weight in the diabetic groups but this was unaltered with sGC modulation (Table 1).

Diabetic mice regardless of treatment exhibited elevated blood glucose levels compared with non-diabetic mice (Table 1; $P < 0.001$). Additionally, diabetic mice (black bars) exhibited elevated cholesterol and LDL/HDL ratios compared with non-diabetic mice (Supplementary Figures S2A–E). Importantly, treatment with either Bay 41 or Bay 60 did not affect lipid parameters (Supplementary Figure S2C).

3.6. Bay 60 but not Bay 41 significantly lessens atherosclerosis

Diabetic aortas displayed an approximately 2.5-fold increase in total aortic plaque compared with non-diabetic aortas (Figure 3;

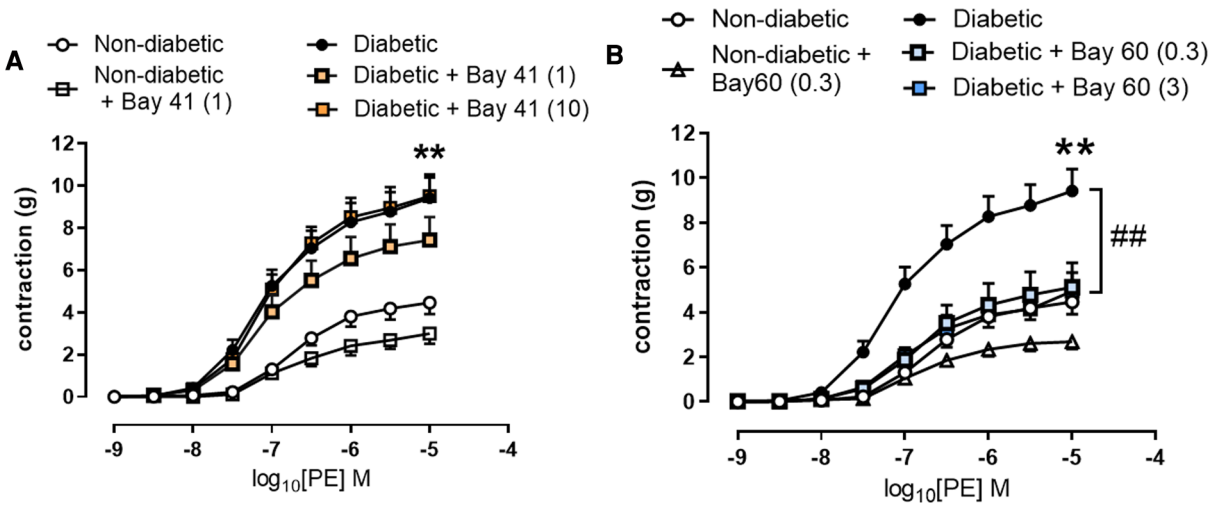

C

Group	Non-diabetic	Non-diabetic + Bay 41 (1)	Non-diabetic + Bay 60 (0.3)	Diabetic	Diabetic + Bay 41 (1)	Diabetic + Bay 41 (10)	Diabetic + Bay 60 (0.3)	Diabetic + Bay 41 (3)
Rmax (%)	4.5 ± 0.5	3.0 ± 0.5	2.7 ± 0.3	9.4 ± 1.0**	7.4 ± 1.0	9.5 ± 1.0	5.1 ± 1.0##	4.9 ± 0.9##
Log EC_{50}	-6.9 ± 0.5	-4.8 ± 2.0	-6.9 ± 0.1	-7.0 ± 0.1	-7.0 ± 0.1	-7.0 ± 0.5	-6.7 ± 0.6	-5.4 ± 1.5

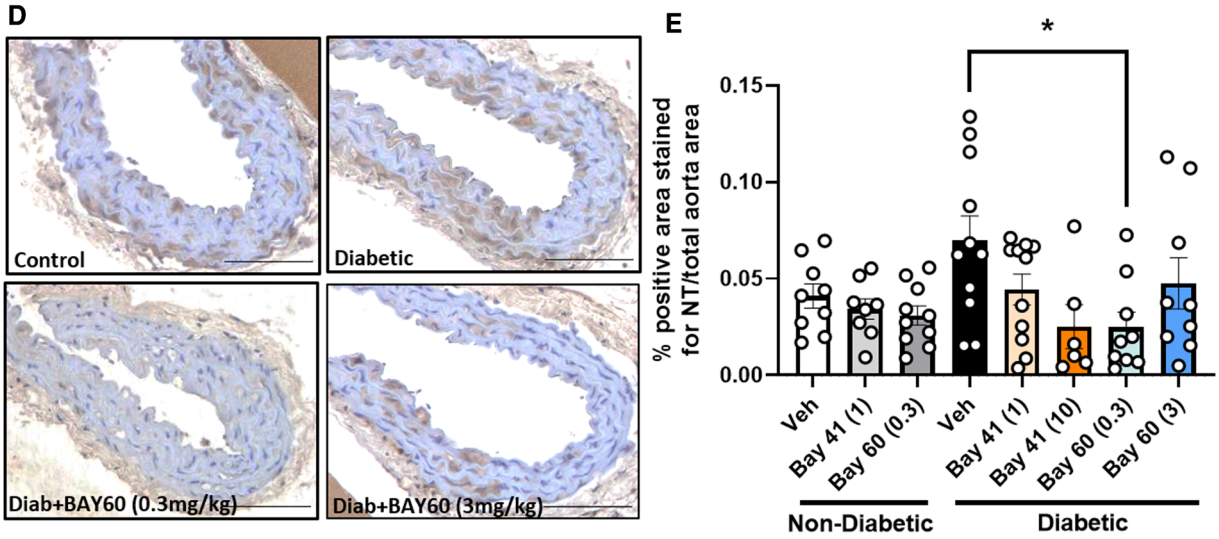

FIGURE 2
(A,B) vascular contraction in response to increasing doses of phenylephrine (PE) in aortic vessels treated with (A) Bay 41 and (B) Bay 60. (C) Rmax and Log EC50 values for PE concentration-response curves were calculated and used for statistics. (D) Representative images of aortic sections stained with nitrotyrosine and (E) quantification of nitrotyrosine stained positive area. Data is presented as mean ± SEM, with individual values plotted. *$P < 0.05$ as indicated, **$P < 0.01$ Diabetic vs. Non diabetic; ##$P < 0.01$ Diabetic + Bay 60 (0.3) vs. Diabetic. $n = 6$-13 per group. Dose (mg/kg) of Bay 41 and Bay 60 indicated in brackets.

TABLE 1 Blood pressure, blood glucose, body weight, height weight and kidney weight at study end point (20 weeks).

Parameter	Non-diabetic	Non-diabetic + Bay41	Non-diabetic + Bay60	Diabetic	Diabetic + Bay41	Diabetic + Bay41	Diabetic + Bay60	Diabetic + Bay41
		1 mg/kg	0.3 mg/kg		1 mg/kg	10 mg/kg	0.3 mg/kg	3 mg/kg
Blood pressure (mmHg)	99.8 ± 4.2	94.0 ± 7.2	116.1 ± 9.0	101.0 ± 3.9	110.4 ± 4.2	96.7 ± 8.8	109.3 ± 5.0	106.5 ± 5.0
Blood glucose (mmol/L)	9.8 ± 0.4	10.9 ± 0.8	9.6 ± 0.5	26.2 ± 2.4*	26.2 ± 2.4*	21.7 ± 3.7*	20.0 ± 3.0*	24.8 ± 3.0*
Body weight (g)	25.1 ± 0.1	28.8 ± 0.1	28.3 ± 0.1	26.4 ± 0.6	26.7 ± 0.6	28.0 ± 0.4	28.6 ± 0.7	27.5 ± 0.7
Heart weight (g)	0.1790 ± 0.0268	0.1414 ± 0.0054	0.1483 ± 0.0071	0.1416 ± 0.0071	0.1276 ± 0.0047	0.1282 ± 0.0044	0.1313 ± 0.0043	0.1261 ± 0.0038
Heart weight/Tibia length (g/mm)	0.0080 ± 0.0004	0.0089 ± 0.0009	0.0084 ± 0.0004	0.0080 ± 0.0004	0.0073 ± 0.0003	0.0072 ± 0.0003	0.0073 ± 0.0002	0.0077 ± 0.0007
Right kidney weight (g)	0.1814 ± 0.0055	0.1735 ± 0.0054	0.1782 ± 0.0074	0.1969 ± 0.0116	0.1954 ± 0.0082	0.1856 ± 0.0119	0.1763 ± 0.0049	0.1886 ± 0.0053
Left kidney weight (g)	0.1739 ± 0.0049	0.1658 ± 0.0061	0.1723 ± 0.0082	0.1818 ± 0.0060	0.1959 ± 0.0103	0.1810 ± 0.0094	0.1701 ± 0.0057	0.1851 ± 0.0055

Data is expressed as mean ± SEM.
*$p < 0.001$ vs. Non-diabetic.

$P < 0.001$). Treatment with Bay 41 did not affect the percentage total plaque (**Figure 3B**), whereas treatment with Bay 60 significantly reduced atherosclerotic lesions in diabetic vessels at 0.3 mg/kg (**Figure 3C**, $P < 0.05$).

3.7. Diabetes-driven myelopoesis is lessened by sGC treatment

Blood from diabetic mice (**Figures 4A,B**; black bars) exhibited significantly elevated total white blood cell (WBC) count at the 10-week time point compared with non-diabetic mice, which was not observed at the 20-week time point (**Figure 4B**). More in-depth analysis of the subtypes of WBCs showed significantly elevated neutrophils in the blood of diabetic mice after 10 weeks of diabetes (**Figure 4E**), whilst other WBCs such as monocytes were unaffected by diabetes (**Figure 4C**). This suggests that diabetes drives an early robust myelopoesis, mainly driven by elevated neutrophils in these mice, in line with published data (34). Treatment with the sGC compounds Bay 41 or Bay 60 tended to prevent the diabetes-driven myelopoesis at the earlier time point (10-weeks after commencement of treatment), although this did not fall within statistical significance (**Figures 4A,C,E**; $P = 0.2$ between diabetic vehicle vs. diabetic + Bay41 (10 mg/kg) and diabetic + Bay60 (3 mg/kg)). Interestingly, neither Bay 41 nor Bay 60 had any impact on WBC count at the 20-week time point (**Figure 4B**), suggesting that these compounds limit early myelopoesis, and in particular neutrophil accumulation in the blood. This is in line with the known function of neutrophils as early responders that migrate towards sites of inflammation where their secretion products activate monocytes that then enter atherosclerotic lesions or release pro-inflammatory mediators (35).

3.8. sGC activation with BAY60 lessens vascular inflammation

Macrophage infiltration, a marker of inflammation, was quantified in aortic sections using a murine-specific antibody against the macrophage marker, F4/80. Diabetic aortae exhibited a trend towards an increase in positively stained cells compared with non-diabetic aortae (**Figures 5A,B**, $P = 0.17$). Treatment with Bay 60 at 0.3 mg/kg and 3 mg/kg significantly reduced the number of macrophages in the diabetic aorta by −75% (**Figures 5A,B**, $P < 0.05$). A trend towards a decrease in macrophage numbers was observed after 1 mg/kg of Bay 41 treatment, however, this failed to reach significance (**Figure 5B**, $P = 0.1$).

Next we assessed a range of inflammatory genes (IL-6, VCAM-1, MCP-1 and IL-1β) by qRT-PCR (**Figures 5C–F**). The expression of IL-6 was significantly elevated in diabetic aortae (black bars) and VCAM-1, MCP-1 and IL-1β trended upward in gene expression in diabetic aortae, whilst treatment with Bay 60 at both doses (0.3 and 3 mg/kg) caused a trend toward reduced expression of these inflammatory genes (**Figures 5C–F**). There was also a trend towards decreased gene expression with Bay 41 at the lower treatment dose of 1 mg/kg although this was not apparent at the higher dose of 10 mg/kg (**Figures 5C–F**, $P = 0.13$ between diabetic vehicle vs. diabetic + Bay 41 (1 mg/kg) and diabetic + Bay 60 (3 mg/kg)).

3.9. Renal function (albuminuria) is improved after sGC activator and stimulator treatment

Elevated proteinuria is a functional marker for the development of diabetic nephropathy. Thus, urine albuminuria levels were measured using ELISA. A highly significant increase in albuminuria (−2-fold) was detected in urine from diabetic mice compared with urine from non-diabetic mice at both the 10 and 20-week time points (**Figure 6**).

Compared to untreated diabetic mice, Bay 41 and Bay 60 showed a trend towards reduced albuminuria levels for all treated groups at both the 10- and 20-week time point. This downward trend was significant after 10 weeks of treatment with Bay 60 at 3 mg/kg ($P < 0.01$). Our data suggest that the sGC activator Bay 60, at a dose of 3 mg/kg, improves renal function in diabetic mice after 10 weeks of treatment.

3.10. Renal structural injury is reduced by BAY60 treatment

Histological examination of periodic acid-Schiff (PAS) stained kidney sections showed extensive glomerular pathology and renal

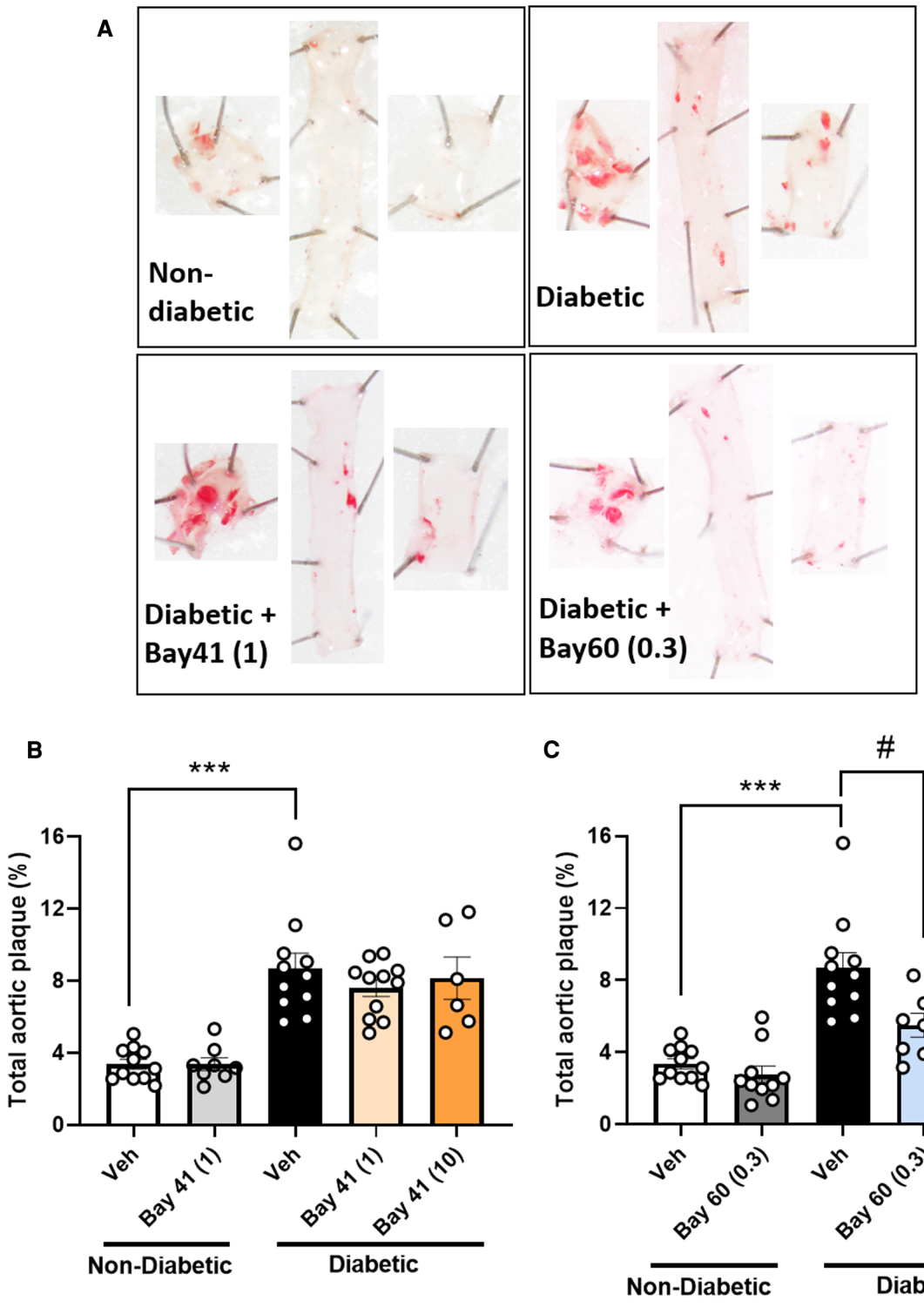

FIGURE 3
Sudan IV-stained aortas and atherosclerotic plaque quantification from mice treated with Bay 41 and Bay 60. (**A**) Representative images and percentage total plaque is shown for (**B**) Bay 41 treated and (**C**) Bay 60 treated ApoE-/- mice. Data is presented as mean ± SEM, with individual values plotted. ***$P < 0.001$ and #$P < 0.05$ as indicated. n = 6-12 aortas analysed per group. Dose (mg/kg) of Bay 41 and Bay 60 indicated in brackets.

injury after 20 weeks of diabetes. Diabetic kidneys showed basement membrane thickening and glomerular hypertrophy due to mesangial expansion and increased extracellular matrix deposition (ECM) compared with non-diabetic kidney sections. This is visualized as dark-magenta stained regions in the glomeruli of the diabetic kidneys (Figure 6C). Histological analysis showed a statistically significant increase in PAS staining in the untreated diabetic group (black bar) compared with

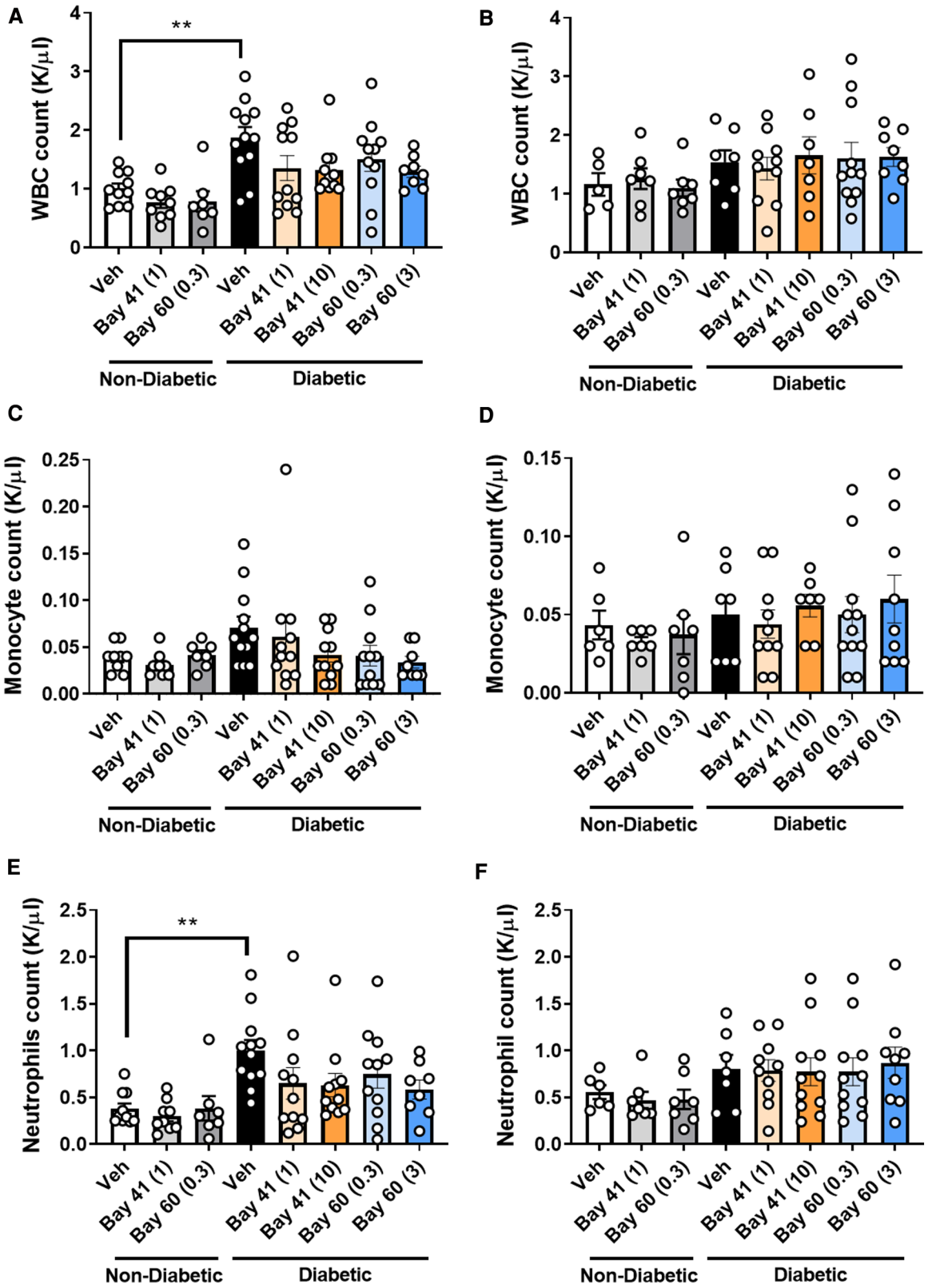

FIGURE 4
White blood cell (WBC), monocytes and neutrophils counts at 10 week (A, C and E respectively) and 20 week time points (B, D and F respectively). Data is presented as mean ± SEM, with individual values plotted. $^{**}P < 0.01$ as indicated. $n = 6–13$ per group. Dose (mg/kg) of Bay 41 and Bay 60 indicated in brackets.

10.3389/fcvm.2023.1220095

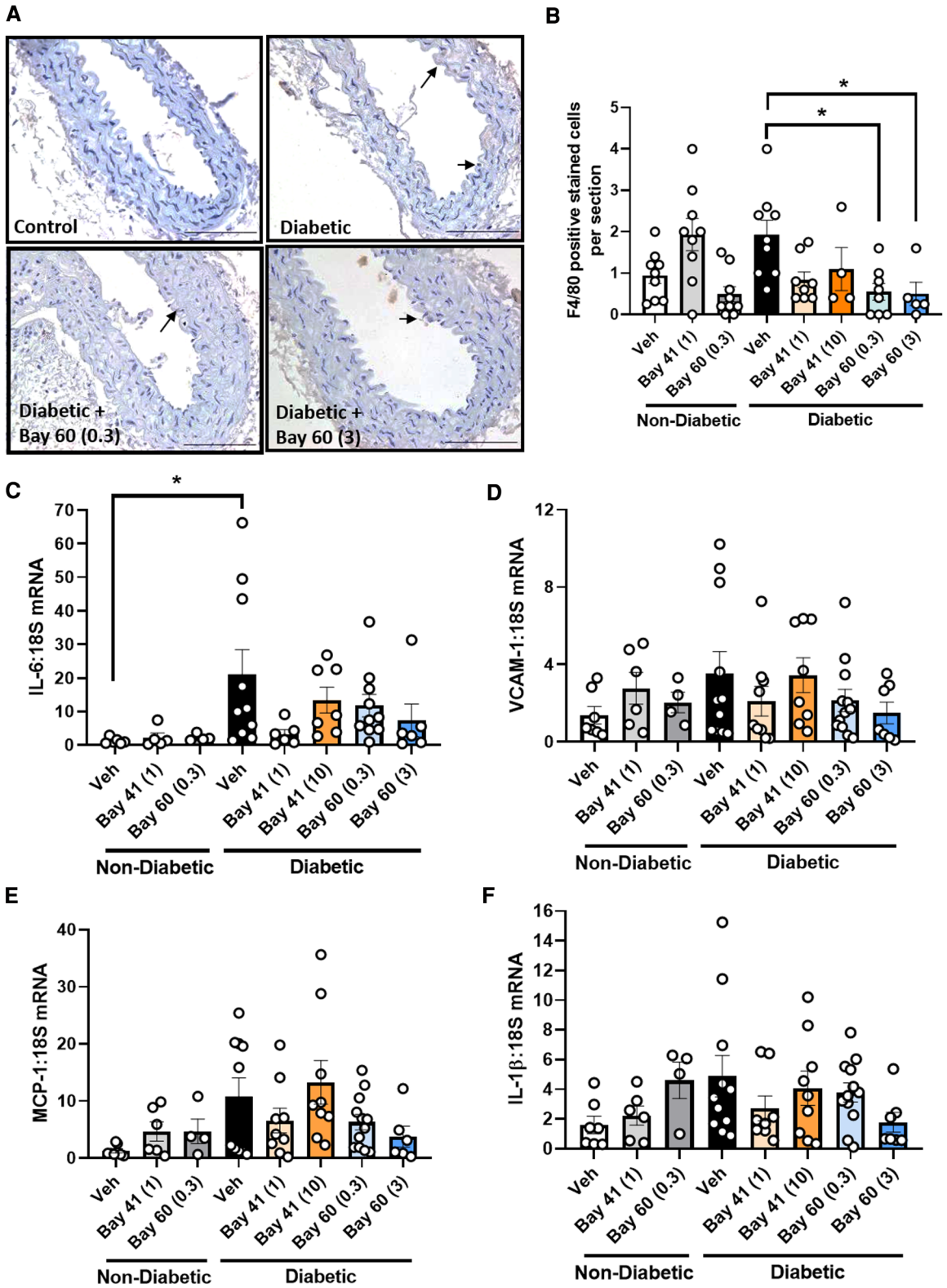

FIGURE 5
(A) Representative images of aortic sections stained with macrophage maker F4/80 and (B) quantification of F4/80 positive cells by averaging cell number across 10 sections per aorta. Gene expression of aortic inflammatory markers: (C) IL-6, (D) VCAM-1, (E) MCP-1 and (F) IL-1β was assessed by qRT-PCR. Data is presented as mean ± SEM, with individual values plotted. *$P < 0.05$ as indicated. n = 6–13 per group. Dose (mg/kg) of Bay 41 and Bay 60 indicated in brackets.

untreated non-diabetic and treated non-diabetic controls (Figures 6C,D; $P < 0.0001$). Treatment with Bay 60 at 3 mg/kg caused a statistically significant decrease in glomerular ECM deposition in the diabetic kidney (Figures 6C,D; $P < 0.001$), suggesting that Bay 60 at 3 mg/kg protects against structural injury in diabetic mice.

3.11. Renal oxidative stress

Diabetes-mediated oxidative stress was detected using immunohistochemical staining for nitrotyrosine. Vehicle-treated diabetic mice showed a significant increase in nitrotyrosine staining compared to all control non-diabetic groups (Figures 6E,F; $P < 0.0001$).

Treatment with Bay 41 at both doses did not significantly alter nitrotyrosine levels despite a strong decreasing trend. Treatment with Bay 60 (3 mg/kg) significantly attenuated nitrotyrosine staining compared to vehicle-treated diabetic mice (Figures 6E,F; $P < 0.001$), suggesting that Bay 60, at 3 mg/kg, protects against diabetes-driven oxidative injury.

3.12. cGMP levels as an indication of sGC activity

cGMP levels, a measure of sGC activity, were analysed in the plasma of diabetic and non-diabetic mice after 20 weeks of treatment with BAY compounds. Compared with non-diabetic untreated controls, cGMP levels were unchanged by 20 weeks of diabetes (Supplementary Figure S1B). Similarly, treatment with Bay 41 and Bay 60 (0.3 mg/kg) did not significantly alter cGMP levels. sGC activation with Bay 60 at a dose of 3 mg/kg showed a tendency towards an increase in cGMP levels in the plasma of diabetic mice when compared to untreated diabetic mice, however this did not reach significance. Additionally, sGC activation with Bay 60 at the 3 mg/kg dose was significantly higher than untreated non-diabetic mice (Supplementary Figure S1B; $P < 0.05$).

4. Discussion

This study aimed to establish whether sGC modulation, using the sGC stimulator Bay 41 and the sGC activator Bay 60, has the potential to protect against diabetes-associated atherosclerosis and renal damage. Using a preventative model where drug treatment commenced at the time of diabetes initiation, we demonstrated that the sGC activator, Bay 60 (0.3 mg/kg), was more efficacious than the stimulator, Bay 41, in reducing atherosclerotic plaque. This was accompanied by significant reductions in inflammation (F4/80 macrophages) and oxidative stress (nitrotyrosine) within the plaque and vasculature of diabetic mice. This atheroprotective effect was complemented by improvements in vascular function as demonstrated by reduced contractility in response to the vasoconstrictor, phenylephrine, as well as a reduction in smooth muscle cell proliferation under diabetic conditions. Additionally, Bay 60 demonstrated strong tendencies to reduce pro-inflammatory cytokines IL-6 and IL-1β, as well as the macrophage recruiting adhesion molecules, ICAM-1 and VCAM-1, under diabetic conditions. On the contrary, even though Bay 41 demonstrated modest decreases in vascular inflammation markers, it did not have an impact on vascular function and the atheroprotective effects were less prominent. The lack of impact of Bay 41 on vascular contraction could explain the differences in atheroprotective effects observed between the sGC stimulator and activator. A more patent vessel is correlated with enhanced and smoother blood flow, reduced endothelial damage due to reduced shear stress, and improved nutrient supply to the underlying vasculature. These factors, as a consequence of greater vessel relaxation by Bay 60, may have contributed to the decrease in plaque size observed. Additionally, it is of interest to note that the higher dose of the activator Bay 60 (3 mg/kg) did not reduce plaque size. Although the precise mechanisms have not been evaluated in this study, our data would suggest that a therapeutic window exists wherein Bay 60 is optimal.

With respect to renal pathology, our study showed significantly increased extracellular matrix protein accumulation and fibrosis under hyperglycaemic conditions. Fibrosis involves vascular smooth muscle cell proliferation, extracellular matrix accumulation and inhibition of matrix degradation (17). In our study, fibrosis in the kidney was lessened by Bay 60 as demonstrated by significant reductions in PAS staining. Additionally, albuminuria, an indicator of renal function, was significantly improved with Bay 60 treatment. These improvements were accompanied by a reduction in oxidative stress as demonstrated by reduced nitrotyrosine staining in the diabetic kidney upon treatment with the sGC activator Bay 60. Interestingly, Bay 60 protected against diabetes-mediated atherosclerosis at the lower dose of 0.3 mg/kg but prevented kidney injury at 3 mg/kg. Thus, we speculate that the metabolism of Bay 60 may be different between these tissues such that a higher dose is required in the kidney to elicit its protective effect.

This anti-fibrotic effect of Bay 60 ties in with the known anti-fibrotic effect of other sGC modulators (36, 37). Mechanistically, sGC modulation and associated cGMP release have been shown to block non-canonical TGFβ signaling and downstream experimental fibrosis (33) as well as attenuating cell proliferation in a variety of cultured cell lines including primary arterial smooth muscle cells (26). This additional anti-fibrotic function of activated sGC and its effector molecule cGMP is expected to limit the progression of atherosclerosis and nephropathy in diabetic patients and would be a highly desirable outcome of early therapy. In support of this, sGC stimulation by BAY 41-2272 has been shown to decrease ventricular interstitial fibrosis and collagen accumulation in a hypertensive rat model (23), while the sGC activator, ataciguat, attenuated extracellular matrix accumulation in the non-infarcted ventricle of rats with heart failure and myocardial infarction (24). Additionally, BAY 41-2272 significantly reduced pulmonary arterial smooth muscle proliferation and migration *in vitro* and reduced neotimal growth post- vascular balloon injury *in vivo* (25, 26).

10.3389/fcvm.2023.1220095

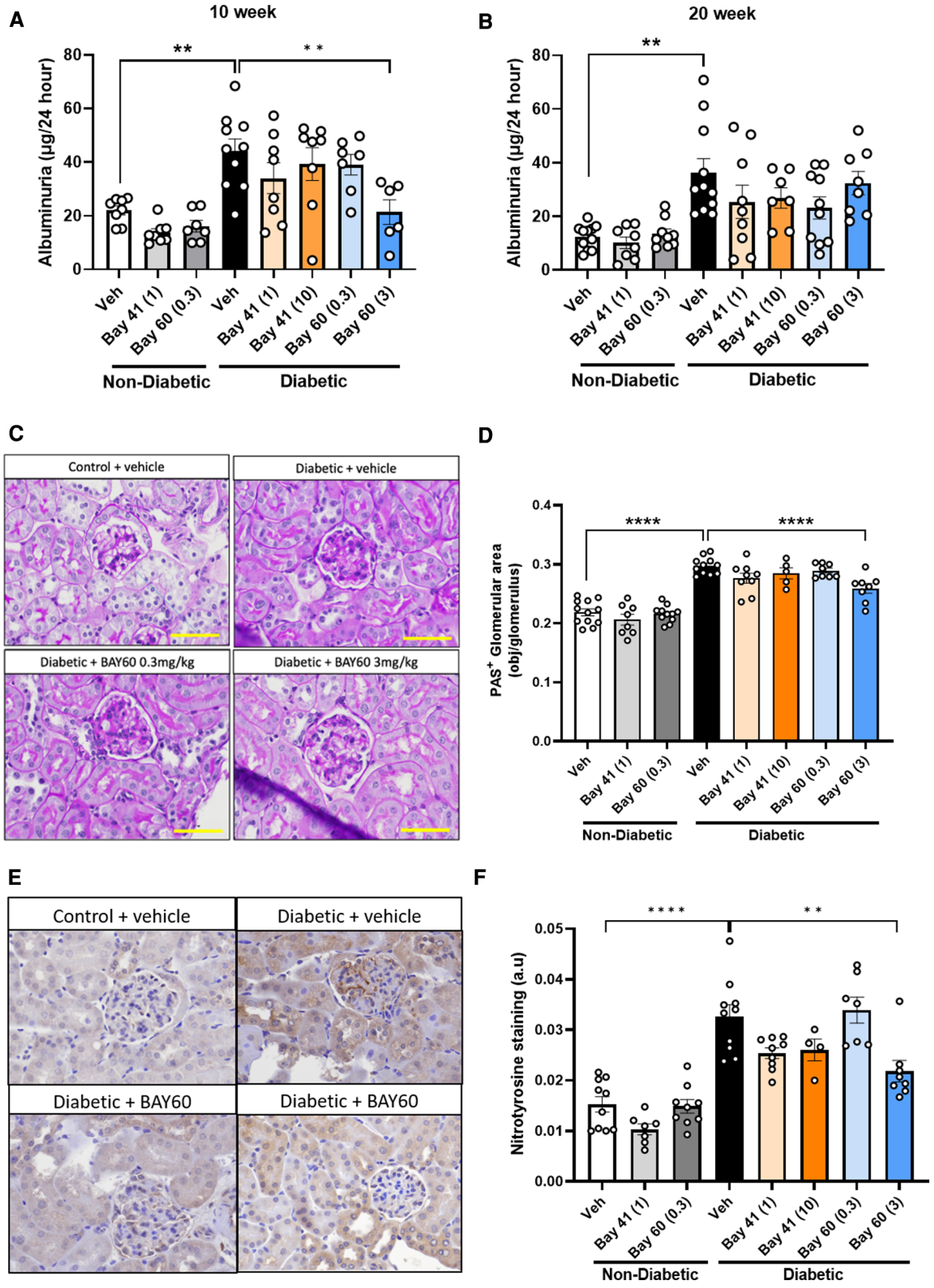

FIGURE 6
Urinary albuminuria was quantified using a commercially available ELISA kit. Total urine production over 24 h was used to determine final albuminuria levels (expressed as µg per 24 h) at (A) 10 weeks and (B) 20 weeks. (C) Representative images and (D) Quantification of kidney sections stained with Periodic acid-Schiff (PAS) in diabetic and non-diabetic mice (Magnification = 400x, scale bar = 50 µm). Results are shown as percentage-positive stained glomerular area and 20 glomeruli per kidney were analyzed. (E) Representative immunohistochemical images and (F) Quantification of glomeruli stained for nitrotyrosine in diabetic and non-diabetic ApoE-/- mice (magnification = 400x, scale bar = 50 µm). Results shown as percentage-positive brown staining per glomerulus area. 20 glomeruli per kidney section were analysed. Data is presented as mean ± SEM, with individual values plotted. $^{**}p < 0.01$ and $^{****}p < 0.0001$ as indicated. $n = 5–11$per group. Dose (mg/kg) of Bay 41 and Bay 60 indicated in brackets.

In another study that compared the efficacy of activators and stimulators under non-diabetic settings, low dose non-hypotensive treatment with the sGC stimulator, BAY 60-4552, improved renal function and survival, whilst the sGC activator, GSK2181236A, reduced cardiac hypertrophy. At high doses, both compounds attenuated cardiac hypertrophy but only the sGC stimulator further improved renal function and attenuated mean arterial pressure. These results suggested that activators and stimulators act preferentially in different tissues. Furthermore, neither sGC stimulation nor activation improved endothelium-dependent vasodilatory responses, suggesting that improvements due to sGC activity act downstream within the smooth muscle cells (19). Our study is in agreement with this finding since we failed to show improvements in vascular function in response to acetylcholine. Collectively, these results suggest that clinical development may need to take into account tissue-specific changes in the oxidation of sGC that are observed in different disease models.

Additionally, recent evidence has highlighted a role for sGC in regulating cholesterol metabolism in macrophages, another prominent cell type involved in the inflammatory component of atherosclerosis development. In atheroprone animal models, sGC inhibition significantly promoted ox-LDL induced cholesterol accumulation in macrophages (22), suggesting that sGC stimulation might prevent macrophage lipid accumulation and cytokine production. Furthermore, evidence from renal biopsies has shown that macrophage accumulation in diabetic kidneys predicts declining renal function (38).

Recent evidence also suggests that the loss of sGC function in platelets contributes to atherosclerotic plaque formation which could be reversed by chronic treatment with a sGC stimulator (21), suggesting that the effects we observed might also be mediated via rescued platelet function. Importantly, our data is in agreement with the anti-atherogenic potential of sGC agonists and it is clear that the sGC enzyme plays a critical role in regulating several cell types and processes involved in atherogenesis and nephropathy, including vascular tone, fibrosis and inflammation, and that targeting this enzyme could prove beneficial for the overall health of the vascular endothelium and prevent renal disease progression.

In conclusion, our head-to-head comparator is the first preclinical study that has shown that the sGC activator Bay 60 is superior to Bay 41 and that Bay 60 has potential therapeutic promise in the treatment of diabetes-associated vascular complications. It is well known that sGC stimulators and activators act via different mechanisms. sGC stimulators act by sensitizing sGC to low levels of NO by stabilizing the nitrosyl-heme complex, whilst sGC activators activate sGC when the enzyme is in an oxidized or in a heme-free state. This advantage of sGC activators is particularly relevant in diabetic patients where endogenous intravascular NO synthesis is markedly decreased and oxidative stress is increased (5, 39). Thus, as highlighted by our study, the sGC activator Bay 60 is more likely to be advantageous in settings of oxidative stress, such as those observed in cardiovascular diseases and diabetes, as a consequence of targeting heme-free sGC. Indeed, our collective data suggest that Bay 60 is the better of the two sGC enhancers at limiting vascular complications under diabetic conditions.

Data availability statement

The original contributions presented in the study are included in the article/**Supplementary Material**, further inquiries can be directed to the corresponding author.

Ethics statement

The animal study was reviewed and approved by AMREP Animal Ethic Committee (E1898).

Author contributions

AS and JD conceived and designed the research and drafted the manuscript. AS, JC, LS, AD and LD performed the experiments. MM, PK and PS provided intellectual input. AS and JBDH prepared the figures. AS, JC, LS, AD, MM, PK, PS, LD and JBDH approved final version of the manuscript. All authors contributed to the article and approved the submitted version.

Funding

This study was funded by the Bayer Grants for New Indications Scheme. The funder provided the sGC modulators and intellectual input for the study.

Conflict of interest

This paper is funded by Bayer Pharmaceuticals. PS and LD who are both co-authors on the paper are employees of Bayer Pharmaceuticals and have assisted with the studies.

The remaining authors declare that the research was conducted in the absence of any commercial or financial relationships that could be construed as a potential conflict of interest.

Publisher's note

Supplementary material

The Supplementary Material for this article can be found online at: https://www.frontiersin.org/articles/10.3389/fcvm.2023.1220095/full#supplementary-material

SUPPLEMENTARY FIGURE S1
(A) Plasma exposure to the sGC activator BAY60 and the sGC stimulator BAY41 in ApoE-/- mice after oral dosing over a 4hr period. (B) cGMP levels, a measure of sGC activity analysed by ELISA in the plasma of diabetic and non-diabetic mice. Data is presented as mean ± SEM with individual values plotted. *$P < 0.05$ as indicated. Dose (mg/kg) of Bay 41 and Bay 60 indicated in brackets.

SUPPLEMENTARY FIGURE S2
Lipid parameters at study end-point (20 weeks) assessed via HPLC. Data is presented as mean ± SEM, with individual values plotted. *$P < 0.05$ and ***$P < 0.001$ as indicated. $n = 6$-13 per group. Dose (mg/kg) of Bay41 and Bay60 indicated in brackets.

SUPPLEMENTARY FIGURE S3
(A,B) Vascular relaxation in response to increasing doses of Acetylcholine (Ach) in aortic vessels treated with (A) Bay 41 and (B) Bay 60. Data is presented as mean ± SEM. Dose (mg/kg) of Bay 41 and Bay 60 indicated in brackets.

References

1. Federation ID. *IDF Diabetes atlas. 10th ed.* Diabetes atlas (2021).

2. Kim SR, Lee YH, Lee SG, Kang ES, Cha BS, Lee BW. The renal tubular damage marker urinary N-acetyl-beta-D-glucosaminidase may be more closely associated with early detection of atherosclerosis than the glomerular damage marker albuminuria in patients with type 2 diabetes. *Cardiovasc Diabetol.* (2017) 16(1):16. doi: 10.1186/s12933-017-0497-7

3. Ishimura E, Shoji T, Emoto M, Motoyama K, Shinohara K, Matsumoto N, et al. Renal insufficiency accelerates atherosclerosis in patients with type 2 diabetes mellitus. *Am J Kidney Dis.* (2001) 38(4 Suppl 1):S186-90. doi: 10.1053/ajkd.2001.2744

4. Lockhart CJ, Hamilton PK, McVeigh KA, McVeigh GE. A cardiologist view of vascular disease in diabetes. *Diabetes Obes Metab.* (2008) 10(4): 279–92. doi: 10.1111/j.1463-1326.2007.00727.x

5. Xu J, Zou MH. Molecular insights and therapeutic targets for diabetic endothelial dysfunction. *Circulation.* (2009) 120(13):1266–86. doi: 10.1161/CIRCULATIONAHA.108.835223

6. Monica FZ, Bian K, Murad F. The endothelium-dependent nitric oxide-cGMP pathway. *Adv Pharmacol.* (2016) 77:1–27. doi: 10.1016/bs.apha.2016.05.001

7. Cannon RO 3rd. Role of nitric oxide in cardiovascular disease: focus on the endothelium. *Clin Chem.* (1998) 44(8 Pt 2):1809–19. doi: 10.1093/clinchem/44.8.1809

8. Forstermann U, Munzel T. Endothelial nitric oxide synthase in vascular disease: from marvel to menace. *Circulation.* (2006) 113(13):1708–14. doi: 10.1161/CIRCULATIONAHA.105.602532

9. Emdin CA, Khera AV, Klarin D, Natarajan P, Zekavat SM, Nomura A, et al. Phenotypic consequences of a genetic predisposition to enhanced nitric oxide signaling. *Circulation.* (2018) 137(3):222–32. doi: 10.1161/CIRCULATIONAHA.117.028021

10. Sharma A, Sellers S, Stefanovic N, Leung C, Tan SM, Huet O, et al. Direct endothelial nitric oxide synthase activation provides atheroprotection in diabetes-accelerated atherosclerosis. *Diabetes.* (2015) 64(11):3937–50. doi: 10.2337/db15-0472

11. Krishnan SM, Kraehling JR, Eitner F, Bénardeau A, Sandner P. The impact of the nitric oxide (NO)/soluble guanylyl cyclase (sGC) signaling cascade on kidney health and disease: a preclinical perspective. *Int J Mol Sci.* (2018) 19(6). doi: 10.3390/ijms19061712

12. Mullen MJ, Wright D, Donald AE, Thorne S, Thomson H, Deanfield JE. Atorvastatin but not L-arginine improves endothelial function in type I diabetes mellitus: a double-blind study. *J Am Coll Cardiol.* (2000) 36(2): p. 410–6. doi: 10.1016/S0735-1097(00)00743-9

13. Elkayam U. Tolerance to organic nitrates: evidence, mechanisms, clinical relevance, and strategies for prevention. *Ann Intern Med.* (1991) 114(8):667–77. doi: 10.7326/0003-4819-114-8-667

14. Sandner P, Follmann M, Becker-Pelster E, Hahn MG, Meier C, Freitas C, et al. Soluble GC stimulators and activators: past, present and future. *Br J Pharmacol.* (2021). doi: 10.1111/bph.15698

15. Martin E, Lee YC, Murad F. YC-1 activation of human soluble guanylyl cyclase has both heme-dependent and heme-independent components. *Proc Natl Acad Sci USA.* (2001) 98(23):12938–42. doi: 10.1073/pnas.231486198

16. Stasch JP, Pacher P, Evgenov OV. Soluble guanylate cyclase as an emerging therapeutic target in cardiopulmonary disease. *Circulation.* (2011) 123(20):2263–73. doi: 10.1161/CIRCULATIONAHA.110.981738

17. Sandner P, Berger P, Zenzmaier C. The potential of sGC modulators for the treatment of age-related fibrosis: a Mini-review. *Gerontology.* (2017) 63(3):216–27. doi: 10.1159/000450946

18. Ghofrani HA, Galiè N, Grimminger F, Grünig E, Humbert M, Jing ZC, et al. Riociguat for the treatment of pulmonary arterial hypertension. *N Engl J Med.* (2013) 369(4):330–40. doi: 10.1056/NEJMoa1209655

19. Costell MH, Ancellin N, Bernard RE, Zhao S, Upson JJ, Morgan LA, et al. Comparison of soluble guanylate cyclase stimulators and activators in models of cardiovascular disease associated with oxidative stress. *Front Pharmacol.* (2012) 3:128. doi: 10.3389/fphar.2012.00128

20. Schmidt HH, Hofmann F, Stasch JP. Handbook of experimental pharmacology 191. cGMP: generators, effectors and therapeutic implications. Preface. *Handb Exp Pharmacol.* (2009) 101(191):v–vi. doi: 10.1007/978-3-540-68964-5

21. Mauersberger C, Sager HB, Wobst J, Dang TA, Lambrecht L, Koplev S, et al. Loss of soluble guanylyl cyclase in platelets contributes to atherosclerotic plaque formation and vascular inflammation. *Nat Cardiovasc Res.* (2022) 1:1174–86. doi: 10.1038/s44161-022-00175-w

22. Tsou CY, Chen CY, Zhao JF, Su KH, Lee HT, Lin SJ, et al. Activation of soluble guanylyl cyclase prevents foam cell formation and atherosclerosis. *Acta Physiol (Oxf).* (2014) 210(4):799–810. doi: 10.1111/apha.12210

23. Masuyama H, Tsuruda T, Sekita Y, Hatakeyama K, Imamura T, Kato J, et al. Pressure-independent effects of pharmacological stimulation of soluble guanylate cyclase on fibrosis in pressure-overloaded rat heart. *Hypertens Res.* (2009) 32(7):597–603. doi: 10.1038/hr.2009.64

24. Fraccarollo D, Galuppo P, Motschenbacher S, Ruetten H, Schäfer A, Bauersachs J. Soluble guanylyl cyclase activation improves progressive cardiac remodeling and failure after myocardial infarction. Cardioprotection over ACE inhibition. *Basic Res Cardiol.* (2014) 109(4):421. doi: 10.1007/s00395-014-0421-1

25. Mendelev NN, Williams VS, Tulis DA. Antigrowth properties of BAY 41-2272 in vascular smooth muscle cells. *J Cardiovasc Pharmacol.* (2009) 53(2):121–31. doi: 10.1097/FJC.0b013e31819715c4

26. Joshi CN, Martin DN, Fox JC, Mendelev NN, Brown TA, Tulis DA. The soluble guanylate cyclase stimulator BAY 41-2272 inhibits vascular smooth muscle growth through the cAMP-dependent protein kinase and cGMP-dependent protein kinase pathways. *J Pharmacol Exp Ther.* (2011) 339(2):394–402. doi: 10.1124/jpet.111.183400

27. Benardeau A, Kahnert A, Schomber T, Meyer J, Pavkovic M, Kretschmer A, et al. Runcaciguat, a novel soluble guanylate cyclase activator, shows renoprotection in hypertensive, diabetic, and metabolic preclinical models of chronic kidney disease. *Naunyn Schmiedebergs Arch Pharmacol.* (2021) 394(12):2363–79. doi: 10.1007/s00210-021-02149-4

28. Stasch JP, Schlossmann J, Hocher B. Renal effects of soluble guanylate cyclase stimulators and activators: a review of the preclinical evidence. *Curr Opin Pharmacol.* (2015) 21:95–104. doi: 10.1016/j.coph.2014.12.014

29. Stasch JP, Becker EM, Alonso-Alija C, Apeler H, Dembowsky K, Feurer A, et al. NO-independent regulatory site on soluble guanylate cyclase. *Nature.* (2001) 410(6825):212–5. doi: 10.1038/35065611

30. Sharma A, Rizky L, Stefanovic N, Tate M, Ritchie RH, Ward KW, et al. The nuclear factor (erythroid-derived 2)-like 2 (Nrf2) activator dh404 protects against diabetes-induced endothelial dysfunction. *Cardiovasc Diabetol.* (2017) 16(1):33. doi: 10.1186/s12933-017-0513-y

31. Chew P, Yuen DY, Koh P, Stefanovic N, Febbraio MA, Kola I, et al. Site-specific antiatherogenic effect of the antioxidant ebselen in the diabetic apolipoprotein E-deficient mouse. *Arterioscler Thromb Vasc Biol.* (2009) 29(6):823–30. doi: 10.1161/ATVBAHA.109.186619

32. Sharma A, Choi JSY, Stefanovic N, Al-Sharea A, Simpson DS, Mukhamedova N, et al. Specific NLRP3 inhibition protects against diabetes-associated atherosclerosis. *Diabetes.* (2021) 70(3):772–87. doi: 10.2337/db20-0357

33. Sharma A, Choi JSY, Watson AMD, Li L, Sonntag T, Lee MKS, et al. Cardiovascular characterisation of a novel mouse model that combines hypertension and diabetes co-morbidities. *Sci Rep.* (2023) 13(1):8741. doi: 10.1038/s41598-023-35680-w

34. Flynn MC, Kraakman MJ, Tikellis C, Lee MKS, Hanssen NMJ, Kammoun HL, et al. Transient intermittent hyperglycemia accelerates atherosclerosis by promoting

myelopoiesis. *Circ Res*. (2020) 127(7):877–92. doi: 10.1161/CIRCRESAHA.120.316653

35. Doring Y, Drechsler M, Soehnlein O, Weber C. Neutrophils in atherosclerosis: from mice to man. *Arterioscler Thromb Vasc Biol*. (2015) 35(2):288–95. doi: 10.1161/ATVBAHA.114.303564

36. Hohenstein B, Daniel C, Wagner A, Stasch JP, Hugo C. Stimulation of soluble guanylyl cyclase inhibits mesangial cell proliferation and matrix accumulation in experimental glomerulonephritis. *Am J Physiol Renal Physiol*. (2005) 288(4):F685–93. doi: 10.1152/ajprenal.00280.2004

37. Kalk P, Godes M, Relle K, Rothkegel C, Hucke A, Stasch JP, et al. NO-independent activation of soluble guanylate cyclase prevents disease progression in rats with 5/6 nephrectomy. *Br J Pharmacol*. (2006) 148(6):853–9. doi: 10.1038/sj.bjp.0706792

38. Tesch GH. Macrophages and diabetic nephropathy. *Semin Nephrol*. (2010) 30(3):290–301. doi: 10.1016/j.semnephrol.2010.03.007

39. Tessari P, Cecchet D, Cosma A, Vettore M, Coracina A, Millioni R, et al. Nitric oxide synthesis is reduced in subjects with type 2 diabetes and nephropathy. *Diabetes*. (2010) 59(9):2152–9. doi: 10.2337/db09-1772

frontiers | Frontiers in Cardiovascular Medicine

TYPE Original Research
PUBLISHED 30 October 2023
DOI 10.3389/fcvm.2023.1234271

OPEN ACCESS

EDITED BY
Mahdi Garelnabi,
University of Massachusetts Lowell,
United States

REVIEWED BY
Michael C. Mahaney,
The University of Texas Rio Grande Valley,
United States
Scott M. Gordon,
University of Kentucky, United States
Chengxue Zhong,
Boehringer Ingelheim, United States

*CORRESPONDENCE
Ming Ren
✉ renming@tjutcm.edu.cn

RECEIVED 05 June 2023
ACCEPTED 04 October 2023
PUBLISHED 30 October 2023

CITATION
Feng W, Guo L, Liu Y and Ren M (2023) Unraveling the role of VLDL in the relationship between type 2 diabetes and coronary atherosclerosis: a Mendelian randomization analysis.
Front. Cardiovasc. Med. 10:1234271.
doi: 10.3389/fcvm.2023.1234271

Unraveling the role of VLDL in the relationship between type 2 diabetes and coronary atherosclerosis: a Mendelian randomization analysis

Wenshuai Feng[1], Liuli Guo[1], Yiman Liu[1] and Ming Ren[2]*

[1]College of Traditional Chinese Medicine, Tianjin University of Traditional Chinese Medicine, Tianjin, China, [2]Baokang Hospital Affiliated to Tianjin University of Traditional Chinese Medicine, Tianjin, China

Background: The causal link between Type 2 diabetes (T2D) and coronary atherosclerosis has been established through wet lab experiments; however, its analysis with Genome-wide association studies (GWAS) data remains unexplored. This study aims to validate this relationship using Mendelian randomization analysis and explore the potential mediation of VLDL in this mechanism.

Methods: Employing Mendelian randomization analysis, we investigated the causal connection between T2D and coronary atherosclerosis. We utilized GWAS summary statistics from European ancestry cohorts, comprising 23,363 coronary atherosclerosis patients and 195,429 controls, along with 32,469 T2D patients and 183,185 controls. VLDL levels, linked to SNPs, were considered as a potential mediating causal factor that might contribute to coronary atherosclerosis in the presence of T2D. We employed the inverse variance weighted (IVW), Egger regression (MR-Egger), weighted median, and weighted model methods for causal effect estimation. A leave-one-out sensitivity analysis was conducted to ensure robustness.

Results: Our Mendelian randomization analysis demonstrated a genetic association between T2D and an increased coronary atherosclerosis risk, with the IVW estimate at 1.13 [95% confidence interval (CI): 1.07–1.20]. Additionally, we observed a suggestive causal link between T2D and VLDL levels, as evidenced by the IVW estimate of 1.02 (95% CI: 0.98–1.07). Further supporting lipid involvement in coronary atherosclerosis pathogenesis, the IVW-Egger estimate was 1.30 (95% CI: 1.06–1.58).

Conclusion: In conclusion, this study highlights the autonomous contributions of T2D and VLDL levels to coronary atherosclerosis development. T2D is linked to a 13.35% elevated risk of coronary atherosclerosis, and within T2D patients, VLDL concentration rises by 2.49%. Notably, each standard deviation increase in VLDL raises the likelihood of heart disease by 29.6%. This underscores the significant role of lipid regulation, particularly VLDL, as a mediating pathway in coronary atherosclerosis progression.

KEYWORDS

type 2 diabetes, very low-density lipoprotein, coronary atherosclerosis, Mendelian randomization, mediation pathway

1. Introduction

1.1. Unraveling the pathogenesis of type 2 diabetes and coronary atherosclerosis

Type 2 diabetes (T2D) stands as a pervasive metabolic disorder affecting a substantial global population (1). Its intricate etiology, devoid of a definitive cure, compels a focus on symptom alleviation and complication prevention (2). Unfortunately, the prevalent chronic complications of T2D, primarily impacting cardiovascular and nerves, pose significant morbidity and mortality risks (3). Among these complications, coronary atherosclerosis emerges as a formidable adversary—characterized by plaque accumulation in the coronary arteries nourishing the heart. Given the pronounced atherogenic tendencies of T2D patients, exploring the mechanisms behind the T2D-coronary atherosclerosis nexus becomes pivotal (4). Thus, deciphering the pathophysiological intricacies driving coronary atherosclerosis in T2D patients is imperative, enabling the formulation of efficacious prevention and management strategies.

In essence, the pervasive prevalence of T2D and its consequential coronary atherosclerosis mandate an in-depth inquiry into the underlying mechanisms. Enhancing our comprehension of T2D's pathophysiology and its cascading complications promises more potent approaches to prevent, manage, and enhance patient well-being.

1.2. Mendelian randomization

Traditional statistical methods for exploring cause-and-effect relationships are flawed due to bias and confounding (5). Mendelian randomization (MR) mitigates confounding and reverse causality issues. Instrumental variables (IVs), linked to exposures but not outcomes or confounding, underpin MR (6–8). Three assumptions—relevance, exchangeability, and exclusion restriction—support MR validity (**Figure 1**) (9). Despite benefits, strict IV requirements limit MR's use. Genome-wide association studies introduce single-nucleotide polymorphisms (SNPs) as robust IVs (10). SNPs serve as popular IVs (11) and uncover novel genetic determinants.

Despite challenges like sample size demands and pleiotropy, MR promises to refine our grasp of complex diseases and their influences. Leveraging MR strengthens causal conclusions, enhancing intervention and management strategies.

1.3. The link between T2D and coronary atherosclerosis

T2D is a pervasive metabolic disorder with a significant global impact. While established links exist between T2D and coronary atherosclerosis (12) gaps remain in comprehending the intricate mechanisms that intricately connect the two (13). The conventional focus on risk factors like hypertension, obesity, and dyslipidemia partially explains the relationship, but an evolving body of research suggests the direct involvement of T2D in atherogenesis, notably impacting coronary atherosclerosis's pathogenesis (14). Central to this relationship is chronic hyperglycemia, a hallmark of T2D, which amplifies cardiovascular risks (15). It impairs endothelium-dependent vasodilation, compromising vascular health (16). Intriguingly, the accumulation of advanced glycation end products (AGEs) amid hyperglycemia plays a pivotal role in T2D-driven coronary atherosclerosis development (17). AGEs activate receptors, inciting inflammation, and cell proliferation, further exacerbating atherosclerosis (18).

1.4. VLDL's role in T2D-coronary atherosclerosis

1.4.1. VLDL is linked to T2D

Elevated fatty acid levels due to hyperinsulinemia are well-documented contributors to metabolic disorders, including T2D (19). These fatty acids trigger immune responses, inducing

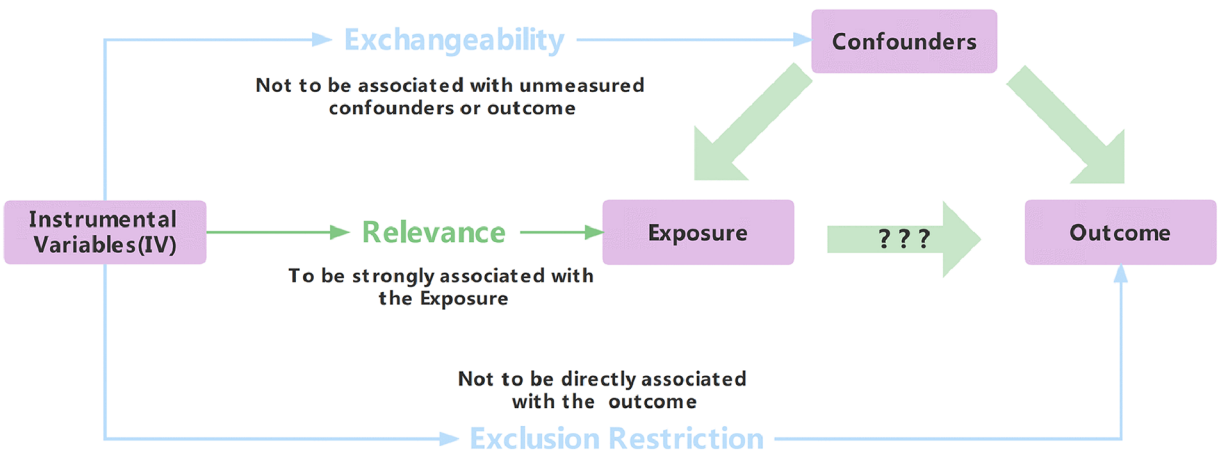

FIGURE 1
Three assumptions about instrumental variables (IV).

inflammatory cytokines like TNF-α, IL-1, and IL-6 (20). This inflammatory milieu drives insulin resistance, disrupts glucose homeostasis, and fosters T2D. Moreover, inhibiting the liver X receptor escalates cholesterol accumulation, inducing CRP, plasminogen inhibitor-1, serum amyloid, fostering fibrinogen synthesis, and hypercoagulability (21). These cytokines catalyze VLDL and free fatty acid production, exacerbating lipid disorders, promoting arterial lipid deposition, and augmenting atherosclerotic risk (22). The complexity of these interactions underscores the multifaceted nature of metabolic disorder pathogenesis, necessitating a comprehensive understanding.

1.4.2. VLDL's role in causing coronary atherosclerosis

Notably, dyslipidemia, particularly the presence of very low-density lipoprotein (VLDL) and elevated triglyceride (TG) levels, has been linked to coronary atherosclerosis (23). It is revealed that elevated levels of very-low-density lipoprotein cholesterol (VLDL-C) are associated with an increased risk of major adverse limb events (MALE) in patients with cardiovascular disease (24). However, there is no correlation between VLDL-C levels and major adverse cardiovascular events (MACE) or all-cause mortality, even after accounting for established risk factors such as LDL-C and lipid-lowering medication (24). Postprandial remnant lipoproteins, especially VLDL remnants, play a significant role in the initiation and progression of atherosclerosis (25). The increase of these lipoproteins in plasma, along with insufficient LPL activity, collectively contribute to the development of coronary atherosclerosis (25).

The intricate interplay between VLDL and coronary atherosclerosis underscores the significance of VLDL metabolism in cardiovascular health, providing valuable insights into potential mechanisms underlying the relationship between metabolic disorders like T2D and the development of atherosclerosis.

1.5. Research landscape and scope of the study

The causal relationships between T2D, VLDL, and coronary atherosclerosis have each been independently established through 2-sample analyses (26–28). However, substantial research gaps persist in elucidating the intricate pathways that connect T2D to coronary atherosclerosis, highlighting the imperative for further investigation. Within this context, investigating the mediating role of VLDL emerges as a promising avenue of exploration.

MR emerges as a robust strategy to probe causal relationships, effectively addressing the gaps in our current understanding (29). This analytical approach, utilizing multiple IVs, holds the potential to unravel the complexity of these relationships. Through the estimation of genetic variant effects on intermediate phenotypes (such as blood glucose) and their subsequent influence on outcomes (such as coronary atherosclerosis), MR offers a pathway to uncover the underlying mechanisms linking T2D to coronary atherosclerosis.

In summary, this study's focus on elucidating the intermediate role of VLDL aims to bridge existing gaps in comprehending the intricate association between T2D and coronary atherosclerosis. Leveraging the capabilities of MR, we aspire to contribute valuable insights into the intricate mechanisms that underscore this relationship, thus advancing our understanding and presenting potential avenues for intervention and management.

2. Materials and methods

2.1. Study selection and data collection

In order to explore how T2D may contribute to the development of coronary atherosclerosis through VLDL regulation, we conducted two-sample MR analyses using data from the IEU openGWAS database (https://gwas.mrcieu.ac.uk/). The aim of these analyses was to verify the consistency of our results. We performed three MR analyses in total. The first two were conducted to investigate the causal relationship between T2D and VLDL, as well as between T2D and coronary atherosclerosis, respectively. The third analysis examined the effect of VLDL levels on coronary atherosclerosis (**Figure 2**). We used GWAS datasets to perform these MR analyses, and there was minimal overlap between them. **Table 1** summarizes the details of the datasets used.

We used a significance threshold of $P < 5e\text{-}8$ to identify SNPs associated with T2D and VLDL, as this is the widely recognized standard for genome-wide association studies (GWAS) (29). To address issues related to linkage disequilibrium (LD) between the two samples, we conducted LD clumping using the TwoSampleMR package in the R language. We applied the following criteria: $R^2 = 0.01$ and kb = 10,000 (30). This procedure enabled the elimination of SNPs exhibiting strong LD with one another, resulting in a subset of independent SNPs for further analysis.

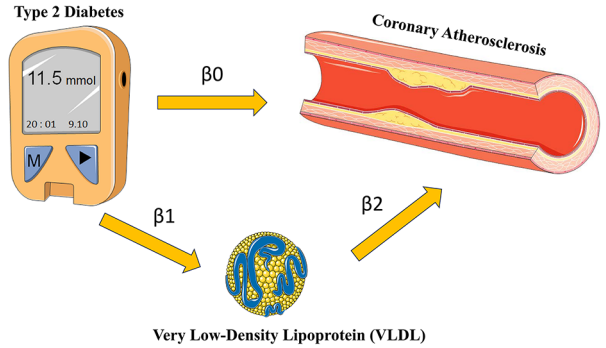

FIGURE 2
Research flow chart. Adapted from Smart Medical Art (Available at: https://smart.servier.com/).

TABLE 1 Summarizes the details of the datasets used.

Trait	Sample size	N SNPs	Sex	Population	Year	ID
T2D	32,469/183,185	16,380,440	Males and females	Europa	2021	finn-b-E4_DM2
VLDL	115,078	12,321,875			2020	met-d-VLDL_L
Coronary atherosclerosis	23,363/195,429	16,380,466			2021	finn-b-I9_CORATHER_EXNONE

2.2. Data analysis methods

2.2.1. Weak instrumental variable test

To ensure the validity of the Mendelian Randomization analysis, we implemented stringent criteria for SNP inclusion, focusing only on SNPs exhibiting strong associations with the respective exposures, namely Type 2 Diabetes or VLDL levels (9). The robustness of individual SNPs or sets of SNPs was assessed through the calculation of the F-statistic, providing a measure of the instrument strength. Additionally, we examined the proportion of variance in the exposure explained by the instrumental variable, as indicated by the R^2 statistic (31). These rigorous metrics were employed to ascertain the reliability and potency of the instrumental variables utilized in our MR analysis.

The *F*-statistic, calculated as $F = \frac{N-K-1}{K} \times \frac{R^2}{1-R^2}$, was employed for the assessment, where "*N*" represents the sample size of the exposure, and "*K*" denotes the number of SNPs associated with both the exposure and the depth of the Genome-Wide Association Study. Furthermore, the determination of R^2 relied on the formula $2 \times (1 - \text{MAF}) \times \text{MAF} \times \beta^2$, with "MAF" representing the Minor Allele Frequency and β^2 signifying the effect size of the SNP on the exposure. This thorough evaluation process served to enhance the confidence in the instrumental variables used for the MR analysis.

2.2.2. Causal effect estimation

In this study, we utilized multiple SNPs as instrumental variables for Mendelian Randomization (MR) analysis. To assess the association of each individual SNP, we employed the Wald statistic with the following formula (31):

$$\widehat{\theta}_i = \frac{\widehat{\beta_i^y}}{\widehat{\beta_i^x}}$$

$\widehat{\theta}_i$ represents the estimated effect size for SNP *i*

$\widehat{\beta_i^y}$ denotes the effect size of the SNP on the outcome variable.

$\widehat{\beta_i^x}$ represents the effect size of the SNP on the exposure variable.

To evaluate the relationship between T2D and coronary atherosclerosis, we combined Wald ratios using the inverse variance weighted (IVW) method (32). In this context, $\widehat{\theta}_i$ represents the estimated causal effect, $\widehat{\beta_i^y}$ denotes the effect size of the SNP on the outcome variable, and $\widehat{\beta_i^x}$ represents the effect size of the SNP on the exposure variable. Additionally, we employed the MR-Egger regression method (33) and the weighted median estimator (WME) (34) to complement and validate the MR results.

It is important to note that the validity assumptions for the three calculation methods used for instrumental variables differ, which helps ensure the robustness of the test results. The IVW method calculates the effect estimate as the slope of a linear regression weighted on the exposure factor for the instrumental variable in the outcome, with the intercepted item constrained to be zero. If all selected SNPs are valid instrumental variables, the IVW rule can provide unbiased effect estimates. In contrast, the MR-Egger method considers the existence of pleiotropy in the instrumental variables by using an intercept term in the weighted regression. The intercept term is used to evaluate the pleiotropy between the instrumental variables, and the slope is estimated accordingly. Finally, the WME method can still estimate the causal effect even when the proportion of invalid instrumental variables is as high as 50% and the estimated precision of the instrumental variables is quite different.

To evaluate the presence of heterogeneity among the instrumental variables, we used Cochran's Q test with both the IVW and MR-Egger methods (35, 36). If there is heterogeneity among the instrumental variables, we used the IVW of the random-effects model for the analysis of the results. In contrast, if there is no heterogeneity, the IVW of the fixed-effects model is used as the main approach (36).

2.2.3. Reliability evaluation

One must bear in mind that when it comes to instrumental variables, they are typically assumed to impact outcomes solely through the exposure factors being investigated. In other words, there is no direct association between these variables and the outcomes themselves. Nonetheless, this assumption becomes increasingly challenging to verify because genetic variation can exhibit pleiotropic effects—meaning that one gene may influence multiple traits or phenotypes simultaneously. Consequently, fully testing the exclusion hypothesis poses difficulties. At present, researchers widely rely on the intercept term of MR-Egger regression as a tool for detecting potential instances of pleiotropy. Essentially, if the Egger intercept (i.e., linear regression intercept) in an MR-Egger model approximates zero closely enough, it indicates a lack of evidence supporting genetic pleiotropy; thus, reinforcing the validity of the exclusionary hypothesis. Moreover, a significantly different result suggests otherwise (32, 37).

To assess the sensitivity of the results, a leave-one-out analysis was performed. This method is widely used to identify potential outliers by removing each SNP one by one and observing whether the results differ significantly before and after the removal. Specifically, if the obtained *P*-value is greater than 0.05 after excluding a particular SNP, it suggests that the SNP does not have a non-specific effect on the estimation of the causal effect (30).

3. Results

3.1. Relevance

The *F*-statistic value is all >10 in every filtering step, indicating strong instrumental variables. The threshold of *r*-squared is 0.01. The low likelihood of weak instrumental variable bias, as suggested by the R^2 and *F* values, further supports the assumption of relevance in MR research.

3.2. Two-step Mendelian randomization results

The study findings, depicted in **Figures 3**, **4** and summarized in **Figure 5**, reveal the established causal links between the exposures and outcomes evaluated through MR-Egger regression, weighted median, and random effects inverse variance weighting methods. In addition, assessments for heterogeneity and horizontal pleiotropy were executed, with the respective outcomes presented in **Figure 5**. While the heterogeneity test results might not align optimally, possibly attributable to the intricate pathogenesis of T2D, they do not undermine the overarching conclusion.

The analysis reveals significant findings across multiple methods and tests investigating the relationships between various factors. Notably, for β^0, which pertains to the causal impact of T2D on the development of coronary atherosclerosis, the inverse variance weighted method indicates a substantial association with an odds ratio (OR) of 1.13 [95% confidence interval (CI): 1.07–1.20], highlighting the elevated risk of coronary atherosclerosis due to T2D. Likewise, the relationship between Type 2 diabetes and VLDL levels, denoted as β^1, exhibited modest associations across the various methods employed. These results imply that while a direct influence of T2D on VLDL levels is observed, it does not reach statistical significance in most analyses. This suggests a nuanced connection that might contribute to the intricate interplay between T2D and VLDL in the context of cardiovascular risk factors. Regarding β^2, which signifies the relationship between VLDL levels and the occurrence of coronary atherosclerosis, the weighted median method demonstrated a significant odds ratio of 1.42, indicating that higher VLDL levels significantly increase the likelihood of developing coronary atherosclerosis. The inverse variance weighted method also presented a meaningful association with an odds ratio of 1.30, further underlining the role of VLDL in the development of coronary atherosclerosis.

The outcomes of horizontal pleiotropy assessment (**Figure 4**) depicted in these three figures serve as a means of mitigating horizontal pleiotropy, a factor that must be accounted for in Mendelian randomization analyses. Horizontal pleiotropy refers to effects that must be eliminated in Mendelian randomization, as each individual SNP locus can potentially exhibit horizontal pleiotropy. The overall pleiotropy fit observed in the images converges closely to zero, thus statistically implying the absence of horizontal pleiotropy.

It is important to note that the conclusions drawn from MR analysis are based on several assumptions, including the validity of instrumental variables, the absence of horizontal pleiotropy, and the absence of unmeasured confounding factors. While

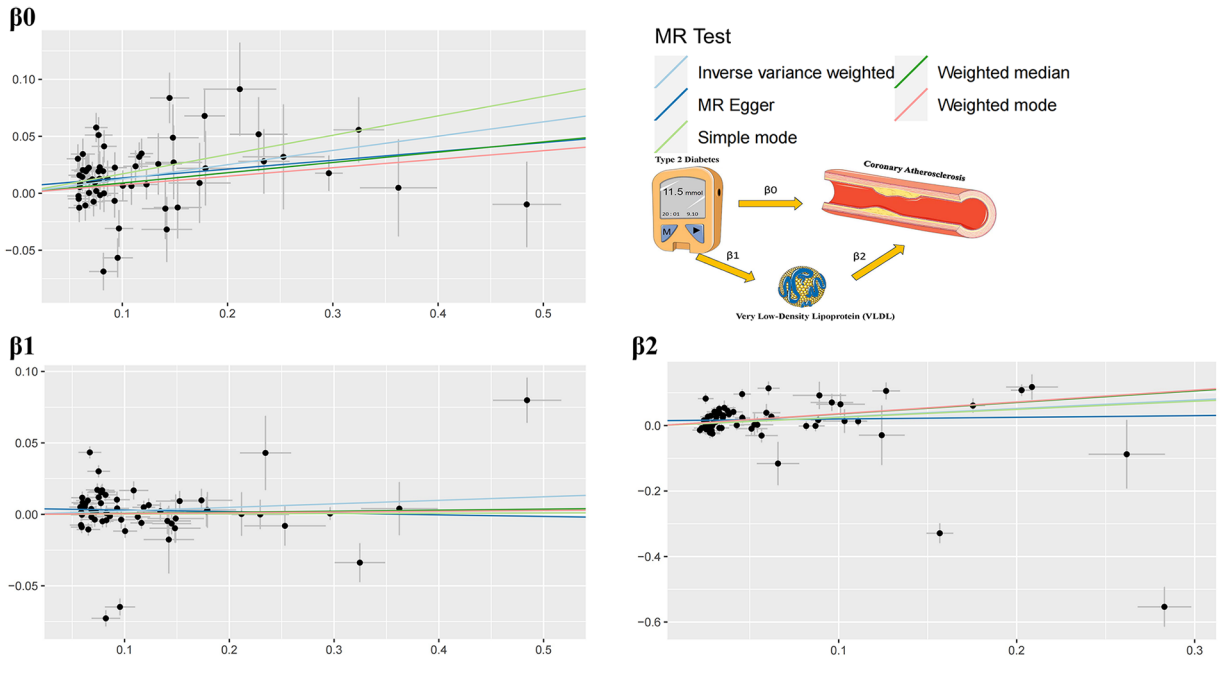

FIGURE 3
MR analysis.

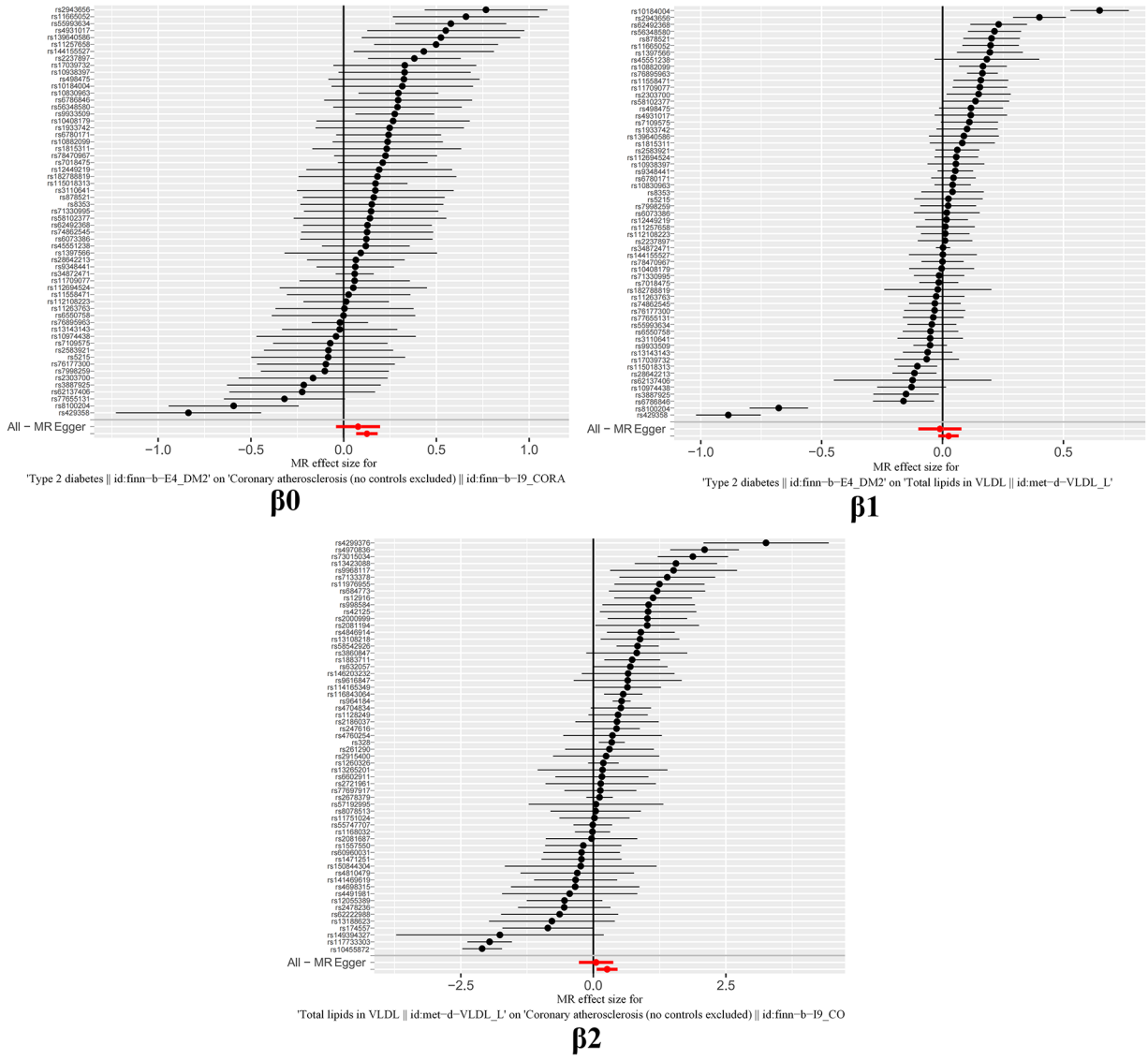

FIGURE 4
Forest plots of MR analysis.

efforts were made to ensure the validity of instrumental variables, it is still possible that some SNPs may have pleiotropic effects or be subject to weak instrument bias. Therefore, the results should be interpreted with caution, and further studies are needed to confirm the causal relationship between T2D, VLDL, and coronary atherosclerosis.

3.3. Reliability evaluation

It is worth highlighting that the "Leave-one-out" sensitivity analysis should be conducted across all instrumental variables employed in the analysis, extending beyond the six groups of data mentioned earlier. Despite the positive outcomes currently depicted in **Figure 6**, this analysis should be iteratively repeated by excluding each individual instrumental variable to assess its impact on the overall results. This meticulous approach offers additional confirmation that the favorable results are not reliant on a single SNP or a limited subset of SNPs.

4. Conclusion

Cardiovascular disease (CVD) is a global health concern with significant morbidity and mortality (38). Within its range, coronary heart disease (CHD) significantly impacts individuals with T2D, being a key contributor to morbidity and mortality (39). T2D is an established risk factor for CHD, with hyperglycemia directly triggering coronary atherosclerosis (40). Elevated blood glucose also contributes to VLDL buildup (41). Particularly important is the link between dyslipidemia—characterized by VLDL and high TG levels—and CHD (42). This investigation aims to uncover VLDL's role, address knowledge

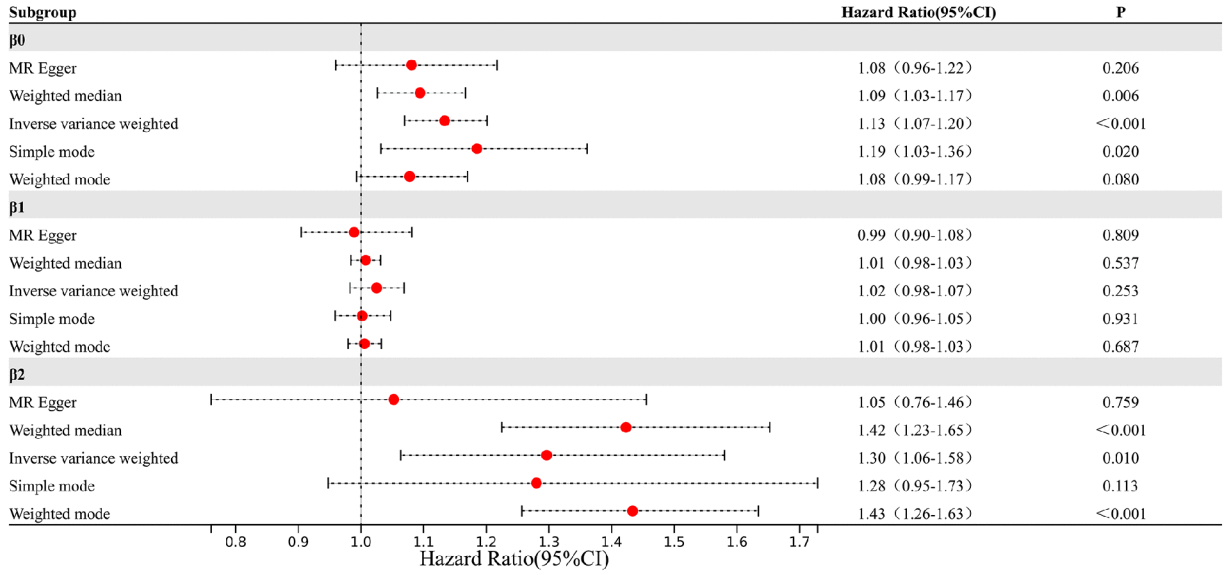

FIGURE 5
The result of 5 methods and 2 tests.

gaps, and enhance understanding of the complex T2D and coronary atherosclerosis relationship via Mendelian randomization.

This study utilized large-scale GWAS meta-analysis data and employed a two-sample Mendelian randomization approach to investigate the causal relationships between T2D, VLDL, and coronary atherosclerosis. T2D increases the risk of developing coronary atherosclerosis, leading to a 13.35% increase in disease occurrence compared to individuals without T2D. Additionally, in the context of patients with T2D, VLDL concentration increases by 2.49%. For every one standard deviation increase in VLDL, the probability of developing heart disease increases by 29.6%. These findings suggest that VLDL may serve as a mediator in the link between T2D and coronary atherosclerosis.

According to reports, coronary atherosclerosis is a significant global health concern, particularly among individuals with T2D due to their elevated risk of CHD (43). VLDL, intricately linked with CHD risk, plays a pivotal role in this context. T2D is known to elevate CHD risk through mechanisms such as chronic inflammation, insulin resistance, and oxidative stress, all of which contribute to the development of atherosclerosis—an underlying factor in CHD progression (44, 45). Moreover, VLDL, a central risk factor for CHD, assumes a crucial role (46). Elevated VLDL levels, characteristic of dyslipidaemia, independently elevate CHD risk by promoting atherosclerosis development (47). This study focused on understanding the individual influences of T2D and VLDL levels on coronary atherosclerosis risk and explored the potential mediating role of VLDL (47). The findings not only delineated the separate contributions of T2D and VLDL levels to coronary atherosclerosis risk but also proposed that VLDL might operate as a mediating pathway. These findings accentuate the significance of managing VLDL levels to mitigate the onset of coronary atherosclerosis among T2D individuals, underlining the need for early intervention to manage CHD risks.

This study possesses several strengths. Firstly, it leveraged large-scale GWAS databases and incorporated hundreds of SNPs in each two-sample Mendelian randomization analysis, minimizing the potential for random outcomes and enhancing the proportion of variance explained by the SNPs. Additionally, the study's robustness is underscored by conducting GWAS for all three variables using European databases with a low overlap probability, effectively addressing the concern of population bias. Furthermore, unlike similar studies focused solely on specific populations, this research significantly broadened its scope by encompassing a diverse European database, contributing to the generalizability of its findings.

While employing the two-sample Mendelian randomization method, this study demonstrates notable strengths as well as certain limitations. Firstly, despite the utilization of GWAS data spanning European databases, the extent of overlap remains low, potentially impacting the external applicability of the findings. Additionally, the assumption of method validity encompasses the effectiveness of instrumental variables; however, the presence of weak instruments might introduce inaccuracies in estimations. On another note, the study might have some shortcomings in controlling for confounding factors, such as lifestyle, genetics, and other potential covariates. This could potentially affect the internal validity of the results, making it challenging to completely exclude the influence of other factors. Furthermore, constrained by sample size and effect magnitude, the study's statistical power could be limited, leading to a potential weakening of result stability. Therefore, careful interpretation of the generalizability of the findings is warranted. These limitations underscore the need for cautious interpretation and highlight avenues for future research.

In conclusion, this study employed three two-sample Mendelian randomization analyses to investigate the relationships

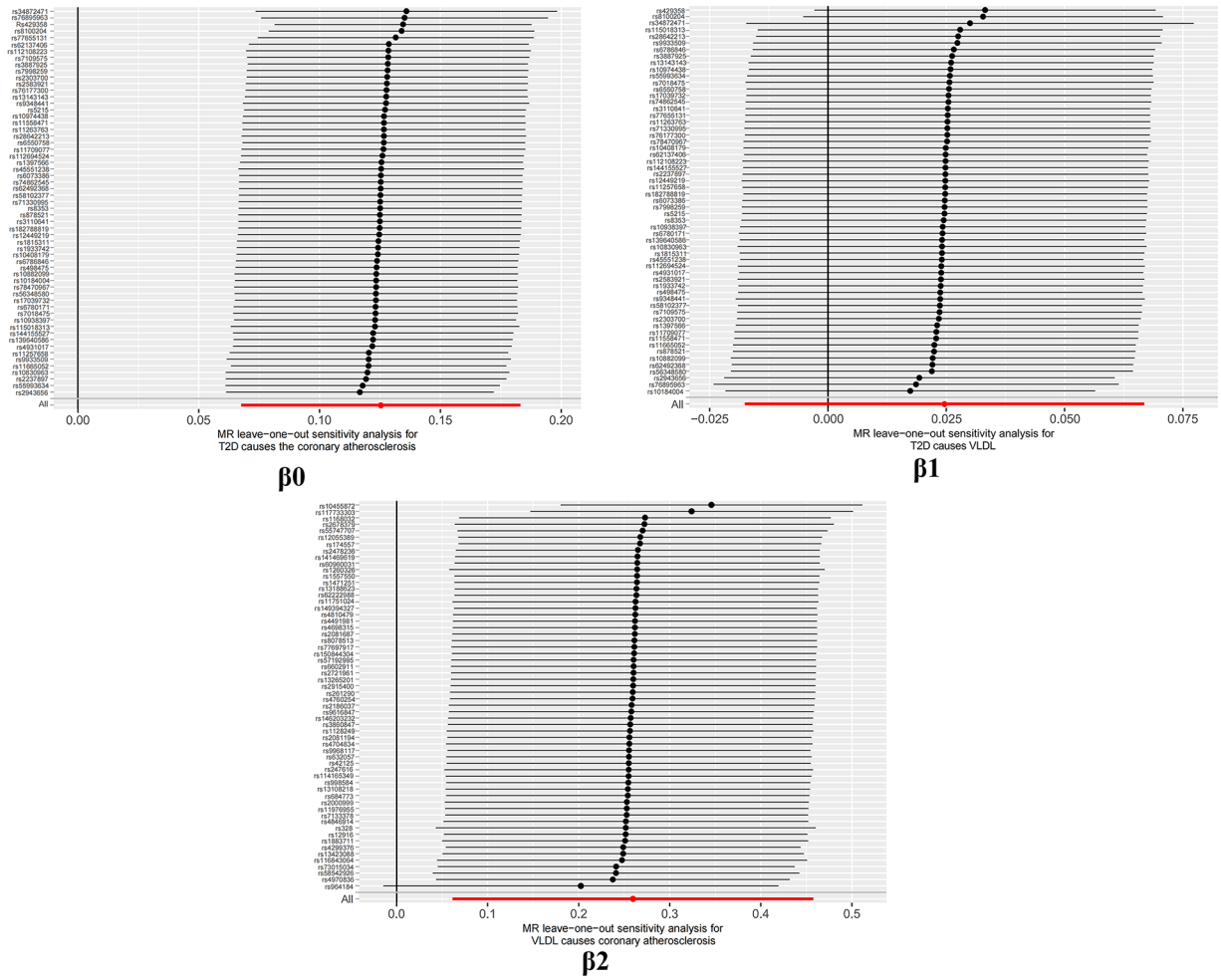

FIGURE 6
"leave one out" sensitivity analysis.

between T2D, VLDL, and coronary atherosclerosis. The results suggest that VLDL may potentially serve as a mediator in the pathway through which T2D leads to coronary atherosclerosis. This innovative approach bridges the gap between experimental and genomic methodologies, providing robust evidence for the causal link between these conditions. By incorporating VLDL levels as a potential mediating factor, it unveils a previously unexplored facet of their interplay, shedding light on the intricate mechanisms underlying this complex association.

The findings of this research have significant implications for clinical practice and public health policy formulation. Confirming the mediating role of VLDL in the T2D-coronary atherosclerosis association underscores the importance of reducing VLDL levels, potentially aiding in coronary atherosclerosis risk reduction. Due to the intricate interplay between T2D and coronary atherosclerosis, these results can guide the development of targeted intervention strategies, facilitating early identification and treatment of abnormal VLDL levels in T2D patients, thereby mitigating cardiovascular risks. Additionally, these discoveries offer a roadmap for future investigations, motivating further exploration into the mechanisms underlying T2D, VLDL, and coronary atherosclerosis, consequently providing more precise and effective approaches for cardiovascular disease prevention and management. This study not only enhances our understanding of the mechanisms underlying relevant diseases but also provides valuable insights for the realms of clinical practice and public health.

Data availability statement

The datasets presented in this study can be found in online repositories. The names of the repository/repositories and accession number(s) can be found in the article/Supplementary Material.

Ethics statement

Ethical approval was not required for the study involving humans in accordance with the local legislation and institutional requirements. Written informed consent to participate in this

study was not required from the participants or the participants' legal guardians/next of kin in accordance with the national legislation and the institutional requirements.

Author contributions

MR and WF designed the study. WF and LG acquired and analyzed all the dates. WF and YL plotted graphics. WF wrote the article. All authors contributed to the article and approved the submitted version.

Funding

This study is subsidized by the Industry Special Project of the National Administration of Traditional Chinese Medicine (201107006), the National key research and development plan (2018YFC1707403), and the Innovation Team Development Plan of the Ministry of Education (IRT_16R54).

Conflict of interest

The authors declare that the research was conducted in the absence of any commercial or financial relationships that could be construed as a potential conflict of interest.

Publisher's note

References

1. Li Y, Guo C, Cao Y. Secular incidence trends and effect of population aging on mortality due to type 1 and type 2 diabetes mellitus in China from 1990 to 2019: findings from the global burden of disease study 2019. *BMJ Open Diabetes Res Care*. (2021) 9(2):e002529. doi: 10.1136/bmjdrc-2021-002529

2. Yun JS, Ko SH. Current trends in epidemiology of cardiovascular disease and cardiovascular risk management in type 2 diabetes. *Metab Clin Exp*. (2021) 123:154838. doi: 10.1016/j.metabol.2021.154838

3. Faselis C, Katsimardou A, Imprialos K, Deligkaris P, Kallistratos M, Dimitriadis K. Microvascular complications of type 2 diabetes mellitus. *Curr Vasc Pharmacol*. (2020) 18(2):117–24. doi: 10.2174/1570161117666190502103733

4. Merino J, Jablonski KA, Mercader JM, Kahn SE, Chen L, Harden M, et al. Interaction between type 2 diabetes prevention strategies and genetic determinants of coronary artery disease on cardiometabolic risk factors. *Diabetes*. (2020) 69 (1):112–20. doi: 10.2337/db19-0097

5. Smith GD, Ebrahim S. Data dredging, bias, or confounding: they can all get you into the BMJ and the Friday papers. *Br Med J*. (2002) 325(7378):1437–8. doi: 10.1136/bmj.325.7378.1437

6. Birney E. Mendelian randomization. *Cold Spring Harb Perspect Med*. (2022) 12 (4):a041302. doi: 10.1101/cshperspect.a041302

7. Burgess S, Small DS, Thompson SG. A review of instrumental variable estimators for mendelian randomization. *Stat Methods Med Res*. (2017) 26(5):2333–55. doi: 10.1177/0962280215597579

8. Markozannes G, Kanellopoulou A, Dimopoulou O, et al. Systematic review of mendelian randomization studies on risk of cancer. *BMC Med*. (2022) 20(1):41. doi: 10.1186/s12916-022-02246-y

9. Deng Y, Wang L, Huang J, Ding H, Wong MCS. Associations between potential causal factors and colorectal cancer risk: A systematic review and meta-analysis of Mendelian randomization studies. *J Dig Dis*. (2022) 23(8–9):435–45. doi: 10.1111/1751-2980.13130

10. Dehghan A. Genome-wide association studies. *Methods Mol Biol*. (2018) 1793:37–49. doi: 10.1007/978-1-4939-7868-7_4

11. Huang D, Lin S, He J, Wang Q, Zhan Y. Association between COVID-19 and telomere length: A bidirectional Mendelian randomization study. *J Med Virol*. (2022) 94(11):5345–53. doi: 10.1002/jmv.28008

12. Abudureyimu M, Luo X, Wang X, Sowers JR, Wang W, Ge J, et al. Heart failure with preserved ejection fraction (HFpEF) in type 2 diabetes mellitus: from pathophysiology to therapeutics. *J Mol Cell Biol*. (2022) 14(5):mjac028. doi: 10.1093/jmcb/mjac028

13. Wakabayashi I. Associations of smoking and drinking with new lipid-related indices in women with hyperglycemia. *Womens Health Rep (New Rochelle)*. (2021) 2(1):23–31. doi: 10.1089/whr.2020.0100

14. Goodarzi MO, Rotter JI. Genetics insights in the relationship between type 2 diabetes and coronary heart disease. *Circ Res*. (2020) 126(11):1526–48. doi: 10.1161/CIRCRESAHA.119.316065

15. Viigimaa M, Sachinidis A, Toumpourleka M, Koutsampasopoulos K, Alliksoo S, Titma T. Macrovascular complications of type 2 diabetes mellitus. *Curr Vasc Pharmacol*. (2020) 18(2):110–6. doi: 10.2174/1570161117666190405165151

16. Juguilon C, Wang Z, Wang Y, Enrick M, Jamaiyar A, Xu Y, et al. Mechanism of the switch from NO to H2O2 in endothelium-dependent vasodilation in diabetes. *Basic Res Cardiol*. (2022) 117(1):2. doi: 10.1007/s00395-022-00910-1

17. Xiao H, Ma Y, Zhou Z, Li X, Ding K, Wu Y, et al. Disease patterns of coronary heart disease and type 2 diabetes harbored distinct and shared genetic architecture. *Cardiovasc Diabetol*. (2022) 21(1):276. doi: 10.1186/s12933-022-01715-1

18. Kosmopoulos M, Drekolias D, Zavras PD, Piperi C, Papavassiliou AG. Impact of advanced glycation end products (AGEs) signaling in coronary artery disease. *Biochim Biophys Acta Mol Basis Dis*. (2019) 1865(3):611–9. doi: 10.1016/j.bbadis.2019.01.006

19. Luong TV, Pedersen MGB, Kjærulff MLBG, Madsen S, Lauritsen KM, Tolbod LP, et al. Ischemic heart failure mortality is not predicted by cardiac insulin resistance but by diabetes per se and coronary flow reserve: a retrospective dynamic cardiac 18F-FDG PET study. *Metab Clin Exp*. (2021) 123:154862. doi: 10.1016/j.metabol.2021.154862

20. Biobaku F, Ghanim H, Batra M, Dandona P. Macronutrient-mediated inflammation and oxidative stress: relevance to insulin resistance, obesity, and atherogenesis. *J Clin Endocrinol Metab*. (2019) 104(12):6118–28. doi: 10.1210/jc.2018-01833

21. Zhao L, Lei W, Deng C, Wu Z, Sun M, Jin Z, et al. The roles of liver X receptor α in inflammation and inflammation-associated diseases. *J Cell Physiol*. (2021) 236 (7):4807–28. doi: 10.1002/jcp.30204

22. Shaya GE, Leucker TM, Jones SR, Martin SS, Toth PP. Coronary heart disease risk: low-density lipoprotein and beyond. *Trends Cardiovasc Med*. (2022) 32 (4):181–94. doi: 10.1016/j.tcm.2021.04.002

23. Sorokin AV, Patel N, Abdelrahman KM, Ling C, Reimund M, Graziano G, et al. Complex association of apolipoprotein E-containing HDL with coronary artery disease burden in cardiovascular disease. *JCI Insight*. (2022) 7(10):e159577. doi: 10.1172/jci.insight.159577

24. Heidemann BE, Koopal C, Bots ML, Asselbergs FW, Westerink J, Visseren FLJ. The relation between VLDL-cholesterol and risk of cardiovascular events in patients with manifest cardiovascular disease. *Int J Cardiol*. (2021) 322:251–7. doi: 10.1016/j.ijcard.2020.08.030

25. Nakajima K, Tanaka A. Atherogenic postprandial remnant lipoproteins; VLDL remnants as a causal factor in atherosclerosis. *Clin Chim Acta*. (2018) 478:200–15. doi: 10.1016/j.cca.2017.12.039

26. Richardson TG, Sanderson E, Palmer TM, Ala-Korpela M, Ference BA, Davey Smith G, et al. Evaluating the relationship between circulating lipoprotein lipids and apolipoproteins with risk of coronary heart disease: a multivariable mendelian randomisation analysis. *PLoS Med*. (2020) 17(3):e1003062. doi: 10.1371/journal.pmed.1003062

27. Holmes MV, Davey Smith G. Can mendelian randomization shift into reverse gear? *Clin Chem*. (2019) 65(3):363–6. doi: 10.1373/clinchem.2018.296806

28. Smith ML, Bull CJ, Holmes MV, Davey Smith G, Sanderson E, Anderson EL, et al. Distinct metabolic features of genetic liability to type 2 diabetes and coronary artery disease: a reverse mendelian randomization study. *EBioMedicine*. (2023) 90:104503. doi: 10.1016/j.ebiom.2023.104503

29. O'Sullivan JW, Ioannidis JPA. Reproducibility in the UK biobank of genome-wide significant signals discovered in earlier genome-wide association studies. *Sci Rep*. (2021) 11(1):18625. doi: 10.1038/s41598-021-97896-y

30. Hemani G, Zheng J, Elsworth B, Wade KH, Haberland V, Baird D, et al. The MR-base platform supports systematic causal inference across the human phenome. *Elife*. (2018) 7:e34408. doi: 10.7554/eLife.34408

31. Boehm FJ, Zhou X. Statistical methods for Mendelian randomization in genome-wide association studies: A review. *Comput Struct Biotechnol J*. (2022) 20:2338–51. doi: 10.1016/j.csbj.2022.05.015

32. Broadbent JR, Foley CN, Grant AJ, Mason AM, Staley JR, Burgess S. Mendelian randomization v0.5.0: updates to an R package for performing mendelian randomization analyses using summarized data. *Wellcome Open Res*. (2020) 5:252. doi: 10.12688/wellcomeopenres.16374.2

33. Bowden J, Davey Smith G, Burgess S. Mendelian Randomization with invalid instruments: effect estimation and bias detection through egger regression. *Int J Epidemiol*. (2015) 44(2):512–25. doi: 10.1093/ije/dyv080

34. Bowden J, Davey Smith G, Haycock PC, Burgess S. Consistent estimation in mendelian randomization with some invalid instruments using a weighted median estimator. *Genet Epidemiol*. (2016) 40(4):304–14. doi: 10.1002/gepi.21965

35. Bowden J, Del Greco MF, Minelli C, Davey Smith G, Sheehan N, Thompson J. A framework for the investigation of pleiotropy in two-sample summary data mendelian randomization. *Stat Med*. (2017) 36(11):1783–802. doi: 10.1002/sim.7221

36. Greco MFD, Minelli C, Sheehan NA, Thompson JR. Detecting pleiotropy in Mendelian randomisation studies with summary data and a continuous outcome. *Stat Med*. (2015) 34(21):2926–40. doi: 10.1002/sim.6522

37. Nazarzadeh M, Pinho-Gomes AC, Bidel Z, Dehghan A, Canoy D, Hassaine A, et al. Plasma lipids and risk of aortic valve stenosis: a Mendelian randomization study. *Eur Heart J*. (2020) 41(40):3913–20. doi: 10.1093/eurheartj/ehaa070

38. Hu Y, Zhang Y, Liu Y, Gao Y, San T, Li X, et al. Advances in application of single-cell RNA sequencing in cardiovascular research. *Front Cardiovasc Med*. (2022) 9:905151. doi: 10.3389/fcvm.2022.905151

39. Guo F, Qiu X, Zhu Y, Tan Z, Li Z, Ouyang D. Association between plasma betaine levels and dysglycemia in patients with coronary artery disease. *Biosci Rep*. (2020) 40(8):BSR20200676. doi: 10.1042/BSR20200676

40. Xu L, Yan X, Tang Z, Feng B. Association between circulating oxidized OxLDL/LDL-C ratio and the severity of coronary atherosclerosis, along with other emerging biomarkers of cardiovascular disease in patients with type 2 diabetes. *Diabetes Res Clin Pract*. (2022) 191:110040. doi: 10.1016/j.diabres.2022.110040

41. Søndergaard E, Nielsen S. VLDL Triglyceride accumulation in skeletal muscle and adipose tissue in type 2 diabetes. *Curr Opin Lipidol*. (2018) 29(1):42–7. doi: 10.1097/MOL.0000000000000471

42. Chen Y, Fu Y, Wang S, Chen P, Pei Y, Zhang J, et al. Clinical significance of neutrophil gelatinase-associated lipocalin and sdLDL-C for coronary artery disease in patients with type 2 diabetes mellitus aged ≥65 years. *Cardiovasc Diabetol*. (2022) 21(1):252. doi: 10.1186/s12933-022-01668-5

43. Pintaudi B, Scatena A, Piscitelli G, Frison V, Corrao S, Manicardi V, et al. Clinical profiles and quality of care of subjects with type 2 diabetes according to their cardiovascular risk: an observational, retrospective study. *Cardiovasc Diabetol*. (2021) 20(1):59. doi: 10.1186/s12933-021-01251-4

44. Zarkasi KA, Abdul Murad NA, Ahmad N, Jamal R, Abdullah N. Coronary heart disease in type 2 diabetes mellitus: Genetic factors and their mechanisms, gene-gene, and gene-environment interactions in the Asian populations. *Int J Environ Res Public Health*. (2022) 19(2):647. doi: 10.3390/ijerph19020647

45. Song J, Xia X, Lu Y, Wan J, Chen H, Yin J. Relationship among insulin therapy, insulin resistance, and severe coronary artery disease in type 2 diabetes mellitus. *J Interv Cardiol*. (2022) 2022:2450024. doi: 10.1155/2022/2450024

46. Manita D, Yoshida H, Hirowatari Y. Cholesterol levels of six fractionated serum lipoproteins and its relevance to coronary heart disease risk scores. *J Atheroscler Thromb*. (2017) 24(19):928–39. doi: 10.5551/jat.34728

47. Khoshandam A, Hedayatian A, Mollazadeh A, Razavi BM, Hosseinzadeh H. Propolis and its constituents against cardiovascular risk factors including obesity, hypertension, atherosclerosis, diabetes, and dyslipidemia: a comprehensive review. *Iran J Basic Med Sci*. (2023) 26(8):853–71. doi: 10.22038/IJBMS.2023.67793.14835

frontiers | Frontiers in Immunology

TYPE Original Research
PUBLISHED 23 February 2024
DOI 10.3389/fimmu.2024.1267963

OPEN ACCESS

EDITED BY
Catherine A. Reardon,
The University of Chicago, United States

REVIEWED BY
Roshni Roy,
Emory University, United States
Xu Peng,
Texas A and M University, United States
Yue Liu,
Xiyuan Hospital, China
Min Xu,
Shanghai Jiao Tong University, China

*CORRESPONDENCE
Huaifang Yao
huaifangyao@163.com
Longyi Zheng
longyizheng111@163.com

†These authors have contributed equally to this work

RECEIVED 21 August 2023
ACCEPTED 22 January 2024
PUBLISHED 23 February 2024

CITATION
Dai C, Wang D, Tao Q, Li Z, Zhai P, Wang Y, Hou M, Cheng S, Qi W, Zheng L and Yao H (2024) CD8$^+$ T and NK cells characterized by upregulation of NPEPPS and ABHD17A are associated with the co-occurrence of type 2 diabetes and coronary artery disease. *Front. Immunol.* 15:1267963. doi: 10.3389/fimmu.2024.1267963

CD8$^+$ T and NK cells characterized by upregulation of NPEPPS and ABHD17A are associated with the co-occurrence of type 2 diabetes and coronary artery disease

Chenyu Dai[1†], Damu Wang[1†], Qianqian Tao[2†], Ziyi Li[2], Peng Zhai[3], Yingying Wang[4], Mei Hou[5], Simin Cheng[1], Wei Qi[2], Longyi Zheng[6*] and Huaifang Yao[1*]

[1]Department of Cadre Cardiology, The First Affiliated Hospital of Anhui University of Chinese Medicine, Hefei, Anhui, China, [2]Department of General Surgery, The First Affiliated Hospital of Anhui University of Chinese Medicine, Anhui Academy of Chinese Medicine, Hefei, Anhui, China, [3]Department of Biomedical Engineering, Boston University, Boston, MA, United States, [4]Anhui Provincial Children's Hospital, Children's Hospital of Fudan University, Hefei, Anhui, China, [5]Cancer Research Center, The First Affiliated Hospital of University of Science and Technology of China (USTC), Division of Life Sciences and Medicine, University of Science and Technology of China, Hefei, Anhui, China, [6]Department of Endocrinology, Changhai Hospital, Naval Medical University, Shanghai, China

Background: Coronary artery disease (CAD) and type 2 diabetes mellitus (T2DM) are closely related. The function of immunocytes in the pathogenesis of CAD and T2DM has not been extensively studied. The quantitative bioinformatics analysis of the public RNA sequencing database was applied to study the key genes that mediate both CAD and T2DM. The biological characteristics of associated key genes and mechanism of CD8$^+$ T and NK cells in CAD and T2DM are our research focus.

Methods: With expression profiles of GSE66360 and GSE78721 from the Gene Expression Omnibus (GEO) database, we identified core modules associated with gene co-expression relationships and up-regulated genes in CAD and T2DM using Weighted Gene Co-expression Network Analysis (WGCNA) and the 'limma' software package. The enriched pathways of the candidate hub genes were then explored using GO, KEGG and GSEA in conjunction with the immune gene set (from the MSigDB database). A diagnostic model was constructed using logistic regression analysis composed of candidate hub genes in CAD and T2DM. Univariate Cox regression analysis revealed hazard ratios (HRs), 95% confidence intervals (CIs), and p-values for candidate hub genes in diagnostic model, while CIBERSORT and immune infiltration were used to assess the immune microenvironment. Finally, monocytes from peripheral blood samples and their immune cell ratios were analyzed by flow cytometry to validate our findings.

Results: Sixteen candidate hub genes were identified as being correlated with immune infiltration. Univariate Cox regression analysis revealed that NPEPPS and ABHD17A were highly correlated with the diagnosis of CAD and T2DM. The

results indicate that $CD8^+$ T cells (p = 0.04) and NK^{bright} cells (p = 3.7e-3) are significantly higher in healthy controls than in individuals with CAD or CAD combined with T2DM. The bioinformatics results on immune infiltration were well validated by flow cytometry.

Conclusions: A series of bioinformatics studies have shown ABHD17A and NPEPPS as key genes for the co-occurrence of CAD and T2DM. Our study highlights the important effect of $CD8^+$ T and NK cells in the pathogenesis of both diseases, indicating that they may serve as viable targets for diagnosis and therapeutic intervention.

KEYWORDS

cardiovascular disease, type 2 diabetes, bioinformatics, hub gene, CD8+T cells, NK cells, immune

Introduction

Diabetes mellitus (DM) is a chronic metabolic disorder characterized by hyperglycemia resulting from defects in insulin secretion, insulin resistance, or a combination of both (1, 2). This condition can lead to the long-term damage to organs, nervous system, and blood vessels, which further develop into organ dysfunction or even failure (3). The global prevalence of DM is increasing each year, with predictions indicating that the number of individuals with DM will reach 5.92 billion by 2035 (4, 5), over 90% of which will be type 2 diabetes mellitus (T2DM) (6). While T2DM can be effectively controlled clinically with antidiabetic drugs such as metformin and insulin (7, 8), the inherent metabolic abnormalities contribute to a wide range of diseases and predisposes to complications that threaten human health (9, 10). For this reason, most medical research has focused on the relationship between T2DM and other diseases (11–13).

Over the past 15 years, coronary artery disease (CAD) has become the leading cause of death worldwide, accounting for 15 million deaths in 2016 alone (14), and it is the primary reason of morbidity and death rate among individuals with T2DM (15, 16). There is a strong correlation between the occurrence of CAD and T2DM (1, 17). In their analysis of the Framingham Heart Study, Fox et al. reported that for each ten-year expand in the duration of T2DM, the morbidity and death rate of CAD in patients with T2DM increased by 1.38 and 1.86 times, respectively, compared to those without T2DM (18). The primary pathology underlying CAD is atherosclerosis, a chronic inflammatory response leading to plaque formation and can result in stable angina, unstable angina, sudden cardiac death, and myocardial infarction (MI) (19, 20). Immune cells including monocytes, macrophages, endothelial cells, smooth muscle cells and adipocytes are attracted to atherosclerotic plaques and are considered critical determinants of the disease progression (21, 22). The transition from stable plaques to unstable, rupture-prone plaques is associated with an increased number of T cells displaying signs of early activation within the plaque (23–25). Studies have shown that the number of apoptotic NK cells in the peripheral blood of patients with CAD is significantly increased (26, 27), and that the phenotype of $CD8^+$ T cells correlates with the rate of disease progression after the onset of T2DM (28–30). Despite the rapidly increasing prevalence of T2DM, which has proved to be a major account of morbidity and death rate in patients with MI (31, 32), research into the associated inflammation and changes in immune cell function between the two conditions is limited. Therefore, it is crucial to investigate the pathogenesis of MI and T2DM as well as determine the mechanisms of inflammation and immune regulation (33).

Drawing on public data and bioinformatics methods, this study identified 16 candidate hub genes linked with immune genes, MI and T2DM. Gene Ontology(GO) and Gene Set Enrichment Analysis (GSEA) were applied to detailed examine the organic procedure and gateways. Stepwise regression and Univariate Cox regression analysis were accomplished to create diagnostic models of CAD and T2DM and examine sixteen candidate hub genes in diagnostic models, which were authenticated in two specimen datasets, GSE66360 and GSE78721. These models have good potential diagnostic performance value in the clinical diagnosis of CAD and T2DM, and the measurement results of Area Under the Curve values indicated this. As T2DM is an important factor influencing cardiovascular disease and have high correlation with immune cell function. Consequently, we additionally investigated the distribution of immunocytes of specimens and the relevance of various immunocytes with these differentially expressed genes (DEGs), then performed correlation validation analyses of the abnormalities of the above DEGs. For further research, we performed correlation validation analyses of the abnormalities of the above candidate hub genes and immune cells in blood samples from 38 clinical CAD, T2DM patients and 9 healthy individuals. The results indicate a strong association between CAD and the prevalence of $CD8^+$ T and NK cells, also suggest the risk of T2DM

combined with CAD, providing insights for targeted treatment and control. The article design is shown in Figure 1.

Results

Identification of CAD and T2DM related gene modules

The Weighted Gene Co-expression Network Analysis (WGCNA) was employed to identify interconnected gene clusters or modules with a close relationship to CAD. The most suitable soft threshold power, β = 16.087, was selected based on scale independence (R^2 = 0.87) and mean connectivity (the minimum of about 0) (Figure 2A). Following this, module merging was performed, resulting in 20 gene co-expression modules related to CAD, each represented by a different color (Figures 2B, C). These colors depict the relationship between the modules and CAD, with turquoise indicating the most positive correlation (232 genes; [CC] = 0.65; P = 6.3e-29) and light green showing the strongest negative correlation (66 genes; [CC]=-0.78; P=4.7e-48) with T2DM. In addition, significant correlations were observed between both the turquoise (r = 0.68) and light green (r = 0.72) module memberships and gene significance for CAD (Figure 2D). Consequently, 298 genes within the turquoise and light green modules, which exhibited the strongest associations with CAD, were chosen for further study. The details of the identification of gene modules associated with T2DM can be found in Supplementary Figure 1.

Identification of hub genes associated with immunological signature genes, CAD, and T2DM

In the comparison between the T2DM and normal population, 1567 DEGs were acknowledged, and the comparison between the CAD and healthy control groups, 1414 DEGs were found. These genes were validated using the "limma" package. In the T2DM group, 1384 of these genes were upregulated and 183 were downregulated, while in the CAD group, 815 were upregulated and 599 were downregulated. The top 20 upregulated and downregulated DEGs are depicted in the heatmap (Figure 3A), and all DEGs are represented by volcano plots, with red or blue grids reflecting genes which were upregulated and downregulated, separately (Figure 3B). Red or green triangles implied genes which were upregulated and downregulated, separately. From the Immunologic Signature gene sets (ImmuneSigDB; MSigDB; Liberzon et al., 2011, Bioinformatics), immune_GENEs were extracted. The ImmuneSigDB contains gene sets representing comprehensive regulatory dynamics of cell types, states, and disturbances within the immune system. These signatures were created through the manual curation of published human immunology studies. Subsequently, an intersection of 298 module genes associated with CAD as identified by WGCNA combined with 1414 DEGs detected by the "limma" package, 3907 immune_GENEs extracted from MSigDB, and 1567 T2DM DEGs associated with T2DM progression led to the selection of 16 candidate hub genes: PI4KA, YWHAZ, ERRFI1, ABHD17, LRRC40, PLSCR4, NPEPPS, SEL1L3, MAP3K2, ZBED5, EIF2B1, CAPN2, ZNF146, BCHE, UQCRC2, USP34. All 16 candidate hub genes are protein-coding and their distribution varies in the human body, mainly concentrated in the brain and lymph nodes (Figure 3C; Table 1).

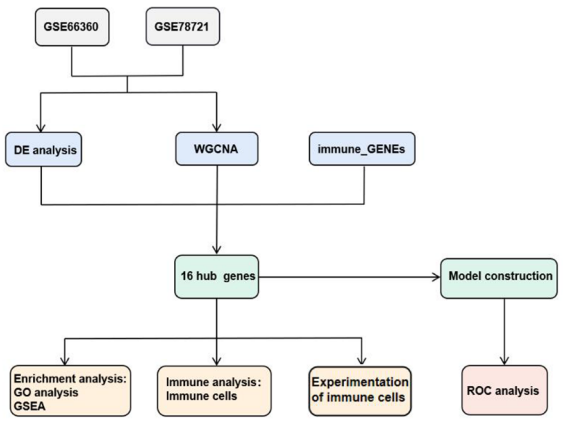

FIGURE 1
Structure of workflow chart.

Functional enrichment analysis and biological process of DEGs

GO and Kyoto Encyclopedia of Genes and Genomes (KEGG) annotations were utilized for more detailed biological research of DEGs. GO manifested that the DEGs were chiefly distributed in several biology procedures including 1) platelet alpha granule, maintenance of DNA methylation, positive regulation of multicellular organism process, and regulation of phosphatidylinositol 3-kinase signaling; 2) ATP binding, secretory granule, enzyme binding, and purine nucleotide binding; and 3) Alzheimer's disease, inositol phosphate metabolism, oxidative phosphorylation, and apoptosis (Figures 4A–C). KEGG pathway enrichment analysis demonstrated that these genes were chiefly enriched in endopeptidase activity, hydrolase activity, and cysteine-type endopeptidase activity (Figure 4D). GSEA was employed to identify activation pathways in CAD and T2DM, and to distinguish differential regulatory pathways between the high and low expression groups of candidate hub genes. GSEA of hub genes suggested that they were associated with several protein biological processes such as ubiquitin-mediated proteolysis, protein export, and RNA polymerase, neurological related activities like neuroactive ligand-receptor interaction, and other biological processes like olfactory transduction, ubiquitin-mediated proteolysis, nucleotide excision repair, endocytosis, and limonene and pinene degradation (Supplementary Figure 2). Among these candidate hub genes, ERRFI1, SEL1L3, ZBED5, ZNF146, ABHD17A, and YWHAZ were implicated in the biological process of protein output. ERRFI1, PI4KA, ZBED5, UQCRC2, and ZNF146 were implicated in the biological process of olfactory transduction. ZNF146 and ABHD17A were implicated in the biological process of the

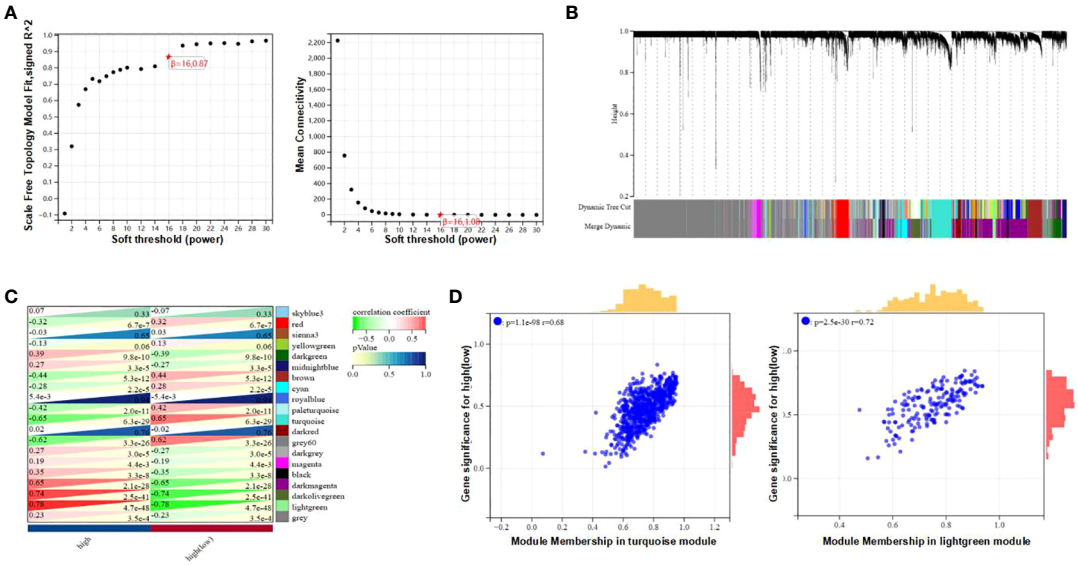

FIGURE 2
Determination of gene modules related to coronary heart disease. **(A)** Constructing Soft Threshold Power (β) based on dimension independence and mean connectivity. **(B)** Gene block mass related to CAD are displayed in various colors under the gather dendrogram. **(C)** The correlation between gene modules and CAD is depicted through heat maps. The upper left side displays the coefficient of correlation, and the lower right side displays the P-value. **(D)** The correlation between the most positively correlated and negatively correlated modules in CAD, different member relationships, and gene conspicuousness.

spliceosome. ERRFI1 was implicated in the biological process of RNA polymerase. Among these candidate hub genes, SEL1L3 was involved in most biological pathways, including ubiquitin-mediated proteolysis, protein export, pyrimidine metabolism, nucleotide excision repair, pathogenic Escherichia coli infection, and neuroactive ligand-receptor interaction. In contrast, PLSCR4 was only involved in the biological process of limonene and pinene degradation.

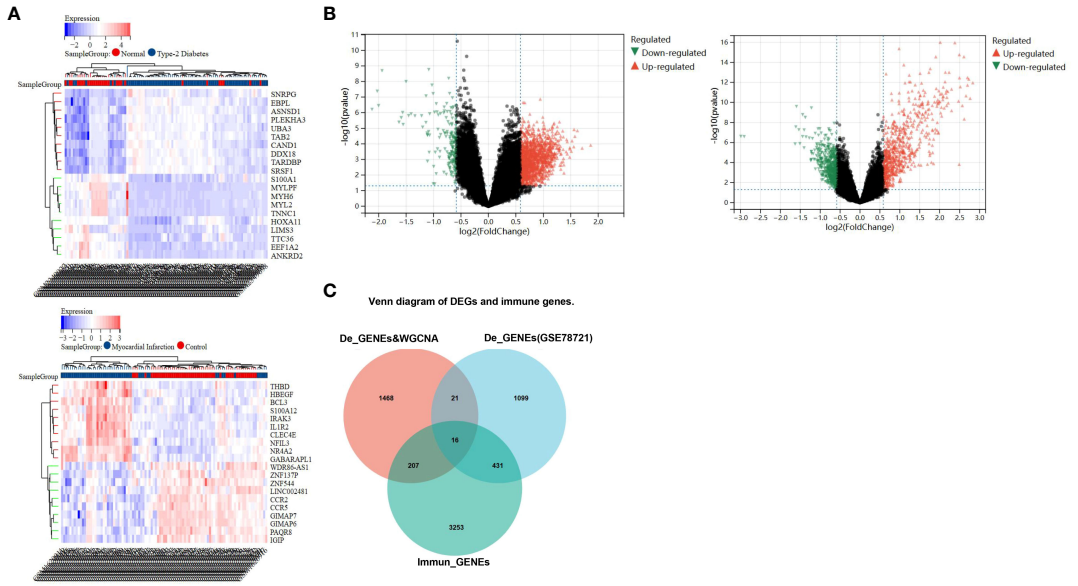

FIGURE 3
Recognition of differential genes associative with CAD patients and healthy cohorts, T2DM patients and healthy cohorts. **(A)** The top 20 up- and down-regulated differential gene discovered between the CAD and healthy groups, as well as T2DM and healthy groups, are represented by red and blue squares in the heat map, respectively. **(B)** The red and green triangles in the volcano map represent the up- and down- differential genes. **(C)** Venn diagram shows gene intersection of immune gene, the differential genes of T2DM and the differential genes of CAD combined with WGCNA-identified module genes.

TABLE 1 The type and expression of the 16 hub genes.

Genes	Gene type	Expression
PI4KA	protein coding	Ubiquitous expression in brain (RPKM 52.3), testis (RPKM 23.0) and 24 other tissues
YWHAZ	protein coding	Ubiquitous expression in esophagus (RPKM 248.0), brain (RPKM 160.0) and 25 other tissues
ERRFI1	protein coding	Broad expression in liver (RPKM 123.7), gall bladder (RPKM 60.1) and 20 other tissues
ABHD17A	protein coding	Ubiquitous expression in spleen (RPKM 12.7), bone marrow (RPKM 10.4) and 25 other tissues
LRRC40	protein coding	Ubiquitous expression in brain (RPKM 8.0), testis (RPKM 8.0) and 25 other tissues
PLSCR4	protein coding	Ubiquitous expression in fat (RPKM 22.0), gall bladder (RPKM 21.1) and 24 other tissues
NPEPPS	protein coding	Ubiquitous expression in esophagus (RPKM 43.2), brain (RPKM 28.6) and 25 other tissues
SEL1L3	protein coding	Broad expression in lymph node (RPKM 28.3), stomach (RPKM 23.4) and 20 other tissues
MAP3K2	protein coding	Ubiquitous expression in bone marrow (RPKM 11.2), thyroid (RPKM 10.3) and 25 other tissues
ZBED5	protein coding	Ubiquitous expression in lymph node (RPKM 23.1), endometrium (RPKM 21.4) and 25 other tissues Ubiquitous expression in lymph node (RPKM 22.1), skin (RPKM 20.5) and 25 other tissues
EIF2B1	protein coding	Ubiquitous expression in lung (RPKM 90.0), gall bladder (RPKM 66.0) and 25 other tissues
CAPN2	protein coding	Ubiquitous expression in thyroid (RPKM 20.8), endometrium (RPKM 19.9) and 25 other tissues
ZNF146	protein coding	Biased expression in liver (RPKM 60.4), brain (RPKM 16.9) and 12 other tissues
BCHE	protein coding	Ubiquitous expression in heart (RPKM 179.2), duodenum (RPKM 111.5) and 25 other tissues
UQCRC2	protein coding	Ubiquitous expression in testis (RPKM 17.6), lymph node (RPKM 17.0) and 25 other tissues
USP34	protein coding	

Construction and validation of diagnostic models and hub genes

Two predictive models incorporating candidate hub genes were developed using the logistic regression algorithm, drawing from GSE66360 and GSE78721 datasets. The prediction model built from the GSE66360 dataset exhibited strong diagnostic capabilities, with an AUC value of 0.80 (Figure 5A). Univariate Cox regression analysis of the expression of candidate hub genes from prediction model was conducted. The results suggested that high expression of ABHD17A (p=2.9e-3) was associated with diagnostic rates of patients with MI compared to that of healthy individuals. (Figure 5B). For the GSE78721 dataset, the model displayed an AUC value of 0.75 (Figure 5C). Univariate Cox regression analysis of the expression of candidate hub genes suggested that high expression of NPEPPS (p=0.04) was associated with diagnostic rates of patients with T2DM compared to that of healthy individuals (Figure 5D). When selecting pathological samples for CAD, blood samples prove to be more appropriate than adipose tissue samples, mainly because peripheral blood samples are easier to obtain *in vivo*. The results from peripheral blood specimens suggest that the GSE66360 dataset has predictive value for CAD

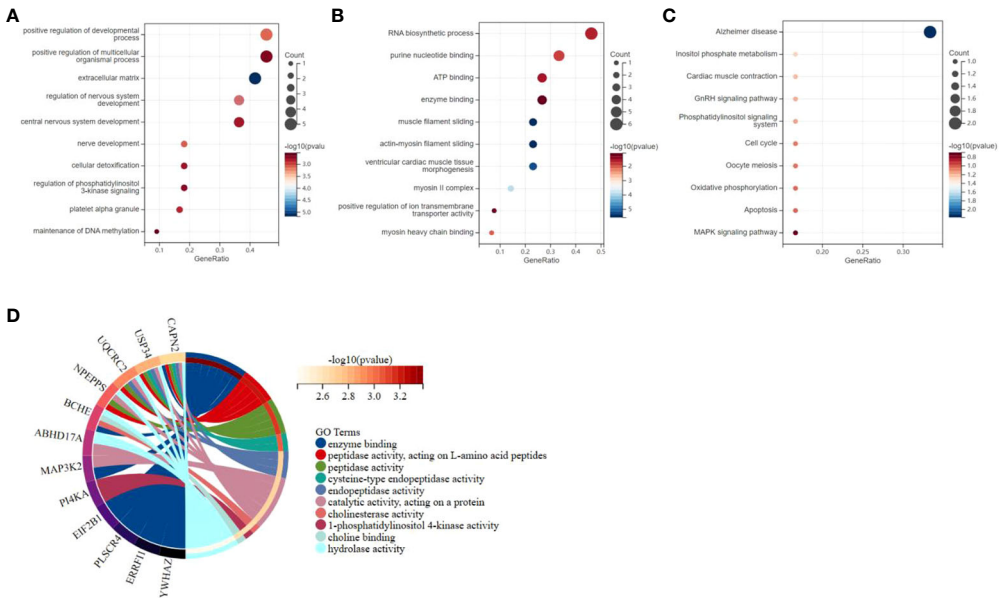

FIGURE 4
Functional enrichment study of differentially expressed genes and hub genes related to CAD and T2DM progression. **(A–C)** Gene Ontology analysis of CAD and T2DM-associated differential gene. The top 10 enriched Gene Ontology sorts (bioprocess, cell constituent, and molecular function) are revealed. Gene proportions and different ontologies are represented by the X and Y coordinates. The circle extent indicates gene count. **(D)** Kyoto Encyclopedia of Genes and Genomes analysis of the candidate hub genes related to CAD and T2DM progression, immune genes. The left and right portion means the enriched differentially expressed genes and most considerable ontologies, respectively.

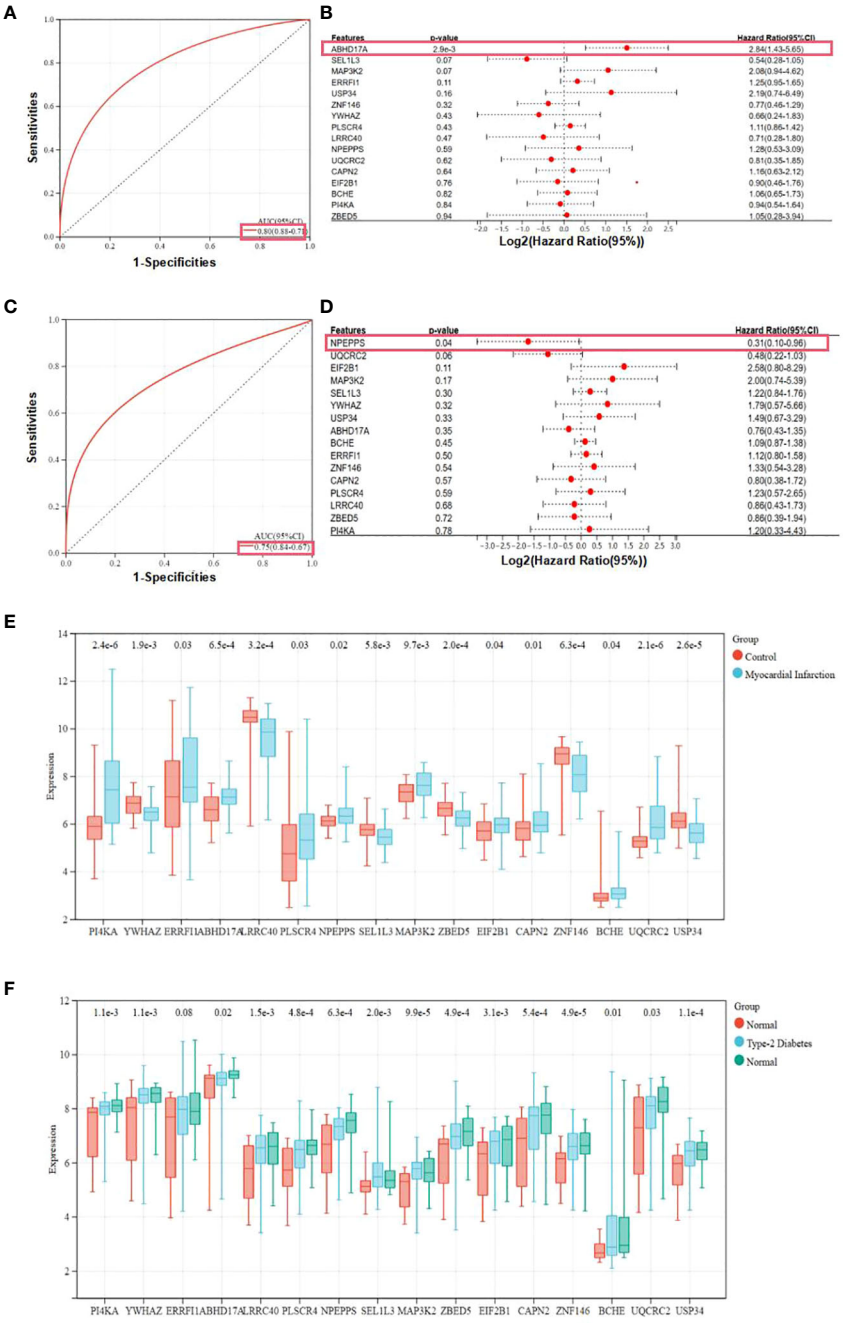

FIGURE 5
Expression and receiver operating characteristic curves values of samples and key genes from two diagnostic models. **(A)** Construction of the candidate genes-based diagnostic prediction model of CAD. **(B)** Univariate Cox regression analysis showing the HRs with 95% CIs and p values for candidate hub genes in CAD. **(C)** Construction of the candidate genes-based diagnostic prediction model of T2DM. **(D)** Univariate Cox regression analysis showing the HRs with 95% CIs and p values for candidate hub genes in T2DM. **(E)** Representation of candidate diagnostic genes in MI individuals of blood specimens in GSE66360. **(F)** Representation of candidate diagnostic genes in T2DM individuals of depots of adipose structure specimens in GSE78721.

diagnosis in practical disease treatment. Using univariate Cox regression analysis to validate candidate hub genes in the GSE66360 prediction models of MI and GSE78721 prediction models of T2DM. This validation revealed that only two hub genes, ABHD17A and NPEPPS, were noticeably up-regulated in CAD and T2DM predictive diagnostic models. Box plots showed that five genes: PI4KA, ERRFI1, LRRC40, ABHD17A and ZNF146 were noticeably expressed in MI, while the remaining eleven genes were expressed to a lesser extent such as SEL1L3, UQCRC2 and USP34. Obviously, the genes expression level of BCHE was the lowest (Figure 5E). In the T2DM dataset, nearly all candidate genes were highly expressed. Among them, the proportion degrees of ABHD17A and UQCRC2 were particularly pronounced, but the proportion degrees of BCHE was again the lowest (Figure 5F).

The composition of immunocytes and immune infiltration

The microenvironment of the sample, consisting of lymphocytes, monocytes, macrophages, granulocytes, and inflammatory factors, has a significant impact on disease diagnosis and clinical therapeutic sensitivity. For this investigation, the composition of 22 types of immunocytes in different sample groups, including 49 MI cases, 50 normal cases, 105 DM cases, and 95 normal cases, were estimated using the CIBERSORT algorithm. This composition is illustrated in the histograms (Figures 6A, B). Comparisons were made between the immunocyte infiltration in the MI and normal groups, as well as between DM and normal specimens, and these comparisons are presented in the box plots (Figures 6C, D). The results suggest that in the GSE66360 dataset, there was a conspicuously higher proportion of CD8 cells (p = 0.04), CD4 memory resting T cells (p = 2.7e-5), and gamma delta T cells (p = 2.3e-4), as well as a lower proportion of activated mast cells (p = 4.2e-10) and neutrophils (p = 9.3e-9) in the normal group compared to the MI group. In the GSE78721 dataset, the normal group exhibited conspicuously higher proportions of resting NK cells (p = 3.7e-3), CD4 naive T cells (p = 1.6e-3), and activated dendritic cells (p = 5.4e-3), but lower proportions of M0 macrophages (p = 6.7e-6) contrast with the DM group. Furthermore, an analysis of the relationship between infiltration estimation and gene expression in gene modules revealed that T-cell $CD4^+$ Th1 in genes ERRFI1, ZBED5, UQCRC2, ZNF146, ABHD17A, YWHAZ, and especially PLSCR4 showed a negative correlation in nearly 40 types of cancer. Many of these cancers are associated with CAD or T2DM, including UCEC, BRCA, PRAD, COAD, PAAD, and others. Modules that investigate the relationship between immune infiltrates and genomic alterations or clinical outcomes in TCGA are displayed in Supplementary Figure 3.

Study of immune cells in CAD, T2DM, and healthy individuals

Following the bioinformatics analysis of immune cell expression in CAD and T2DM, clinical samples were collected for the clinical validation of immune cells using flow cytometry. Prior to the flow cytometry analysis, suitable gating strategies were utilized to identify cells with live/dead staining in CD8 T cells and NK cells using fresh cells (freshly isolated from peripheral blood), as some biomarkers such as CD16 may undergo downregulation or detachment after thawing. Blood counts of $CD8^+$ T and NK cell lymphocytes were detected by flow cytometry in 38 patients from the First Affiliated Hospital of Anhui University of Chinese Medicine, categorized as those with CAD, T2DM, CAD Combined with T2DM, and 9 healthy subjects (Tables 2–4). The $CD8^+$T and NK cells in CAD, CAD Combined with T2DM, and normal venous blood were observed through flow cytometry (Figures 7A–D). Combined with Tables 3 and 4, the results demonstrated that noticeably higher percentages of $CD8^+$T cells are typically present in healthy subjects (Figure 7A) compared to those with CAD (Figure 7B), and higher levels of NK^{bright} cells in healthy subjects compared to those with CAD or T2DM (Figure 7C). It was observed that healthy subjects typically have conspicuously higher proportions of NK^{bright} cells than those with CAD combined with T2DM (Figure 7D).

Discussion

Early diagnosis of CAD combined with T2DM is challenging due to its complicated etiology and risk factors. Therefore, it is crucial to develop new diagnostic models to identify the drivers of

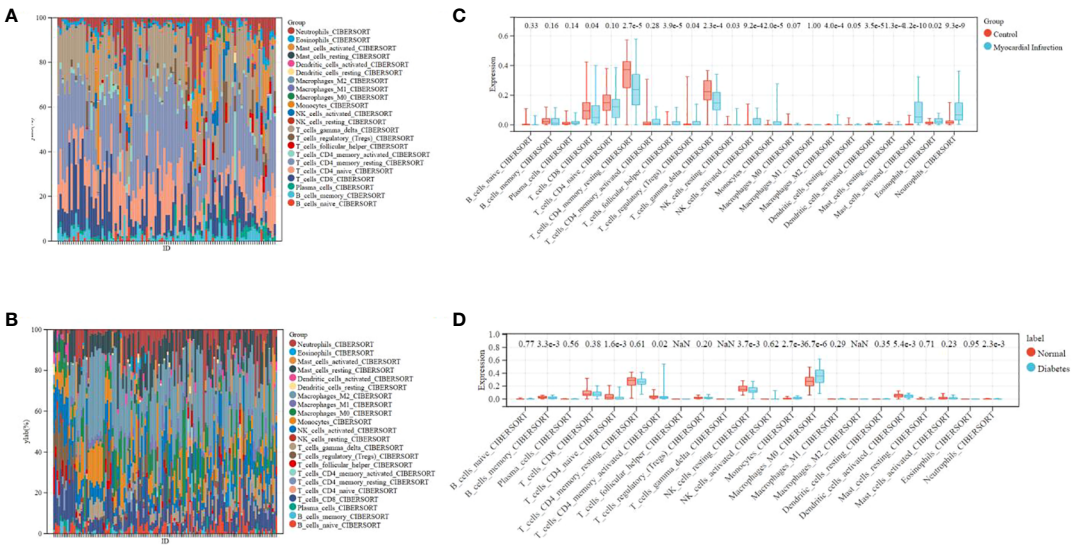

FIGURE 6
Distribution of immunocytes between diseased and normal specimens. **(A)** Relational proportion of 22 immunocytes in each specimen in GSE66360. **(B)** Relative proportion of 22 immunocytes in each specimen in GSE78721. **(C)** Variation in Immunocyte proportion expression between MI and Normal specimens. **(D)** Variation in Immunocyte proportion expression between T2DM and Normal specimens.

TABLE 2 The demographics and clinical characteristics of individuals.

	NOR Control (n=9)	CAD (n=13)	T2DM (n=11)	CAD-T2DM (n=14)
Female/Male	4/5	7/6	6/5	7/7
Mean age	62.8 ± 4.5	61.8 ± 4.6	64.1 ± 4.4	62.7 ± 5.0
BMI	22.5 ± 2.5	24.3 ± 2.1	25.4 ± 3.0	23.0 ± 2.6
HbA1c, %	5.32 ± 0.55	5.29 ± 0.44	8.90 ± 1.57	7.49 ± 1.18
TC, mmol/L	5.18 ± 1.09	4.91 ± 0.73	6.21 ± 1.05	6.16 ± 1.21
TG, mmol/L	1.81 ± 0.68	1.61 ± 0.79	3.3 ± 0.96	3.17 ± 1.38
LDL-c, mmol/L	2.78 ± 0.96	2.65 ± 0.94	3.03 ± 1.27	2.89 ± 1.31

CAD associated with T2DM. In this study, bioinformatics research identified 16 candidate hub genes associated with gene co-expression relationships and up-regulated genes in CAD and T2DM. NPEPPS and ABHD17A were identified as key genes in CAD combined with T2DM patients and were highly associated with the diagnosis of CAD and T2DM. Subsequently, we highlighted the important roles of $CD8^+$ T cells and NK cells in the pathogenesis of these two diseases using CIBERSORT and immune infiltration, suggesting that they may be viable targets for diagnosis and therapeutic intervention. The discovery of key diagnostic genes and significant changes in immune cells, specifically $CD8^+$ cells and NK cells, in CAD combined with T2DM provides new insights into potential targets for diagnostic and therapeutic interventions.

Further bioinformatics analysis revealed that these 16 candidate hub genes were associated with various protein biological processes. The key diagnostic gene, ABHD17A, is associated with the biological process of protein export and ubiquitin-mediated proteolysis. ABHD17A has significant catalytic activity to play a key role in membrane localization, and promotes N-Ras deacylation, leading to changes in the subcellular localization of N-Ras. Additionally, it promotes palmitate turnover on proteins such as PSD95 and N-Ras, which are important processes that control protein localization and signal transduction (34). The other diagnostic key gene, aminopeptidase (NPEPPS) is an important zinc metallopeptidase belonging to the oxytocinase subfamily of the M1 aminopeptidase family (35, 36). It contributes to the machining of the proteosome-acquired peptide pool, following closely behind pruning of antigen peptides by ERAP1 and ERAP2 for emergence on major histocompatibility complex (MHC) class I molecules (35, 37). Several GWAS analysis have presented relevances of these NPEPPS with multifarious immunity-induced disorders for instance inflammatory bowel disease, and diabetes mellitus, the genetic interactions between some aminopeptidases and HLA class I loci are closely related to these diseases (38–43). In this study, multiple bioinformatic analyses have established that CAD and T2DM are tightly associated through the hub genes ABHD17A and NPEPPS. Unfortunately, these analyses and subsequent validation, by applying clinical samples, are not sufficient to elucidate whether ABHD17A and NPEPPS are a cause or a consequence of T2DM or CAD. Both ABHD17A and NPEPPS are related to cell metabolism and play important roles in phosphatidylinositol metabolism, which may be significant in promoting T2DM progression. In addition, NPEPPS is closely associated with various autoimmune diseases. Despite these findings, since T2DM is a long-term chronic metabolism disease, it affects the metabolic changes in the body, which will affect the function of the immune system, and the progression of CAD, especially the occurrence of MI, is closely related to the abnormal function of the immune system. Therefore, when focusing on ABHD17A and NPEPPS in $CD8^+$ T cells and NK cells, we tend to believe that the abnormalities of these hub genes in these immune cells are caused by long-term metabolic changes caused by T2DM. Subsequently, these abnormalities in immune cells caused by T2DM contribute to the progression of CAD and increase the risk of MI. These are considerations based on disease characteristics and known hub gene functions. Additional research is required to clarify the pathogenic mechanisms of ABHD17A and NPEPPS in CAD and T2DM and establish specific causal relationships.

This study found that $CD8^+$ T cell ratios was higher in healthy individuals than in CAD patients and CAD complicated with T2DM patients. Notably, the proportion of NK^{bright} cells in healthy individuals is usually significantly higher than CAD or T2DM

TABLE 3 The levels of $CD8^+$ T and NK cells in patients.

Group	$CD8^+$T Cell		NK Cell	
	High	low	$CD56^{bright}$	$CD56^{dim}$
Normal	7(77.8%)	2(22.2%)	6(66.7%)	3(33.3%)
CAD	5(38.5%)	8(61.5%)	4(31.0%)	9(60.0%)
T2DM	8(72.7%)	3(27.3%)	4(36.4%)	7(63.3%)
CAD & T2DM	4(28.6%)	10(71.4%)	3(21.4%)	11(78.6%)

10.3389/fimmu.2024.1267963

TABLE 4 Changes in $CD8^+$ T and NK cell levels in peripheral blood (%).

Group	n	$CD8^+$T Cell	NK^{bright} Cell
Normal	9	26.77±2.96	89.02±2.87
CAD	13	14.71±4.22	40.81±3.98
T2DM	11	31.45±3.76	42.05±2.80
CAD-T2DM	14	11.64±4.33	17.87±6.08

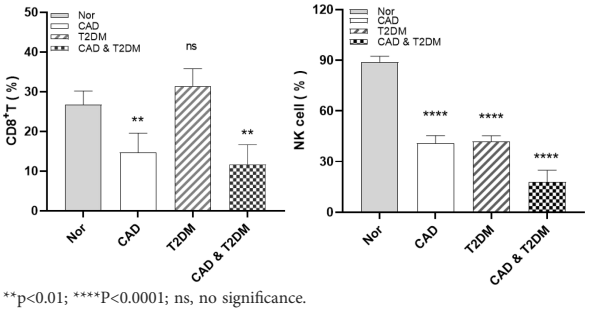

**p<0.01; ****P<0.0001; ns, no significance.

patients. Recent studies revealed that CAD patients have a high number of $CD8^+$ T cells expressing CD56 or CD57, which exhibited typical pro-inflammatory features (44–46). Dilated CD8 IL-6Rα^+ low T cells were associated with increased incidence of failure, cytotoxic CD8CD57 T cells, and elevated IL-6 levels. The expression of IL-6Rα by human $CD8^+$ T cells has been considered to define a distinct T cell subset that produces Th2 cytokines (47). Simultaneously, In patients with CAD, NK cell apoptosis, a key factor in initiating and regulating the immune response, is reduced (48). Furthermore, a potential negative impact on immunomodulatory defenses during the development of atherosclerosis may result from the sustained loss of NK cells (26, 49, 50). NK cells from the patients had suppressed both TNF-α secretion and particle capability as evidenced by CD107a reflection (51).

T2DM is known to be a major risk factor for CAD. Among T2DM patients, CAD is more likely to be a complicated disorder characterized by small, extensive, calcified, multivessel disease (MVD) and often requires coronary revascularization apart from definitive medical treatment to control angina pectoris (52). Research has shown that insulin resistance, hyperinsulinemia, and vascular calcification are common complications in diabetes patients (53). Promotive factors, such as diabetes-induced ROS overexpression, secretion of inflammatory factors, improved conversion rate of aldose reductase (AKR1B1) basement (54), and activation of protein kinase C β, δ, and θ, can accelerate the transformation of stable plaque into unstable plaque or plaque rupture (51, 52), which subsequently leads to thrombosis and the manifestation of adverse coronary events (51).

Inevitably, the above study has limitations. Diagnostic models were constructed for the diagnostic prediction of patients with CAD combined with T2DM based on retrospective data from the GEO database. The model is based on 16 candidate hub genes. Prospective data is needed to validate the clinical application value of the model. Further investigation is needed to determine the specific mechanism of action of ABHD17A and NPEPPS in $CD8^+$ and NK cells.

Materials and methods

Study design and data collection

The NCBI Gene Expression Comprehensive Public Database (GEO) provides source support for data collection and subsequent analysis. GSE66360 annotated HG-133U from GPL570 in peripheral blood_PLUS_2 microarray measurement of gene expression, which included 49 myocardial infarction groups and 50 healthy cohorts. GSE78721 was annotated by GPL15207 from different adipose depots (thigh, visceral and subcutaneous) of patients suffering from type 2 diabetes.

WGCNA of T2DM and CAD

The Sangerbox 3.0 software package, which includes "WGCNA," was used to produce a gene co-expression network to explore the co-expression relevances between genes in the sample and the relevance of genes and their expressions. This process required a Pearson correlation matrix and an average linkage method for all pairs of genes. A weighted adjacency matrix was constructed using the power function A_Mn = |C_Mn|^β. When the soft threshold is 16.087, the R^2 has a significant improvement, reaching 0.9. At this point, the network has already followed a scale-free distribution. After choosing a power of 16.087, the contiguity was changed into a Topological Overlap Matrix (TOM). This matrix determined the network relevancy of genes, considered as the summation of their contiguity to all others in the network relative to the gene proportion, and calculated the associated diversity (1-TOM). To group genes with comparable description characteristics into gene modules, mean integration collecting was conducted according to the TOM-based diversity estimation. The minimal size for the gene dendrogram (tree) was set at 30. For further module analysis, we evaluated the module's own genetic diversity, picked a cut-off for the module dendrogram, and combined certain modules. Each module was represented by a different color. The gene expression profile of each module was expressed by three factors: module eigengene (ME), module membership (MM), and gene significance (GS). MEs were applied to estimate the relevance between different modules and phenotypes. Module membership (MM) indicates the correlation between a gene and its corresponding module. Gene significance (GS) represented the relationship between a gene and phenotype, and was determined by the log10 transformation of the P value in the linear regression between gene expression and phenotype.

Identification of differentially expressed genes

Perform expression analysis of diverse genes on CAD (GSE66360) and T2DM (GSE78721) samples using the "limma" software package from the online website Sangerbox 3.0. P_ Genes with adj < 0.05 and multiple variation (FC) | > 1.5 were regarded as distinctively described genes. Create heat maps and volcanic maps

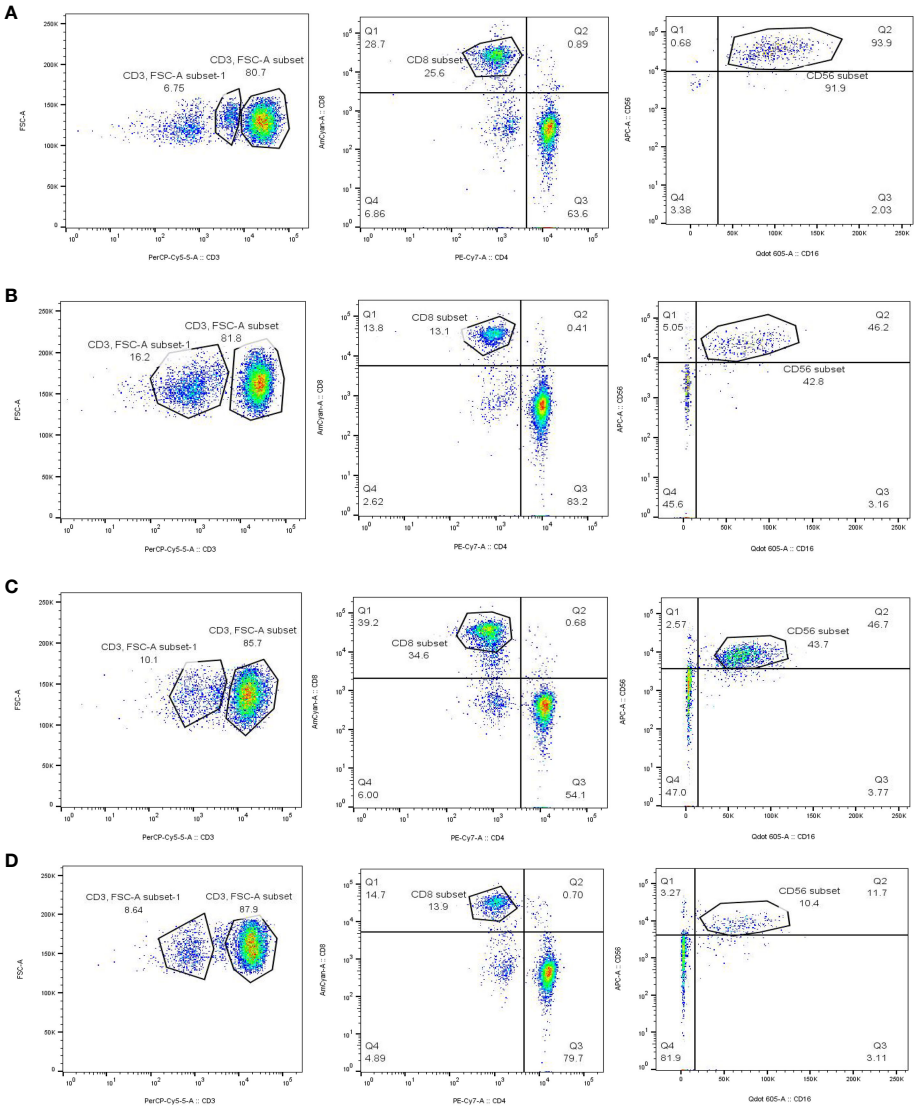

FIGURE 7
Gating strategy for immune cells of CAD, T2DM patients and healthy people. **(A)** The blood count of $CD8^{+}$T and NK cells in healthy people. **(B)** The blood count of $CD8^{+}$ T and NK cells in CAD patients. **(C)** The blood count of $CD8^{+}$ T and NK cells in T2DM patients. **(D)** The blood count of $CD8^{+}$ T and NK cells in CAD combined with T2DM individuals.

of differentially expressed genes using the "pheatmap" and "ggplot2" software packages. Use the online Venn chart tool to obtain their common 16 DEGs.

Functional enrichment analysis

The online website sangerbox carries out GO analysis and KEGG analysis, in which GO analysis includes BP (Biological Process), MF (Molecular function), CC (Cellular configuration), cardiovascular disease samples and diabetes samples, as well as hub gene enrichment investigation. GSEA was served as reveal the respective functions of central genes. Using the Gene Ontology footnote in R program procedure (edition 3.1.0) for the technical support, enrichment analysis of gene set functions was conducted, genes are plotted to the backdrop set, Enrichment investigation was conducted enacting R program clustering archive (edition 3.14.3) to derive gene set enrichment outcomes. Setting the minimum gene set to 5 and the maximum gene set to 5000, with a P value of < 0.05 and an FDR value of < 0.25, is considered statistically relevantly.

Production of receiver operating characteristic curves and description of hub genes in samples

We operated R program pROC (edition 1.15.0.1) to conduct ROC estimation to acquire AUC. Specifically, we obtained the CAD and T2DM gene expression of patients, used the ROC function of pROC to conduct ROC analysis at 365 time points, and used the ci ability of pROC to estimate AUC and confidence intermission to acquire the final AUC outcomes.

Gene set enrichment investigation

We assembled GSEA (http://software.broadinstitute.org/gsea/index.jsp). The web page obtained GSEA program (edition 3.0) and separated the models into two series according to disease types. The various immune gene samples were collected from the immunologic signature gene sets (http://www.gsea-msigdb.org/gsea/downloads.jsp). The kegg characters subset was downloaded to estimate relative pathways and molecular mechanisms of action. According to gene reflection profiling and phenotype subsets, set the minimal genomes and utmost genomes, and collect samples again, P numerial number of < 0.05 and an FDR of < 0.25 were consistent statistically significance relevant.

Immunocyte infiltration and level in diverse cancer types

CIBERSORT is used to evaluate the infiltration of immunocytes in the human microenvironment. This reagent includes 547 biomarkers and 22 humanity immunocytes, comprising lymphocytes (T cells and B cells), Monocyte, neutrophils, macrophages, etc. The figures were Presented as stacked bar charts through the online platform Sangerbox (http://vip.sangerbox.com/home.html). Various cancer types in Immune infiltration level were presented as heatmap, and figures will indicate the fineness-restructured spearman's rho pass through assorted cancer categories through the online platform (http://timer.comp-genomics.org/timer/).

Diagnosis standard for CAD and T2DM

According to the diagnostic criteria by the American Diabetes Association and International Society of Hypertension, our study employed an case–control design, which included the selection of the 38 most rapidly progressing CAD, T2DM and CAD combined with T2DM cases from the clinical study. CAD was defined as: (1) Male patients aged over 40 and female patients aged 45 and above; (2)Coronary artery stenosis≥50% based on CAG or CCTA examination; (3)Symptoms such as chest tightness or chest pain undergo a comprehensive evaluation on admission. T2DM was defined as: (1)FPG ≥ 7.0mmol/L; (2)PBG ≥11.1mmol/L; (3) HbA1c≥6.5%. Controls included participants with no evidence of T2DM and no evidence of CAD by 65 years of age.

Detection of immunocytes infiltration in patients and healthy cohorts

We screened 38 patients with CAD or T2DM from the Department of Cardiology of the First Affiliated Hospital of Anhui University of Chinese Medicine, as well as 9 eligible healthy volunteers, and conducted flow cytometry immune examinations. Firstly, blood is taken from the human body to prepare samples, prepare cell suspension, count cells, use EP (1.5ml) tube for sub packaging, level rotor 800g, 4°C centrifugation. After completion, use a Pap pipette to remove the middle white membrane layer, add 5ml PBS for resuspension, level rotor 250g, 4°C centrifugation and add appropriate fluorescence-labelled antibodies. Mix well, avoid light and incubate at 4°C for 30 minutes. After completion, add 1ml PBS to wash twice and finally resuspend with 200ul PBS. Then adjust the laser light source, detector and flow rate, and load the prepared cell sample into the flow cytometer (BD LSR Fortessa) to detect the expression of $CD8^+$T and NK cells, collect and count the proportion of $CD8^+$T and NK cells in CAD, T2DM and healthy samples, and obtain the final results.

Numerical statement manipulation

The data processing were manipulated in R program and loads of online websites. The selection and use of data in the article are based on the criterion of significance $P < 0.05$.

Data availability statement

The original contributions presented in the study are included in the article/Supplementary Material. Further inquiries can be directed to the corresponding authors.

Ethics statement

All human blood samples were collected with informed consent from patients, and all related procedures were performed with the approval of ethics boards of the The First Affiliated Hospital of Anhui University of Chinese Medicine.

Author contributions

CD: Data curation, Methodology, Software, Writing – original draft, Supervision. DW: Data curation, Methodology, Writing – original draft, Supervision. QT: Supervision, Writing – original draft. ZL: Formal analysis, Writing – review & editing. PZ: Investigation, Writing – original draft. YW: Writing – original draft, Conceptualization, Data curation, Visualization. MH: Investigation, Validation, Writing – original draft. SC: Validation, Conceptualization, Writing – original draft. WQ: Data curation, Supervision, Writing – original draft. LZ: Writing – review & editing. HY: Funding acquisition, Visualization, Writing – review & editing.

Funding

The author(s) declare financial support was received for the research, authorship, and/or publication of this article. This work was supported by Clinical Research Project of the First Affiliated Hospital of Anhui University of Chinese Medicine (yfyzc04).

Conflict of interest

The authors declare that the research was conducted in the absence of any commercial or financial relationships that could be construed as a potential conflict of interest.

Publisher's note

All claims expressed in this article are solely those of the authors and do not necessarily represent those of their affiliated organizations, or those of the publisher, the editors and the reviewers. Any product that may be evaluated in this article, or claim that may be made by its manufacturer, is not guaranteed or endorsed by the publisher.

Supplementary material

The Supplementary Material for this article can be found online at: https://www.frontiersin.org/articles/10.3389/fimmu.2024.1267963/full#supplementary-material

References

1. Shah AD, Langenberg C, Rapsomaniki E, Denaxas S, Pujades-Rodriguez M, Gale CP, et al. Type 2 diabetes and incidence of cardiovascular diseases: a cohort study in 1.9 million people. *Lancet Diabetes Endocrinol* (2015) 3:105–13. doi: 10.1016/S2213-8587(14)70219-0

2. Gillespie KM. Type 1 diabetes: pathogenesis and prevention. *CMAJ* (2006) 175:165–70. doi: 10.1503/cmaj.060244

3. American Diabetes Association Professional Practice, C. 2. Classification and diagnosis of diabetes: standards of medical care in diabetes-2022. *Diabetes Care* (2022) 45:S17–38. doi: 10.2337/dc22-S002

4. Guariguata L, Whiting DR, Hambleton I, Beagley J, Linnenkamp U, Shaw JE. Global estimates of diabetes prevalence for 2013 and projections for 2035. *Diabetes Res Clin Pract* (2014) 103:137–49. doi: 10.1016/j.diabres.2013.11.002

5. Chen L, Magliano DJ, Zimmet PZ. The worldwide epidemiology of type 2 diabetes mellitus–present and future perspectives. *Nat Rev Endocrinol* (2011) 8:228–36. doi: 10.1038/nrendo.2011.183

6. Kharroubi AT, Darwish HM. Diabetes mellitus: The epidemic of the century. *World J Diabetes* (2015) 6:850–67. doi: 10.4239/wjd.v6.i6.850

7. Maruthur NM, Tseng E, Hutfless S, Wilson LM, Suarez-Cuervo C, Berger Z, et al. Diabetes medications as monotherapy or metformin-based combination therapy for type 2 diabetes: A systematic review and meta-analysis. *Ann Intern Med* (2016) 164:740–51. doi: 10.7326/M15-2650

8. Katsarou A, Gudbjörnsdottir S, Rawshani A, Dabelea D, Bonifacio E, Anderson BJ, et al. Type 1 diabetes mellitus. *Nat Rev Dis Primers* (2017) 3:17016. doi: 10.1038/nrdp.2017.16

9. Thong EP, Codner E, Laven JSE, Teede H. Diabetes: a metabolic and reproductive disorder in women. *Lancet Diabetes Endocrinol* (2020) 8:134–49. doi: 10.1016/S2213-8587(19)30345-6

10. Forbes JM, Cooper ME. Mechanisms of diabetic complications. *Physiol Rev* (2013) 93:137–88. doi: 10.1152/physrev.00045.2011

11. Cole JB, Florez JC. Genetics of diabetes mellitus and diabetes complications. *Nat Rev Nephrol* (2020) 16:377–90. doi: 10.1038/s41581-020-0278-5

12. Tomic D, Shaw JE, Magliano DJ. The burden and risks of emerging complications of diabetes mellitus. *Nat Rev Endocrinol* (2022) 18:525–39. doi: 10.1038/s41574-022-00690-7

13. Zheng Y, Ley SH, Hu FB. Global aetiology and epidemiology of type 2 diabetes mellitus and its complications. *Nat Rev Endocrinol* (2018) 14:88–98. doi: 10.1038/nrendo.2017.151

14. Collaborators, G.B.D.C.o.D. Global, regional, and national age-sex-specific mortality for 282 causes of death in 195 countries and territories, 1980-2017: a systematic analysis for the Global Burden of Disease Study 2017. *Lancet* (2018) 392:1736–88. doi: 10.1016/S0140-6736(18)32203-7

15. International Hypoglycaemia Study, G. Hypoglycaemia, cardiovascular disease, and mortality in diabetes: epidemiology, pathogenesis, and management. *Lancet Diabetes Endocrinol* (2019) 7:385–96. doi: 10.1016/S2213-8587(18)30315-2

16. Wong ND, Sattar N. Cardiovascular risk in diabetes mellitus: epidemiology, assessment and prevention. *Nat Rev Cardiol* (2023) 20:685–695. doi: 10.1038/s41569-023-00877-z

17. Paneni F, Beckman JA, Creager MA, Cosentino F. Diabetes and vascular disease: pathophysiology, clinical consequences, and medical therapy: part I. *Eur Heart J* (2013) 34:2436–43. doi: 10.1093/eurheartj/eht149

18. Fox CS, Sullivan L, D'Agostino RB Sr, Wilson PW. The significant effect of diabetes duration on coronary heart disease mortality: the Framingham Heart Study. *Diabetes Care* (2004) 27:704–8. doi: 10.2337/diacare.27.3.704

19. Bhatnagar P, Wickramasinghe K, Williams J, Rayner M, Townsend N. The epidemiology of cardiovascular disease in the UK 2014. *Heart* (2015) 101:1182–9. doi: 10.1136/heartjnl-2015-307516

20. Malakar AK, Choudhury D, Halder B, Paul P, Uddin A, Chakraborty S. A review on coronary artery disease, its risk factors, and therapeutics. *J Cell Physiol* (2019) 234:16812–23. doi: 10.1002/jcp.28350

21. Spirig R, Tsui J, Shaw S. The emerging role of TLR and innate immunity in cardiovascular disease. *Cardiol Res Pract* (2012) 2012:181394. doi: 10.1155/2012/181394

22. Hansson GK. Inflammation, atherosclerosis, and coronary artery disease. *N Engl J Med* (2005) 352:1685–95. doi: 10.1056/NEJMra043430

23. Gao P, Rong H-H, Lu T, Tang G, Si L-Y, Lederer JA, et al. The CD4/CD8 ratio is associated with coronary artery disease (CAD) in elderly Chinese patients. *Int Immunopharmacol* (2017) 42:39–43. doi: 10.1016/j.intimp.2016.11.007

24. Hansson GK, Libby P. The immune response in atherosclerosis: a double-edged sword. *Nat Rev Immunol* (2006) 6:508–19. doi: 10.1038/nri1882

25. Shimokawa C, Kato T, Takeuchi T, Ohshima N, Furuki T, Ohtsu Y, et al. CD8(+) regulatory T cells are critical in prevention of autoimmune-mediated diabetes. *Nat Commun* (2020) 11:1922. doi: 10.1038/s41467-020-15857-x

26. Li W, Lidebjer C, Yuan X-M, Szymanowski A, Backteman K, Ernerudh J, et al. NK cell apoptosis in coronary artery disease: relation to oxidative stress. *Atherosclerosis* (2008) 199:65–72. doi: 10.1016/j.atherosclerosis.2007.10.031

27. Jonasson L, Backteman K, Ernerudh J. Loss of natural killer cell activity in patients with coronary artery disease. *Atherosclerosis* (2005) 183:316–21. doi: 10.1016/j.atherosclerosis.2005.03.011

28. Wiedeman AE, Muir VS, Rosasco MG, DeBerg HA, Presnell S, Haas B, et al. Autoreactive CD8+ T cell exhaustion distinguishes subjects with slow type 1 diabetes progression. *J Clin Invest* (2020) 130:480–90. doi: 10.1172/JCI126595

29. Kumar NP, Sridhar R, Nair D, Banurekha VV, Nutman TB, Babu S. Type 2 diabetes mellitus is associated with altered CD8(+) T and natural killer cell function in pulmonary tuberculosis. *Immunology* (2015) 144:677–86. doi: 10.1111/imm.12421

30. Donath MY, Shoelson SE. Type 2 diabetes as an inflammatory disease. *Nat Rev Immunol* (2011) 11:98–107. doi: 10.1038/nri2925

31. Aronson D, Rayfield EJ, Chesebro JH. Mechanisms determining course and outcome of diabetic patients who have had acute myocardial infarction. *Ann Intern Med* (1997) 126:296–306. doi: 10.7326/0003-4819-126-4-199702150-00006

32. Cui J, Liu Y, Li Y, Xu F, Liu Y. Type 2 diabetes and myocardial infarction: recent clinical evidence and perspective. *Front Cardiovasc Med* (2021) 8:644189. doi: 10.3389/fcvm.2021.644189

33. Yao Z, Zhang B, Niu G, Yan Z, Tong X, Zou Y, et al. Neutrophil infiltration characterized by upregulation of S100A8, S100A9, S100A12 and CXCR2 is associated with the co-occurrence of Crohn's disease and peripheral artery disease. *Front Immunol* (2022) 13:896645. doi: 10.3389/fimmu.2022.896645

34. Lin DT, Conibear E. ABHD17 proteins are novel protein depalmitoylases that regulate N-Ras palmitate turnover and subcellular localization. *Elife* (2015) 4:e11306. doi: 10.7554/eLife.11306

35. Agrawal N, Brown MA. Genetic associations and functional characterization of M1 aminopeptidases and immune-mediated diseases. *Genes Immun* (2014) 15:521–7. doi: 10.1038/gene.2014.46

36. Reddi R, Ganji RJ, Marapaka AK, Bala SC, Yerra NV, Haque N, et al. Puromycin, a selective inhibitor of PSA acts as a substrate for other M1 family aminopeptidases: Biochemical and structural basis. *Int J Biol Macromol* (2020) 165:1373–81. doi: 10.1016/j.ijbiomac.2020.10.035

37. Breban M, Costantino F, André C, Chiocchia G, Garchon HJ. Revisiting MHC genes in spondyloarthritis. *Curr Rheumatol Rep* (2015) 17:516. doi: 10.1007/s11926-015-0516-1

38. Li Z, Brown MA. Progress of genome-wide association studies of ankylosing spondylitis. *Clin Transl Immunol* (2017) 6:e163. doi: 10.1038/cti.2017.49

39. Sollid LM, Pos W, Wucherpfennig KW. Molecular mechanisms for contribution of MHC molecules to autoimmune diseases. *Curr Opin Immunol* (2014) 31:24–30. doi: 10.1016/j.coi.2014.08.005

40. Genetic Analysis of Psoriasis Consortium & the Wellcome Trust Case Control Consortium 2, Strange A, Capon F, Spencer CCA, Knight J, Weale ME, et al. A genome-wide association study identifies new psoriasis susceptibility loci and an interaction between HLA-C and ERAP1. *Nat Genet* (2010) 42:985–90. doi: 10.1038/ng.694

41. Franke A, McGovern DPB, Barrett JC, Wang K, Radford-Smith GL, Ahmad T, et al. Genome-wide meta-analysis increases to 71 the number of confirmed Crohn's disease susceptibility loci. *Nat Genet* (2010) 42:1118–25. doi: 10.1038/ng.717

42. Wellcome Trust Case Control Consortium., The Australo-Anglo-American Spondylitis Consortium (TASC). Association scan of 14,500 nonsynonymous SNPs in four diseases identifies autoimmunity variants. *Nat Genet* (2007) 39:1329–37. doi: 10.1038/ng.2007.17

43. Shirakawa K, Sano M. T cell immunosenescence in aging, obesity, and cardiovascular disease. *Cells* (2021) 10:2435. doi: 10.3390/cells10092435

44. Touch S, Clement K, Andre S. T cell populations and functions are altered in human obesity and type 2 diabetes. *Curr Diabetes Rep* (2017) 17:81. doi: 10.1007/s11892-017-0900-5

45. SantaCruz-Calvo S, Bharath L, Pugh G, SantaCruz-Calvo L, Lenin RR, Lutshumba J, et al. Adaptive immune cells shape obesity-associated type 2 diabetes mellitus and less prominent comorbidities. *Nat Rev Endocrinol* (2022) 18:23–42. doi: 10.1038/s41574-021-00575-1

46. Nishimura S, Manabe I, Nagasaki M, Eto K, Yamashita H, Oshugi M, et al. CD8+ effector T cells contribute to macrophage recruitment and adipose tissue inflammation in obesity. *Nat Med* (2009) 15:914–20. doi: 10.1038/nm.1964

47. Hwang Y, Yu HT, Kim D-H, Jang J, Kim HY, Kang I, et al. Expansion of CD8(+) T cells lacking the IL-6 receptor alpha chain in patients with coronary artery diseases (CAD). *Atherosclerosis* (2016) 249:44–51. doi: 10.1016/j.atherosclerosis.2016.03.038

48. Backteman K, Ernerudh J, Jonasson L. Natural killer (NK) cell deficit in coronary artery disease: no aberrations in phenotype but sustained reduction of NK cells is associated with low-grade inflammation. *Clin Exp Immunol* (2014) 175:104–12. doi: 10.1111/cei.12210

49. Jabir NR, Firoz CK, Ahmed F, Kamal MA, Hindawi S, Damanhouri GA, et al. Reduction in CD16/CD56 and CD16/CD3/CD56 natural killer cells in coronary artery disease. *Immunol Invest* (2017) 46:526–35. doi: 10.1080/08820139.2017.1306866

50. Szymanowski A, Li W, Lundberg A, Evaldsson C, Nilsson L, Backteman K, et al. Soluble Fas ligand is associated with natural killer cell dynamics in coronary artery disease. *Atherosclerosis* (2014) 233:616–22. doi: 10.1016/j.atherosclerosis.2014.01.030

51. Zhu Y, Xian X, Wang Z, Bi Y, Chen Q, Han X, et al. Research progress on the relationship between atherosclerosis and inflammation. *Biomolecules* (2018) 8:80. doi: 10.3390/biom8030080

52. Qi B, Song L, Hu L, Guo D, Ren G, Peng T, et al. Cardiac-specific overexpression of Ndufs1 ameliorates cardiac dysfunction after myocardial infarction by alleviating mitochondrial dysfunction and apoptosis. *Exp Mol Med* (2022) 54:946-60. doi: 10.1038/s12276-022-00800-5

53. Sordo-Bahamonde C, Lorenzo-Herrero S, Payer ÁR, Gonzalez S, López-Soto A. Mechanisms of apoptosis resistance to NK cell-mediated cytotoxicity in cancer. *Int J Mol Sci* (2020) 21:3726. doi: 10.3390/ijms21103726

54. Naito R, Miyauchi K. Coronary artery disease and type 2 diabetes mellitus. *Int Heart J* (2017) 58:475–80. doi: 10.1536/ihj.17-191

frontiers | Frontiers in Cardiovascular Medicine

TYPE Original Research
PUBLISHED 09 May 2024
DOI 10.3389/fcvm.2024.1340602

OPEN ACCESS

EDITED BY
Catherine A. Reardon,
The University of Chicago, United States

REVIEWED BY
Peijun Liu,
The Central Hospital of Enshi Tujia and Miao Autonomous Prefecture, China
Hala Shokr,
The University of Manchester, United Kingdom

*CORRESPONDENCE
Songbo Fu
✉ fusb@lzu.edu.cn

†These authors have contributed equally to this work and share first authorship

RECEIVED 18 November 2023
ACCEPTED 01 April 2024
PUBLISHED 09 May 2024

CITATION
Liu Q, Chang X, Lian R, Chen Q, Wang J and Fu S (2024) Evaluation of bi-directional causal association between obstructive sleep apnoea syndrome and diabetic microangiopathy: a Mendelian randomization study.
Front. Cardiovasc. Med. 11:1340602.
doi: 10.3389/fcvm.2024.1340602

Evaluation of bi-directional causal association between obstructive sleep apnoea syndrome and diabetic microangiopathy: a Mendelian randomization study

Qianqian Liu[1,2†], Xingyu Chang[3†], Rongna Lian[4†], Qi Chen[1,2], Jialei Wang[1,2] and Songbo Fu[1,2*]

[1]Department of Endocrinology, First Hospital of Lanzhou University, Lanzhou, Gansu, China, [2]Gansu Provincial Endocrine Disease Clinical Medicine Research Center, Lanzhou, Gansu, China, [3]Department of Gynecology, Obstetrics and Gynecology Hospital, Fudan University, Shanghai, China, [4]Center of Gerontology and Geriatrics, West China Hospital, Sichuan University, Chengdu, China

Background: The relationship between obstructive sleep apnea syndrome (OSAS) and diabetic microangiopathy remains controversial.
Objective: This study aimed to use bidirectional two-sample Mendelian Randomization (MR) to assess the causal relationship between OSAS and diabetic microangiopathy.
Methods: First, we used the Linkage Disequilibrium Score Regression(LDSC) analysis to assess the genetic correlation. Then, the bidirectional two-sample MR study was conducted in two stages: OSAS and lung function-related indicators (forced vital capacity (FVC) and forced expiratory volume in 1 s (FEV1)) were investigated as exposures, with diabetic microangiopathy as the outcome in the first stage, and genetic tools were used as proxy variables for OSAS and lung function-related measures in the second step. Genome-wide association study data came from the open GWAS database. We used Inverse-Variance Weighted (IVW), MR-Egger regression, Weighted median, Simple mode, and Weighted mode for effect estimation and pleiotropy testing. We also performed sensitivity analyses to test the robustness of the results. Furthermore, we performed multivariate and mediation MR analyses.
Results: In the LDSC analysis, We found a genetic correlation between OSAS, FVC, FEV 1, and diabetic microangiopathy. In the MR analysis, based on IVW analysis, genetically predicted OSAS was positively correlated with the incidence of diabetic retinopathy (DR), diabetic kidney disease (DKD), and diabetic neuropathy (DN). In the subgroup analysis of DR, there was a significant causal relationship between OSAS and background diabetic retinopathy (BDR) and proliferative diabetic retinopathy (PDR). The reverse MR did not show a correlation between the incidence of diabetic microangiopathy and OSAS. Reduced FVC had a potential causal relationship with increased incidence of DR and PDR. Reduced FEV1 had a potential causal relationship with the increased incidence of BDR, PDR, and DKD. Multivariate MR analysis showed that the association between OSAS and diabetic microangiopathy remained significant after adjusting for confounding factors. However, we did not find the significant mediating factors.

Conclusion: Our results suggest that OSAS may be a cause of the development of diabetic microangiopathy, and OSAS may also be associated with a high risk of diabetic microangiopathy, providing a reference for a better understanding of the prevention of diabetic microangiopathy.

KEYWORDS

obstructive sleep apnea syndrome, diabetic microangiopathy, Mendelian randomization, forced vital capacity, forced expiratory volume in 1 s

1 Introduction

Diabetic microangiopathy is one of the major complications of diabetes, with over 4.59 billion adults worldwide having diabetes, and over a third developing diabetic microangiopathy (1–4). Diabetic microvascular complications include diabetic retinopathy (DR), diabetic kidney disease (DKD), and diabetic neuropathy (DN) (5). Among them, DR is the most common, with a prevalence of 35.4% (6) and DR can be divided into background diabetic retinopathy (BDR) and proliferative diabetic retinopathy (PDR). The overall health of diabetic patients is severely affected by microvascular complications, leading to various adverse health consequences. Studies have shown that the combination of DKD and hypoglycemic events results in a significantly increased risk of falls and fractures and significant challenges in performing daily tasks such as walking and housework (7, 8). Furthermore, their incidence of chronic and acute health events is also higher than the general population (9). Most critically, patients with diabetic microangiopathy also have a significantly increased risk of death from cardiovascular complications and renal failure (10). The early prevention and management of diabetic microangiopathy are therefore essential.

OSAS is widely recognized worldwide as a significant respiratory disorder, with an estimated prevalence of 5%–15% in the general population and positively correlated with age, showing a gradual growth trend (11). The primary characteristic of OSAS recurrent episodes of sleep-dependent apnea and reduced airflow. Persistent OSAS can have detrimental effects on respiratory function, which is typically quantified using forced vital capacity (FVC) and forced expiratory volume in 1 s (FEV1) values. More critically, this respiratory disorder is closely related to increased risks of hypertension, coronary heart disease, and heart failure (12).

Previous observational studies have found a close connection between OSAS and diabetic microangiopathy (13–18). However, due to potential confounding biases and reverse causality in observational studies, their causal relationship is still unclear and requires further research to fully understand the potential mechanisms and establish the relationship between these diseases.

MR uses single nucleotide polymorphisms (SNPs) as instrumental variables (IVs) to infer the causal relationship between two traits, treating genetic variations as a "natural" randomized controlled trial. Individuals are randomly assigned to different exposure levels throughout their lives, minimizing biases caused by confounding factors and reverse causality (19–21). Therefore, this study aims to use samples based on the GWAS database for MR analysis to explore the causal relationship between OSAS and diabetic microangiopathy, which may guide the prevention and treatment of diabetic microangiopathy.

2 Materials and methods

2.1 Study design

We employed a bidirectional two-sample MR study design, utilizing two-sample MR methods and varying GWAS summary-level datasets to elucidate the causal relationship and pathogenic direction between OSAS and lung function indicators (FVC, FEV1) with diabetic microvascular complications in European populations. This investigation was split into two phases. Initially, we probed whether OSAS had a causal relationship with diabetic microvascular complications. In the second stage, we evaluated if diabetic microangiopathy was associated with OSAS. The primary flow of our study is illustrated in Figure 1. We then conducted supplementary analyses, including a multivariate MR analysis to mitigate potential confounding factors and a mediation MR analysis to explore potential mediating factors. The MR design is based on three assumptions: (1) genetic variants are strongly associated with the exposure; (2) genetic variants are unrelated to other confounding factors; (3) genetic variants are associated with the outcomes solely through the investigated exposure. The association data of SNPs with OSAS and diabetic microangiopathy derive from recently published genome-wide association studies (GWAS).

2.2 Data source

For OSAS, we utilized the published GWAS summary statistics from the FinnGen study, which includes 217,955 European patients (22). FVC and FEV1 data were extracted from UKB. The sample size for FVC (GWAS ID: ukb-b-7953) was 421,986 and for FEV1 (GWAS ID: ukb-b-19657) was also 421,986. The summary statistics for GWAS of diabetic microvascular complications were taken from FinnGen (https://r5.finngen.fi/). DR (GWAS ID: finn-b-DM_RETINOPATHY_EXMORE) analysis involved 14,584 cases and 176,010 controls. BDR is an early stage of DR. The analysis for BDR (GWAS ID: finn-b-DM_BCKGRND_RETINA) included 2,026 cases and 204,208 controls; PDR (GWAS ID: finn-b-DM_RETINA_PROLIF) consisted of 8,681 cases and 204,208 controls. DKD (GWAS ID:

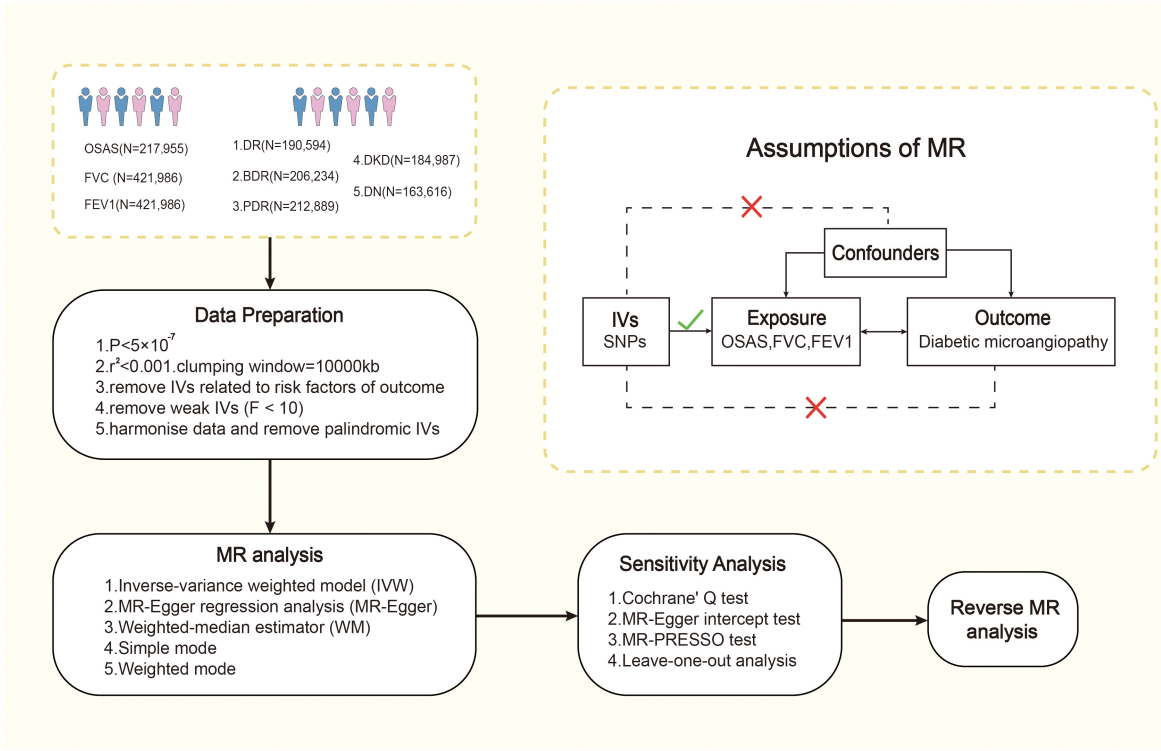

FIGURE 1
The process of Mendel randomization research. FVC, forced vital capacity; FEV1, forced expiratory volume in one second; IV, instrumental variable; MR-PRESSO, Mendelian randomization pleiotropy residual sum and outlier; MR, Mendelian randomization; OSAS, obstructive sleep apnea syndrome; SNP, single nucleotide polymorphism.

finn-b-DM_NEPHROPATHY_EXMORE) had 3,283 cases and 181,704 controls. DN (GWAS ID: finn-b-DM_NEUROPATHY) included 1,415 cases and 162,201 controls. The diagnoses for these conditions are based on their respective International Classification of Diseases(ICD) codes, and we have meticulously organized detailed inclusion and exclusion criteria for each study mentioned above. See Supplementary Materials Tables S1–S3 for details.

2.3 Instrument variable selection

Single nucleotide polymorphisms (SNPs) were selected based on the following criteria: (1) SNPs are strongly associated with exposure and reach genome-wide significance ($P < 5 \times 10^{-7}$); SNPs were not associated with any potential confounders and were independent of each other to avoid bias caused by linkage disequilibrium ($r^2 < 0.0001$, clustering distance = 10,000 kb); (2) SNPs are associated with outcomes only through exposure. F statistics ($F = \frac{R^2 \times (N-2)}{1-R^2}$, R^2 (SNP < 10) $= 2 \times EAF \times (1 - EAF) \times beta^2$, R^2 (SNP ≥ 10) $= \frac{2 \times EAF \times (1-EAF) \times beta^2}{(2 \times EAF \times (1-EAF) \times beta^2) + (2 \times EAF \times (1-EAF) \times N \times SE^2)}$); SNP exposure-associated beta (β); variance (SE)). Since an empirical threshold above 10 indicates that the SNP has sufficient validity, SNPs with F statistics less than 10 were removed. We provide information on F statistics, SNPs using the supplementary datasheet. Details of the screened SNP are provided in Supplementary Materials Tables S4–S11.

2.4 Data analysis

Linkage Disequilibrium Score Regression (LDSC) analysis is a new method for estimating genetic correlations that require only GWAS summary statistics. Even if there are overlapping individuals between the two GWAS, the regression slope of LDSC provides an unbiased estimate of the genetic correlation (23). LDSC analysis in this study was used to evaluate the genetic correlation of OSAS, FVC, FEV1, and diabetic microvascular disease. First, it is used to reformat summary statistics and remove non-SNP variants (such as indels), chain-ambiguous SNPs, and duplicate SNPs. SNPs with imputation quality scores >0.9 and Minor Allele Frequency (MAF) > 0.01 were selected in our study to prevent bias due to variable imputation quality (24). Second, LD scores were estimated using the 1,000 Genomes Project as the linkage disequilibrium reference panel, following standard methods recommended by the developers. Third, we studied the genetic correlation between OSAS, FVC, FEV1, and diabetic microangiopathy using LDSC (https://github.com/bulik/ldsc). And the strict Bonferroni threshold was set at $P < 0.0033$ (0.05/15). However, after the Bonferroni correction, there was no significant correlation.

Therefore, we set the candidate threshold of LDSC regression analysis at $P < 0.0033$ and used MR analysis to verify the causal relationship between OSAS, FVC, FEV1, and diabetic microangiopathy.

Two-sample MR is used to analyze the causal relationship between OSAS, FVC, FEV1, and diabetic microvascular complications. In the absence of horizontal pleiotropy, the IVW method can be used as the main method to analyze causal relationships in MR analysis. Before this, we used Cochrane's Q test to assess heterogeneity among IVs. If heterogeneity is detected ($P < 0.05$), the random-effects IVW model provides a more conservative estimate; otherwise, the fixed-effects IVW model will be used (25). Other MR analysis methods, including Weighted mode, MR-Egger regression, Simple mode, and Weighted mode methods (26), can supplement the IVW method and provide wider confidence intervals (27). The IVW method is applicable when horizontal pleiotropy does not exist (28); If the results of the MR analysis are nominally significant ($P < 0.05$), we consider a possible causal relationship between the exposure and the outcome (29). As the basic model of MR analysis, the IVW method shows good robustness and reliability when dealing with pleiotropic effects. It assumes that all genetic variants contribute uniformly to the causal effect, and obtains an overall causal estimate by weighting the average of the causal estimates of different single nucleotide polymorphisms (SNPs) (30). By comprehensively considering the weights of different genetic variants for analysis, the IVW method can more effectively control possible pleiotropic effects and provide relatively reliable causal estimates (31–34). The IVW method is widely used in MR research and has been widely recognized and accepted in academia and scientific research fields. Its universality as a basic model makes it easier for researchers to understand and use. In addition, the IVW method is one of the simplest and most intuitive methods in MR analysis and does not require overly complex statistical models and calculation processes, allowing researchers to perform analysis and result interpretation more quickly (35). When comparing other methods, the Weighted median is similar to IVW, the Weighted mode method assumes that less than 50% of IVs have horizontal pleiotropy (36), but it uses median weighting instead of inverse variance weighting. Weighted median may be more robust to some skewed or outlier data sets, but may control pleiotropy slightly less than IVW in some cases (34). MR-Egger regression assumes that more than 50% of IVs are affected by horizontal pleiotropy, considers the relationship between the impact of genetic variation on exposure and its impact on outcomes, and can detect and correct biases caused by reverse causation (31, 32). However, the MR-Egger method may not be robust enough to strong horizontal skew (37). Simple mode and Weighted mode methods have poor control over pleiotropic effects and are not as robust as IVW and MR-Egger (38, 39).

We conducted a reverse MR analysis between diabetic microvascular complications and OSAS to examine the possibility of a reverse causal relationship. The procedure for the reverse MR analysis was the same as the aforementioned analysis.

We employed several methods to monitor the possible presence of horizontal pleiotropy. Specifically, P values from the MR-Egger intercept test and MR pleiotropy residual sum and outlier (MR-PRESSO) global test could be used to assess the presence of horizontal pleiotropy, and $P < 0.05$ was considered statistically significant (32, 40). The MR-PRESSO outlier test can adjust horizontal pleiotropy by detecting and removing outliers (34). Additionally, we performed a leave-one-out analysis on the identified significant results to determine whether the causal role of the MR analysis was due to a single SNP (41).

Multivariable MR extends the capabilities of MR, akin to evaluating the effects of multiple treatments independently within a single randomized control trial (42). In this approach, the genetic instrument need not be exclusively associated with a single risk factor but can instead relate to a set of measured risk factors, while still adhering to equivalent instrumental-variable assumptions (43). This method accommodates multiple genetic variants, which may not necessarily be linked to every exposure in the model, as well as several causally dependent or independent exposures in an instrumental-variable analysis, thereby disentangling the direct causal effect of each risk factor included in the model (42, 44). Consequently, multivariate MR analysis allows the simultaneous consideration of multiple potential confounding factors, aiding researchers in mitigating the interference of these factors with observed associations and enhancing the accuracy of causal inference (45). In this study, possible confounding factors include obesity, elevated BMI, hyperlipidemia, hypercholesterolemia, etc (46–50). As the main method, we employed a robust IVW method with multiplicative random effects (51).

Given that OSAS is a complicated disease and previous studies have revealed that inflammatory factors and hypertension might mediate the development of diabetic microangiopathy (52–55), we performed a mediation MR analysis using the two-step MR method (56). Based on the literature review, we selected 15 variables that may serve as mediators that may lie on the pathway from sleep apnea syndrome to diabetic microangiopathy with available genetic tools from GWAS, including BMI, triglycerides, cholesterol, High-Density Lipoprotein (HDL), Low-Density Lipoprotein(LDL), apolipoprotein A, apolipoprotein B, blood glucose, C-reactive protein, heart rate, sleep duration, heme oxygenase 1 (53, 54, 57). Then, we screened the mediating factors of the relationship between OSAS and diabetic microangiopathy according to the following criteria: (1) There should be a causal relationship between OSAS and the mediator, and the effect of OSAS on the mediator should be unidirectional, because if the mediation analysis between Bidirectionality exists and the validity of the mediation analysis may be affected (24). (2) Regardless of whether OSAS is adjusted for, the causal relationship between mediators and diabetic microvasculopathy always exists; (3) Based on current scientific evidence, in practice, the relationship between OSAS and mediators, and the association between mediators and diabetic microvasculopathy, should be the other way around. Finally, only one mediating factor, blood glucose level, met all criteria and was included in the mediation analysis to evaluate its mediating effect on the causal relationship between OSAS and diabetic microangiopathy. We then conducted a mediation analysis using a two-step

approach. In the first step, we calculated the causal effect of OSAS on mediators (β_1), and in the second step, we estimated the causal effect of mediators on diabetic microangiopathy (β_2). The significance of the mediating effects (β_1*β_2) and the proportion of the mediation effect in the total effect were estimated using the delta method (58).

All statistical analyses were conducted using R version 4.2.1 (R Foundation for Statistical Computing, Vienna, Austria) along with the "TwoSampleMR", "MendelianRandomization", and "MRPRESSO" packages.

2.5 Ethics

The ethical data used in our study are publicly available pooled data and their analysis does not require ethical approval.

3 Results

3.1 Linkage disequilibrium score regression

Regression of LD score between OSAS and diabetic microvasculopathy using summary statistics from the FinnGin database. The results showed a moderate genetic correlation between OSAS and diabetic microangiopathy ($r_g = 0.142$, SE = 0.044, $P = 0.0011$; $r_g = 0.414$, SE = 0.077, $P < 0.001$; $r_g = 0.398$, SE = 0.062, $P < 0.001$). For FVC and FEV1 and diabetic microvasculopathy, we used summary statistics from the UKB and Finnish databases, respectively, to calculate genetic correlations. The results showed a significant genetic correlation between FVC and diabetic microangiopathy ($r_g = -0.117$, SE = 0.016, $P < 0.001$; $r_g = -0.205$, SE = 0.028, $P < 0.001$; $r_g = -0.153$, SE = 0.023, $P < 0.001$). The results also showed a genetic correlation between FEV1 and diabetic microangiopathy ($r_g = -0.086$, SE = 0.023, $P = 0.0002$; $r_g = -0.121$, SE = 0.040, $P = 0.0028$; $r_g = -0.148$, SE = 0.032, $P < 0.001$), as shown in Supplementary Materials Table S12.

3.2 Causal effects of OSAS, FVC, and FEV1 on DR

Regarding OSAS, as depicted in Figure 2, we observed a potential causal association between OSAS and an increased incidence of DR (OR = 1.248, 95% CI: 1.079–1.442, $P = 0.003$) and also with an increased incidence of BDR and PDR (OR = 1.390, 95% CI: 1.023–1.889, $P = 0.035$; OR = 1.176, 95% CI: 1.009–1.371, $P = 0.038$). In the sensitivity analysis of the IVs, no significant heterogeneity was observed through both the IVW test (Q = 9.703, $P = 0.206$; Q = 2.398, $P = 0.935$; Q = 4.288, $P = 0.746$) and the MR-Egger regression test (Q = 9.643, $P = 0.141$; Q = 2.332, $P = 0.887$; Q = 4.267, $P = 0.641$). The results of the MR–Egger regression analysis indicated that there was no horizontal pleiotropy among the IVs (all $P > 0.05$). The MR-PRESSO test ensured the accuracy of the results (all $P < 0.05$).

We also found that the respiratory-related indicators FVC and FEV1 were positive exposures for diabetic retinopathy, and FVC reduction has a potential causal relationship with the increased incidence of DR and PDR (OR = 0.862, 95% CI: 0.765–0.972, $P = 0.015$; OR = 0.838, 95% CI: 0.725–0.969, $P = 0.017$). There is either no heterogeneity (Q = 423.304, $P = 0.062$; Q = 422.036, $P = 0.063$) or horizontal pleiotropy ($P > 0.05$) in the PDR. Minor heterogeneity could be observed in the DR by IVW testing (Q = 448.273, $P = 0.009$) and MR-Egger testing (Q = 447.105, $P = 0.009$). According to the intercept of MR–Egger regression, it can be found that IVs do not have horizontal pleiotropy ($P > 0.05$), and the MR-PRESSO test ensures the accuracy of the results (all $P < 0.05$). Reduced FEV1 will also increase the risk of BDR and PDR (OR = 0.627, 95% CI: 0.466–0.844, $P = 0.002$; OR = 0.830, 95% CI: 0.708–0.974, $P = 0.022$). There is either no heterogeneity (Q = 321.439, $P = 0.592$; Q = 321.420, $P = 0.577$) or horizontal pleiotropy ($P > 0.05$) in the BDR. However, minor heterogeneity could be observed in the PDR by IVW testing (Q = 377.673, $P = 0.030$) and MR-Egger testing (Q = 373.099, $P = 0.040$). Based on the leave-one-out analysis, no SNP significantly altered the overall results, and the MR-PRESSO test ensures the accuracy of the results (all $P < 0.05$). The MVMR analysis was conducted to assess the direct effect of OSAS on DR with the adjustment of multiple other risk factors for diabetic complications. The results obtained from the two-sample univariable MR analysis were consistent with the findings from the MVMR, but the associations of OSAS with BDR and PDR were no longer significant, as shown in Supplementary Materials Table S14. Detailed results of the MR analysis are presented in Supplementary Materials Tables S13, S15 and the sensitivity analysis results are shown in Supplementary Materials Table S15. Based on the recent MR analysis, we infer that patients with OSAS exhibit an elevated risk for DR development. Individuals with pulmonary function abnormalities are advised to undergo periodic lung function evaluations and implement preventive measures against DR.

3.3 Causal effects of OSAS, FVC, and FEV1 on DKD

Next, as shown in Figure 3, we evaluated the causal relationship between OSAS and DKD. IVW, Weighted median, and Weighted mode analyses indicated that genetically predicted OSAS is associated with a higher risk of DKD (OR = 1.570, 95% CI: 1.233–1.999, $P < 0.001$; OR=1.678, 95% CI: 1.215–2.319, $P = 0.002$; OR = 1.774, 95% CI: 1.142–2.757, $P = 0.038$). Both the IVW test (Q = 5.853, $P = 0.557$) and the MR-Egger regression test (Q = 5.673, $P = 0.461$) showed no evident heterogeneity. The MR-Egger regression results suggested that there's no horizontal pleiotropy in the IVs ($P > 0.05$), and the MR-PRESSO test confirmed the accuracy of the results ($P < 0.05$). There was no significant correlation between the decrease in FVC and DKD. However, a decrease in FEV1 showed a significant correlation with DKD (OR = 0.710, 95% CI: 0.553–0.911, $P = 0.007$). Although there was slight heterogeneity, our MR–Egger

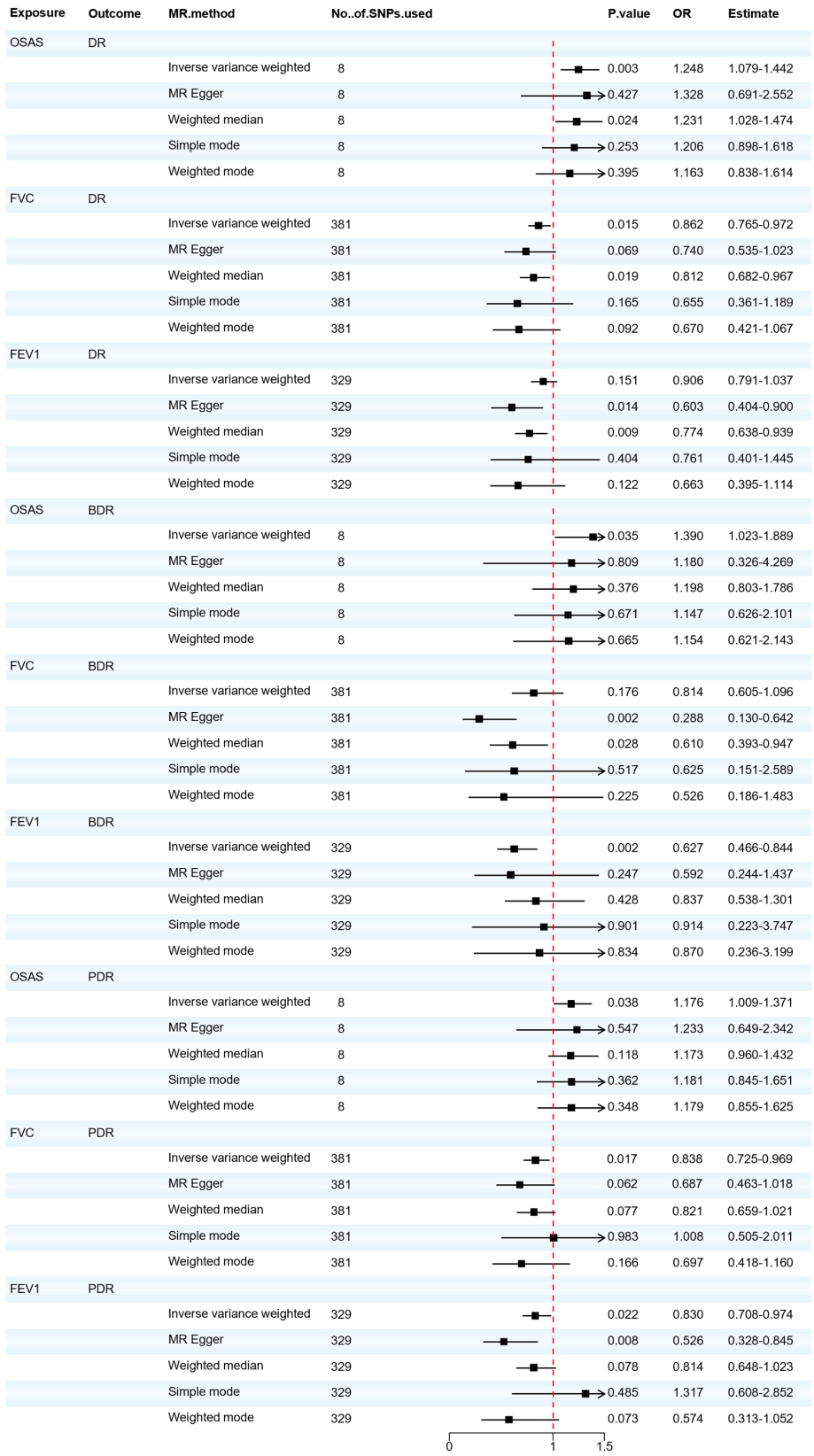

FIGURE 2
Forest plot of OSAS, FVC, and FEV1 associated with the risk of DR, BDR, and PDR. BDR, background diabetic retinopathy; DR, diabetic retinopathy; FVC, forced vital capacity; FEV1, forced expiratory volume in one second; MR, Mendelian randomization; MR-Eggcr, MR-Egger regression analysis; OSAS, obstructive sleep apnea syndrome; PDR, proliferative diabetic retinopathy; SNP, single nucleotide polymorphism.

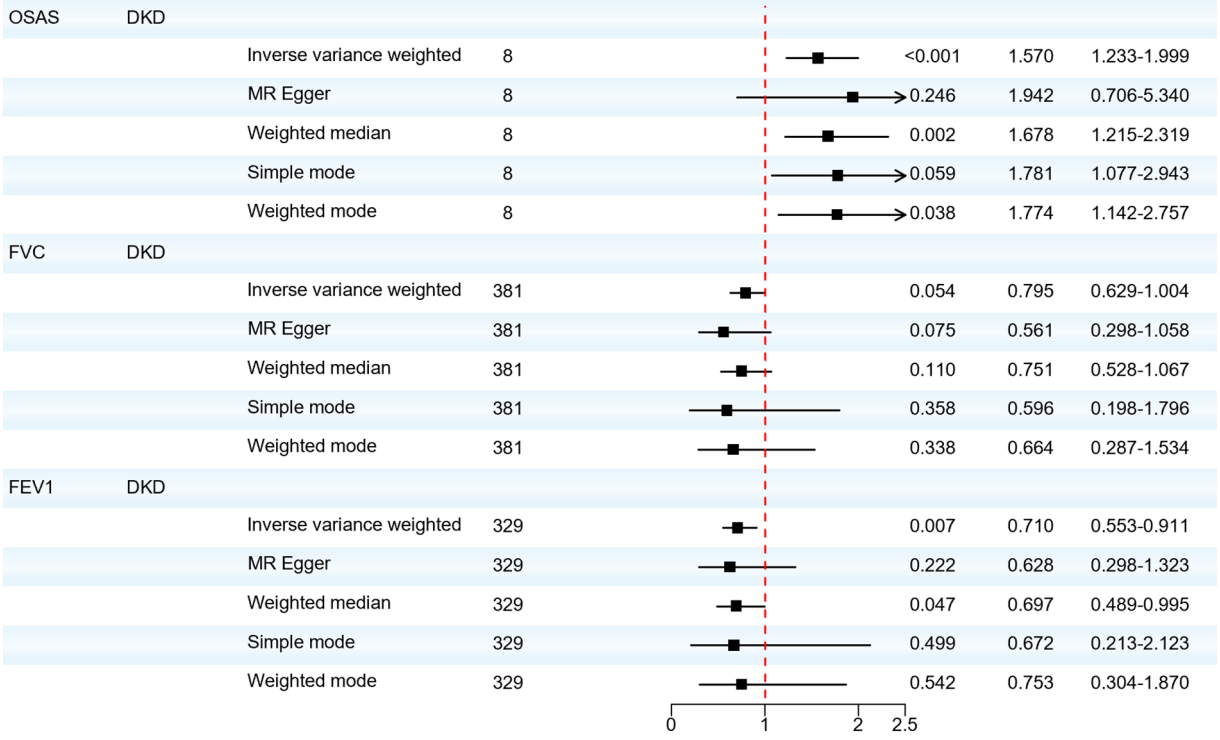

FIGURE 3
Forest plot of OSAS, FVC, FEV1 associated with the risk of DKD. DKD, diabetic kidney disease; FVC, forced vital capacity; FEV1, forced expiratory volume in one second; MR, Mendelian randomization; MR-Eggcr, MR-Egger regression analysis; OSAS, obstructive sleep apnea syndrome; SNP, single nucleotide polymorphism.

regression results indicated that there was no horizontal pleiotropy in the IVs ($P > 0.05$). The MR-PRESSO test also proved the accuracy of the results ($P < 0.05$), and no SNP significantly altered the overall results, so our results are relatively robust. After adjusting for possible confounding factors including obesity, elevated BMI, hyperlipidemia and hypercholesterolemia, OSAS was still associated with DKD, as shown in Supplementary Materials Table S14. The detailed results of the MR analysis are presented in Supplementary Materials Table S13 and the results of the sensitivity analysis are shown in Supplementary Materials Table S15. This suggests that the FEV1 level plays a pivotal role in the pathogenesis of DKD. Concurrently, patients with OSAS should be vigilant in taking preventive measures against the onset of DKD.

3.4 Causal effects of OSAS, FVC, and FEV1 on DN

We also analyzed the causal relationship between OSAS and DN. The IVW and Weighted median analyses indicated that genetically predicted OSAS is associated with a high risk of DN (OR = 1.912, 95% CI: 1.325–2.760, $P = 0.001$). Both the IVW test (Q = 1.141, $P = 0.992$) and the MR-Egger regression test (Q = 1.047, $P = 0.984$) showed that there is no heterogeneity among the IVs. The MR-Egger regression revealed no horizontal pleiotropy for the IVs ($P > 0.05$). However, there was no significant association between the risk of DN and either FVC or FEV1. As shown in Figure 4. OSAS was still associated with DN after adjusting for possible confounding factors such as obesity, elevated BMI, hyperlipidemia, and hypercholesterolemia, as shown in Supplementary Materials Table S14. The results of the sensitivity analysis can be found in Supplementary Materials Table S15. This reminds us that attention should be paid to the possibility of developing DN when patients with OSAS.

3.5 Causal effects of diabetic microvascular complications on OSAS

When considering OSAS as the outcome, we found no significant association between DR, DKD, and the risk of developing OSAS. Although the Weighted median analysis suggested that DN might increase the risk of OSAS (OR = 1.045; 95% CI: 1.005–1.086; $P = 0.027$), our primary analysis method, the IVW analysis, indicated no significant association between DN and OSAS (OR = 1.022; 95% CI: 0.986–1.061; $P = 0.234$). The IVW test (Q = 4.459, $P = 0.216$) and the MR-Egger test (Q = 3.479, $P = 0.176$) did not observe significant heterogeneity. The MR-Egger regression analysis indicated no horizontal

10.3389/fcvm.2024.1340602

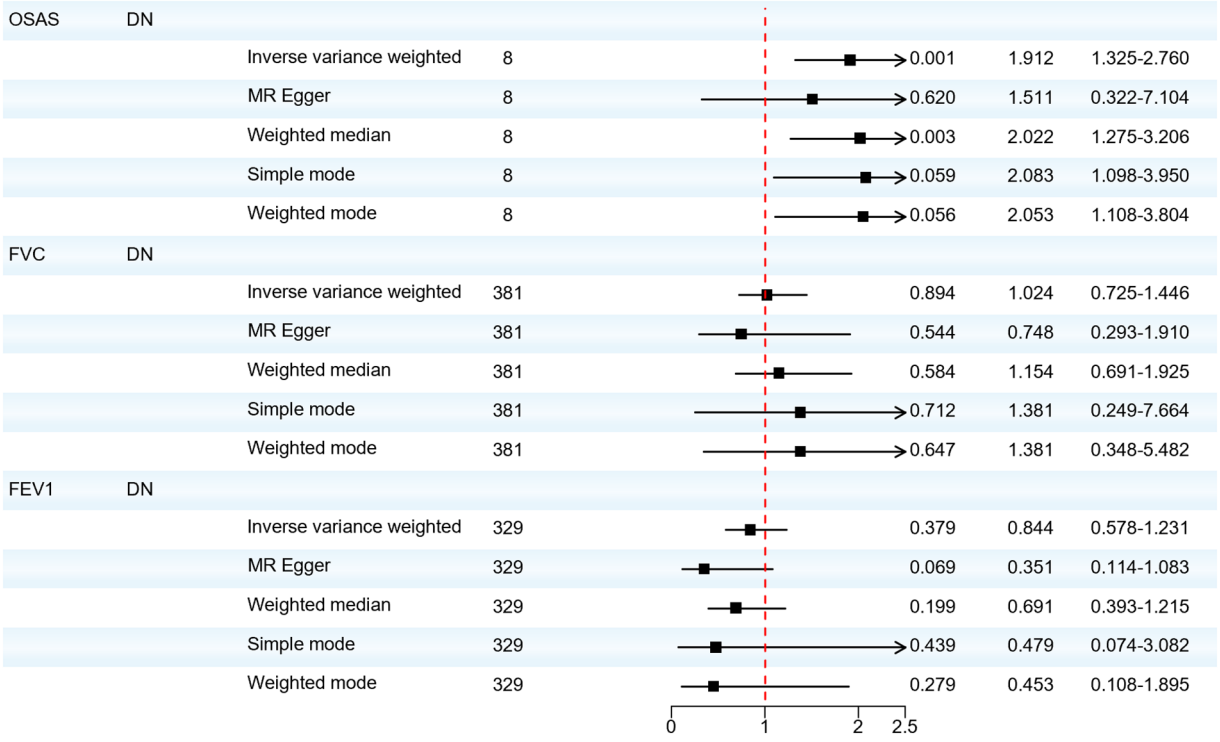

FIGURE 4
Forest plot of OSAS, FVC, FEV1 associated with the risk of DN. DN, diabetic neuropathy; MR, Mendelian randomization; MR-Eggcr, MR-Egger regression analysis; FVC, forced vital capacity; FEV1, forced expiratory volume in one second; OSAS, obstructive sleep apnea syndrome; SNP, single nucleotide polymorphism.

pleiotropy between the exposure and the outcome ($P > 0.05$). Thus, the reverse MR suggests there's no significant association between diabetic microvascular complications and OSAS, as shown in Figure 5. Furthermore, we found that there's no reverse causal relationship between FVC and diabetic microvascular complications. In the IVW analysis, when using FEV1 as the outcome, there was a reverse causal relationship between FEV1 and DR, BDR, and PDR (OR = 0.981; 95% CI: 0.966–0.997; $P = 0.021$; OR = 0.990; 95% CI: 0.980–0.999; $P = 0.029$; OR = 0.984; 95% CI: 0.972–0.998; $P = 0.020$), as shown in Supplementary Materials Table S16. The results of the sensitivity analysis can be found in Supplementary Materials Table S17. Subsequently, we performed a mediation MR analysis, and unfortunately, in the current sample and data conditions, we were unable to determine that blood glucose levels played a significant mediator between OSAS and diabetic microangiopathy. This finding suggests that a larger sample size or finer statistical methods may be needed to further explore this mediation effect, as shown in Supplementary Materials Table S18.

4 Discussion

Our study found that a genetic correlation between OSAS, FVC, FEV1 and diabetic microangiopathy exists and genetically predicted OSAS leads to an increased incidence of diabetic microangiopathy. Among them, the impact of OSAS on DN is the most significant. Patients with OSAS have a risk of developing DN that is 1.91 times that of normal individuals, while the risks of developing DR and DKD for such patients are 1.25 and 1.57 times respectively compared to normal individuals. In terms of DR, the effect of OSAS on BDR is more pronounced than on PDR. Furthermore, the lung function indicators FVC and FEV1 are protective factors against diabetic microangiopathy, and a bidirectional causality exists between FEV1 and DR, BDR and PDR. After adjusting for possible confounding factors such as obesity, elevated BMI, hyperlipidemia, and hypercholesterolemia using MVMR, OSAS is still associated with DR, DKD, and DN, but the association with BDR and PDR is no longer significant. The results of the LDSC analysis also showed a genetic correlation between OSAS and DR, but this correlation was no longer significant in the BDR and PDR. It may be because BDR and PDR are specific subtypes of DR. It may have different risk factors or causal pathways than DR overall. The genetic variants used in analyses may capture the causal effects of BDR and PDR less effectively than DR overall. In addition, as subgroups of DR, BDR, and PDR have smaller samplesizes than DR, the smaller sample sizes may result in reduced statistical power to detect true associations, which may explain the loss of significance (59, 60).

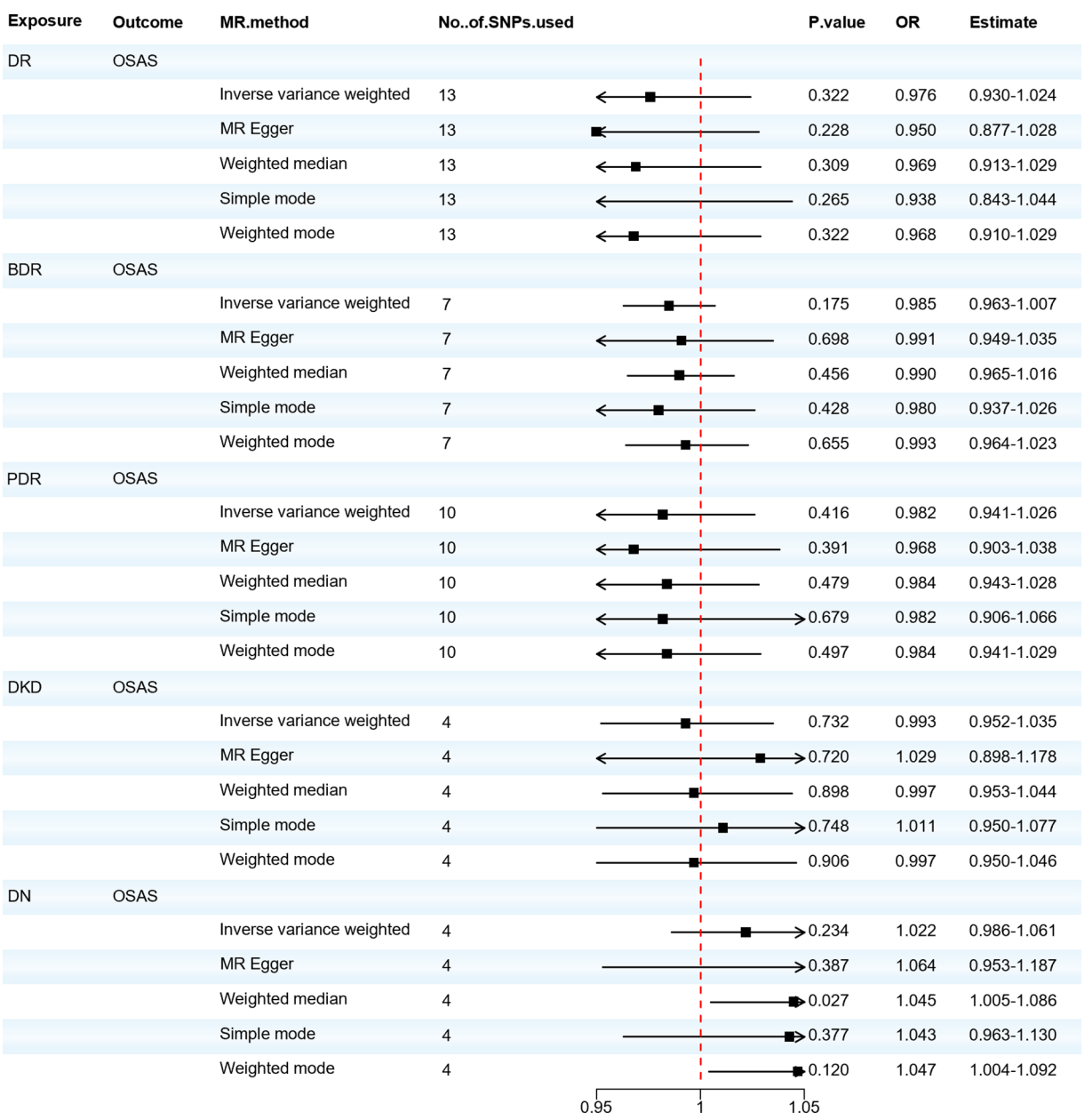

FIGURE 5
Forest plot of DR, BDR, PDR, DKD, DN associated with the risk of OSAS. BDR, background diabetic retinopathy; DKD, diabetic kidney disease; DN, diabetic neuropathy; DR, diabetic retinopathy; MR, Mendelian randomization; MR-Eggcr, MR-Egger regression analysis; PDR, proliferative diabetic retinopathy; OSAS, obstructive sleep apnea syndrome; SNP, single nucleotide polymorphism.

The application of pulmonary function testing in OSAS patients is for a comprehensive evaluation of the respiratory system (61). Although the diagnosis of OSAS mainly relies on polysomnography (PSG), pulmonary function testing is of great significance for evaluating the patient's respiratory function status (30). There is literature showing that FEV1 and FVC in pulmonary function tests are related to the severity of OSAS, which reflects the ventilatory dysfunction that occurs in OSAS patients during sleep and its impact on the respiratory system (62). In addition, through pulmonary function testing, we can evaluate the patient's vital capacity, ventilatory function, airflow limitation, and other indicators (63). These indicators can provide a comprehensive understanding of the respiratory function status of OSAS patients (30, 64). In clinical practice, pulmonary function test results can not only guide the selection of treatment strategies. For example, OSAS patients with abnormal pulmonary function may require different treatment options, such as continuous positive airway pressure (CPAP) therapy or physical exercise, but also Treatment effects and changes in condition can be monitored (30). Therefore, pulmonary function testing plays an important role in the management of OSAS. It can not only help doctors comprehensively evaluate the patient's respiratory function, but also guide the selection and

adjustment of treatment options to ensure that the patient's respiratory function is optimally controlled and managed.

Diabetic microangiopathy represents hallmark manifestations of the chronic progression of diabetes. During the non-proliferative phase, DR manifests as microaneurysms and retinal hemorrhages. As it progresses to the proliferative phase, ischemia or edema in the macular region, vitreous hemorrhage, and tractional or rhegmatogenous retinal detachment can lead to significant visual impairment, even blindness (65). DKD is characterized by proteinuria and a decline in glomerular filtration rate (66), often advancing to uremia (67). DN is a complex neurologic disorder affecting both peripheral and autonomic nervous systems. Symptoms may include pain, numbness, balance issues, and foot ulcers (2, 68, 69), increasing the risk of diabetic foot and amputation. In summary, diabetic microangiopathy can impair bodily functions, potentially leading to disability, and reducing employment opportunities and the work capacity of patients (70, 71).

In previous observational studies, Chang and colleagues found an association between the presence and severity of OSAS and DR (72). After adjusting for all possible confounding factors, Tahrani et al. found that OSAS remained an independent risk factor for Diabetic Peripheral Neuropathy (DPN) (73). Leong et al. conducted a comprehensive analysis of 2 longitudinal and 10 cross-sectional studies. Multivariate analysis indicated a significant correlation between OSAS and DKD, which was confirmed through a meta-analysis of another 7 studies (74). Furthermore, Ouardighi et al. compared the prevalence of OSAS in patients with diabetic microangiopathy and assessed the potential effects of diabetic microangiopathy on OSAS. The results showed no correlation between diabetic microangiopathy and OSAS (75). Hsin-Chieh et al. found that a decrease in FVC and FEV1 could increase the risk of diabetes, and chronic hyperglycemia and tissue hypoxia could promote the onset of microangiopathy (76). Our bidirectional MR study further supplements previous research and provides evidence for the potential causal relationship between OSAS and diabetic microangiopathy.

The development of diabetic microvascular complications may be attributed to OSAS and its associated cyclical drops in oxygen saturation and disruptions in sleep structure. This leads to several biological changes, including the activation of ADP-ribose polymerase, protein kinase C, and the polyol pathway. Additionally, there's an increase in the production of advanced glycation end-products, oxidative and nitrosative stress, as well as the activation of the sympathetic nervous system and the renin-angiotensin-aldosterone system (RAAS) (11, 77). All these biological changes can lead to endothelial dysfunction, triggering inflammatory responses and cell apoptosis, resulting in damage to the vascular wall, increased permeability, white blood cell infiltration, and cell death. These conditions stimulate the production of hypoxia-inducible factors, leading to an increased expression of vascular endothelial growth factor (VEGF) and a higher rate of neovascularization. These factors collectively contribute to the progression of diabetic microvascular complications (73, 78, 79). Additionally, ventilation abnormalities can lead to decreased FVC and dynamic lung compliance (80), the decline in lung function, leading to a cumulative loss of pulmonary reserves, ultimately exacerbates tissue hypoxia associated with vascular lesions in distant organs. This is the fundamental cause of diabetic microvascular complications (81). At the same time, reductions in FVC and FEV1 are correlated with increased levels of Hypoxia-Inducible Factor-1 (HIF-1) and VEGF (51), thereby heightening the likelihood of endothelial vascular lesions related to diabetes.

From a clinical perspective, as the first MR study on the role of OSAS in the etiology of diabetic microangiopathy, this study suggests that the genetic susceptibility to OSAS may account for variations in diabetic microangiopathy in people of European descent. Although OSAS has a genetic component, it is also influenced by environmental and lifestyle factors and is possibly preventable (82). Although there is still uncertainty about the exact functions of the 8 SNPs, their polygenic effects on diabetic microvascular complications, and the mechanisms by which these gene variants operate, current evidence still suggests that reduced blood oxygen saturation plays a significant role in diabetic microvascular complications. It seems prudent to recommend that people at high risk of diabetic microangiopathy strengthen the management of OSAS and take measures including lifestyle changes by strengthening social publicity and education and improving residents' health awareness. In addition, detecting self-oxygen saturation, monitoring pulmonary function parameters, and timely adjustment for abnormal pulmonary function seem to have unexpected effects on the prevention of clinical DR and its subtypes. Future work should try to clarify potential mechanisms, aiming to intervene, provide information for public health research, or further enhance our understanding of the etiology of diabetic microvascular complications. Instrumental variable SNPs can be incorporated as genetic predictors in predictive models aimed at identifying populations most likely to benefit from specific interventions. In our study, there were 8 SNPs for diabetic microangiopathy as instrumental variables for OSAS. Future research could consider building predictive models based on these SNPs and validating them in longitudinal cohorts for early detection and intervention in individuals at risk of diabetic microvascular complications. As our understanding of human genetics and the interactions between genes, metabolomics, proteomics, and transcriptomics grows, future MR studies should integrate these aspects to identify new biomarkers predicting the onset of diabetic microvascular complications and screen potential therapeutic targets. By screening SNP-related protein factors as instrumental variables to estimate the causal impact of this protein factor on specific results, MR studies can be used to assess whether the drug is likely to be effective in the study of compounds targeting specific proteins, guiding clinical decision-making and treatment planning. Lastly, in this study, we adopted a comprehensive dataset derived from public databases encompassing cases of microvascular complications induced by both Type 1 diabetes mellitus (T1DM) and Type 2 diabetes mellitus (T2DM). Given that sustained hyperglycemic conditions in both types of diabetes can trigger a series of intricate metabolic and molecular cascades, leading to endothelial dysfunction within the microvasculature, this constitutes the primary pathological mechanism (83). We posit that merging and analyzing datasets

from T1DM and T2DM collectively, as opposed to separate analyses, significantly enhances the statistical power of the study. This analytical strategy aids in uncovering universal characteristics of DR across the entire diabetic population, rather than focusing solely on specific diabetic subtypes (84). Furthermore, through the amalgamation analysis, we can circumvent potential issues of reduced statistical significance due to insufficient sample sizes, thereby enhancing the generalizability and credibility of study findings (85). The central objective of this study is to capture the overall trends of DR, rather than distinguishing between specific subtypes of diabetes. Through this comprehensive analytical approach, we aim to provide a more thorough and profound scientific basis for the prevention and therapeutic intervention of microvascular complications in diabetes.

Our current research has several advantages. Firstly, few studies have comprehensively investigated the relationship between OSAS and the incidence of diabetic microvascular complications. We are the first to examine their potential causal relationship using the MR method and a large amount of GWAS data. Secondly, because we used a two-sample MR analysis, our results are less likely to be confounded and reverse causality compared to traditional observational studies. In addition, we utilized large-scale samples to improve the statistical power of the study and make the findings more convincing. MR designs estimate the causal effects of independent variables on dependent ones rather than merely observing their correlation. Thus, the advantages of MR analysis may enhance the reliability of our findings, provide stronger evidence for clinical decision-making, and assist doctors and patients in making more informed medical choices.

However, some limitations were identified in our study. First, MR requires three strict core assumptions to be met: relevance, independence, and exclusion restriction. While we employed a rigorous study design to avoid violating these assumptions and identified closely related genetic tools for exposure (P-value $< 5 \times 10^{-7}$) with F-statistics > 10, and replicated results with multiple sensitivity analyses. Additionally, we used MR-Egger to identify potential horizontal pleiotropy, but it's impossible to completely rule out residual pleiotropy. In our study, no horizontal pleiotropy was found between OSAS with diabetic microvascular complications. However, horizontal pleiotropy exists between FEV1 and PDR, indicating that their relationship might be influenced by pleiotropic factors and warrants further validation. Second, there may be some sample overlap in our study, the direction and extent of any bias remain uncertain. Recent simulation studies also suggest that two-sample MR methods can be safely applied to single-sample MR performed in large biobanks. Hence, any bias due to sample overlap, if present, might be minimal (82). Third, clinical trials typically assess short-term intervention effects over shorter durations. This implies that our findings might not provide information about short-term intervention effects, which could be crucial for questions directly related to clinical interventions. Although our research can reveal the relationship between OSAS and DR, the application of the findings in real-world clinical settings might require additional research to determine whether treatment or interventions for OSAS are needed and how they should be conducted. Lastly, since the UK Biobank represents a biased sample of healthy older individuals from the UK, the Finnish database population also has specific demographic characteristics, including genetic background, genetic diversity, lifestyle, dietary habits, and genomic features, among others. These characteristics might differ from those of other countries or populations, making the research findings potentially inapplicable to other groups (86). Due to the lack of individual-level data, it's not possible to evaluate the relationship between the severity of OSAS and other parameters. Therefore, our findings should be interpreted with caution and validated in further studies.

5 Conclusion

Our study offers suggestive causal evidence indicating a potential causal relationship between OSAS and diabetic microvascular complications. Lung function might also be associated with the risk of diabetic microvascular disease onset. Our findings suggest that lifestyle interventions related to OSAS could serve as preventive strategies for potential populations at risk of diabetic microvascular complications. Our research is comprehensive and lays the groundwork for further large-scale longitudinal studies or randomized controlled trials

Data availability statement

Publicly available datasets were analyzed in this study. This data can be found here: https://gwas.mrcieu.ac.uk/.

Author contributions

QL: Writing – original draft, Writing – review & editing, Conceptualization, Methodology, Software. XC: Writing – original draft, Conceptualization, Methodology, Software. RL: Writing – original draft, Conceptualization, Methodology, Software. QC: Writing – original draft, Visualization, Data curation. JW: Writing – original draft, Visualization, Data curation, Software. SF: Writing – review & editing, Conceptualization, Resources.

Funding

The author(s) declare financial support was received for the research, authorship, and/or publication of this article.

This work was supported by Gansu Province Natural Science Foundation Project (22JR5RA914); Lanzhou Municipal Science and Technology Development Guidance Plan Project (2019-ZD-38); Gansu Province Joint Research Fund Project, Number (23JRRA1490).

Acknowledgments

Thanks to everyone who assisted with this project. We are grateful to Jiahui Liu for her assistance in obtaining materials

and in the intermediate methodology section. We are also grateful to Buyu Guo for his help with the multivariate MR methodology and data analysis aspects. We sincerely thank all GWAS consortia for providing summary data related to obstructive sleep apnea characteristics, lung function features, and diabetic microvascular complications for this study. Additionally, we are grateful to FinnGen and UK Biobank for the provision of their extensive genetic data.

Conflict of interest

The authors declare that the research was conducted in the absence of any commercial or financial relationships that could be construed as a potential conflict of interest.

Publisher's note

Supplementary material

The Supplementary Material for this article can be found online at: https://www.frontiersin.org/articles/10.3389/fcvm.2024.1340602/full#supplementary-material

References

1. Afkarian M, Sachs MC, Kestenbaum B, Hirsch IB, Tuttle KR, Himmelfarb J, et al. Kidney disease and increased mortality risk in type 2 diabetes. *J Am Soc Nephrol*. (2013) 24:302–8. doi: 10.1681/ASN.2012070718

2. Pop-Busui R, Boulton AJ, Feldman EL, Bril V, Freeman R, Malik RA, et al. Diabetic neuropathy: a position statement by the American diabetes association. *Diabetes Care*. (2017) 40:136–54. doi: 10.2337/dc16-2042

3. Sun H, Saeedi P, Karuranga S, Pinkepank M, Ogurtsova K, Duncan BB, et al. IDF diabetes atlas: global, regional and country-level diabetes prevalence estimates for 2021 and projections for 2045. *Diabetes Res Clin Pract*. (2022) 183:109119. doi: 10.1016/j.diabres.2021.109119

4. Yau JW, Rogers SL, Kawasaki R, Lamoureux EL, Kowalski JW, Bek T, et al. Global prevalence and major risk factors of diabetic retinopathy. *Diabetes Care*. (2012) 35:556–64. doi: 10.2337/dc11-1909

5. Scherer PE, Hill JA. Obesity, diabetes, and cardiovascular diseases: a compendium. *Circ Res*. (2016) 118:1703–5. doi: 10.1161/CIRCRESAHA.116.308999

6. Solomon SD, Chew E, Duh EJ, Sobrin L, Sun JK, VanderBeek BL, et al. Diabetic retinopathy: a position statement by the American diabetes association. *Diabetes Care*. (2017) 40:412–18. doi: 10.2337/dc16-2641

7. Kautzky-Willer A, Harreiter J, Pacini G. Sex and gender differences in risk, pathophysiology and complications of type 2 diabetes Mellitus. *Endocr Rev*. (2016) 37:278–316. doi: 10.1210/er.2015-1137

8. Janghorbani M, Van Dam RM, Willett WC, Hu FB. Systematic review of type 1 and type 2 diabetes mellitus and risk of fracture. *Am J Epidemiol*. (2007) 166:495–505. doi: 10.1093/aje/kwm106

9. Sarwar N, Gao P, Seshasai SR, Gobin R, Kaptoge S, Di Angelantonio E, et al. Diabetes mellitus, fasting blood glucose concentration, and risk of vascular disease: a collaborative meta-analysis of 102 prospective studies. *Lancet*. (2010) 375:2215–22. doi: 10.1016/S0140-6736(10)60484-9

10. Zoungas S, Woodward M, Li Q, Cooper ME, Hamet P, Harrap S, et al. Impact of age, age at diagnosis and duration of diabetes on the risk of macrovascular and microvascular complications and death in type 2 diabetes. *Diabetologia*. (2014) 57:2465–74. doi: 10.1007/s00125-014-3369-7

11. Lévy P, Kohler M, McNicholas WT, Barbé F, McEvoy RD, Somers VK, et al. Obstructive sleep apnoea syndrome. *Nat Rev Dis Primers*. (2015) 1:15015. doi: 10.1038/nrdp.2015.15

12. Marin JM, Carrizo SJ, Vicente E, Agusti AG. Long-term cardiovascular outcomes in men with obstructive sleep apnoea-hypopnoea with or without treatment with continuous positive airway pressure: an observational study. *Lancet*. (2005) 365:1046–53. doi: 10.1016/S0140-6736(05)71141-7

13. Zhang R, Zhang P, Zhao F, Han X, Ji L. Association of diabetic microvascular complications and parameters of obstructive sleep apnea in patients with type 2 diabetes. *Diabetes Technol Ther*. (2016) 18:415–20. doi: 10.1089/dia.2015.0433

14. Schipper SBJ, Van Veen MM, Elders PJM, van Straten A, Van Der Werf YD, Knutson KL, et al. Sleep disorders in people with type 2 diabetes and associated health outcomes: a review of the literature. *Diabetologia*. (2021) 64:2367–77. doi: 10.1007/s00125-021-05541-0

15. Kurnool S, McCowen KC, Bernstein NA, Malhotra A. Sleep apnea, obesity, and diabetes—an intertwined trio. *Curr Diab Rep*. (2023) 23:165–71. doi: 10.1007/s11892-023-01510-6

16. Misra A, Shrivastava U. Obstructive sleep apnea and diabetic nephropathy. *Diabetes Technol Ther*. (2016) 18:405–7. doi: 10.1089/dia.2016.0147

17. Shiba T, Takahashi M, Hori Y, Saishin Y, Sato Y, Maeno T. Relationship between sleep-disordered breathing and iris and/or angle neovascularization in proliferative diabetic retinopathy cases. *Am J Ophthalmol*. (2011) 151:604–9. doi: 10.1016/j.ajo.2010.10.002

18. Wei DYW, Chew M, Sabanayagam C. Obstructive sleep apnoea, other sleep parameters and diabetic retinopathy. *Curr Diab Rep*. (2021) 21:58. doi: 10.1007/s11892-021-01425-0

19. Emdin CA, Khera AV, Kathiresan S. Mendelian randomization. *Jama*. (2017) 318:1925–26. doi: 10.1001/jama.2017.17219

20. Burgess S, Davey Smith G, Davies NM, Dudbridge F, Gill D, Glymour MM, et al. Guidelines for performing Mendelian randomization investigations: update for summer 2023. *Wellcome Open Res*. (2019) 4:186. doi: 10.12688/wellcomeopenres.15555.1

21. Davies NM, Holmes MV, Davey Smith G. Reading Mendelian randomisation studies: a guide, glossary, and checklist for clinicians. *Br Med J*. (2018) 362:k601. doi: 10.1136/bmj.k601

22. Strausz S, Ruotsalainen S, Ollila HM, Karjalainen J, Kiiskinen T, Reeve M, et al. Genetic analysis of obstructive sleep apnoea discovers a strong association with cardiometabolic health. *Eur Respir J*. (2021) 57(5):2003091. doi: 10.1183/13993003.03091-2020

23. Bulik-Sullivan B, Finucane HK, Anttila V, Gusev A, Day FR, Loh PR, et al. An atlas of genetic correlations across human diseases and traits. *Nat Genet*. (2015) 47:1236–41. doi: 10.1038/ng.3406

24. Zhang M, Qiao J, Zhang S, Zeng P. Exploring the association between birthweight and breast cancer using summary statistics from a perspective of genetic correlation, mediation, and causality. *J Transl Med*. (2022) 20:227. doi: 10.1186/s12967-022-03435-2

25. Greco MF, Minelli C, Sheehan NA, Thompson JR. Detecting pleiotropy in Mendelian randomisation studies with summary data and a continuous outcome. *Stat Med*. (2015) 34:2926–40. doi: 10.1002/sim.6522

26. Bowden J, Davey Smith G, Burgess S. Mendelian Randomization with invalid instruments: effect estimation and bias detection through Egger regression. *Int J Epidemiol*. (2015) 44:512–25. doi: 10.1093/ije/dyv080

27. Slob EAW, Burgess S. A comparison of robust Mendelian randomization methods using summary data. *Genet Epidemiol*. (2020) 44:313–29. doi: 10.1002/gepi.22295

28. Burgess S, Butterworth A, Thompson SG. Mendelian Randomization analysis with multiple genetic variants using summarized data. *Genet Epidemiol*. (2013) 37:658–65. doi: 10.1002/gepi.21758

29. Liu B, Ye D, Yang H, Song J, Sun X, Mao Y, et al. Two-sample Mendelian randomization analysis investigates causal associations between gut microbial genera and inflammatory bowel disease, and specificity causal associations in ulcerative colitis or Crohn's disease. *Front Immunol*. (2022) 13:921546. doi: 10.3389/fimmu.2022.921546

30. Lee JJ, Sundar KM. Evaluation and management of adults with obstructive sleep apnea syndrome. *Lung*. (2021) 199:87–101. doi: 10.1007/s00408-021-00426-w

31. Bowden J, Del Greco MF, Minelli C, Davey Smith G, Sheehan NA, Thompson JR. Assessing the suitability of summary data for two-sample Mendelian randomization analyses using MR-Egger regression: the role of the I2 statistic. *Int J Epidemiol*. (2016) 45:1961–74. doi: 10.1093/ije/dyw252

32. Burgess S, Thompson SG. Interpreting findings from Mendelian randomization using the MR-Egger method. *Eur J Epidemiol*. (2017) 32:377–89. doi: 10.1007/s10654-017-0255-x

33. Hemani G, Bowden J, Davey Smith G. Evaluating the potential role of pleiotropy in Mendelian randomization studies. *Hum Mol Genet*. (2018) 27:R195–r208. doi: 10.1093/hmg/ddy163

34. Verbanck M, Chen CY, Neale B, Do R. Detection of widespread horizontal pleiotropy in causal relationships inferred from Mendelian randomization between complex traits and diseases. *Nat Genet*. (2018) 50:693–98. doi: 10.1038/s41588-018-0099-7

35. Bowden J, Holmes MV. Meta-analysis and Mendelian randomization: a review. *Res Synth Methods*. (2019) 10:486–96. doi: 10.1002/jrsm.1346

36. Jiang X, O'Reilly PF, Aschard H, Hsu YH, Richards JB, Dupuis J, et al. Genome-wide association study in 79,366 European-ancestry individuals informs the genetic architecture of 25-hydroxyvitamin D levels. *Nat Commun*. (2018) 9:260. doi: 10.1038/s41467-017-02662-2

37. Lin Z, Pan I, Pan W. A practical problem with Egger regression in Mendelian randomization. *PLoS Genet*. (2022) 18:e1010166. doi: 10.1371/journal.pgen.1010166

38. Yang M, Wan X, Zheng H, Xu K, Xie J, Yu H, et al. No evidence of a genetic causal relationship between ankylosing spondylitis and gut Microbiota: a two-sample Mendelian randomization study. *Nutrients*. (2023) 15(4):1057. doi: 10.3390/nu15041057

39. Lin L, Luo P, Yang M, Wang J, Hou W, Xu P. A bidirectional Mendelian randomized study of classical blood lipids and venous thrombosis. *Sci Rep*. (2023) 13:3904. doi: 10.1038/s41598-023-31067-z

40. Ni JJ, Xu Q, Yan SS, Han BX, Zhang H, Wei XT, et al. Gut Microbiota and psychiatric disorders: a two-sample Mendelian randomization study. *Front Microbiol*. (2021) 12:737197. doi: 10.3389/fmicb.2021.737197

41. Xiang K, Wang P, Xu Z, Hu YQ, He YS, Chen Y, et al. Causal effects of gut microbiome on systemic lupus erythematosus: a two-sample Mendelian randomization study. *Front Immunol*. (2021) 12:667097. doi: 10.3389/fimmu.2021.667097

42. Burgess S, Thompson SG. Multivariable Mendelian randomization: the use of pleiotropic genetic variants to estimate causal effects. *Am J Epidemiol*. (2015) 181:251–60. doi: 10.1093/aje/kwu283

43. Sanderson E, Davey Smith G, Windmeijer F, Bowden J. An examination of multivariable Mendelian randomization in the single-sample and two-sample summary data settings. *Int J Epidemiol*. (2019) 48:713–27. doi: 10.1093/ije/dyy262

44. Rasheed H, Zheng J, Rees J, Sanderson E, Thomas L, Richardson TG, et al. The causal effects of serum lipids and apolipoproteins on kidney function: multivariable and bidirectional Mendelian-randomization analyses. *Int J Epidemiol*. (2021) 50:1569–79. doi: 10.1093/ije/dyab014

45. Karami S, Daugherty SE, Schonfeld SJ, Park Y, Hollenbeck AR, Grubb RL 3rd, et al., Reproductive factors and kidney cancer risk in 2 US cohort studies, 1993–2010. *Am J Epidemiol*. (2013) 177(12):1368–77. doi: 10.1093/aje/kws406. Urol Oncol (2014) **32**:932–3. Commentary on Occupational and Environmental Epidemiology Branch, Division of Cancer Epidemiology and Genetics, Department of Health and Human Services, National Cancer Institute, National Institutes of Health, Bethesda, MD.

46. Ward ZJ, Bleich SN, Cradock AL, Barrett JL, Giles CM, Flax C, et al. Projected U.S. state-level prevalence of adult obesity and severe obesity. *N Engl J Med*. (2019) 381(25):2440–50. doi: 10.1056/NEJMsa1909301

47. Stone NJ, Robinson JG, Lichtenstein AH, Bairey Merz CN, Blum CB, Eckel RH, et al. 2013 ACC/AHA guideline on the treatment of blood cholesterol to reduce atherosclerotic cardiovascular risk in adults: a report of the American college of cardiology/American heart association task force on practice guidelines. *J Am Coll Cardiol*. (2014) 63(25 Pt B):2889–934. doi: 10.1016/j.jacc.2013.11.002. Erratum in: J Am Coll Cardiol. (2014) 63(25 Pt B):3024-3025. Erratum in: J Am Coll Cardiol. (2015) 66(24):2812. PMID: 24239923.

48. Freuer D, Linseisen J, Meisinger C. Association between inflammatory bowel disease and both psoriasis and psoriatic arthritis: a bidirectional 2-sample Mendelian randomization study. *JAMA Dermatol*. (2022) 158:1262–8. doi: 10.1001/jamadermatol.2022.3682

49. Grundy SM, Cleeman JI, Daniels SR, Donato KA, Eckel RH, Franklin BA, et al. Diagnosis and management of the metabolic syndrome: an American heart association/national heart, lung, and blood institute scientific statement. *Circulation*. (2005) 112:2735–52. doi: 10.1161/CIRCULATIONAHA.105.169404

50. Afshin A, Forouzanfar MH, Reitsma MB, Sur P, Estep K, Lee A, et al. Health effects of overweight and obesity in 195 countries over 25 years. *N Engl J Med*. (2017) 377:13–27. doi: 10.1056/NEJMoa1614362

51. Zhang L, Jiang F, Xie Y, Mo Y, Zhang X, Liu C. Diabetic endothelial microangiopathy and pulmonary dysfunction. *Front Endocrinol*. (2023) 14:1073878. doi: 10.3389/fendo.2023.1073878

52. Zhang W, Si LY. Obstructive sleep apnea syndrome (OSAS) and hypertension: pathogenic mechanisms and possible therapeutic approaches. *Ups J Med Sci*. (2012) 117:370–82. doi: 10.3109/03009734.2012.707253

53. Li Y, Liu Y, Liu S, Gao M, Wang W, Chen K, et al. Diabetic vascular diseases: molecular mechanisms and therapeutic strategies. *Signal Transduct Target Ther*. (2023) 8(1):152. doi: 10.1038/s41392-023-01400-z

54. Madonna R, Balistreri CR, Geng YJ, De Caterina R. Diabetic microangiopathy: pathogenetic insights and novel therapeutic approaches. *Vascul Pharmacol*. (2017) 90:1–7. doi: 10.1016/j.vph.2017.01.004

55. Greco C, Spallone V. Obstructive sleep apnoea syndrome and diabetes. Fortuitous association or interaction? *Curr Diabetes Rev*. (2015) 12:129–55. doi: 10.2174/1573399811666150319112611

56. Sanderson E. Multivariable Mendelian randomization and mediation. *Cold Spring Harb Perspect Med*. (2021) 11(2):a038984. doi: 10.1101/cshperspect.a038984

57. Fang F, Wang J, Wang YF, Peng YD. Microangiopathy in diabetic polyneuropathy revisited. *Eur Rev Med Pharmacol Sci*. (2018) 22:6456–62. doi: 10.26355/eurrev_201810_16058

58. MacKinnon DP, Fairchild AJ, Fritz MS. Mediation analysis. *Annu Rev Psychol*. (2007) 58:593–614. doi: 10.1146/annurev.psych.58.110405.085542

59. Milne BJ, Atkinson J, Blakely T, Day H, Douwes J, Gibb S, et al. Data resource profile: the New Zealand Integrated Data Infrastructure (IDI). *Int J Epidemiol*. (2019) 48:1027. doi: 10.1093/ije/dyz014

60. Cuijpers P, Griffin JW, Furukawa TA. The lack of statistical power of subgroup analyses in meta-analyses: a cautionary note. *Epidemiol Psychiatr Sci*. (2021) 30:e78. doi: 10.1017/S2045796021000664

61. Stavrou VT, Astara K, Tourlakopoulos KN, Papayianni E, Boutlas S, Vavougios GD, et al. Obstructive sleep apnea syndrome: the effect of acute and chronic responses of exercise. *Front Med*. (2021) 8:806924. doi: 10.3389/fmed.2021.806924

62. Baiardi S, Cirignotta F. The clinical diagnosis of Obstructive Sleep Apnea Syndrome (OSAS). *Med Lav*. (2017) 108:267–75. doi: 10.23749/mdl.v108i4.6414

63. Ruaro B, Baratella E, Confalonieri M, Antonaglia C, Salton F. Editorial: obstructive sleep apnea syndrome (OSAS). What's new? *Front Med*. (2022) 9:1009410. doi: 10.3389/fmed.2022.1009410

64. Lv R, Liu X, Zhang Y, Dong N, Wang X, He Y, et al. Pathophysiological mechanisms and therapeutic approaches in obstructive sleep apnea syndrome. *Signal Transduct Target Ther*. (2023) 8:218. doi: 10.1038/s41392-023-01496-3

65. Flaxel CJ, Adelman RA, Bailey ST, Fawzi A, Lim JI, Vemulakonda GA, et al. Diabetic retinopathy preferred practice pattern®. *Ophthalmology*. (2020) 127:P66–p145. doi: 10.1016/j.ophtha.2019.09.025

66. Cole JB, Florez JC. Genetics of diabetes mellitus and diabetes complications. *Nat Rev Nephrol*. (2020) 16:377–90. doi: 10.1038/s41581-020-0278-5

67. Teo ZL, Tham YC, Yu M, Chee ML, Rim TH, Cheung N, et al. Global prevalence of diabetic retinopathy and projection of burden through 2045: systematic review and meta-analysis. *Ophthalmology*. (2021) 128:1580–91. doi: 10.1016/j.ophtha.2021.04.027

68. Earle K, Walker J, Hill C, Viberti G. Familial clustering of cardiovascular disease in patients with insulin-dependent diabetes and nephropathy. *N Engl J Med*. (1992) 326:673–7. doi: 10.1056/NEJM199203053261005

69. Rosenberger DC, Blechschmidt V, Timmerman H, Wolff A, Treede RD. Challenges of neuropathic pain: focus on diabetic neuropathy. *J Neural Transm*. (2020) 127:589–624. doi: 10.1007/s00702-020-02145-7

70. Tomic D, Shaw JE, Magliano DJ. The burden and risks of emerging complications of diabetes mellitus. *Nat Rev Endocrinol*. (2022) 18(9):525–39. doi: 10.1038/s41574-022-00690-7

71. Seuring T, Archangelidi O, Suhrcke M. The economic costs of type 2 diabetes: a global systematic review. *Pharmacoeconomics*. (2015) 33:811–31. doi: 10.1007/s40273-015-0268-9

72. Chang AC, Fox TP, Wang S, Wu AY. Relationship between obstructive sleep apnea and the presence and severity of diabetic retinopathy. *Retina*. (2018) 38:2197–206. doi: 10.1097/IAE.0000000000001848

73. Tahrani AA, Ali A, Raymond NT, Begum S, Dubb K, Mughal S, et al. Obstructive sleep apnea and diabetic neuropathy: a novel association in patients with type 2 diabetes. *Am J Respir Crit Care Med*. (2012) 186:434–41. doi: 10.1164/rccm.201112-2135OC

74. Leong WB, Jadhakhan F, Taheri S, Thomas GN, Adab P. The association between obstructive sleep apnea on diabetic kidney disease: a systematic review and meta-analysis. *Sleep*. (2016) 39:301–8. doi: 10.5665/sleep.5432

75. Ouardighi HE, Poppe KG, Kleynen P, Grabzcan L, Veltri F, Bruyneel AV, et al. Obstructive sleep apnea is not associated with diabetic retinopathy in diabetes: a prospective case-control study. *Sleep Breath*. (2023) 27:121–28. doi: 10.1007/s11325-022-02578-2

76. Yeh HC, Punjabi NM, Wang NY, Pankow JS, Duncan BB, Cox CE, et al. Cross-sectional and prospective study of lung function in adults with type 2 diabetes: the Atherosclerosis Risk in Communities (ARIC) study. *Diabetes Care*. (2008) 31:741–6. doi: 10.2337/dc07-1464

77. Adeseun GA, Rosas SE. The impact of obstructive sleep apnea on chronic kidney disease. *Curr Hypertens Rep*. (2010) 12:378–83. doi: 10.1007/s11906-010-0135-1

78. Altaf QA, Ali A, Piya MK, Raymond NT, Tahrani AA. The relationship between obstructive sleep apnea and intra-epidermal nerve fiber density, PARP activation and foot ulceration in patients with type 2 diabetes. *J Diabetes Complications*. (2016) 30:1315–20. doi: 10.1016/j.jdiacomp.2016.05.025

79. Lavie L. Oxidative stress inflammation and endothelial dysfunction in obstructive sleep apnea. *Front Biosci (Elite Ed)*. (2012) 4:1391–403. doi: 10.2741/e469

80. Lange P, Groth S, Mortensen J, Appleyard M, Nyboe J, Schnohr P, et al. Diabetes mellitus and ventilatory capacity: a five year follow-up study. *Eur Respir J*. (1990) 3:288–92. doi: 10.1183/09031936.93.03030288

81. Hsia CC, Raskin P. Lung involvement in diabetes: does it matter? *Diabetes Care*. (2008) 31:828–9. doi: 10.2337/dc08-0103

82. Mokdad AH, Ford ES, Bowman BA, Dietz WH, Vinicor F, Bales VS, et al. Prevalence of obesity, diabetes, and obesity-related health risk factors, 2001. *Jama*. (2003) 289:76–9. doi: 10.1001/jama.289.1.76

83. Zhao X, Ouyang W, Hao F, Lin C, Wang F, Han S, et al. Properties comparison of biochars from corn straw with different pretreatment and sorption behaviour of atrazine. *Bioresour Technol*. (2013) 147:338–44. doi: 10.1016/j.biortech.2013.08.042

84. American Diabetes Association Professional Practice Committee. 2. Classification and Diagnosis of Diabetes: Standards of Medical Care in Diabetes-2022. *Diabetes Care*. (2022) 45(Suppl 1):S17–38. doi: 10.2337/dc22-S002

85. Quinn TP, Erb I. Amalgams: data-driven amalgamation for the dimensionality reduction of compositional data. *NAR Genom Bioinform*. (2020) 2:lqaa076.

86. Munafò MR, Tilling K, Taylor AE, Evans DM, Davey Smith G. Collider scope: when selection bias can substantially influence observed associations. *Int J Epidemiol*. (2018) 47:226–35. doi: 10.1093/ije/dyx206

frontiers | Frontiers in Cardiovascular Medicine

TYPE Original Research
PUBLISHED 24 May 2024
DOI 10.3389/fcvm.2024.1345421

OPEN ACCESS

EDITED BY
Catherine A. Reardon,
The University of Chicago, United States

REVIEWED BY
Xiaohan Mei,
NewYork-Presbyterian, United States
Jun Yu,
Temple University, United States

*CORRESPONDENCE
Ayotunde O. Dokun
✉ ayotunde-dokun@uiowa.edu

RECEIVED 27 November 2023
ACCEPTED 14 May 2024
PUBLISHED 24 May 2024

CITATION
Singh MV, Wong T, Moorjani S, Mani AM and Dokun AO (2024) Novel components in the nuclear factor-kappa B (NF-κB) signaling pathways of endothelial cells under hyperglycemic-ischemic conditions. Front. Cardiovasc. Med. 11:1345421. doi: 10.3389/fcvm.2024.1345421

Novel components in the nuclear factor-kappa B (NF-κB) signaling pathways of endothelial cells under hyperglycemic-ischemic conditions

Madhu V. Singh, Thomas Wong, Sonia Moorjani, Arul M. Mani and Ayotunde O. Dokun*

Division of Endocrinology and Metabolism, Carver College of Medicine, University of Iowa, Iowa City, IA, United States

Diabetes worsens the outcomes of a number of vascular disorders including peripheral arterial disease (PAD) at least in part through induction of chronic inflammation. However, in experimental PAD, recovery requires the nuclear factor-kappa B (NF-κB) activation. Previously we showed that individually, both ischemia and high glucose activate the canonical and non-canonical arms of the NF-κB pathway, but prolonged high glucose exposure specifically impairs ischemia-induced activation of the canonical NF-κB pathway through activation of protein kinase C beta (PKCβ). Although a cascade of phosphorylation events propels the NF-κB signaling, little is known about the impact of hyperglycemia on the canonical and non-canonical NF-κB pathway signaling. Moreover, signal upstream of PKCβ that lead to its activation in endothelial cells during hyperglycemia exposure have not been well defined. In this study, we used endothelial cells exposed to hyperglycemia and ischemia (HGI) and an array of approximately 250 antibodies to approximately 100 proteins and their phosphorylated forms to identify the NF-κB signaling pathway that is altered in ischemic EC that has been exposed to high glucose condition. Comparison of signals from hyperglycemic and ischemic cell lysates yielded a number of proteins whose phosphorylation was either increased or decreased under HGI conditions. Pathway analyses using bioinformatics tools implicated BLNK/BTK known for B cell antigen receptor (BCR)-coupled signaling. Inhibition of BLNK/BTK in endothelial cells by a specific pharmacological inhibitor terreic acid attenuated PKC activation and restored the IκBα degradation suggesting that these molecules play a critical role in hyperglycemic attenuation of the canonical NF-κB pathway. Thus, we have identified a potentially new component of the NF-κB pathway upstream of PKC in endothelial cells that contributes to the poor post ischemic adaptation during hyperglycemia.

KEYWORDS

endothelial cells, hyperglycemia, BLNK/BTK, peripheral artery disease, NF-κB, inflammation, diabetes, protein kinase C

Introduction

Diabetes significantly worsens the outcomes of a number of vascular disorders including peripheral arterial disease (PAD) (1–6). This poor outcome is attributed in part to the inflammatory milieu of the diabetic condition (1, 7–10). The NF-κB signaling pathway is one of the most studied inflammatory pathways under multiple

stress and disease related conditions including diabetes (11–13). The NF-κB transcription factor is a heterogeneous group of five transcription factor subunits that form dimers in various combinations to regulate transcription of their various target genes (14, 15).

The commonly described NF-κB signaling pathway, also known as the canonical pathway, involves phosphorylation dependent tagging and subsequent proteosomal degradation of the inhibitory IκBα subunit to allow nuclear translocation of the p65 subunit containing NF-κB dimer (14). NF-κB signaling is activated under ischemic conditions and is required for arteriogenesis following an ischemic injury (16). Inhibition of NF-κB signaling pathway in endothelial cells shows aberrant endothelial function and poor post-ischemic perfusion recovery (16). Recently, we have shown that chronic activation of NF-κB pathway by hyperglycemia in diabetes impairs activation of the canonical NF-κB pathway as measured by increased IκBα levels (1). Moreover, we showed that, this process involves activated PKCβ and contributes to poor reperfusion recovery in a preclinical model of peripheral artery disease (PAD) in type I diabetes (1). Inhibition of PKCβ by ruboxistaurin (Rbx) restored the canonical NF-κB signaling pathway both *in vitro* and *in vivo* suggesting a pivotal role of PKCβ activity in post ischemic adaptation in the setting of hyperglycemia. However, the molecular signals and pathways that lead to PKCβ activation under hyperglycemic ischemic conditions are not well understood. To elucidate the pathway involved, we used a combined approach of bioinformatics and unbiased screening of the phosphorylation states of approximately 100 proteins known to participate in various pathways of NF-κB activation. Here we report a previously unknown signaling pathway of NF-κB activation in endothelial cells that resembles B cell receptor signaling.

Materials and methods

Cell cultures

All experiments were performed using pooled human vascular endothelial cells (HUVEC, ATCC, Cat # PCS-100-011, USA) and human aortic endothelial cells (HAEC) from Cell Applications (Cat # 304-05a, San Diego, CA, USA) or mouse microvascular endothelial cells from skeletal muscles (MMEC, Cat#T4991, Applied Biological Materials, Richmond, British Columbia, Canada) between passage 4 and 7 as described previously (1). The complete endothelial cell growth medium (ECGM) was obtained from Cell Applications, Inc. (Cat # 211-500, San Diego, CA, USA). All endothelial cells were grown on gelatin coated (Cat # 6950, Cell Biologics) plastic culture dishes in the above medium under 95% humidity and 20% O_2. For simulated ischemia, culture medium was removed, cells were washed with Dulbecco's PBS and medium was replaced with endothelial cell starvation medium (Cell Applications, San Diego, Cat# 209–250) and incubated for 24 h in a hypoxia chamber with 95% humidity and 2% O_2 (6). Cell cultures were maintained in normal glucose (5 mM D-glucose). For experiments, the medium was supplemented with 20 mM D-glucose (high glucose medium, HG) or with 20 mM metabolically inert L-glucose (normal glucose medium, NG). For inhibitor studies, cultured cells were treated with terreic acid at described concentrations shown in results (Cat# 1405, Tocris). For BLNK knockdown by shRNA, MMEC were transfected with plasmid containing shRNA sequence (TRCN0000329213, Millipore-Sigma) or corresponding empty plasmid vector using Lipofectamine3000 (Thermo-Fisher). Cell lysates were prepared in RIPA buffer and immunoblotting performed.

Phosphoprotein array

Antibodies arrays were used to detect differences in phosphorylation of signaling molecules involved in the NF-κB pathway (NF-κB Phospho Antibody Array, Cat# PNK215, Full Moon Biosystems, Sunnyvale, CA, USA) as described previously (1). These arrays contained 215 antibodies to approximately 100 proteins and their phosphorylated forms that are known to participate in the NF-κB signaling pathways. Cell extracts from HUVEC exposed to either normal glucose (NG, 5 mM D-Glucose), normal glucose with ischemia (NGI), 25 mM D-glucose (HG), or 25 mM D-glucose with ischemia (HGI) were analyzed for the phosphoprotein levels according to the manufacturer's suggested protocol. A microarray scanner was used to record and digitize the fluorescence signals. Raw data were analyzed by manufacturer's recommendations using ImageJ (17) and transferred to Excel worksheet (Microsoft Office suite) for further analyses. Background corrections were performed, and the signals normalized against the median intensity of all the experimental spots on the array. Fold change in protein phosphorylation was calculated by dividing the intensity of the phosphorylated spot by the signal intensity of the corresponding non-phosphorylated spot for each protein. Differential expression between NG and NGI samples, and HG and HGI were calculated by dividing the phosphorylation ratio of the NGI and HGI with that of the NG and HG controls, respectively. Significant change was taken as greater than 1.5- or less than 0.67-fold. This experiment was carried out with three samples for each experimental group, and the array contained six spots for each antibody.

Immunoblotting

Cell and tissue lysates were prepared in RIPA buffer (Thermo Scientific, Cat# 89901) as described previously (1). Equal amounts of protein in each sample were separated on NuPAGE gels and transferred to nitrocellulose membranes (BioRad, Cat# 1620094). After blocking non-specific binding in Intercept blocking buffer (LiCor, Cat# 927-60001), the membranes were probed with primary antibodies overnight at 4°C. The primary antibodies used were anti-IκBα (Cat#9242, Cell Signaling Technology, Danvers, MA, USA), anti-pSer661-PKC (Cat# DBOA15543, Vita Scientific, Beltsville, Maryland), anti-BTK (Cat# 8547, Cell Signaling Technology, Danvers, MA, USA), anti-BLNK (Cat# 36438, Cell Signaling), phospho-BLNK-Tyr84 (Cat # 26528, Cell Signaling),

anti-GAPDH (Cat# 2118), and anti-β-actin (Cat# 3700, Cell Signaling). Following washes with Tris-buffered saline-0.1% Tween20 (TBST), secondary antibodies either Donkey-anti-rabbit-HRP (Cat # NA93AV, Cytiva), Goat-anti-rabbit-IR800, or Goat-anti-mouse-IR680 (both Li-COR Biosciences, Lincoln NE, USA) were used at 1:5,000 dilution in blocking buffer for 1 h at room temperature. Membranes were washed in TBST and signals were captured by iBright 1500 (Invitrogen) imager either directly for IR antibodies or by enhanced chemiluminescence (ECL) method. Quantification of the protein bands on immunoblots were performed using Image Studio Lite version 5.2 (Li-COR Biotechnology, Lincoln, Nebraska). Abundance of phosphoproteins was determined as the ratio of band intensity of target protein bands to β-actin.

RNA isolation and real-time QPCR

RNA was isolated from cultured cells using Direct-zol RNA mini prep kit (Zymo Research, USA, Cat. R2052)) using Tri Reagent for cell lysis. Quality of isolated RNA (A260/280 ≥2.0) and quantification was done on a NanoDrop instrument. Aliquots of 200 ng RNA samples were reverse transcribed using a High-Capacity RNA to cDNA kit (AppliedBiosystems, Cat 4388950). For QPCR of BTK RNA, 10 ng RNA equivalent cDNA was used in each reaction with Power SYBR Green reagent (AppliedBiosystems, Cat 4367659) on a QuantStudio 3 thermocycler (ThermoFisher). One picomoles of forward and reverse primers were used for *BTK* (Forward 5′-AGCACAACTCTGCAGGACTC-3′ and Reverse 5′-TGCAGTGGAAGGTGCATTCT-3′) and *GAPDH* (Forward 5′-GTCTCCTCTGACTTCAACAGCG-3′ and Reverse 5′-ACCACCC TGTTG CTGTAGCCAC-3′). *GAPDH* was used as a loading control (1 ng RNA equivalent for GAPDH QPCR) and expression analysis was done by ΔΔCt method (18).

Statistical analysis

The measurements are expressed as mean ± SEM. Statistical comparisons between two groups (e.g., treated vs. untreated) were performed by *t*-test, whereas for more than two groups, we used one-way analysis of variance. A *P* value of <0.05 was considered statistically significant.

Results

In hyperglycemic mice with type 1 diabetes, perfusion recovery and post ischemic adaption is poor following experimental PAD or induction of hind limb ischemia (HLI) (1, 19, 20). We have shown that ischemic activation of the canonical NF-κB pathway, is impaired under hyperglycemic conditions (1). Therefore, we investigated endothelial cells for an increase or decrease in phosphorylation of proteins associated with NF-κB signaling under hyperglycemic-ischemic conditions. Using HUVECs grown either in normal glucose with ischemia (NGI) or high D-glucose with ischemia (HGI), we compared the phosphorylation state of 98 protein sites representing about 48 distinct proteins. These proteins are known to be modulated in various pathways of the NF-κB signaling. We used an array of antibodies and selected the protein phosphorylation sites whose signals were increased greater than 1.5-folds or decreased greater than 0.67-fold change.

We first analyzed the increase or decrease in phosphorylation of signaling proteins in cells grown in normal glucose concentration and exposed to either normoxia (NG) or ischemia (NGI). In NGI samples, when compared to normoxic samples (NG), 26 protein phosphorylation sites were identified to undergo increased phosphorylation whereas 36 sites had decreased phosphorylation (Figure 1A). Similarly, when cell cultured in high D-glucose (HG) and exposed to normoxia were compared to cells exposed to ischemia (HGI) increased phosphorylation of 25 protein sites and decreased phosphorylation of 40 sites (Figure 1B) were identified. Additionally, a direct comparison of NGI and HGI results showed increased phosphorylation on 15 sites and decreased phosphorylation on 41 sites (Figure 1C, also see Supplementary Material Table S1). Thus, ischemia modulates phosphorylation of a different number of sites in proteins that are involved in NF-κB signaling pathway under normal glucose compared to high glucose.

To identify protein phosphorylation in ischemic ECs that could be attributed to exposure to high glucose we compared the list of sites that had increased phosphorylation in either NGI or HGI. A Venn-diagram analysis showed that out of the 25 sites whose phosphorylation was increased in HGI, 17 sites were common to both NGI and HGI, suggesting that these increases were related to ischemia, independent of glucose levels (Figure 2A). There were 9 out of 26 sites that had increased phosphorylation specifically in NGI, suggesting ischemia induced changes under normal glucose conditions. In addition, 8 sites had increased phosphorylation only in HGI samples indicating their unique role in hyperglycemic ischemia.

Similarly, comparison of the list of sites with decreased phosphorylation in either NGI or HGI showed that 28 sites had decreased phosphorylation under ischemic conditions irrespective of the glucose concentration in the growth medium. There were 8 sites with decreased phosphorylation only in NGI and 12 sites whose phosphorylation decreased only in HGI (Figure 2B).

Since high D-glucose alone can induce NF-κB signaling, we further compared these increases or decrease in protein phosphorylation with the respective protein sites observed in high D-glucose-specific conditions (NG/HG) (Figure 3A). There was increased phosphorylation of 15 protein sites attributable to HG, 3 of these sites showed increased phosphorylation also in ischemic conditions with NG while 2 other sites showed increased phosphorylation in HGI. Of the 8 phospho-sites identified in HGI/HG (Figure 2A), all were specific for high D-glucose with ischemia (HGI, Figure 3A). However, of the 12 decreased phospho-proteins in HGI (Figure 2B), 10 protein sites were specific for high D-glucose with ischemia, whereas 2 protein sites also had decreased phosphorylation in high D-glucose (HG/NG) without ischemia (Figure 3B). Thus, high glucose, ischemia, or combinations of these conditions result in specific changes at different phosphorylation sites of proteins in the NF-κB signaling pathways (Table 1).

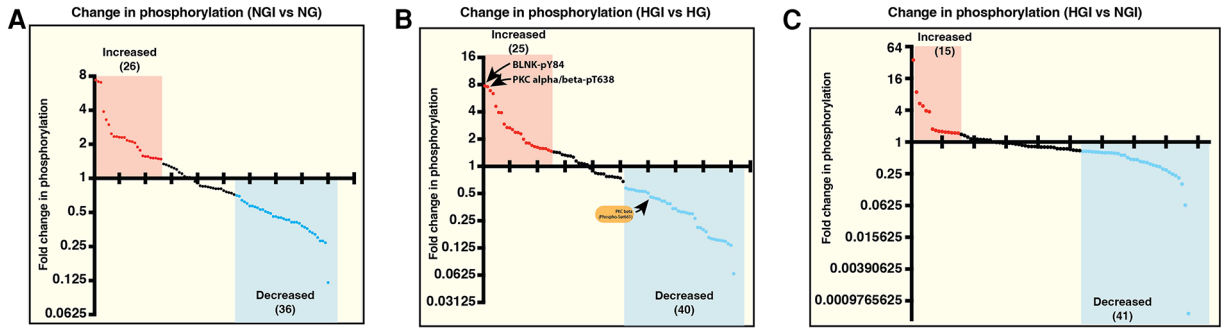

FIGURE 1
Measurement of relative changes in the phosphorylation state of proteins involved in the signaling pathways of NF-κB activation using printed arrays of antibodies. The graphs show fold-changes as ratios of phosphorylated/total signal in human endothelial cell lysates. (**A**) The plot shows fold-change in phosphorylation of specific epitopes of proteins in human endothelial cells under normal D-glucose and ischemic condition (5 mM D-glucose + 20 mM L-glucose, NGI) compared to the control cells grown under normal D-glucose and normoxic condition (5 mM D-glucose + 20 mM L-glucose, NG). Each dot represents a phospho-protein site. Red and blue dots represent greater than 1.5-folds increase or greater than 0.67-fold decreased phosphorylation, respectively. (**B**) Comparison of changes in protein phosphorylation in hyperglycemic-ischemic endothelial cells. The plot shows protein sites with 1.5-folds increased (red dots) or 0.67-fold decreased (blue dots) phosphorylation in high D-glucose and ischemia (25 mM D-glucose + ischemia, HGI) compared to high D-glucose and normoxia (25 mM D-glucose, HG). (**C**) Phospho-proteins comparison of NGI and HGI (1.5-folds increase or 0.67-fold decrease cutoff) revealed increased phosphorylation at 15 sites (red dots) and decreased phosphorylation at 41 sites (blue dots). *N* = 3 antibody arrays per group, 1 array/sample.

Multiple signaling pathways related to environmental stress affect development, growth, cell death and post-ischemic adaption through activation of the NF-κB pathway (37). To identify the pathway leading to NF-κB activation in hyperglycemic-ischemic condition in endothelial cells, we employed a bioinformatics approach. We hypothesized that any protein that has undergone a change in phosphorylation under HGI, irrespective of the direction of change, must participate in the NF-κB signaling pathway. Moreover, change in environmental condition may not necessarily recruit an entirely

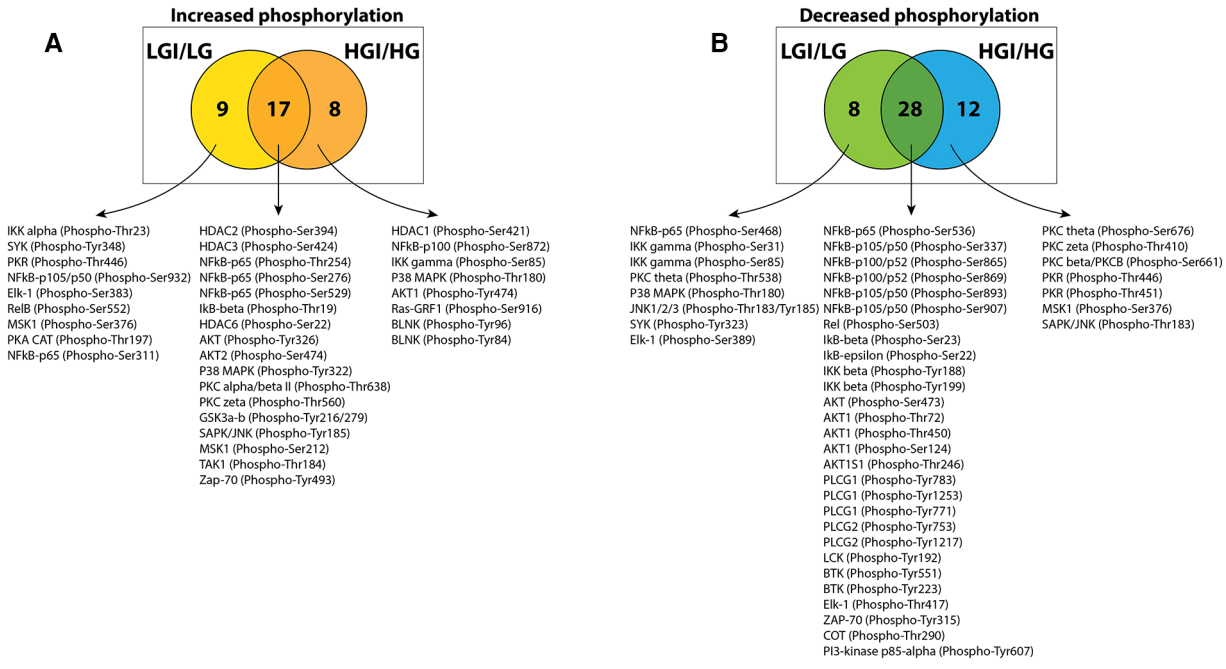

FIGURE 2
Venn diagram analysis of protein phosphorylation sites with 1.5-folds changes in normal D-glucose with ischemia (NGI) and high D-glucose with ischemia (HGI) to identify specific protein phosphorylation sites in hyperglycemic-ischemic conditions. (**A**) Comparison of the protein sites with increased phosphorylation in NGI and ischemic HGI showed 9 NGI-specific and 8 HGI-specific protein phosphorylation sites. (**B**) Comparison of sites with decreased phosphorylation showed 8 NGI-specific sites and 12 HGI-specific sites.

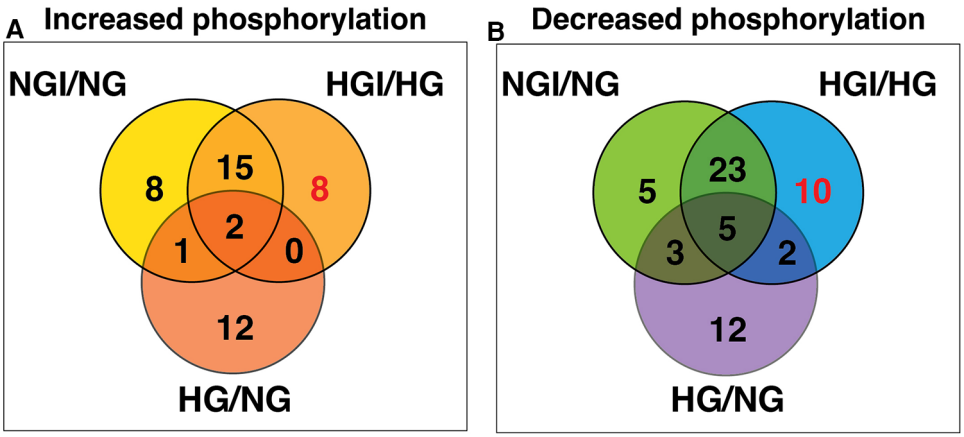

FIGURE 3
Venn diagram analyses to impose a higher level of specificity of phosphorylation changes by eliminating high D-glucose-related phosphorylation sites (HG). The 15 HG-related increased and 22 decreased phosphorylation sites were obtained from our published results (1). These analyses eliminated sites that whose phosphorylation is either increased (A) or decreased (B) in the presence of high D-glucose alone. The analysis yielded 8 HGI-specific sites with increased phosphorylation and 10 HGI-specific sites that had decreased phosphorylation (shown in red).

new signaling pathway; instead, modification of even a single key protein may potentially alter the signaling outcome. Therefore, to identify the signaling pathway involved in hyperglycemic-ischemic condition (HGI), we obtained a list of genes representing all phosphoproteins that were modulated in HGI (Figure 1B). The 65 modulated phospho-sites (25 increased and 40 decreased) in HGI (Figure 1B) were represented by 35 genes (Table 2). We then performed an over-representation test on this set of representative genes using PANTHER molecular classification system (38).

Among the predicted pathways, the toll-like receptor pathway, B cell activation and T cell activation pathways were prominent for their fold-enrichment (TLR >100-folds, T cell activation 81.71-folds, and B-cell activation 80.56-folds) and low probability of false discovery rate (Table 3). Similar results were obtained from the Reactome database (www.reactome.org) for enrichment of genes related to the TLR and B cell receptor signaling (BCR) pathways. Together, these results suggest that in addition to the TLR pathway, the endothelial cells may also have an operative BCR like pathway (Figure 4). Although BCR pathway was originally thought to be limited to the B lymphocytes, it has now been known to operate in several non-B cells as well (39, 40). However, since this pathway or its components have not been reported in endothelial cells, we decided to investigate this pathway.

TABLE 1 Hyperglycemia-ischemia (HGI) specific change in phosphorylation of signaling proteins involved in the NF-κB pathway.

Phospho-protein site	Change in phosphorylation	Reference to NF-κB involvement
P38 MAPK (Phospho-Thr180)	Up	(21–23)
AKT1 (Phospho-Tyr474)	Up	(24)
Ras-GRF1 (Phospho-Ser916)	Up	(25, 26)
HDAC1 (Phospho-Ser421)	Up	(27)
NF-κB-p100 (Phopho-Ser872)	Up	(28)
BLNK (Phopho-Tyr96)	Up	(29)
BLNK (Phopho-Tyr84)	Up	
IKK gamma (Phopho-Ser85)	UP	(30)
PKC theta (Phopho-Ser676)	Down	(31, 32)
PKR (Phospho-Thr446)	Down	(33)
PKR (Phopho-Thr451)	Down	
PKC beta (Phospho-Ser661)	Down	
PKC zeta (Phospho-Thr410)	Down	(31, 32, 34)
HDAC5 (Phopho-Ser259)	Down	
SAPK/JNK (Phospho-Thr183)	Down	
IκB-alpha (Phopho-Ser32/36)	Down	(35)
NF-κB-p65 (Phopho-Thr435)	Down	(36)
LCK (Phopho-Tyr505)	Down	

BLNK/BTK-dependent NF-κB signaling in endothelial cells

Our screening showed a role of B-cell linker protein (BLNK) in the predicted B-cell receptor activation pathway. BLNK is responsible for B-cell receptor (BCR) signaling pathway leading to B-cell development (41). BLNK is a scaffold protein that bridges BCR signaling components with downstream signaling pathways including activation of the NF-κB signaling pathway (42). In addition, BLNK has also been shown to play a role in growth of cancer cells (39, 40). However, their presence and role in endothelial cell signaling is not known. We used antibody to BLNK in immunoblotting experiments with several primary endothelial cells from human and mouse. We found that BLNK protein is expressed in human (HUVEC, HAEC, Figure 5A) as well as mouse (MVECsk, MVEC) endothelial cells (Figure 5B). In addition, BLNK protein undergoes increased phosphorylation at the Tyr84 residue (pY84-BLNK) under ischemic conditions both in normal glucose (NGI) and high glucose (HGI) as predicted from the phosphoarray screening (Figures 5C,D). These

TABLE 2 The list of 35 distinct endothelial cell proteins within the NF-κB signaling pathway showing change in phosphorylation under hyperglycemic-ischemic conditions (HGI).

Proteins in HGI	Genes in HGI
AKT1	AKT1
AKT2	AKT2
BLNK	BLNK
BTK	BTK
CSNK2B	CSNK2B
PKR	EIF2AK2
ELK-1	ELK1
GSK3a	GSK3A
GSK3b	GSK3B
HDAC1	HDAC1
HDAC5	HDAC5
IκB beta	IKBKB
IKK gamma	IKBKG
LCK	LCK
TAK1	MAP3K7
COT	MAP3K8
P38 MAPK	MAPK14
SAPK/JNK	MAPK8
NF-κB p105/p50	NFKB1
NF-κB p100/p52	NFKB2
IκB-alpha	NFKBIA
IKK beta	IKBKB
IκB epsilon	NFKBIE
PI3-kinase p85 alpha	PIK3R1
PLCG1	PLCG1
PLCG2	PLCG2
PKC alpha	PRKCA
PKC beta II	PRKCB
PRKCQ	PRKCQ
PKC zeta	PRKCZ
RAS-GRF1	RASGRF1
REL	REL
NF-κB p65	RELA
MSK1	RPS6KA5
ZAP-70	ZAP70

results validated the results from the phosphoarray screening that BLNK protein is expressed in endothelial cells and its phosphorylation is modulated under ischemic conditions. To test the effect of BLNK on the NF-κB pathway, we used shRNA-mediated knockdown of BLNK protein in MVECsk cells (Figures 6A,B). Decrease in BLNK resulted in decreased NF-κB basal activity reflected by increase in steady state levels of IκBα protein (Figures 6A–C) suggesting that BLNK participates in the NF-κB signaling pathway in endothelial cells.

As a scaffold protein, BLNK recruits multiple proteins to propagate downstream signaling pathways including PLCγ activation (43). Bruton's tyrosine kinase (BTK) is a BLNK-associated non-receptor tyrosine kinase that is important for this signaling (44). Therefore, we tested the expression of BTK mRNA and protein in cultured human endothelial cells (HUVEC and HAEC) by RT-QPCR and immunoblotting, respectively. In RT-QPCR analysis using BTK-specific primers, the expression of BTK was detected both in HUVEC and peripheral blood mononuclear cells (PBMC) as seen by melt curve analysis of SYBR green based RT-QPCR products of BTK and GAPDH. Result showed similar peaks in PBMC and HUVECS with similar Tm values (Figure 7A). Agarose gel electrophoresis of the RT-QPCR reaction products showed single specific band of expected molecular size (77 bp) for BTK amplicon and 131 bp amplicon for GAPDH (Figure 7B). Immunoblotting of cell lysates also showed BTK protein expression in human as well as mouse cultured primary endothelial cells (Figure 7C). Together, these results strongly suggested that BLNK and BTK are expressed in HUVEC as well as other endothelial cells from human and mouse and validate the results of the phosphoarray screening.

Previously, we have shown that high glucose conditions impair the canonical NF-κB signaling resulting in increased steady state levels of IκBα (1) which was related to increased phosphorylation of PKCβ-Ser661. To test whether BLNK/BTK axis might be upstream of this pathway, we treated high D-glucose grown primary mouse endothelial cells (MVECsk) with terreic acid (TA, 20 and 30 μM), a selective inhibitor of BTK. Compared to the control cells grown in high L-glucose (normal D-glucose), cells grown in high D-glucose had increased IκBα protein (46.7% increase from control), an observation consistent with decreased NF-κB activity as we showed previously (Figures 8A,B) (1). Treatment with terreic acid significantly decreased accumulation of IκBα suggesting a net increase in NF-κB activity.

We further tested the effect of inhibiting BLNK/BTK signaling in primary mouse endothelial cells on PKC activation by phosphorylation. PKC phosphorylation was increased in high D-glucose conditions and treatment with terreic acid decreased this phosphorylation (Figures 8C,D). These results suggest that a BLNK/BTK mediated signaling pathway plays a role upstream of PKCβ in high glucose-related NF-κB signaling in endothelial cells.

TABLE 3 Identified NF-κB signaling pathways based on PANTHER pathways over-representation (*homo sapiens*) analysis of proteins whose phosphorylation was modulated by hyperglcemic-ischemic (HGI) condition. Top 5 pathways are shown. PANTHER overrepresentation test (released 20240226; PANTHER version 18.0 (released 2023-08-01).

PANTHER pathway	Number of genes	Fold enrichment	P value	FDR (false discovery rate)
Toll receptor signaling pathway	12	>100	8.78E-23	7.07E-21
T cell activation	12	81.71	1.08E-20	4.35E-19
B cell activation	10	80.56	2.90E-17	7.79E-16
Insulin/IGF pathway-protein kinase B signaling cascade	5	75.26	5.89E-09	4.51E-08
Histamine H1 receptor mediated signaling pathway	6	74.61	1.64E-10	1.76E-09

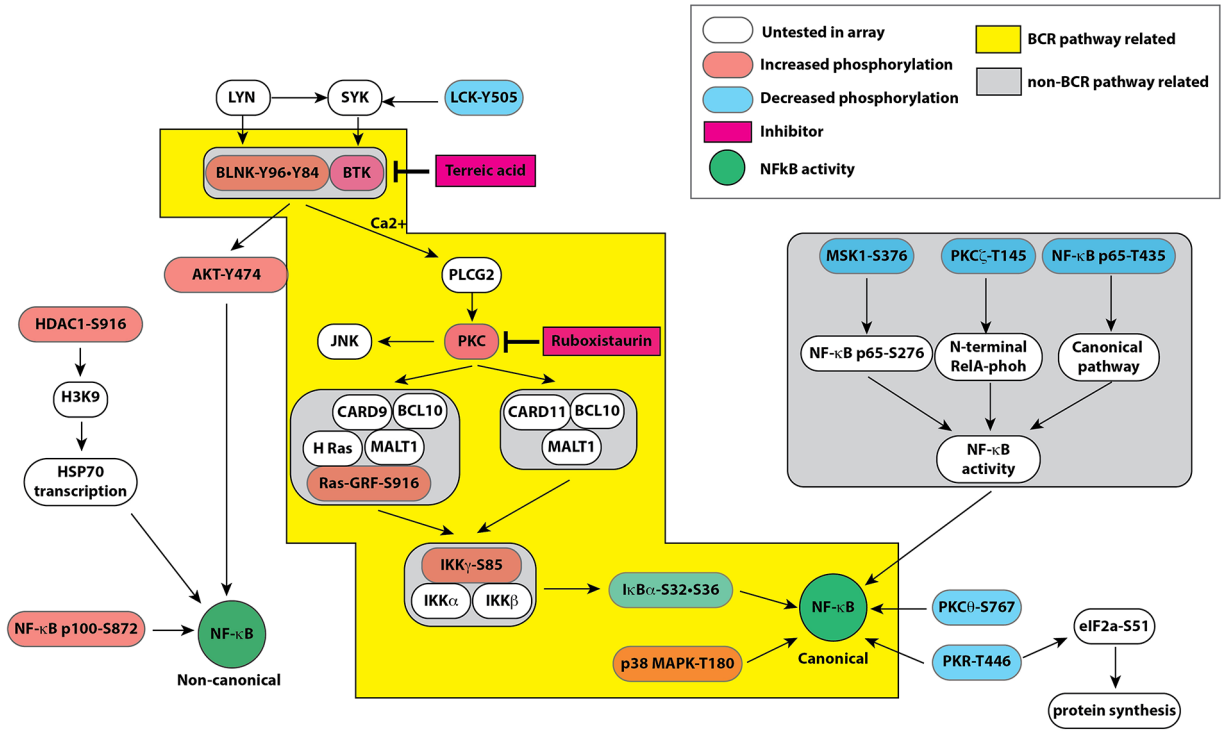

FIGURE 4
Pathway map based on combined results obtained from bioinformatic analyses of signaling protein phosphorylation sites using PANTHER molecular classification system and reactome database. Both databases strongly suggested a role of B cell receptor like pathway in endothelial cells leading to modulation of the canonical and non-canonical pathways of NF-κB activation by hyperglycemic-ischemic conditions. The colored boxes show proteins represented in the experimental data. The components highlighted in orange show increased phosphorylation whereas components highlighted in blue represent decreased phosphorylation on the depicted proteins. Please see the text for description.

Discussion

In this study, using an antibody array for proteins and bioinformatics tools, we have identified BLNK and BTK proteins as novel upstream signaling components of hyperglycemic-ischemic NF-κB responses in endothelial cells. Phosphorylation and dephosphorylation are important biochemical modifications in propagation of NF-κB signaling. Functional NF-κB pathway is required for recovery from ischemic conditions (16), but prolonged high glucose and ischemic conditions impair the canonical pathway of the NF-κB signaling (1). We used an array of about 215 specific antibodies representing 100 distinct phospho-protein sites related to the NF-κB signaling. We compared the changes in phosphorylation of these proteins in the lysates from endothelial cells that were grown in normal D-glucose or high D-glucose under normoxic or ischemic conditions. Our results revealed a novel pathway of endothelial cells under hyperglycemic-ischemic conditions that utilizes proteins involved in B cell receptor signaling. Moreover, our analysis suggests that in accordance with our published results, hyperglycemic conditions alter the phosphorylation of various proteins participating in the NF-κB signaling to downregulate the canonical pathway (Figure 4). BLNK is a scaffold protein that can nucleate a large protein complex of several proteins including Tec family kinases of which BTK is a member (45). Although originally described in B-cell receptor signaling, BLNK/BTK pathway also functions in non-hematopoietic cells (39, 40). Thus, modulation of IκBα by knocking down BLNK expression and by a selective inhibitor of BTK suggest an important role of this pathway in hyperglycemia related inflammatory response. Further studies will elucidate the contribution of other proteins that function upstream of BLNK in impairment of the canonical NF-κB signaling in endothelial cells chronically exposed to high glucose.

Both high glucose concentration and ischemia elicit stress response in cells through activation of the NF-κB pathway. Accordingly, a set of common protein sites had increased phosphorylation in both cells grown in normal or high D-glucose when exposed to ischemic condition. Similarly, a set of protein sites had decreased phosphorylation under ischemic condition with normal or high D-glucose. However, we also identified protein phosphorylation sites that were uniquely modulated in cells exposed to normal glucose with ischemia or to high glucose with ischemia.

Based on our findings, we have constructed a schematic of putative signaling pathways that depicts interactions of components operating in balancing the canonical and non-canonical pathways of the NF-κB-mediated transcription activation (Figure 4). Here we discuss the phosphorylation events that were upregulated or downregulated specifically in HGI

10.3389/fcvm.2024.1345421

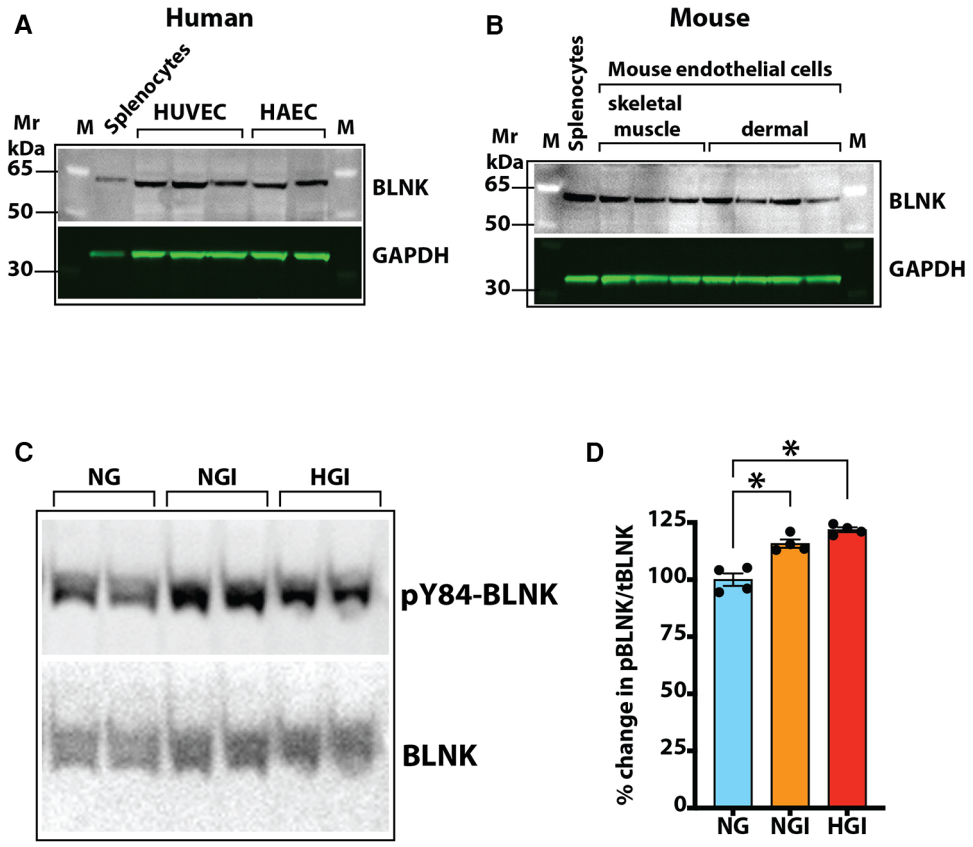

FIGURE 5
Expression of BLNK in endothelial cells. (**A**) Immunoblotting of primary cultures of human umbilical vein endothelial cells (HUVEC) and human aortic endothelial cells (HAEC) for BLNK protein. Each lane represents a replicate cell culture of the labeled primary cell type. (**B**) Immunoblotting of mouse primary endothelial cells of skeletal muscle or dermal origin for BLNK protein. GAPDH was used as a loading control in the lanes. Each lane represents a replicate culture of the respective primary cell type. (**C**) Immunoblots showing phosphorylated BLNK protein on Tyr84 residue (pY84-BLNK) under normal glucose plus ischemia (NGI) and high glucose plus ischemia (HGI) in mouse skeletal muscle endothelial cells, (**D**) pY84-BLNK in mouse skeletal muscle endothelial cells is increased under both NGI and HGI conditions ($n = 4$ each group, asterisks denote $p < 0.05$).

samples. We show that the upregulated phosphoproteins promote the non-canonical NF-κB pathway whereas the downregulated phosphoproteins limit the activation of the canonical NF-κB pathway. These changes in turn may have a net adverse effect of attenuating the canonical NF-κB pathway in hyperglycemic ischemic conditions.

Upregulated phosphorylation sites

BLNK (p-Tyr96 and p-Tyr84)

B cell linker protein (BLNK) serves a scaffolding function to coordinate second messenger generation and signal transduction upon activation of B cell receptor (BCR). BLNK does not have an intrinsic enzyme activity; instead, it functions as a scaffold protein to assemble multiple proteins including kinases and PLCβ. In mouse, $BLNK^{-/-}$ B cells show intact activation of AKT but impaired activation of the canonical nuclear factor NF-κB due to a failure to degrade IκBα protein (46). In accordance, we observed that shRNA-mediated knockdown of BLNK in mouse endothelial cells increased IκBα levels suggesting an impaired canonical NF-κB pathway (Figure 6). In this pathway, phospholipase C (PLC)-gamma2 has also been demonstrated to be essential for NF-κB activation. BLNK is required for PLCγ2 phosphorylation and Ca^{2+} influx through BCR activation (47). Peptide containing phosphorylated-Tyr96 residue specifically bind to BTK that leads to Ca^{2+} influx and PLCγ binding and phosphorylation upon BCR activation (29). Thus, the presence of BLNK in cultured primary endothelial cells (passage 4–7), that are devoid of B cells, suggests the presence of a B cell like signaling pathway. Consistent with our previous report of decreased canonical NF-κB pathway activation, we observed decreased PLCγ phosphorylation, whereas increased AKT1 phosphorylation leads to sustained or increased non-canonical activation of NF-κB pathway.

We also observed expression of BTK in both mouse and human primary endothelial cells from different tissue sources. We verified the expression of BTK transcripts in endothelial cells using QPCR based method. In addition, inhibition of BTK activity led to change in IκBα levels. These findings further suggest a functional role of BLNK/BTK pathway in inflammatory response in endothelial cells under hyperglycemic conditions. Interestingly, knocking down of BLNK or inhibition of BTK, both resulted in

10.3389/fcvm.2024.1345421

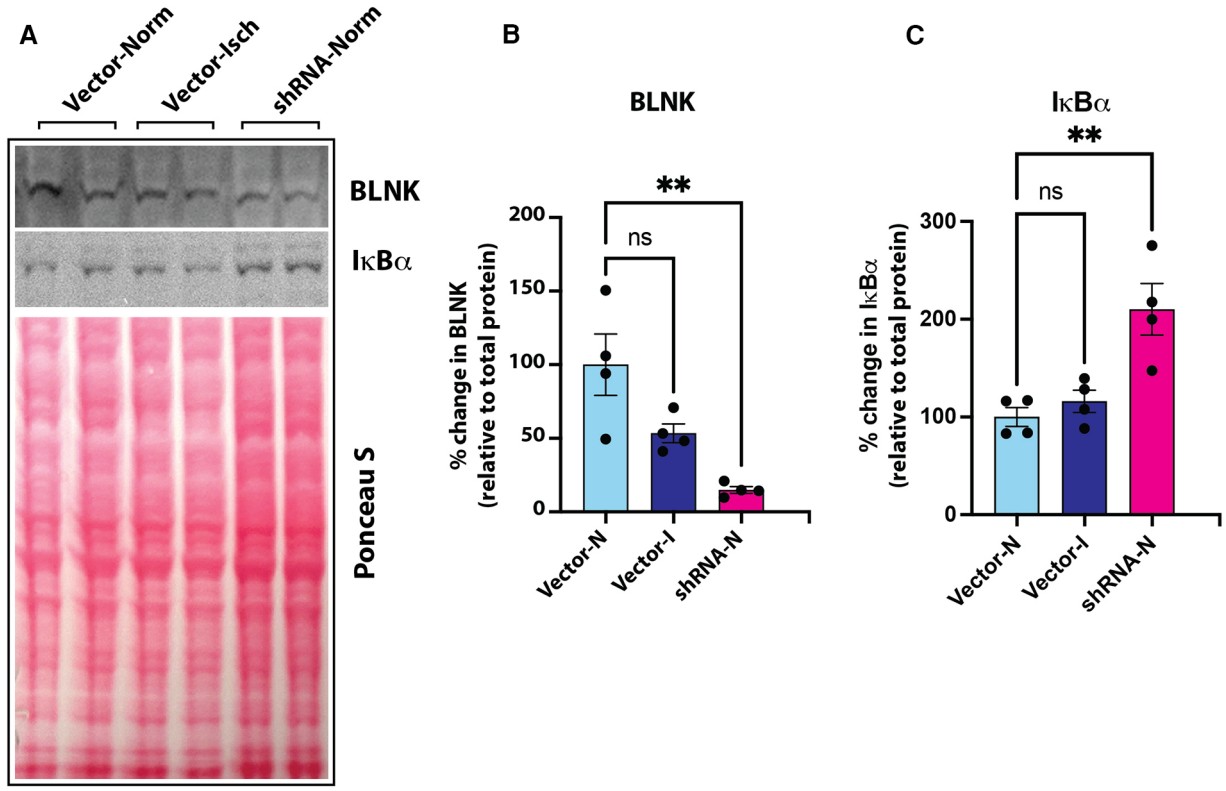

FIGURE 6
(A) Immunoblot of BLNK and IκBα proteins in culture grown primary mouse skeletal microvascular endothelial cells (MVECsk). Intensity of protein bands was normalized to total loaded protein in corresponding lanes (Ponceau S staining). (B) BLNK protein was significantly knocked down by transfection of shRNA harboring plasmid (shRNA-Norm) compared to control plasmid vector transfected cells and kept under normoxic or ischemic conditions (Vector-Norm and Vector-Isch, respectively). (C) Knockdown of BLNK resulted in increased IκBα protein in corresponding samples probed on the same blot. $N = 4$ each group, $p < 0.05$ by One Way ANOVA).

activated NF-κB as measured by changes in IκBa levels. Since the outcome of signaling through both BLNK and BTK depends on phosphorylation status of their different amino acid residues, future experiments will elucidate how these post-translational modifications relate to hyperglycemic and ischemic conditions.

AKT1 (p-Tyr474)

Akt1 is a key serine/threonine-protein kinase that regulates a number of cellular processes including cell survival, proliferation, metabolism, and angiogenesis by phosphorylating a number of protein substrate. However, the kinase activity of AKT1 itself is dependent on the phosphorylation of three specific sites (Thr308, Ser473 and Tyr474). Phosphorylation of Tyr474 residue, which was increased in our HGI samples, is the major determinant of AKT1 activity (24). The upstream signaling events leading to membrane localization and phosphorylation of AKT1 are coordinated by BTK, a non-receptor tyrosine kinase that acts as a scaffold protein to nucleate several signaling proteins. Active AKT1 positively affects a role in NF-κB-dependent gene transcription. Overexpression of constitutively active AKT1 increases non-canonical NF-κB activity by increasing IKKα activity that in turn results in increased production of p52 subunit of NF-κB (48). Our finding of increased Tyr474 phosphorylation of AKT1 in HGI cell lysates is consistent with our previous finding of increased non-canonical NF-κB activity in hyperglycemia both *in vitro* in HUVEC and *in vivo* in DM (1).

Ras-GRF1 (p-Ser916)

Ras-GRF1 (Ras-specific guanine nucleotide-releasing factor 1), also known as CDC25, is an exchange factor that promotes exchange of Ras-bound GDP by GTP. Ras-GRF1 is phosphorylated in an LCK-Syk dependent manner (49). Ras-GRF1 is linked to H-Ras and participates in activation pathway of ERK and canonical pathway of the NF-κB through CARD9-BCL10-MALT1 complex (25, 26).

HDAC1 (p-Ser916)

Histone deacetylase 1 (HDAC1) is a class I histone deacetylase that exists in multi protein complexes and modulates transcription through its enzyme activity. The phosphorylation of Ser421 residue of HDAC1 promotes its enzyme activity and complex formation (50). HDAC1 is thought to be associated with NF-κB activation since treatment of RAW264.7 cells with lovastatin inhibited IκBα phosphorylation as well as HDAC1 expression (27). Thus, HDAC1 in likely involved in down-regulating the canonical NF-κB pathway.

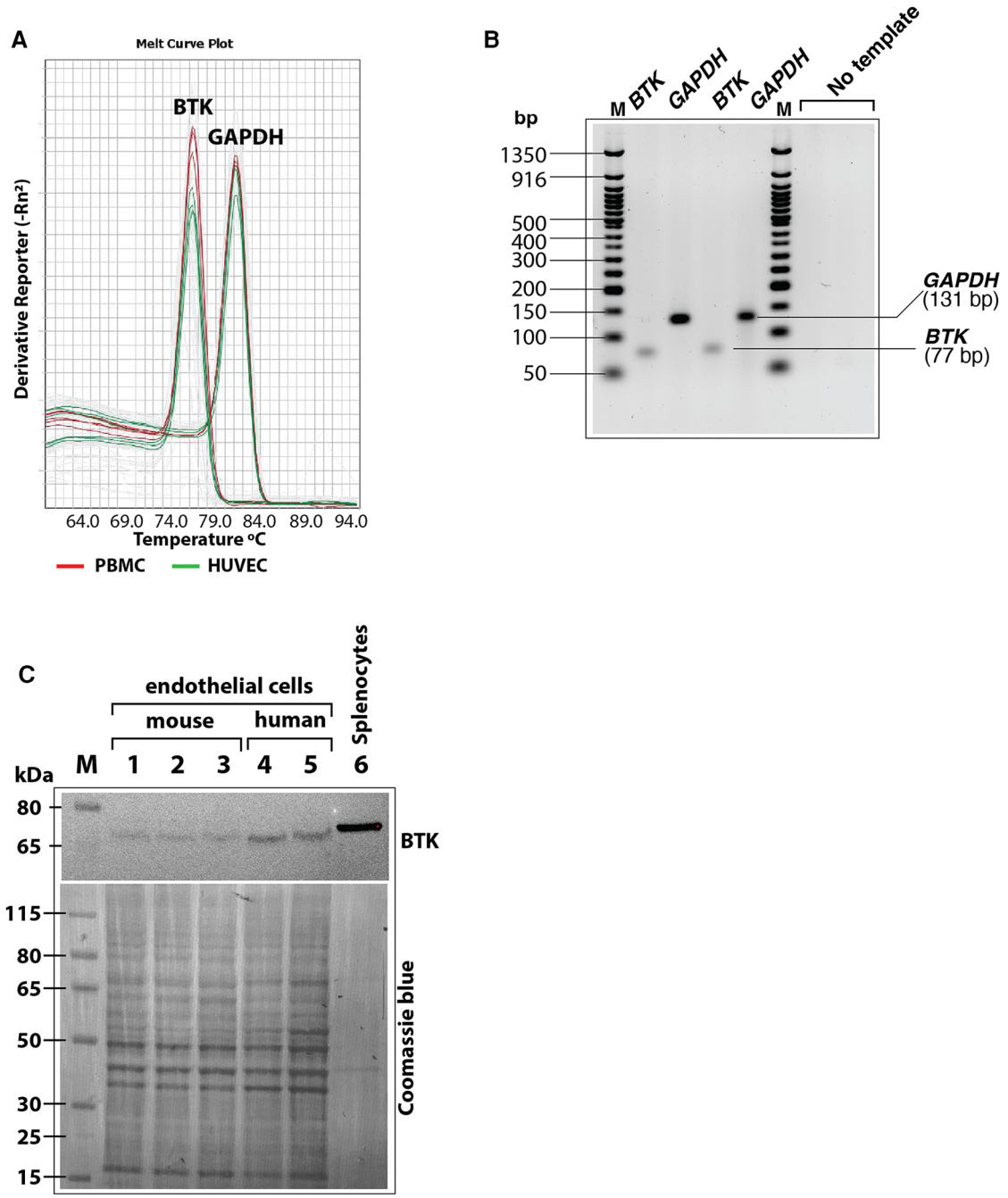

FIGURE 7
(A) Melt curves of BTK and GAPDH amplicons after RT-QPCR run showing similar *BTK* and *GAPDH* PCR product peaks from human peripheral blood mononuclear cells (PBMC, red lines) and HUVEC (green lines). (B) RT-QPCR reaction products were analyzed by agarose gel electrophoresis (3% agarose-TBE gel) to show the BTK amplicon (77 bp) and GAPDH amplicon (131 bp) in two different reactions were of specific and of expected size. Each lane represents samples loaded from an RT-QPCR reaction product. (C) Immunoblot of mouse and human primary endothelial cell lysates showing BTK protein expression. After probing with antibody, the blot was stained with Coomasie blue stain to visualize loading of protein bands in each lane. Less total protein was loaded in the mouse splenocytes lysate (positive control). Protein molecular size marker locations are shown on the left.

IKK gamma (p-Ser85)

IKKγ, also known as NEMO (NF-κB Essential Modulator), is a regulatory subunit of the cytoplasmic IKK complex. The IKK complex undergoes multiple post-translational modifications including phosphorylation. IKKγ is phosphorylated by PKCα (51). Phosphorylation of Ser85 of IKKγ enhances the kinase activity of IKKβ that results in increased phosphorylation of IκB. However, Ser85 alone is not sufficient for this activation; a combination of Ser85 and Ser141 is required for this enhancement. Moreover, IKKγ-Ser85 does not play a role in all

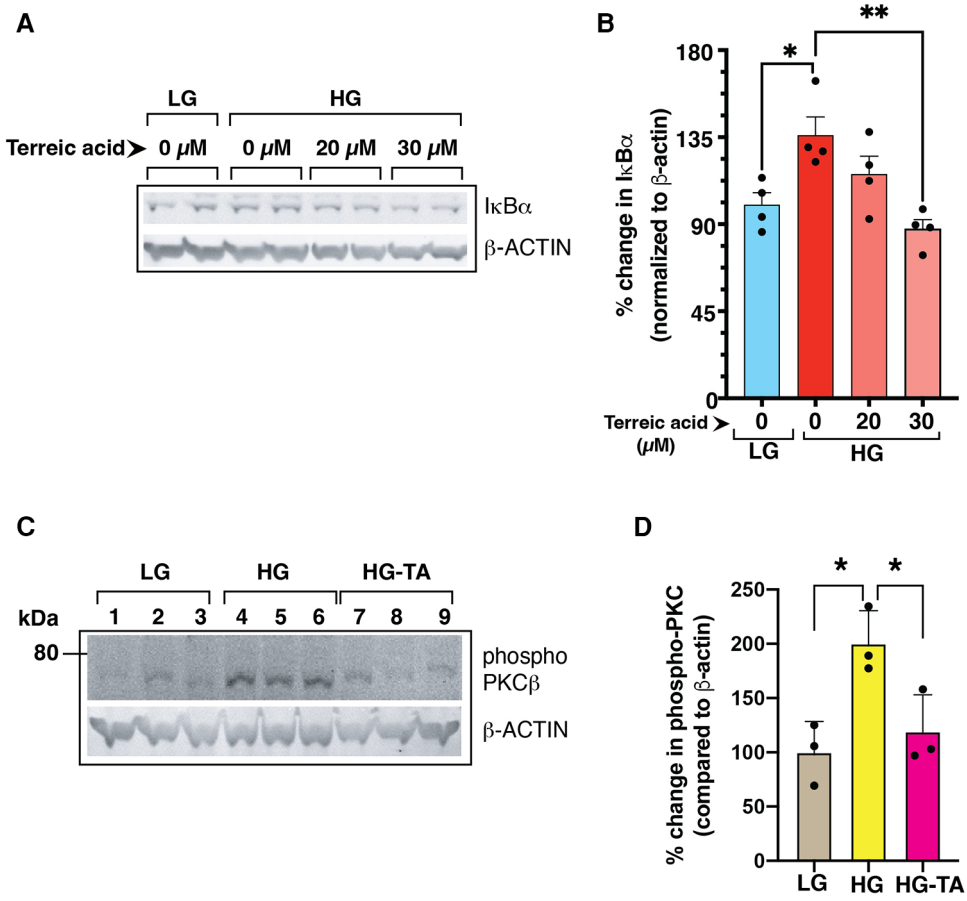

FIGURE 8
(A) Mouse primary endothelial cell cultures were subjected to normal glucose (NG, 5 mM D-glucose) or high D-glucose (HG, 25 mM D-glucose) exposure for 3 days in the presence or absence of a selective BTK inhibitor terreic acid (0, 20 and 30 μM final concentration). Cell lysates were subjected to immunoblotting with antibodies against IκBα. β-actin was used as a loading control in the corresponding lanes. (B) Signal intensity of IκBα bands were normalized by the signal intensity of β-actin band. High D-glucose (HG) increased the IκBα protein levels in the cells, an observation previously described by US (1). Treatment with terreic acid restored the IκBα levels similar to the control cells (NG-grown cells). $N = 4$ each group, Asterisks represent $p \leq 0.05$. (C) BTK-inhibitor terreic acid (30 μM final concentration) decreased the elevated phosphorylation on Ser661 site of PKCβ in mouse primary endothelial cells grown in high D-glucose (HG) condition for 3 days. Cells were exposed to either normal glucose (NG, 5 mM D-glucose), high glucose (HG, 25 mM D-glucose), or high glucose with terreic acid (HG-TA, 25 mM D-glucose + 30 μM terreic acid). The lower part of the membrane was probed with antibody against β-actin (loading control). Results are presented as the ratio of PKC-Ser661 normalized by the signal intensity of β-actin in corresponding lanes. $N = 3$ samples for each condition. Asterisks denote statistically significant difference of $p \leq 0.05$.

NF-κB activation pathways (30). Our array did not contain antibody to Ser141, limiting a conclusion based only on IKKγ-Ser85 phosphorylation.

NF-κB-p100 (p-Ser872)

The p100 protein is the precursor of the p52 NF-κB subunit that undergoes phosphorylation-dependent inducible processing. Phosphorylation results in ubiquitination and proteosomal processing of p100 to generate p52 subunit that is translocated to the nucleus (52). The Ser872 site of p100 is phosphorylated by IKKα and is a requirement for ubiquitination and proteosomal processing of p100 protein (28). We have previously shown that under hyperglycemic conditions, the non-canonical NF-κB pathway preferentially remains active in HUVEC (1). The current finding of increased phosphorylation of p100 NF-κB subunit in HGI samples is consistent with increased role of the non-canonical NF-κB pathway.

P38 MAPK (p-Thr180)

The p38 MAPK is involved in expression of proinflammatory cytokines (53). Several environmental factors specifically induce p38 MAPK in signal specific manner by dual phosphorylation of Thr180 and Tyr182 residues (21). The NF-κB activity is affected by p38 MAPK since inhibitors of p38 result in diminished expression of NF-κB dependent genes (54) likely through post translational modification of the NF-κB subunits by phosphorylation or acetylation (22, 23) or by promoting transcription initiation complex on the target genes (55).

Downregulated phosphorylation sites

LCK (p-Tyr505)

Lymphocyte cell kinase (LCK) is a Src-family kinase expressed predominantly in T cells and plays a key role in T-cell receptor (TCR) signaling pathway. However, LCK is expressed in endothelial cells, where its inhibition promoted endothelial proliferation and blocked apoptosis (56). Both structural and biochemical studies show that phosphorylation of the C-terminal 505 tyrosine residue (Y505) of LCK confers a closed molecular conformation, leading to inactivation of the kinase domain (57). In contrast, deletion or mutation of Y505 in LCK results in a constitutively active enzyme (58). Thus, decreased Tyr505 phosphorylation in high D-glucose plus ischemia would suggest an increase enzymatic activity of LCK (59).

I kappa B alpha (p-Ser32, Ser36)

Under the normal conditions, I kappa B alpha (IκBα) is an unstable protein that binds and retains the NF-κB transcription factor in the cytoplasm of the cells. Upon stimulation by appropriate signal, IκBα is rapidly degraded allowing the NF-κB transcription factor to migrate to the nucleus. The degradation of IκBα is dependent on phosphorylation at its Serine 32 and Serine 36 predominantly by IKKalpha/beta kinases. In addition to IKK complex, other kinases also phosphorylate IκBα on S32 and S36 (35). For the canonical pathway mediated NF-κB activation, phosphorylation of these two amino acid residues, S32 and S36, is an obligatory step. Thus, decreased phosphorylation of these residues on IκBα under our experimental conditions, i.e., high glucose with ischemia, suggests a decreased signaling through the canonical pathway. This finding is consistent with our published results that prolonged exposure of HUVEC to high D-glucose attenuated degradation of IκBα (1).

NF-κB-p65 (p-Thr435)

The inducing or repressing transcription activity of the p65 (RelA) subunit of the NF-κB transcription factor is modulated by phosphorylation. The p65 subunit is phosphorylated at multiple sites. TNF-α, a potent activator of the canonical NF-κB signaling pathway, induces phosphorylation of Thr435 residue of the p65 in the transcription activation domain. This phosphorylation increases occupancy by p65 in a highly promoter-specific manner (36) to increase the expression of proinflammatory chemokine. Thus, a decreased phosphorylation of p65-T435 would effectively decrease the induction of certain genes affected by the canonical NF-κB pathway.

PKCtheta (p-Ser676) and PKCzeta (p-Thr410)

Protein kinase C-theta (PKCθ) and PKCzeta are members of atypical serine/threonine kinase PKC family that plays a role in NF-κB activation in T lymphocytes (31) for adequate immune response. The function of the PKC family members is regulated by phosphorylation at several different residues. PKC are phosphorylated on at least 3 sites after T cell receptor stimulation (60). The p-Ser676 site in PKCθ is in the turn-motif of the enzyme that is autophosphorylated (61). Thus, a decrease in phosphorylation at this site might reflect the decreased enzyme activity. Overexpression of PKCζ specifically increases IKKβ activity without affecting IKKα. The Thr410 residue of PKCζ is located in its activation domain and its phosphorylation is critical for PKCζ activity (62). Since both PKCθ and PKCζ are involved in induction of NF-κB by phosphorylating IKK (32). In addition, PKCζ can directly phosphorylated the RelA subunit of NF-κB transcription factor (34). Taken together, decreased enzyme activity of PKCθ and PKCζ would result in a decline in canonical NF-κB activation.

PKR (p-Thr446 and p-451)

PKR is a double stranded RNA (dsRNA)-activated serine/threonine protein kinase that potentiates the activation of NF-κB by phosphorylating IκB (33). PKR is autophosphorylated at multiple residues including Thr446 that is associated with stabilization of homodimeric form and increased catalytic activity (63). Decreased phosphorylation of Thr446 is consistent with concomitant decrease in canonical NF-κB activity.

SAPK/JNK (p-Thr183)

Stress activated protein kinase/c-Jun-N-terminal kinase 1 (SAPK/JNK) is activated by phosphorylation at positions Thr183 and Tyr185 (64). JNK may participate in inflammatory process by promoting NF-κB action on specific promoters (65).

Thus, we have demonstrated that hyperglycemia and ischemia, either alone or in combination, cause profound changes in the phosphorylation states of the components of the key inflammatory pathway- the NF-κB. Importantly, we have identified BLNK and BTK as novel upstream components of the NF-κB inflammatory pathway in hyperglycemic-ischemic condition. In the future, it will be important to study how BLNK/BTK are activated by diabetes-related hyperglycemia.

Data availability statement

The raw data supporting the conclusions of this article will be made available by the authors, without undue reservation.

Ethics statement

Ethical approval was not required for the studies on humans in accordance with the local legislation and institutional requirements because only commercially available established cell lines were used. Ethical approval was not required for the studies on animals in accordance with the local legislation and institutional

requirements because only commercially available established cell lines were used.

Author contributions

MS: Conceptualization, Data curation, Formal Analysis, Investigation, Methodology, Validation, Visualization, Writing – original draft, Writing – review & editing. TW: Data curation, Visualization, Writing – review & editing. SM: Data curation, Investigation, Writing – original draft. AM: Data curation, Visualization, Writing – review & editing. AD: Conceptualization, Funding acquisition, Investigation, Methodology, Project administration, Resources, Supervision, Writing – review & editing, Writing – original draft.

Funding

The author(s) declare financial support was received for the research, authorship, and/or publication of this article.

This work was supported by the National Heart, Lung, and Blood Institute (R01 HL130399 to AOD).

Conflict of interest

The authors declare that the research was conducted in the absence of any commercial or financial relationships that could be construed as a potential conflict of interest.

Publisher's note

Supplementary material

The Supplementary Material for this article can be found online at: https://www.frontiersin.org/articles/10.3389/fcvm.2024.1345421/full#supplementary-material

References

1. Alleboina S, Wong T, Singh MV, Dokun AO. Feature article: inhibition of protein kinase C beta phosphorylation activates nuclear factor-kappa B and improves postischemic recovery in type 1 diabetes. *Exp Biol Med (Maywood)*. (2020) 245 (9):785–96. doi: 10.1177/1535370220920832

2. Dokun, AO, Duggan NN, Maddux RA, Areiter E, Annex BH. *Glycemic Control and Peripheral Arterial Disease (PAD) in Diabetes: Insulin Treatment Results in Enhanced Perfusion Recovery and Increased Vascular Endothelial Growth Factor (VEGF) Receptor 2 Expression in Experimental PAD*. San Diego Califonia: 71th scientific session of American Diabetes Association (ADA) (2011).

3. Fadini GP, Spinetti G, Santopaolo M, Madeddu P. Impaired regeneration contributes to poor outcomes in diabetic peripheral artery disease. *Arterioscler Thromb Vasc Biol*. (2020) 40(1):34–44. doi: 10.1161/ATVBAHA.119.312863

4. Fitridge R, Pena G, Mills JL. The patient presenting with chronic limb-threatening ischaemia. Does diabetes influence presentation, limb outcomes and survival? *Diabetes Metab Res Rev*. (2020) 36(Suppl. 1):e3242. doi: 10.1002/dmrr.3242

5. Lamin V, Verry J, Eigner-Bybee I, Fuqua JD, Wong T, Lira VA, et al. Modulation of miR-29a and ADAM12 reduces post-ischemic skeletal muscle injury and improves perfusion recovery and skeletal muscle function in a mouse model of type 2 diabetes and peripheral artery disease. *Int J Mol Sci*. (2021) 23 (1):429. doi: 10.3390/ijms23010429

6. Mani AM, Dhanabalan K, Lamin V, Wong T, Singh MV, Dokun AO. BAG3 Attenuates ischemia-induced skeletal muscle necroptosis in diabetic experimental peripheral artery disease. *Int J Mol Sci*. (2022) 23(18):10715. doi: 10.3390/ijms231810715

7. Casale GP, Thompson JR, Carpenter LC, Kim J, Lackner TJ, Mietus CJ, et al. Cytokine signature of inflammation mediated by autoreactive th-cells, in calf muscle of claudicating patients with fontaine stage II peripheral artery disease. *Transl Res*. (2021) 228:94–108. doi: 10.1016/j.trsl.2020.08.008

8. Cauley JA, Kassem AM, Lane NE, Thorson S. Osteoporotic fractures in men study research G. Prevalent peripheral arterial disease and inflammatory burden. *BMC Geriatr*. (2016) 16(1):213. doi: 10.1186/s12877-016-0389-9

9. Gardner AW, Montgomery PS, Zhao YD, Ungvari Z, Csiszar A, Sonntag WE. Endothelial cell inflammation and antioxidant capacity are associated with 6-minute walk performance in patients with symptomatic peripheral artery disease. *Angiology*. (2018) 69(5):416–23. doi: 10.1177/0003319717726934

10. Ozaki Y, Imanishi T, Akasaka T. Inflammatory biomarkers in peripheral artery disease: diagnosis, prognosis, and therapeutic challenges. *Curr Med Chem*. (2015) 22 (23):2744–53. doi: 10.2174/0929867322666150630141200

11. Almowallad S, Alqahtani LS, Mobashir M. NF-κB in signaling patterns and its temporal dynamics encode/decode human diseases. *Life (Basel)*. (2022) 12(12):2012. doi: 10.3390/life12122012

12. Singh S, Singh TG. Role of nuclear factor kappa B (NF-kappaB) signalling in neurodegenerative diseases: an mechanistic approach. *Curr Neuropharmacol*. (2020) 18(10):918–35. doi: 10.2174/1570159X18666200207120949

13. Zinatizadeh MR, Schock B, Chalbatani GM, Zarandi PK, Jalali SA, Miri SR. The nuclear factor kappa B (NF-κB) signaling in cancer development and immune diseases. *Genes Dis*. (2021) 8(3):287–97. doi: 10.1016/j.gendis.2020.06.005

14. Baldwin AS J. The NF-kappa B and I kappa B proteins: new discoveries and insights. *Annu Rev Immunol*. (1996) 14:649–83. doi: 10.1146/annurev.immunol.14.1.649

15. Ghosh S, May MJ, Kopp EB. NF-kappa B and rel proteins: evolutionarily conserved mediators of immune responses. *Annu Rev Immunol*. (1998) 16:225–60. doi: 10.1146/annurev.immunol.16.1.225

16. Tirziu D, Jaba IM, Yu P, Larrivee B, Coon BG, Cristofaro B, et al. Endothelial nuclear factor-kappaB-dependent regulation of arteriogenesis and branching. *Circulation*. (2012) 126(22):2589–600. doi: 10.1161/CIRCULATIONAHA.112.119321

17. Schindelin J, Arganda-Carreras I, Frise E, Kaynig V, Longair M, Pietzsch T, et al. Fiji: an open-source platform for biological-image analysis. *Nat Methods*. (2012) 9 (7):676–82. doi: 10.1038/nmeth.2019

18. Livak K, Schmittgen T. Analysis of relative gene expression data using real-time quantitative PCR and the 2(-Delta Delta C(T)) method. *Methods*. (2001) 25(4):402–8. doi: 10.1006/meth.2001.1262

19. Peravali R, Gunnels L, Alleboina S, Gerling IC, Dokun AO. Type 1 diabetes alters ischemia-induced gene expression. *J Clin Transl Endocrinol*. (2019) 15:19–24. doi: 10.1016/j.jcte.2018.11.003

20. Singh MV, Dokun AO. Diabetes mellitus in peripheral artery disease: beyond a risk factor. *Front Cardiovasc Med*. (2023) 10:1148040. doi: 10.3389/fcvm.2023.1148040

21. Raingeaud J, Gupta S, Rogers JS, Dickens M, Han J, Ulevitch RJ, et al. Pro-inflammatory cytokines and environmental stress cause p38 mitogen-activated protein kinase activation by dual phosphorylation on tyrosine and threonine. *J Biol Chem*. (1995) 270(13):7420–6. doi: 10.1074/jbc.270.13.7420

22. Guo RM, Xu WM, Lin JC, Mo LQ, Hua XX, Chen PX, et al. Activation of the p38 MAPK/NF-kappaB pathway contributes to doxorubicin-induced inflammation

and cytotoxicity in H9c2 cardiac cells. *Mol Med Rep*. (2013) 8(2):603–8. doi: 10.3892/mmr.2013.1554

23. Saha RN, Jana M, Pahan K. MAPK P38 regulates transcriptional activity of NF-kappaB in primary human astrocytes via acetylation of p65. *J Immunol*. (2007) 179 (10):7101–9. doi: 10.4049/jimmunol.179.10.7101

24. Conus NM, Hannan KM, Cristiano BE, Hemmings BA, Pearson RB. Direct identification of tyrosine 474 as a regulatory phosphorylation site for the Akt protein kinase. *J Biol Chem*. (2002) 277(41):38021–8. doi: 10.1074/jbc.M203387200

25. Jia XM, Tang B, Zhu LL, Liu YH, Zhao XQ, Gorjestani S, et al. CARD9 mediates dectin-1-induced ERK activation by linking ras-GRF1 to H-ras for antifungal immunity. *J Exp Med*. (2014) 211(11):2307–21. doi: 10.1084/jem.20132349

26. Zhao XQ, Zhu LL, Chang Q, Jiang C, You Y, Luo T, et al. C-type lectin receptor dectin-3 mediates trehalose 6,6′-dimycolate (TDM)-induced mincle expression through CARD9/Bcl10/MALT1-dependent nuclear factor (NF)-kappaB activation. *J Biol Chem*. (2014) 289(43):30052–62. doi: 10.1074/jbc.M114.588574

27. Choi HW, Shin PG, Lee JH, Choi WS, Kang MJ, Kong WS, et al. Anti-inflammatory effect of lovastatin is mediated via the modulation of NF-kappaB and inhibition of HDAC1 and the PI3K/akt/mTOR pathway in RAW264.7 macrophages. *Int J Mol Med*. (2018) 41(2):1103–9. doi: 10.3892/ijmm.2017.3309

28. Xiao G, Fong A, Sun SC. Induction of p100 processing by NF-kappaB-inducing kinase involves docking IkappaB kinase alpha (IKKalpha) to p100 and IKKalpha-mediated phosphorylation. *J Biol Chem*. (2004) 279(29):30099–105. doi: 10.1074/jbc.M401428200

29. Chiu CW, Dalton M, Ishiai M, Kurosaki T, Chan AC. BLNK: molecular scaffolding through "cis"-mediated organization of signaling proteins. *EMBO J*. (2002) 21(23):6461–72. doi: 10.1093/emboj/cdf658

30. Wu ZH, Shi Y, Tibbetts RS, Miyamoto S. Molecular linkage between the kinase ATM and NF-kappaB signaling in response to genotoxic stimuli. *Science*. (2006) 311 (5764):1141–6. doi: 10.1126/science.1121513

31. Lin X, O'Mahony A, Mu Y, Geleziunas R, Greene WC. Protein kinase C-theta participates in NF-kappaB activation induced by CD3-CD28 costimulation through selective activation of IkappaB kinase beta. *Mol Cell Biol*. (2000) 20(8):2933–40. doi: 10.1128/MCB.20.8.2933-2940.2000

32. Lallena MJ, Diaz-Meco MT, Bren G, Paya CV, Moscat J. Activation of IkappaB kinase beta by protein kinase C isoforms. *Mol Cell Biol*. (1999) 19(3):2180–8. doi: 10.1128/MCB.19.3.2180

33. Kumar A, Haque J, Lacoste J, Hiscott J, Williams BR. Double-stranded RNA-dependent protein kinase activates transcription factor NF-kappa B by phosphorylating I kappa B. *Proc Natl Acad Sci U S A*. (1994) 91(14):6288–92. doi: 10.1073/pnas.91.14.6288

34. Anrather J, Csizmadia V, Soares MP, Winkler H. Regulation of NF-kappaB RelA phosphorylation and transcriptional activity by p21(ras) and protein kinase czeta in primary endothelial cells. *J Biol Chem*. (1999) 274(19):13594–603. doi: 10.1074/jbc.274.19.13594

35. Taylor JA, Bren GD, Pennington KN, Trushin SA, Asin S, Paya CV. Serine 32 and serine 36 of IkappaBalpha are directly phosphorylated by protein kinase CKII in vitro. *J Mol Biol*. (1999) 290(4):839–50. doi: 10.1006/jmbi.1999.2912

36. O'Shea JM, Perkins ND. Thr435 phosphorylation regulates RelA (p65) NF-kappaB subunit transactivation. *Biochem J*. (2010) 426(3):345–54. doi: 10.1042/BJ2009163

37. O'Dea E, Hoffman A. The regulatory logic of the NF-κB signaling system. In: Karin M, Staud LM, editors. *NF-κB: A Network Hub Controlling Immunity, Inflammation, and Cancer*. Cold Spring Harbor, New York: Cold Spring Harbor Laboratory Press (2010). p. 127–38.

38. Mi H, Thomas P. PANTHER pathway: an ontology-based pathway database coupled with data analysis tools. *Methods Mol Biol*. (2009) 563:123–40. doi: 10.1007/978-1-60761-175-2_7

39. Pathmanathan S, Yao Z, Coelho P, Valla R, Drecun L, Benz C, et al. B cell linker protein (BLNK) is a regulator of met receptor signaling and trafficking in non-small cell lung cancer. *iScience*. (2022) 25(11):105419. doi: 10.1016/j.isci.2022.105419

40. Shinohara M, Koga T, Okamoto K, Sakaguchi S, Arai K, Yasuda H, et al. Tyrosine kinases Btk and Tec regulate osteoclast differentiation by linking RANK and ITAM signals. *Cell*. (2008) 132(5):794–806. doi: 10.1016/j.cell.2007.12.037

41. Kurosaki T. Functional dissection of BCR signaling pathways. *Curr Opin Immunol*. (2000) 12(3):276–81. doi: 10.1016/S0952-7915(00)00087-X

42. Khan WN. Regulation of B lymphocyte development and activation by bruton's tyrosine kinase. *Immunol Res*. (2001) 23(2-3):147–56. doi: 10.1385/IR:23:2-3:147

43. Ishiai M, Kurosaki M, Pappu R, Okawa K, Ronko I, Fu C, et al. BLNK required for coupling Syk to PLC gamma 2 and Rac1-JNK in B cells. *Immunity*. (1999) 10 (1):117–25. doi: 10.1016/S1074-7613(00)80012-6

44. Lagresle-Peyrou C, Millili M, Luce S, Boned A, Sadek H, Rouiller J, et al. The BLNK adaptor protein has a nonredundant role in human B-cell differentiation. *J Allergy Clin Immunol*. (2014) 134(1):145–54. doi: 10.1016/j.jaci.2013.12.1083

45. Wu JN, Koretzky GA. The SLP-76 family of adapter proteins. *Semin Immunol*. (2004) 16(6):379–93. doi: 10.1016/j.smim.2004.08.018

46. Tan JE, Wong SC, Gan SK, Xu S, Lam KP. The adaptor protein BLNK is required for B cell antigen receptor-induced activation of nuclear factor-kappa B and cell cycle entry and survival of B lymphocytes. *J Biol Chem*. (2001) 276 (23):20055–63. doi: 10.1074/jbc.M010800200

47. Taguchi T, Kiyokawa N, Takenouch H, Matsui J, Tang WR, Nakajima H, et al. Deficiency of BLNK hampers PLC-gamma2 phosphorylation and Ca2+influx induced by the pre-B-cell receptor in human pre-B cells. *Immunology*. (2004) 112(4):575–82. doi: 10.1111/j.1365-2567.2004.01918.x

48. Gustin JA, Korgaonkar CK, Pincheira R, Li Q, Donner DB. Akt regulates basal and induced processing of NF-kappaB2 (p100) to p52. *J Biol Chem*. (2006) 281 (24):16473–81. doi: 10.1074/jbc.M507373200

49. Giglione C, Gonfloni S, Parmeggiani A. Differential actions of p60c-Src and Lck kinases on the Ras regulators p120-GAP and GDP/GTP exchange factor CDC25Mm. *Eur J Biochem*. (2001) 268(11):3275–83. doi: 10.1046/j.1432-1327.2001.02230.x

50. Pflum MK, Tong JK, Lane WS, Schreiber SL. Histone deacetylase 1 phosphorylation promotes enzymatic activity and complex formation. *J Biol Chem*. (2001) 276(50):47733–41. doi: 10.1074/jbc.M105590200

51. Tarassishin L, Horwitz MS. Sites on FIP-3 (NEMO/IKKgamma) essential for its phosphorylation and NF-kappaB modulating activity. *Biochem Biophys Res Commun*. (2001) 285(2):555–60. doi: 10.1006/bbrc.2001.5197

52. Beinke S, Ley SC. Functions of NF-kappaB1 and NF-kappaB2 in immune cell biology. *Biochem J*. (2004) 382(Pt 2):393–409. doi: 10.1042/BJ20040544

53. Lee JC, Laydon JT, McDonnell PC, Gallagher TF, Kumar S, Green D, et al. A protein kinase involved in the regulation of inflammatory cytokine biosynthesis. *Nature*. (1994) 372(6508):739–46. doi: 10.1038/372739a0

54. Bhat NR, Feinstein DL, Shen Q, Bhat AN. P38 MAPK-mediated transcriptional activation of inducible nitric-oxide synthase in glial cells. Roles of nuclear factors, nuclear factor kappa B, cAMP response element-binding protein, CCAAT/enhancer-binding protein-beta, and activating transcription factor-2. *J Biol Chem*. (2002) 277(33):29584–92. doi: 10.1074/jbc.M204994200

55. Carter AB, Knudtson KL, Monick MM, Hunninghake GW. The p38 mitogen-activated protein kinase is required for NF-kappaB-dependent gene expression. The role of TATA-binding protein (TBP). *J Biol Chem*. (1999) 274(43):30858–63. doi: 10.1074/jbc.274.43.30858

56. Betapudi V, Shukla M, Alluri R, Merkulov S, McCrae KR. Novel role for p56/Lck in regulation of endothelial cell survival and angiogenesis. *FASEB J*. (2016) 30 (10):3515–26. doi: 10.1096/fj.201500040

57. Sicheri F, Kuriyan J. Structures of Src-family tyrosine kinases. *Curr Opin Struct Biol*. (1997) 7(6):777–85. doi: 10.1016/S0959-440X(97)80146-7

58. Marth JD, Cooper JA, King CS, Ziegler SF, Tinker DA, Overell RW, et al. Neoplastic transformation induced by an activated lymphocyte-specific protein tyrosine kinase (pp56lck). *Mol Cell Biol*. (1988) 8(2):540–50. doi: 10.1128/mcb.8.2.540-550.1988

59. Palacios EH, Weiss A. Function of the Src-family kinases, Lck and Fyn, in T-cell development and activation. *Oncogene*. (2004) 23(48):7990–8000. doi: 10.1038/sj.onc.1208074

60. Freeley M, Kelleher D, Long A. Regulation of protein kinase C function by phosphorylation on conserved and non-conserved sites. *Cell Signal*. (2011) 23 (5):753–62. doi: 10.1016/j.cellsig.2010.10.013

61. Liu Y, Graham C, Li A, Fisher RJ, Shaw S. Phosphorylation of the protein kinase C-theta activation loop and hydrophobic motif regulates its kinase activity, but only activation loop phosphorylation is critical to in vivo nuclear-factor-kappaB induction. *Biochem J*. (2002) 361(Pt 2):255–65. doi: 10.1042/bj3610255

62. Le Good JA, Brindley DN. Molecular mechanisms regulating protein kinase Czeta turnover and cellular transformation. *Biochem J*. (2004) 378(Pt 1):83–92. doi: 10.1042/bj20031194

63. Gal-Ben-Ari S, Barrera I, Ehrlich M, Rosenblum K. PKR: a kinase to remember. *Front Mol Neurosci*. (2018) 11:480. doi: 10.3389/fnmol.2018.00480

64. Bardeleben R, Kaina B, Fritz G. Ultraviolet light-induced apoptotic death is impaired by the HMG-CoA reductase inhibitor lovastatin. *Biochem Biophys Res Commun*. (2003) 307(2):401–7. doi: 10.1016/S0006-291X(03)01205-1

65. Ip YT, Davis RJ. Signal transduction by the c-Jun N-terminal kinase (JNK)–from inflammation to development. *Curr Opin Cell Biol*. (1998) 10(2):205–19. doi: 10.1016/S0955-0674(98)80143-9

frontiers | Frontiers in Cardiovascular Medicine

TYPE Original Research
PUBLISHED 17 July 2024
DOI 10.3389/fcvm.2024.1435246

OPEN ACCESS

EDITED BY
Catherine A. Reardon,
The University of Chicago, United States

REVIEWED BY
Hongya Han,
Capital Medical University, China
Meng Jia,
University of Pennsylvania, United States

*CORRESPONDENCE
Yue Deng
dyue7138@sina.com
Liping Chang
ZSFL_TCM@163.com

RECEIVED 20 May 2024
ACCEPTED 04 July 2024
PUBLISHED 17 July 2024

CITATION
Dong H, Liu Z, Chen H, Ba J, Shi R, Jin Q, Shao X, Tian T, Yin J, Chang L and Deng Y (2024) Association between glycemia and multi-vessel lesion in participants undergoing coronary angiography: a cross-sectional study. Front. Cardiovasc. Med. 11:1435246. doi: 10.3389/fcvm.2024.1435246

Association between glycemia and multi-vessel lesion in participants undergoing coronary angiography: a cross-sectional study

Hezeng Dong[1], Zhaozheng Liu[2], Hao Chen[2], Jin Ba[1], Rui Shi[2], Qu Jin[2], Xiao Shao[2], Tenghui Tian[2], Jinzhu Yin[2], Liping Chang[2]* and Yue Deng[2]*

[1]College of Traditional Chinese Medicine, Changchun University of Traditional Chinese Medicine, Changchun, Jilin, China, [2]Cardiology Center, Affiliated Hospital of Changchun University of Traditional Chinese Medicine, Changchun, Jilin, China

Background: This study aims to elucidate the association between glycemia and the occurrence of multi-vessel lesions in participants undergoing coronary angiography.
Methods: We analyzed 2,533 patients with coronary artery disease who underwent coronary angiography. Of these, 1,973 patients, identified by the endpoint of multi-vessel lesions, were examined using univariate and multivariate logistic regression analyses to determine the relationship between glycemia levels and multi-vessel lesion occurrence.
Results: The analysis included 1,973 participants, among whom 474 patients were identified with coronary multi-vessel lesions. Univariate logistic regression analysis demonstrated a positive correlation between glycemia and the occurrence of coronary multi-vessel lesions (OR 1.04; 95% CI 1.01–1.08; $p = 0.02$). The adjusted model indicated that for each unit increase in glycemia, the risk of developing coronary multi-vessel lesions increased by 4%, showing a significant correlation ($p < 0.05$). Subgroup analyses revealed that the impact of glycemia on multi-vessel lesions in patients with PCI varied according to gender, age, and smoking status, with the effect being more pronounced in men, older patients, and smokers.
Conclusion: Our findings establish a significant association between glycemia and the incidence of multi-vessel lesions, particularly pronounced in male patients, individuals over 45, and smokers.

KEYWORDS

glycemia, multi-vessel lesion, coronary angiography, diabetes, Asian

Background

Advances in intravascular imaging and functional techniques, as well as coronary interventions (1), have led to a gradual increase in the detection rate of multi-vessel lesions in today's clinics. The European Society of Cardiology (ESC) has reported that more than 50% of patients with ST-segment elevation myocardial infarction (STEMI) have concomitant multibranch vasculopathy (2). Multi-vessel lesions often predict more serious adverse cardiovascular events (3). The risk of recurrent cardiovascular events is high even after interventional or pharmacological treatment (4). However, there are

relatively few clinical studies on multi-vessel lesions, and there is a lack of effective predictive indicators for multi-vessel lesions (5), except for performing coronary angiography or intravascular ultrasound. We believe that it is crucial to identify and address the key factors in clinical practice. Timely intervention at an early stage is essential to prevent multi-vessel lesions and reduce the occurrence of acute coronary syndromes, lowering the risk of cardiovascular death. Individualized prevention and treatment protocols must be developed.

It is well established that diabetes mellitus and its complications represent a significant risk factor for coronary artery disease (6). Djupsjo, Kuhl, et al. demonstrated that patients with hyperglycemia exhibited a twofold increased risk of long-term cardiovascular death and a rate of cardiovascular events that were more than one times higher than that observed in patients with pre-diabetes (7). Jie Yang et al.'s study also found that glycosylated hemoglobin (HbA1c) and fasting blood glucose (FBG) are better at assessing the severity of coronary heart disease (CHD) in patients undergoing elective percutaneous coronary intervention (PCI) (8). Furthermore, Tütün U et al. demonstrated that uncontrolled glycemia levels not only increase perioperative complications but also the incidence of distal and middle coronary artery lesions. It is imperative to diagnose and aggressively control hyperglycemia before performing CABG (9). These studies confirm that glycemia aggravates the process of coronary atherosclerosis. However, direct clinical evidence of glycemia and multi-vessel lesions, a serious lesion in cardiovascular disease, is currently lacking, especially in Asia. This study is vital given the unique lifestyle and genetic characteristics of Asian populations. Our study will fill this gap by exploring the association between glycemia and multivessel disease in patients undergoing coronary angiography. The aim is to provide clinicians with more precise treatment options and to provide a scientific basis for cardiovascular risk management in diabetic patients.

Method

The participants in our study were all derived from patients who underwent coronary angiography between July 2009 and August 2011 at the First Affiliated Hospital of Zhengzhou University. Based on strict inclusion criteria, 1973 patients were included in this analysis after excluding incomplete and unclear data (Figure 1).

The primary endpoint of this study was a multi-vessel lesion, defined as the presence of ≥50% stenosis in at least two of the three major epicardial vessels. All participants underwent coronary angiography and quantitative analyses to characterize lesions according to standard methods. Furthermore, we collected comprehensive demographic and clinical data, which we then analyzed. All data was derived from a database containing demographic, clinical, angiographic, and procedural information. We also obtained data through patient visits, telephone interviews, and chart reviews, or by conducting clinical follow-ups. We then entered the data independently, and an independent committee adjudicated clinical events. The definitions of diabetes mellitus and hypertension as important risk factors for cardiovascular disease were based solely on clinical guidelines. Patients were defined as diabetic if they had a fasting blood glucose concentration of more than 6.1 mmol/L, a glycated hemoglobin level of more than 6.5%, or were receiving insulin or oral hypoglycaemic agents. Hypertension was defined as a systolic blood pressure of 140 mmHg or more and a diastolic blood pressure of 90 mmHg or more, or the current use of antihypertensive medications. A history of smoking was considered to be the presence of smoking within the previous ten years. Glycemia values were obtained from fasting blood samples at the time of admission, along with other laboratory tests including (Cr, UA, BIL, TC, TG, HDL-C, and LDL-C). All laboratory tests were collected and analyzed in compliance with the criteria (10).

The data that support the findings of this study are from Long-term follow-up results in patients undergoing percutaneous coronary intervention (PCI) with drug-eluting stents: results from a single high-volume PCI center [Dataset]. Dryad. https://doi.org/10.5061/dryad.13d31.

Statistical analysis

In our study, we averaged participants' glycemia levels into four quartiles: quartile 1 ($n = 482$), quartile 2 ($n = 500$), quartile 3 ($n = 496$) and quartile 4 ($n = 495$). We expressed categorical variables as numbers (n) and percentages (%) and assessed them using the chi-square test. Continuous variables are expressed as the mean ± standard deviation of normally distributed data. In addition, multiple imputation with multivariate imputation by chained equation was used for handling the missing values. We used univariate and multivariate regression analyses to examine the association between glycemia and multi-vessel lesions. In univariate analyses, we selected variables with a p-value <0.05, including age, gender, smoking, hypertension, DBP, HR, UA, and TG. We then adjusted for a variety of influences in multivariate analyses to validate the robustness of the results. Subgroup analyses were conducted using logistic models to determine the relationship between glycemia and multi-vessel lesions among subgroups, including gender, age, smoking status, and presence of diabetes. All analyses were performed using Free Statistics Approximation software version 1.9. A two-sided P-value of less than 0.05 was considered statistically significant.

Result

Study population and baseline characteristics

Our study involved 2,533 patients with coronary artery disease who underwent coronary angiography. After rigorous data screening, 1,973 participants were included in the final analysis. The cohort included 1,341 men and 632 women. The mean age

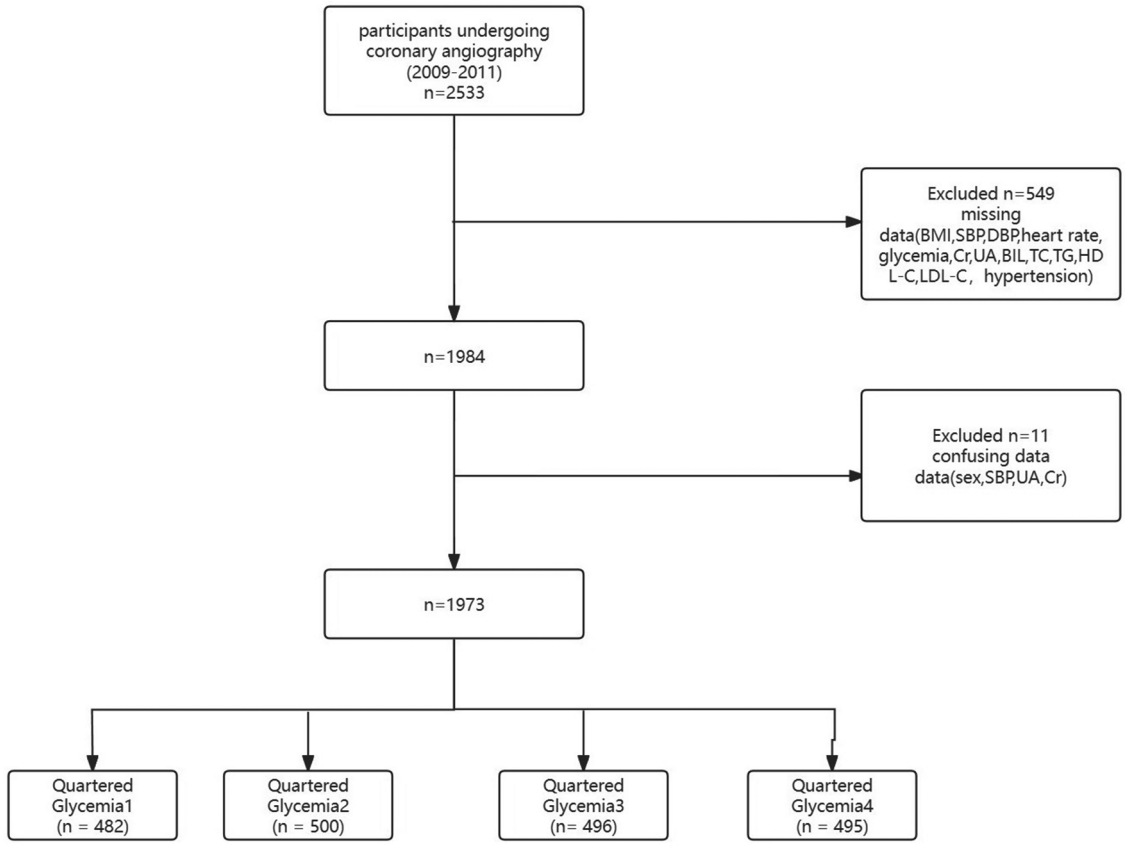

FIGURE 1
Flowchart of participant selection.

was 59 years, and 474 participants were defined as having multi-vessel lesions. Glycemia was categorized into four quartiles, and a description of baseline characteristics revealed significant associations between glycemia and several key factors, including gender, age, BMI,hypertension, diabetes mellitus, and prevalence of multi-vessel lesions (Table 1).

Univariate and multifactorial analysis

In univariate analysis, age, hypertension, diabetes mellitus, glycemia level, uric acid level, and triglycerides were significantly associated with coronary multi-vessel lesion (Table 2).

To further elucidate the relationship between participants' glycemia and multi-vessel lesions, we performed a multifactorial logistic analysis. In the unadjusted model, there was a significant correlation between glycemia and coronary multivessel disease, with a 4% increase in the risk of multi-vessel lesions for each unit increase in glycemia (OR: 1.04, $P = 0.02$). This relationship remained significant after adjusting for sex, age, smoking, hypertension, diastolic blood pressure, heart rate, uric acid, and triglycerides. (Adj. OR: 1.04, $P = 0.039$) (Table 3).

These results are clear: glycemia is an important risk factor for the development of coronary multi-vessel lesion. After adjusting for various covariates, we observed a linear relationship between glycemia and multi-vessel lesions, with the risk of developing multi-vessel lesions progressively increasing with increasing glycemia levels (Figure 2).

Subgroup analysis

To clarify the relationship between glycemia and multi-vessel lesion in different age, gender and smoking status, we conducted further subgroup analyses. These showed that glycemia and multi-vessel lesion had a more significant association in males ($p = 0.031$) compared to females. The analyses showed a significant association between glycemia and multi-vessel lesion in those aged ≥ 45 years ($p = 0.008$). Furthermore, smokers showed a stronger correlation ($p = 0.038$) compared to non-smokers ($p = 0.085$). Due to the lack of information on medications taken by patients prior to admission, diabetic patients who were regularly taking hypoglycaemic medications prior to admission would have resulted in relatively low fasting glycemia values on admission, which would have had an impact on our findings. Consequently, we grouped the patients by previous diabetes or not, and found that compared to diabetic patients, blood glucose and multi-vessel lesion were yet more

TABLE 1 Baseline characteristics of the study participants.

	All participants (n = 1,973)	Quartile glycemia1 (n = 482)	Quartile glycemia2 (n = 500)	Quartile glycemia3 (n = 496)	Quartile glycemia4 (n = 495)	p	Statistic
Sex, n (%)						**0.004**	13.241
Female	632 (32.0)	135 (28)	144 (28.8)	168 (33.9)	185 (37.4)		
Male	1,341 (68.0)	347 (72)	356 (71.2)	328 (66.1)	310 (62.6)		
Age (years)	59.9 ± 11.1	58.7 ± 12.1	59.7 ± 11.0	60.6 ± 10.9	60.8 ± 10.2	**0.013**	3.592
Mean ± SD							
Hypertension n (%)						**0.001**	16.082
No	975 (49.4)	264 (54.8)	261 (52.2)	238 (48)	212 (42.8)		
Yes	998 (50.6)	218 (45.2)	239 (47.8)	258 (52)	283 (57.2)		
DM, n (%)						**<0.001**	492.204
No	1,553 (78.7)	448 (92.9)	466 (93.2)	422 (85.1)	217 (43.8)		
Yes	420 (21.3)	34 (7.1)	34 (6.8)	74 (14.9)	278 (56.2)		
Heart.failure, n (%)						0.723	1.324
No	1,744 (88.4)	427 (88.6)	445 (89)	442 (89.1)	430 (87)		
Yes	228 (11.6)	55 (11.4)	55 (11)	54 (10.9)	64 (13)		
Angina, n (%)						0.313	3.561
No	1,745 (88.4)	415 (86.1)	444 (88.8)	444 (89.5)	442 (89.3)		
Yes	228 (11.6)	67 (13.9)	56 (11.2)	52 (10.5)	53 (10.7)		
AMI, n (%)						0.307	3.604
No	1,880 (95.3)	465 (96.5)	476 (95.2)	474 (95.6)	465 (93.9)		
Yes	93 (4.7)	17 (3.5)	24 (4.8)	22 (4.4)	30 (6.1)		
Smoking, n (%)						0.06	7.398
No	1,322 (67.0)	312 (64.7)	319 (63.8)	340 (68.5)	351 (70.9)		
Yes	651 (33.0)	170 (35.3)	181 (36.2)	156 (31.5)	144 (29.1)		
SBP (mmHg)	104.5 ± 28.5	108.8 ± 28.1	102.5 ± 28.2	106.6 ± 29.0	100.1 ± 28.0	**<0.001**	9.372
Mean ± SD							
DBP (mmHg)	77.3 ± 11.9	78.0 ± 11.6	76.0 ± 11.6	77.4 ± 12.1	78.0 ± 12.2	**0.031**	2.964
Mean ± SD							
EF, Mean ± SD	61.0 ± 7.8	61.8 ± 7.4	60.8 ± 8.1	61.0 ± 7.3	60.4 ± 8.2	**0.024**	3.166
BMI (kg/m^2), Mean ± SD	24.1 ± 3.6	24.0 ± 3.3	23.8 ± 3.6	24.4 ± 3.6	24.3 ± 3.8	**0.027**	3.068
Heart.rate,	72.1 ± 11.5	69.8 ± 10.8	71.1 ± 10.1	73.0 ± 11.6	74.4 ± 12.9	**<0.001**	15.778
Mean ± SD							
Cr (μmol/L)	72.0 ± 30.2	73.3 ± 25.5	72.3 ± 20.5	73.0 ± 40.1	69.2 ± 31.1	0.133	1.867
Mean ± SD							
UA (μmol/L)	304.2 ± 92.5	306.4 ± 87.0	308.0 ± 84.3	310.4 ± 100.5	291.9 ± 96.3	**0.007**	4.034
Mean ± SD							
BIL (mg/dl)	9.8 ± 7.6	9.4 ± 4.6	9.5 ± 5.2	10.4 ± 12.3	10.0 ± 5.7	0.160	1.723
Mean ± SD							
TC (Mmol/L)	4.3 ± 1.1	4.1 ± 1.0	4.2 ± 1.0	4.3 ± 1.1	4.4 ± 1.1	**<0.001**	9.736
Mean ± SD							
TG (Mmol/L)	1.9 ± 1.4	1.6 ± 0.8	1.8 ± 1.2	2.1 ± 1.9	2.2 ± 1.4	**<0.001**	14.313
Mean ± SD							
HDL,C (Mmol/L)	1.1 ± 0.3	1.1 ± 0.3	1.1 ± 0.3	1.1 ± 0.3	1.0 ± 0.3	0.215	1.493
Mean ± SD							
LDL.C (Mmol/L)	2.7 ± 0.9	2.5 ± 0.9	2.7 ± 0.9	2.7 ± 0.9	2.8 ± 1.0	**<0.001**	6.921
Mean ± SD							
Multi-vessel lesion n (%)						**0.003**	13.998
No	1,499 (76.0)	392 (81.3)	379 (75.8)	376 (75.8)	352 (71.1)		
Yes	474 (24.0)	90 (18.7)	121 (24.2)	120 (24.2)	143 (28.9)		

Data are shown as mean ± standard deviation (SD) or median (IQR) for continuous variables and proportions (%) for categorical variables. Sex, Age, Hypertension, DM, Heart failure, Angina, Acute myocardial infarction, Smoking, SBP, DBP, EF,BMI,Heart rate, Cr, UA, BIL, TC, HDL, C, LDL.C, Multi-vessel lesion P-values in bold are <0.05.

significantly associated among non-diabetic patients. This shows that even non-diabetics should be aware of glycemia changes. The association between glycemia and multi-vessel lesion was stronger in non-diabetics among the participants who underwent coronary angiography. Therefore, close monitoring of glycemia is essential to prevent adverse cardiovascular events, regardless of previous diagnosis of diabetes mellitus. In conclusion, the findings demonstrate the complexity of

TABLE 2 Univariate analysis for overall population.

Variable	OR_95CI	*P*_value
Sex = female, *n* (%)	0.94 (0.75~1.17)	0.56
Age (years)	1.03 (1.02~1.04)	**<0.001**
Hypertension, *n* (%)	1.31 (1.06~1.61)	**0.011**
DM, *n* (%)	1.85 (1.46~2.34)	**<0.001**
Smoking, *n* (%)	0.97 (0.78~1.21)	0.788
SBP (mmHg)	1 (1~1.01)	0.317
DBP (mmHg)	1.01 (1~1.02)	**0.012**
Heart.rate (Bpm)	1.01 (1~1.02)	0.13
Glycemia (Mmol/L)	1.04 (1.01~1.08)	**0.02**
Cr (μmol/L)	1 (1~1)	0.358
UA (μmol/L)	1 (1~1)	**0.023**
BIL (mg/dl)	1.01 (0.99~1.02)	0.394
TC (Mmol/L)	1.02 (0.93~1.12)	0.693
TG (Mmol/L)	1.09 (1.01~1.17)	**0.018**
HDL.C (Mmol/L)	1.06 (0.76~1.46)	0.746
LDL.C (Mmol/L)	1.02 (0.91~1.14)	0.713

OR, odds ratio; CI, confidence interval; SD, standard deviation. Abbreviations as in Table 1. *P* values in bold are <0.05.

TABLE 3 Multivariate analysis for overall population.

Variable	Model 1	Model 2	Model 3	Model 4
n total	1,973	1,973	1,973	1,973
n event_%	474 (24)	474 (24)	474 (24)	474 (24)
crude OR (95%CI)	1.04 (1.01~1.08)	1.04 (1.01~1.08)	1.04 (1.01~1.08)	1.04 (1.01~1.08)
crude *P*_value	**0.02**	0.02	0.02	0.02
adj. OR (95%CI)		1.04 (1~1.07)	1.04 (1~1.07)	1.04 (1~1.07)
adj. *P*_value		**0.024**	**0.025**	**0.039**

Model 1: no adjusted.
Model 2: Adj: Model 1 + Sex + age.
Model 3: Adj: Model 2 + smoking + hypertension.
Model 4: Adj: Model 3 + DBP + HR + UA + TG.
P values in bold are <0.05.

cardiovascular risk factors and their differential impact in different patient subgroups. This stratified analysis will help to develop a more personalised management strategy for patients (Figure 3 and Table 4).

Epidemiology and significance of multivessel lesions

The incidence of multi-vessel lesions is increasing in clinical practice and is a matter of considerable concern in current clinical cardiovascular disease research. There is a clear association between multi-vessel lesions and a wide range of adverse cardiovascular outcomes (11). Dziewierz, Siudak et al. reported that multi-vessel lesions were present in approximately 40%–65% of patients with ST-segment elevation myocardial infarction (STEMI) or complete coronary occlusion, as well as other coronary artery disease (12). A prospective randomised, multicentre, open-label and controlled clinical trial enrolled 396 patients and found that 52% had multivessel disease (13). Furthermore, Tindale A et al. demonstrated that patients with multi-vessel lesion treated with CR who developed STEMI with cardiogenic shock (defined as lactic acid ≥2 mmol/L) had a higher mortality rate (14). This finding is in line with Sorajja, Bernard J. et al., who observed that three-vessel disease significantly predicted cardiovascular mortality and risk of reinfarction (15). These findings demonstrate that multi-vessel lesion is a serious and widespread cardiovascular disease process, that the number of patients who develop multi-vessel lesions is enormous, and that understanding and managing multi-vessel lesions to avoid adverse cardiovascular events is of the utmost importance.

Glycaemia is clearly associated with several cardiovascular diseases (16). Our study definitively confirms the link between elevated glycaemia and cardiovascular disease. This observation is in line with the findings of Xiang Wang et al. who concluded that the TyG index can be a valuable predictor of CAD severity, especially for patients with prediabetes (17). Furthermore, a study by Iijima R, et al. demonstrated that Patients with diabetes often accelerate atherosclerotic thrombosis, resulting in early, widespread, and rapidly progressing coronary artery disease (18). Tong Zhao et al. concluded that hyperglycaemia was an independent predictor of severe coronary artery disease in non-diabetic patients (19). Our study definitively confirms that the association of glycemia with multi-vessel lesions is more significant in non-diabetic patients. Clinicians must be aware of this and provide appropriate early intervention to prevent adverse cardiovascular events.

Unique considerations for Asian populations

It is crucial to note that our study differs from previous studies in two key ways. Firstly, we have a larger sample size. Secondly, we only include Asian populations. This is because Asia is an important region for the development of cardiovascular disease and diabetes worldwide. This may be due to unique lifestyle and genetic influences, among other factors. Expert discussions at the WHO have made it clear that, at a BMI below the existing WHO overweight threshold (≥25 kg/m^2), Asians are at a much higher risk of developing type 2 diabetes and cardiovascular disease (20). It is therefore of great importance to conduct a study of diabetes and cardiovascular disease in Asia. By identifying the link between glycemia and multivessel disease, physicians will be able to more accurately assess a patient's risk of developing multivessel disease.

Limitations and outlook

Our study is comprehensive, but it has limitations. Our study was a cross-sectional investigation, so even after rigorous

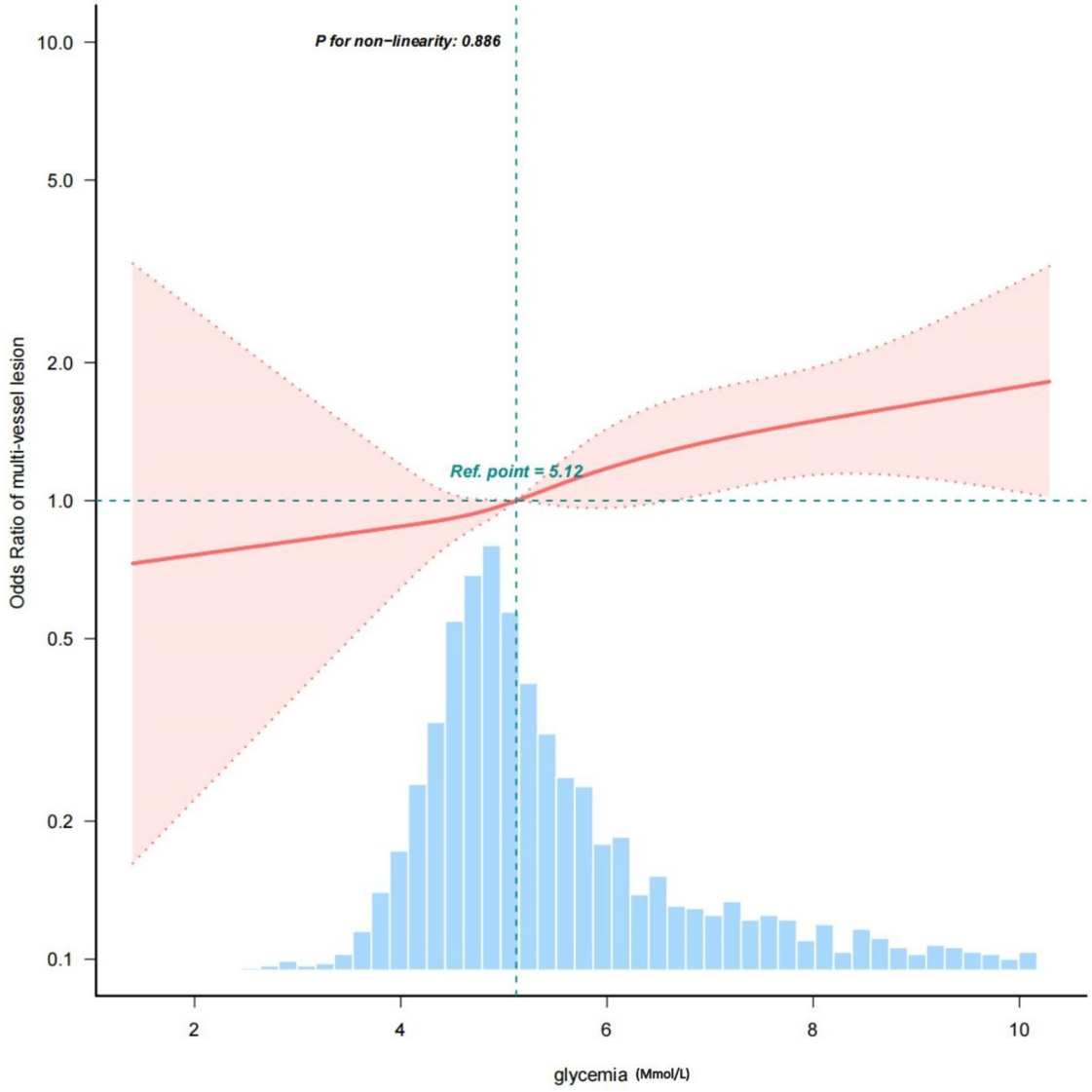

FIGURE 2
A linear relationship between glycemia and multi-vessel mesion.

data screening, potential confounders could not be completely eliminated. This may limit the generalisability of the findings, but we included a relatively large number of participants, and the results are still instructive for future studies to provide a basis for a deeper understanding of the relationship between diabetes mellitus and cardiovascular disease. Longitudinal studies are needed to understand the long-term effects of glycemia on cardiovascular occurrence and prognosis in patients with multivessel disease. It is also crucial to include participants from more regions and ethnicities to raise awareness of glycaemic control in all regions. Clinicians must be vigilant about the glycaemic status of their patients, as this is a key factor in the assessment and management of cardiovascular risk.

Conclusion

Our study definitively demonstrated a linear relationship between glycemia and multivessel disease in patients undergoing coronary angiography. Even after adjusting for study-related confounders, the results remained significant. This indicates that the risk of multi-vessel lesion increases progressively with increasing glycemia levels. Our study provides unquestionable evidence that glycemia control is crucial for the prevention and treatment of multi-vessel lesions. It also offers invaluable insights for improving risk assessment and management of cardiovascular disease. These findings have significant implications for public health policy development and optimisation of clinical care, particularly in areas with a high prevalence of diabetes and cardiovascular disease.

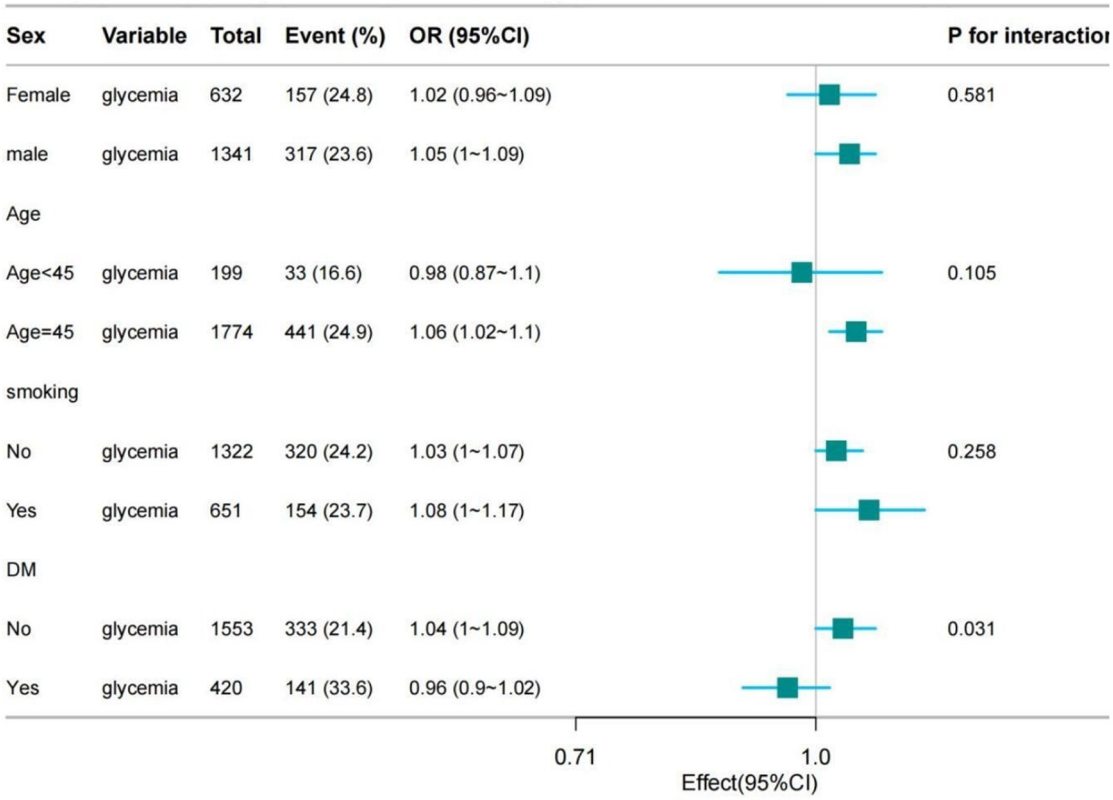

FIGURE 3
Strtification analysis on the association between glycemia and multi-vessel lesion.

TABLE 4 Subgroup analysis for association between glycemia and multi-vessel lesion.

Subgroup	*n* total	*n* event_%	crude OR_95CI	crude *P*_value	P for interaction_1	P for interaction_2
Sex						
Female	632.0	157 (24.8)	1.02 (0.96~1.09)	0.477	0.581	0.585
Male	1,341.0	317 (23.6)	1.05 (1~1.09)	0.031		
Age (years)						
Age < 45	199.0	33 (16.6)	0.98 (0.87~1.1)	0.688	0.105	0.208
Age ≥ 45	1,774.0	441 (24.9)	1.06 (1.02~1.1)	0.008		
Smoking						
No	1,322.0	320 (24.2)	1.03 (1~1.07)	0.085	0.258	0.253
Yes	651.0	154 (23.7)	1.08 (1~1.17)	0.038		
DM						
No	1,553.0	333 (21.4)	1.04 (1~1.09)	0.074	0.031	0.038
Yes	420.0	141 (33.6)	0.96 (0.9~1.02)	0.191		

OR, odds ratio; CI, confidence interval; SD, standard deviation; Other abbreviations as in Table 1.

Data availability statement

The datasets presented in this study can be found in online repositories. The names of the repository/repositories and accession number(s) can be found below: https://doi.org/10.5061/dryad.13d31.

Ethics statement

The studies involving humans were approved by the ethics committee of The First Affiliated Hospital of Zhengzhou University. The studies were conducted in accordance with the local legislation and institutional requirements. The participants provided their written informed consent to participate in this study. Written informed consent was obtained from the individual(s) for the publication of any potentially identifiable images or data included in this article.

Author contributions

HD: Conceptualization, Writing – original draft. ZL: Data curation, Writing – original draft. HC: Formal Analysis, Writing –

original draft. JB: Data curation, Writing – review & editing. RS: Formal Analysis, Writing – review & editing. QJ: Data curation, Writing – review & editing. XS: Writing – review & editing. TT: Writing – review & editing. JY: Supervision, Writing – review & editing. LC: Data curation, Writing – review & editing. YD: Conceptualization, Funding acquisition, Supervision, Writing – review & editing.

Funding

The author(s) declare financial support was received for the research, authorship, and/or publication of this article.

This work was supported by the National Natural Science Foundation of China, (82174350).

Acknowledgments

We gratefully thank Haimu Yao (Department of Cardiology, The First Affiliated Hospital of Zhengzhou University) for providing the datasets. We are also grateful to Dr. Jie Liu (Department of Vascular and Endovascular Surgery, Chinese PLA General Hospital) and Dr. Wentao Ni (Department of Respiration, Peking University People's Hospital) for their contribution to the statistical support, and study design consultations.

Conflict of interest

The authors declare that the research was conducted in the absence of any commercial or financial relationships that could be construed as a potential conflict of interest.

Publisher's note

References

1. Serruys PW, Ono M, Garg S, Hara H, Kawashima H, Pompilio G, et al. Percutaneous coronary revascularization: JACC historical breakthroughs in perspective. *J Am Coll Cardiol.* (2021) 78(4):384–407. doi: 10.1016/j.jacc.2021.05.024

2. Widimsky P, Holmes DR Jr. How to treat patients with ST-elevation acute myocardial infarction and multi-vessel disease? *Eur Heart J.* (2011) 32(4):396–403. doi: 10.1093/eurheartj/ehq410

3. Sheth T, Pinilla-Echeverri N, Moreno R, Wang J, Wood DA, Storey RF, et al. Nonculprit lesion severity and outcome of revascularization in patients with STEMI and multivessel coronary disease. *J Am Coll Cardiol.* (2020) 76(11):1277–86. doi: 10.1016/j.jacc.2020.07.034

4. Hemetsberger R, Abdelghani M, Toelg R, Garcia-Garcia HM, Farhan S, Mankerious N, et al. Complex vs. Non-complex percutaneous coronary intervention with newer-generation drug-eluting stents: an analysis from the randomized BIOFLOW trials. *Clin Res Cardiol.* (2022) 111(7):795–805. doi: 10.1007/s00392-022-01994-4

5. Baumann AAW, Mishra A, Worthley MI, Nelson AJ, Psaltis PJ. Management of multivessel coronary artery disease in patients with non-ST-elevation myocardial infarction: a complex path to precision medicine. *Ther Adv Chronic Dis.* (2020) 11:2040622320938527. doi: 10.1177/2040622320938527

6. Hong KN, Fuster V, Rosenson RS, Rosendorff C, Bhatt DL. How low to go with glucose, cholesterol, and blood pressure in primary prevention of CVD. *J Am Coll Cardiol.* (2017) 70(17):2171–85. doi: 10.1016/j.jacc.2017.09.001

7. Djupsjö C, Kuhl J, Andersson T, Lundbäck M, Holzmann MJ, Nyström T. Admission glucose as a prognostic marker for all-cause mortality and cardiovascular disease. *Cardiovasc Diabetol.* (2022) 21(1):258. doi: 10.1186/s12933-022-01699-y. Erratum in: Cardiovasc Diabetol. 2022 December 29;21(1):292. PMID: 36435766; PMCID: PMC9701417.

8. Yang J, Zhou Y, Zhang T, Lin X, Ma X, Wang Z, et al. Fasting blood glucose and HbA1c correlate with severity of coronary artery disease in elective PCI patients with HbA1c 5.7% to 6.4. *Angiology.* (2020) 71(2):167–74. doi: 10.1177/0003319719887655

9. Tütün U, Çiçekçioğlu F, Budak B, Temürtürkan M, Parlar AI, Seren M, et al. Coronary atherosclerosis distribution and the effect of blood glucose level on operative mortality/morbidity in diabetic patients undergoing coronary artery bypass grafting surgery: a single center experience. *Anadolu Kardiyol Derg.* (2007) 7 (2):158–63.

10. Cheng Y, Fang Z, Zhang X, Wen Y, Lu J, He S, et al. Association between triglyceride glucose-body mass index and cardiovascular outcomes in patients undergoing percutaneous coronary intervention: a retrospective study. *Cardiovasc Diabetol.* (2023) 22(1):75. doi: 10.1186/s12933-023-01794-8

11. Toma A, Stähli BE, Gick M, Gebhard C, Nührenberg T, Mashayekhi K, et al. Impact of multi-vessel versus single-vessel disease on outcomes after percutaneous coronary interventions for chronic total occlusions. *Clin Res Cardiol.* (2017) 106 (6):428–35. doi: 10.1007/s00392-016-1072-z

12. Dziewierz A, Siudak Z, Rakowski T, Zasada W, Dubiel JS, Dudek D. Impact of multivessel coronary artery disease and noninfarct-related artery revascularization on outcome of patients with ST-elevation myocardial infarction transferred for primary percutaneous coronary intervention (from the EUROTRANSFER registry). *Am J Cardiol.* (2010) 106(3):342–7. doi: 10.1016/j.amjcard.2010.03.029

13. Werner GS, Martin-Yuste V, Hildick-Smith D, Boudou N, Sianos G, Gelev V, et al. A randomized multicentre trial to compare revascularization with optimal medical therapy for the treatment of chronic total coronary occlusions. *Eur Heart J.* (2018) 39(26):2484–93. doi: 10.1093/eurheartj/ehy220

14. Tindale A, Cretu I, Meng H, Panoulas V. Complete revascularization is associated with higher mortality in patients with ST-elevation myocardial infarction, multi-vessel disease and shock defined by hyperlactataemia: results from the harefield shock registry incorporating explainable machine learning. *Eur Heart J Acute Cardiovasc Care.* (2023) 12(9):615–23. doi: 10.1093/ehjacc/zuad062

15. Sorajja P, Gersh BJ, Cox DA, McLaughlin MG, Zimetbaum P, Costantini C, et al. Impact of multivessel disease on reperfusion success and clinical outcomes in patients undergoing primary percutaneous coronary intervention for acute myocardial infarction. *Eur Heart J.* (2007) 28(14):1709–16. doi: 10.1093/eurheartj/ehm184

16. Chen Y, Xu L, Cheng Z, Zhang D, Yang J, Yin C, et al. Progression from different blood glucose states to cardiovascular diseases: a prospective study based on multi-state model. *Eur J Prev Cardiol.* (2023) 30(14):1482–91. doi: 10.1093/eurjpc/zwad196

17. Wang X, Xu W, Song Q, Zhao Z, Meng X, Xia C, et al. Association between the triglyceride-glucose index and severity of coronary artery disease. *Cardiovasc Diabetol.* (2022) 21(1):168. doi: 10.1186/s12933-022-01606-5

18. Iijima R, Ndrepepa G, Kujath V, Harada Y, Kufner S, Schunkert H, et al. A pan-coronary artery angiographic study of the association between diabetes mellitus and progression or regression of coronary atherosclerosis. *Heart Vessels.* (2017) 32 (4):376–84. doi: 10.1007/s00380-016-0889-8

19. Zhao T, Gong HP, Dong ZQ, Du YM, Lu QH, Chen HQ. Predictive value of fasting blood glucose for serious coronary atherosclerosis in non-diabetic patients. *J Int Med Res.* (2019) 47(1):152–8. doi: 10.1177/0300060518798252

20. Expert Consultation WHO. Appropriate body-mass index for Asian populations and its implications for policy and intervention strategies. *Lancet.* (2004) 363 (9403):157–63. doi: 10.1016/S0140-6736(03)15268-3 Erratum in: Lancet. 2004 March 13;363(9412):902. PMID: 14726171.

frontiers | Frontiers in Cardiovascular Medicine

TYPE Original Research
PUBLISHED 31 March 2025
DOI 10.3389/fcvm.2025.1446675

OPEN ACCESS

EDITED BY
Catherine A. Reardon,
The University of Chicago, United States

REVIEWED BY
Gobinath Shanmugam,
University of Alabama at Birmingham, United States
Masaki Mizuno,
University of Texas Southwestern Medical Center, United States

*CORRESPONDENCE
Xingping Zhang
194955495@qq.com

RECEIVED 10 June 2024
ACCEPTED 19 March 2025
PUBLISHED 31 March 2025

CITATION
Lou J, Lang H, Xia Y, Jiang H, Li K and Zhang X (2025) Reduced heart rate response to exercise in patients with type 2 diabetes. Front. Cardiovasc. Med. 12:1446675. doi: 10.3389/fcvm.2025.1446675

Reduced heart rate response to exercise in patients with type 2 diabetes

Jingfeng Lou[1], Hongmei Lang[1], Yuhan Xia[2], Hui Jiang[3,4], Kun Li[3,5] and Xingping Zhang[1]*

[1]Department of General Medicine, Chengdu Second People's Hospital, Chengdu, China, [2]Department of Endocrinology, North Sichuan Medical College, Nan Chong, China, [3]Department of General Medicine, Chengdu Second People's Hospital, Clinical Medical College of Chengdu Medical College, Chengdu, China, [4]Department of General Medicine, Qiyang People's Hospital, Yongzhou, China, [5]Department of General Medicine, Hongpailou Community Health Care Center, Chengdu, China

Background: Recent studies have found that heart rate response is impaired in patients with type 2 diabetes. However, it remains unclear how chronotropic competence changes in these patients and which chronotropic index is more closely related to type 2 diabetes. This study aims to investigate the changes in chronotropic competence in type 2 diabetes and compares the association of two different chronotropic indices with type 2 diabetes.
Patients and methods: Patients who underwent cardiopulmonary exercise testing at the Chengdu Second People's Hospital from October 2022 to October 2023, we included. Logistic regression was used to analyze the relationship between chronotropic indices and type 2 diabetes, comparing which of the two chronotropic indices is more closely related to type 2 diabetes.
Results: A total of 166 patients were included in our study, of which 42.8% had type 2 diabetes and 57.2% did not have type 2 diabetes. After adjusting for confounders, the OR for chronotropic index 1 with type 2 diabetes was 0.001 (95% CI: 0.0001–0.521, $P = 0.03$), and the OR for chronotropic index 2 with type 2 diabetes was 0.665 (95% CI: 0.479–0.923, $P = 0.015$), both showing a negative correlation with type 2 diabetes. When chronotropic index 2 was included in the model as quartiles, it still showed a negative correlation with type 2 diabetes (OR: 0.388; 95% CI: 0.173–0.869; $P = 0.021$), while chronotropic index 1 showed no significant correlation.
Conclusion: Heart rate response is reduced in patients with type 2 diabetes, and a low chronotropic index 2 is independently associated with type 2 diabetes.

KEYWORDS

heart rate response, chronotropic index, cardiopulmonary exercise testing, type 2 diabetes, correlation

1 Introduction

Type 2 diabetes (T2DM) is a significant cardiovascular risk factor and increases the risk of mortality. Globally, diabetes affects 6.1% of the population, with T2DM constituting 96% of these cases, thereby representing a significant global health challenge (1). Patients with T2DM may develop several complications, including autonomic neuropathy, which is a dysfunction of the sympathetic and parasympathetic nervous systems (2, 3). The entire process of physical activity reflects the dynamic balance between the parasympathetic and sympathetic nerves. At rest, the maintenance of resting heart rate primarily relies on the parasympathetic nervous system. During the recovery period after exercise, the

parasympathetic nervous system is gradually activated, and the sympathetic nervous system is suppressed, leading to a gradual decrease in heart rate (2). However, during exercise, the sympathetic nervous system is activated, the parasympathetic nervous system is inhibited, and the heart rate increases. The increase in heart rate reflects the balance of parasympathetic and sympathetic nervous system function, known as chronotropic competence, and how this competence changes in patients with T2DM is not yet well understood.

Chronotropic incompetence, characterized by the heart's failure to adequately increase its rate in response to activity or demand, is common among patients with cardiovascular diseases. It reduces exercise tolerance, adversely affecting quality of life, and serves as an independent predictor of major cardiovascular events and overall mortality (4). The mechanisms underlying impaired chronotropic function in T2DM remain unclear; however, studies suggest it may be associated with hyperglycemia, dyslipidemia, and abnormalities in insulin signaling pathways (5, 6). Cardiopulmonary exercise testing (CPET), as a vital diagnostic and assessment tool, can evaluate and measure the heart's chronotropic competence. In CPET, chronotropic incompetence is defined as the failure to reach 85% of the age-predicted maximal heart rate, or a low chronotropic index (heart rate adjusted to the MET level) (7, 8). However, there is no definitive, unified standard for calculating chronotropic competence. Some studies represent it as (HRpeak-HRrest) (220-age-HRrest) (9), while the 2012 CPET guidelines suggest using the change in heart rate per increase of 1 MET to assess chronotropic competence (10). It remains unclear which indicator is more closely related to chronotropic competence in patients with T2DM.

Although the relationship between T2DM and cardiovascular complications has been extensively explored, the variations in chronotropic competence among patients with T2DM remain unclear. It is crucial to determine which of the previously mentioned calculation methods is more accurate for assessing chronotropic competence in these patients. Therefore, this study aims to investigate the relationship between T2DM and chronotropic competence, and to compare the associations of two different chronotropic indices with T2DM.

2 Materials and methods

2.1 Participants

In this study, we included adult patients who underwent CPET at the Chengdu Second People's Hospital from October 2022 to October 2023. We excluded the following patients: (1) those who did not follow the protocol; (2) those who were unable to complete submaximal exercise; (3) patients taking β-blockers and (4) patients under the age of 18. Ultimately, 166 patients (mean age 56 years old) were included in our study, comprising 71 individuals with diabetes and 95 without diabetes. Among them, middle-aged and older patients constituted the majority, comprising 83% of the total individuals (the specific age distribution of participants provided in Supplementary Figure S1). This study was approved by the Ethics Committee of the Chengdu Second People's Hospital, and all participants provided written informed consent.

2.2 Clinical data

All data were obtained from the database of the Chengdu Second people's Hospital. Demographic and clinical information included: gender, age, height, weight, waist circumference, smoking history, hypertension, coronary artery disease, and heart failure. BMI was calculated as weight divided by the square of height. Smoking history was defined as having smoked continuously or cumulatively for more than six months. T2DM was diagnosed based on at least one of the following criteria: use of diabetes medications or insulin, a physician diagnosis of T2DM, fasting blood glucose ≥7 mmol/L, or a 2-hour oral glucose tolerance test blood glucose ≥11.1 mmol/L. Hypertension is defined as having a blood pressure greater than 140/90 mmHg on at least three separate occasions, or a history of hypertension. Coronary artery disease was defined as a history of stable or unstable angina, acute myocardial infarction, or ischemic cardiomyopathy. Heart failure was defined as being classified as NYHA II or higher, or having a history of decompensated heart failure. The test indicators include: blood glucose, troponin, NT-proBNP, total cholesterol, and low-density lipoprotein.

2.3 Exercise test protocol

The CPETs were conducted at the Chengdu Second People's Hospital, with all testing environments meeting the required standards, including pre-test gas calibration. According to the guidelines of the American College of Cardiology/American Heart Association, all participants underwent symptom-limited cardiopulmonary bicycle exercise testing using the standard Ramp protocol (11, 12). The Ramp protocol is a linear incremental exercise test where the workload is gradually increased, with the power incrementing progressively every second. The test includes a 3-minute rest period, a 3-min warm-up period, followed by exercise, with the duration of the exercise varying according to the patient's condition. The recovery period lasts 6–8 min. During the exercise, the pedaling rate is maintained at 60–70 revolutions per minute. The workload is increased progressively every minute based on a predefined power increment per minute. The power increment per second is calculated by dividing the predefined power increment per minute by 60 s. Endpoints for exercise testing included: a rating of perceived exertion (6–20 scale) >17 (very hard) or a peak respiratory exchange ratio (RER) >1.15; participant request to stop the test due to volitional fatigue; systolic blood pressure ≥240 mmHg or diastolic blood pressure ≥110 mmHg; significant chest discomfort during exercise; severe arrhythmias; or horizontal or downsloping ST-segment depression greater than 2 mm or ST-segment elevation greater than 1 mm.

2.4 Exercise test variables

Resting period blood pressure and heart rate were measured after at least 5 min of rest. Peak systolic blood pressure, peak diastolic blood pressure, peak heart rate, and METs were recorded at peak VO2. Heart rate recovery was defined as the peak heart rate minus the heart rate after 1 min of recovery. CI 1 was calculated as (peak HR - resting HR)/(220 - age - resting HR). CI 2 was calculated as (peak HR - resting HR)/(peak METs - resting METs). Peak VO2 was defined as the highest 10-second average VO2 during the final stage of a symptom-limited exercise test. The VE/VCO2 slope represented gas exchange from rest to the peak of exercise. Heart rhythm was monitored using continuous 12-lead electrocardiography.

2.5 Statistical analysis

Continuous variables with normal distributions were described as mean ± standard deviation, while those with non-normal distributions were expressed as median and interquartile range. Categorical variables were presented as frequencies and percentages. To compare continuous variables between different groups, the two-sided independent or paired *t*-test was used for normally distributed data; for non-normally distributed data, the Wilcoxon rank-sum test was employed. Pearson's Chi-square test was used to compare frequency distributions. To explore the relationship between diabetes and various indices of chronotropic competence, univariate logistic regression analysis was conducted in the first model. Subsequently, we performed multivariate logistic regression analysis, including all variables that were significantly associated with T2DM in the univariate analysis. In the second model, we adjusted for age, gender, BMI, and smoking history; in the third model, we additionally adjusted for hypertension, heart failure, and coronary artery disease, beyond the factors in the first model; in the fourth model, besides the factors adjusted in the first two models, we also adjusted for blood glucose, NT-proBNP, VO2/Kg, and VE/VCO2 slope. All statistical analyses were performed using SPSS software, version 26, and two-sided probability values <0.05 were considered statistically significant.

3 Results

3.1 Participant characteristics

Initially, we collected data from 216 patients, of which 166 met the criteria and were included in our study (Figure 1). Among these patients, 71 (42.8%) had T2DM and 95 (57.2%) did not. Baseline data and test results are shown in Table 1. The average age was 55.9 ± 14.4 years, approximately 51.8% were female, the BMI was 24.4 ± 4.0 kg/m^2, waist circumference was 85.8 ± 11.1 cm, and 21.7% had a history of smoking. The T2DM group had higher blood glucose and lower NT-proBNP, while there were no significant differences between the two groups in terms of troponin, total cholesterol, and low-density lipoprotein. The detailed characteristics of the study population are shown in Table 1.

3.2 Heart rate responses by T2DM

All exercise test results are shown in Table 2. At rest, patients with T2DM had higher systolic blood pressure, heart rate, and metabolic equivalents (METs) compared to those without T2DM, while their diastolic pressure was lower. However, these differences were not statistically significant. During the exercise load, patients with T2DM had a significantly lower peak heart rate than those without T2DM ($P < 0.001$). The peak systolic blood pressure and peak METs of patients with T2DM were lower than those of individuals without T2DM, while their peak diastolic pressure was higher, but these indicators were not statistically significant. The heart rate recovery for patients with T2DM was 14.65 ± 11.89 s, compared to 20.26 ± 8.58 s for those

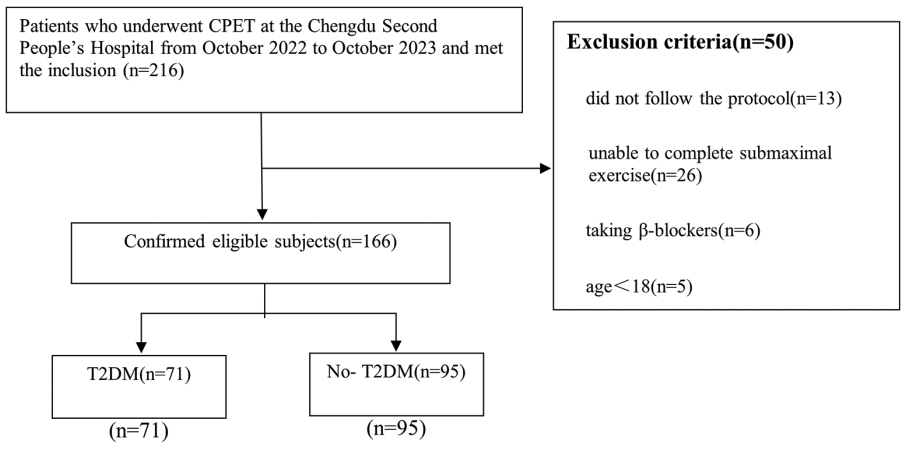

FIGURE 1
Flow chart of inclusion and exclusion.

TABLE 1 Baseline characteristics of the patients with and without T2DM.

Variable	Overall (166)	2T2DM (71)	No-T2DM (95)	*P*-value
Age (years)	55.9 ± 14.4	57.9 ± 13.2	54.4 ± 15.1	0.11
Sex (% female)	86 (51.8)	26 (36.6)	60 (63.2)	0.001
BMI ($kg \times m^{-2}$)	24.4 ± 4.0	24.2 ± 4.0	24.6 ± 4.8	0.66
Waist circumference (cm)	85.8 ± 11.1	86.3 ± 11.9	85.4 ± 10.5	0.67
Smoking history, *n* (%)	36 (21.7)	21 (29.6)	15 (15.8)	0.033
Hypertension, *n* (%)	8 (4.8)	5 (7.0)	3 (3.2)	0.43
Heart failure, *n* (%)	4 (2.4)	0 (0)	4 (4.2)	0.14
Coronary artery disease, *n* (%)	7 (4.2)	5 (7.0)	2 (2.1)	0.24
Glucose (mmol/L)	7.5 ± 3.1	9.7 ± 3.1	5.9 ± 1.7	<0.001
Troponin (ng/ml)	7.1 (5.6, 9.6)	8.0 (5.9, 11.6)	6.2 (5.1, 8.1)	0.170
NT-proBNP (ng/L)	61.0 (25.5, 126.5)	41.0 (18.0, 92.5)	72.5 (40.0, 250.0)	0.012
TC (mmol/L)	4.8 ± 1.0	4.7 ± 1.0	4.9 ± 1.0	0.202
LDL-C (mmol/L)	2.7 ± 0.8	2.7 ± 0.8	2.7 ± 0.7	0.793

BMI, body mass index; TC, total cholesterol; LDL-C, low-density lipoprotein cholesterol. Continuous data were presented as mean ± SD or median and interquartile range, and categorical data as a percentage of the sample.

TABLE 2 Exercise test variables of the patients with and without T2DM.

Variable	T2DM	No-T2DM	*P*-value
Reasting systolic BP (mmHg)	117.50 ± 15.44	117.39 ± 14.00	0.96
Resting diastolic BP (mmHg)	71.63 ± 10.13	71.68 ± 11.75	0.98
Peak systolic BP (mmHg)	155.19 ± 26.91	162.96 ± 25.77	0.07
Peak diastolic BP (mmHg)	77.58 ± 13.01	75.62 ± 11.32	0.31
Reasting METs	1.45 ± 0.26	1.40 ± 0.27	0.26
Peak METs	5.99 ± 1.89	6.29 ± 1.33	0.22
Reasting HR (beats/min)	82.49 ± 12.89	80.43 ± 10.54	0.27
Peak HR (beats/min)	118.85 ± 23.66	133.26 ± 21.48	<0.001
Heart rate recovery (beats/min)	14.65 ± 11.89	20.26 ± 8.58	0.001
CI 1	0.46 ± 0.23	0.63 ± 0.21	<0.001
CI 2	7.88 ± 3.19	10.91 ± 2.75	<0.001
VO_2/Kg (ml/min/kg)	20.95 ± 6.60	22.09 ± 4.80	0.22
VE/VCO_2 slop	29.41 ± 2.86	28.07 ± 2.30	0.001
RER	1.12 ± 1.07	1.03 ± 0.09	0.41
VC (L)	3.01 ± 0.64	3.13 ± 0.86	0.33
FEV1/FVC	83.67 ± 12.66	3.13 ± 0.86	0.04
VEmax (L)	44.80 ± 18.41	46.39 ± 15.78	0.56

BP, blood pressure; METs, metabolic equivalents; CI, chronotropic index. Continuous data were presented as mean ± SD.

without T2DM ($P < 0.001$). In terms of chronotropic competence, the chronotropic index 2 for patients with T2DM was 7.88 ± 3.19, significantly lower than the 10.91 ± 2.75 for those without T2DM ($P < 0.001$). The chronotropic index 1 for patients with T2DM was also significantly lower than that for individuals without T2DM ($P < 0.001$). There were no significant differences between the two groups in VO2/Kg, RER, VC, or VEmax.

Table 3 shows the impact of T2DM on chronotropic competence. Initial univariate logistic regression analyses were conducted to clarify the relationship between chronotropic competence and T2DM. This was followed by multivariate logistic regression analyses to exclude potential confounding factors affecting the relationship between chronotropic competence and T2DM. In the unadjusted Model 1, both chronotropic index 1 (OR: 0.023; 95% CI: 0.004–0.126; $P < 0.001$) and chronotropic index 2 (OR: 0.705; 95% CI: 0.620–0.801; $P < 0.001$) were negatively correlated with T2DM, with lower values of both indices associated with T2DM. Model 2, adjusted for age, gender, BMI, and smoking history, showed that the OR for chronotropic index 1 with T2DM was 0.043 (95% CI: 0.007–0.253; $P < 0.001$), while the OR for chronotropic index 2 with T2DM was 0.718 (95% CI: 0.621–0.831; $P < 0.001$). Model 3, building on Model 2, included adjustments for hypertension, heart failure, and coronary artery disease, and showed that the OR for chronotropic index 1 with T2DM was 0.062 (95% CI: 0.010–0.374; $P < 0.001$), while the OR for chronotropic index 2 with T2DM was 0.732 (95% CI: 0.630–0.852; $P < 0.001$). Model 4, based on Model 3, included additional adjustments for blood glucose, BNP, VO2/Kg, and VE/VCO2 slope, and the correlation remained significant. The chronotropic index 1 and chronotropic index 2 showed a consistent negative association with T2DM, remaining significant even after adjusting for various potential confounding factors. Subsequently, chronotropic index 2 was included in the model as a quartile variable. After adjusting for confounding factors, chronotropic index 2 still showed a negative correlation with T2DM (OR: 0.388; 95% CI: 0.173–0.869; $P = 0.021$), while the chronotropic index 1 itself was not associated with T2DM (OR: 0.414; 95% CI: 0.147–1.165; $P = 0.095$).

4 Discussion

Our study primarily found that patients with T2DM exhibited a lower heart rate response during exercise compared to individuals without T2DM. Even after adjusting for age, gender, BMI, smoking history, comorbidities, and other variables, this result remained unchanged. We also discovered that chronotropic index 2 is more closely related to T2DM than chronotropic index 1, with a lower chronotropic index 2 significantly associated with T2DM. These results remained consistent even after adjusting for other confounding factors.

We thoroughly analyzed heart rate response indicators in patients with T2DM, specifically focusing on their response during exercise. For the first time, we compared the change in heart rate per 1 MET increase during exercise between patients with T2DM and those without (chronotropic index 2). We confirmed that chronotropic index 2, as opposed to chronotropic index 1, is more closely related to T2DM and may more accurately assess the heart rate response of T2DM during exercise.

Previous studies have found that patients with diabetes may have impaired heart rate recovery. Seshadri et al. discovered that, in a healthy cohort without known coronary artery disease, diabetes was associated with abnormal heart rate recovery after exercise. This association persisted even after adjusting for several potential confounding factors (13). Yu et al. also found that delayed heart rate recovery after exercise is an independent risk factor for T2DM in men, even after adjusting for biochemical indicators such as glucose metabolism (14). These studies suggested that impaired heart rate recovery may be an early

TABLE 3 Odds ratios and 95% CI of type 2 diabetes and chronotropic index.

Variable	Model 1	Model 2	Model 3	Model 4
CI 1	0.023 (0.004–0.126)*	0.043 (0.007–0.253)*	0.062 (0.010–0.374)*	0.001 (0.0001–0.521)*
CI 2	0.705 (0.620–0.801)*	0.718 (0.621–0.831)*	0.732 (0.630–0.852)*	0.665 (0.479–0.923)*
CI 1 group	0.522 (0.384–0.710)*	0.586 (0.424–0.808)*	0.634 (0.455–0.883)*	0.414 (0.147–1.165)
CI 2 group	0.374 (0.265–0.568)*	0.393 (0.265–0.582)*	0.415 (0.275–0.624)*	0.388 (0.173–0.869)*

CI, chronotropic index; CI group, the quartiles of the chronotropic index; Model 1: univariate logistic regression; Model 2: additionally adjusted for Model 1 variables plus age, sex, BMI, smoking history; Model3: additionally adjusted for Model 2 variables plus hypertension, heart failure, coronary artery disease; Model4: additionally adjusted for Model 3 variables plus Glucose, NT-proBNP, VO_2/Kg, VE/VCO_2 slop.
Data were presented as odds ratios and 95% confidence intervals.
*$P < 0.05$.

manifestation of diabetes and could predict the onset of diabetes. However, other studies have found that impaired heart rate recovery is not independently associated with the occurrence of diabetes. Jae et al. discovered that while slowed heart rate recovery is related to the development of T2DM, this relationship became insignificant after adjusting for diabetes risk factors and fasting blood glucose. They believed that this relationship could largely be explained by baseline fasting blood glucose in healthy males (15). Numerous studies have also found that patients with diabetes tend to have an increased resting heart rate. Park et al. found that for every 10 beats per minute increase in resting heart rate, the risk of diabetes increases by 1.39 times for men and 1.28 times for women (16). A meta-analysis shows a strong positive association between high resting heart rate and the risk of T2DM (17). A prospective cohort study conducted by Lee found that an increase of 10 beats per minute in resting heart rate is associated with a 19% increase in the risk of T2DM (18). Additionally, some studies have found the association between resting heart rate and diabetes to be unclear. An increase of 12 beats per minute in resting heart rate is associated with approximately a 10% higher risk of developing diabetes. However, this association becomes statistically insignificant after adjusting for BMI and postprandial blood glucose (19).

Heart rate recovery after exercise is primarily related to the activation of the parasympathetic nervous system, while the heart rate response during exercise is mainly associated with the activation of the sympathetic nervous system. Previous studies have shown that patients with diabetes exhibit significant sympathetic nervous responses during exercise, but the direction of this response varies across studies. Some studies have found that patients with T2DM have significantly enhanced sympathetic responses during isometric handgrip exercises (20). Additionally, animal experiments have shown that T2DM rats exhibit significantly stronger heart rate responses during muscle contraction and tendon stretch compared to healthy controls (21, 22). However, other studies have found weaker sympathetic activation responses in diabetic patients during exercise. Sydó et al. found in a cohort study of 21,396 patients without cardiovascular disease that diabetic patients had a lower chronotropic index, and this low heart rate response independently predicted long-term survival in diabetic patients (23). Our study similarly found a decrease in heart rate response during exercise in patients with T2DM, reflecting impaired sympathetic activation. It is noteworthy that our study is more comprehensive, especially focusing on T2DM patients, with a more detailed study design. The differences in these study results may be related to the choice of exercise mode in the studies—some focused on static exercises (e.g., handgrip tests), while others focused on dynamic exercises (e.g., aerobic exercise). Additionally, the duration of exercise may also be a factor influencing heart rate response. Whether the heart rate response is enhanced or diminished, it indicates abnormal cardiovascular responses during exercise in T2DM patients. This abnormal response may be an important marker of the increased cardiovascular risk in diabetic patients.

At any time, the heart rate reflects the function of the autonomic nervous system, which is the dynamic balance between the parasympathetic and sympathetic nerves. During exercise, sympathetic nerve tension increases and parasympathetic nerve tension decreases, leading to a gradual increase in heart rate (24, 25). Therefore, if the heart rate does not increase correspondingly with the intensity of exercise, it indicates a dysfunction of the autonomic nervous system (9).

The overt clinical symptoms of autonomic nervous system dysfunction in patients with T2DM often appear in the late stages, but subclinical dysfunction may already be present in the early stages. Hypotheses about the etiology of diabetic neuropathy include metabolic injury to nerve fibers, inadequate neurovascular function, autoimmune damage, and deficiency of neurotrophic growth factors. This pathogenic process involves multiple factors. Hyperglycemia leads to the accumulation of sorbitol and NAD by activating the polyol pathway. The activation of protein kinase C causes vasoconstriction and reduces nerve blood flow. Increased oxidative stress can cause endothelial damage and reduce the bioavailability of nitric oxide. Alternatively, excessive production of nitric oxide may lead to the formation of peroxynitrite and damage to the endothelium and neurons, a process known as nitric oxide stress. In the subgroup with neuropathy, immune mechanisms may also be involved. The reduction in nerve growth factor, deficiency of essential fatty acids, and the formation of advanced glycation end products also lead to decreased intraneural blood flow and nerve hypoxia, altering nerve function. The result of this multifactorial process may be the activation of ADP-ribosylation, leading to the depletion of ATP, which in turn causes cell necrosis and activates genes associated with neuronal injury (21, 22). Therefore, we can assess autonomic nervous dysfunction in patients with T2DM by evaluating their early chronotropic function status.

Our study also has several limitations. (1) This is a single-center study with a relatively small sample size, and we cannot

avoid selection bias, which may limit the generalizability of the results. Additionally, our study subjects are Chinese, and larger studies are needed to extend the findings to other ethnic groups. Therefore, larger multi-center studies are necessary. (2) This is a cross-sectional study, which does not effectively establish the causal relationship between T2DM and chronotropic competence. Thus, large cohort studies are needed to further confirm this relationship. (3) Because this is retrospective data, some laboratory test results are missing. To minimize the impact of missing data, we used statistical methods for imputation, but this may still lead to some bias. Therefore, we should be more cautious when interpreting these related indicators. (4) Because of the retrospective design of this study, we did not consider the impact of the duration of T2DM, blood glucose control, and the use of antidiabetic medications on the results. These factors may influence heart rate responses in patients with T2DM.

5 Conclusion

Our study suggests that heart rate response is significantly reduced in patients with T2DM, and a low chronotropic index is independently associated with T2DM. This finding highlights the importance of monitoring heart rate dynamics as a potential strategy for managing and identifying diabetes. However, since our study may have limitations in establishing causality, further prospective studies and randomized controlled trials are recommended to investigate the causal relationships of these associations and determine their clinical significance in patients with T2DM.

Data availability statement

The original contributions presented in the study are included in the article/Supplementary Material, further inquiries can be directed to the corresponding author.

Ethics statement

The studies involving humans were approved by the Ethics Committee of Chengdu Second People's Hospital. The studies were conducted in accordance with the local legislation and institutional requirements. The participants provided their written informed consent to participate in this study.

Author contributions

JL: Conceptualization, Data curation, Formal analysis, Writing – original draft. HL: Methodology, Writing – review & editing. YX: Software, Writing – review & editing. HJ: Data curation, Writing – review & editing. KL: Data curation, Writing – review & editing. XZ: Supervision, Writing – review & editing.

Funding

The author(s) declare that financial support was received for the research and/or publication of this article. This research was funded by Research Project of Sichuan Medical and Health Promotion Institute (no. KY2022QN0385) and Chengdu Second People's Hospital Research Project Fund (grant number 2023-RC-002).

Conflict of interest

The authors declare that the research was conducted in the absence of any commercial or financial relationships that could be construed as a potential conflict of interest.

Publisher's note

Supplementary material

The Supplementary Material for this article can be found online at: https://www.frontiersin.org/articles/10.3389/fcvm.2025.1446675/full#supplementary-material

References

1. GBD 2021 Diabetes Collaborators. Global, regional, and national burden of diabetes from 1990 to 2021, with projections of prevalence to 2050: a systematic analysis for the global burden of disease study 2021. *Lancet*. (2023) 402:203–34. doi: 10.1016/S0140-6736(23)01301-6

2. Vinik AI, Maser RE, Mitchell BD, Freeman R. Diabetic autonomic neuropathy. *Diabetes Care*. (2003) 26:1553–79. doi: 10.2337/diacare.26.5.1553

3. Vinik AI, Nevoret ML, Casellini C, Parson H. Diabetic neuropathy. *Endocrinol Metab Clin North Am*. (2013) 42:747–87. doi: 10.1016/j.ecl.2013.06.001

4. Cheng YJ, Macera CA, Church TS, Blair SN. Heart rate reserve as a predictor of cardiovascular and all-cause mortality in men. *Med Sci Sports Exerc*. (2002) 34:1873–8. doi: 10.1097/00005768-200212000-00003

5. Feldman EL, Callaghan BC, Pop-Busui R, Zochodne DW, Wright DE, Bennett DL, et al. Diabetic neuropathy. *Nat Rev Dis Primers*. (2019) 5:42. doi: 10.1038/s41572-019-0097-9

6. Pfeifer MA, Weinberg CR, Cook DL, Reenan A, Halter JB, Ensinck JW, et al. Autonomic neural dysfunction in recently diagnosed diabetic subjects. *Diabetes Care*. (1984) 7:447–53. doi: 10.2337/diacare.7.5.447

7. Balady GJ, Arena R, Sietsema K, Myers J, Coke L, Fletcher GF, et al. Clinician's guide to cardiopulmonary exercise testing in adults: a scientific statement from the American Heart Association. *Circulation*. (2010) 122:191–225. doi: 10.1161/CIR.0b013e3181e52e69

8. Lauer MS, Okin PM, Larson MG, Evans JC, Levy D. Impaired heart rate response to graded exercise. Prognostic implications of chronotropic incompetence in the Framingham heart study. *Circulation*. (1996) 93:1520–6. doi: 10.1161/01.cir.93.8.1520

9. Brubaker PH, Kitzman DW. Chronotropic incompetence: causes, consequences, and management. *Circulation*. (2011) 123:1010–20. doi: 10.1161/circulationaha.110.940577

10. Guazzi M, Adams V, Conraads V, Halle M, Mezzani A, Vanhees L, et al. EACPR/AHA joint scientific statement. Clinical recommendations for cardiopulmonary exercise testing data assessment in specific patient populations. *Eur Heart J*. (2012) 33:2917–27. doi: 10.1093/eurheartj/ehs221

11. Gibbons RJ, Balady GJ, Bricker JT, Chaitman BR, Fletcher GF, Froelicher VF, et al. ACC/AHA 2002 guideline update for exercise testing: summary article. A report of the American College of Cardiology/American Heart Association task force on practice guidelines (committee to update the 1997 exercise testing guidelines). *J Am Coll Cardiol*. (2002) 40:1531–40. doi: 10.1016/s0735-1097(02)02164-2

12. Gibbons RJ, Balady GJ, Beasley JW, Bricker JT, Duvernoy WF, Froelicher VF, et al. ACC/AHA guidelines for exercise testing. A report of the American College of Cardiology/American Heart Association task force on practice guidelines (committee on exercise testing). *J Am Coll Cardiol*. (1997) 30:260–311. doi: 10.1016/s0735-1097(97)00150-2

13. Seshadri N, Acharya N, Lauer MS. Association of diabetes mellitus with abnormal heart rate recovery in patients without known coronary artery disease. *Am J Cardiol*. (2003) 91:108–11. doi: 10.1016/s0002-9149(02)03014-x

14. Yu TY, Jee JH, Bae JC, Hong WJ, Jin SM, Kim JH, et al. Delayed heart rate recovery after exercise as a risk factor of incident type 2 diabetes mellitus after adjusting for glycometabolic parameters in men. *Int J Cardiol*. (2016) 221:17–22. doi: 10.1016/j.ijcard.2016.06.149

15. Jae SY, Carnethon MR, Heffernan KS, Fernhall B, Lee MK, Park WH. Heart rate recovery after exercise and incidence of type 2 diabetes in men. *Clin Auton Res*. (2009) 19:189–92. doi: 10.1007/s10286-009-0007-4

16. Park DH, Goo SY, Hong SH, Min JH, Byeon JY, Lee MK, et al. Prognostic value of resting heart rate in predicting undiagnosed diabetes in adults: Korean national health and nutrition examination survey 2008–2018. *Nutr Metab Cardiovasc Dis*. (2023) 33:141–50. doi: 10.1016/j.numecd.2022.09.012

17. Aune D, Ó Hartaigh B, Vatten LJ. Resting heart rate and the risk of type 2 diabetes: a systematic review and dose-response meta-analysis of cohort studies. *Nutr Metab Cardiovasc Dis*. (2015) 25:526–34. doi: 10.1016/j.numecd.2015.02.008

18. Lee DH, de Rezende LFM, Hu FB, Jeon JY, Giovannucci EL. Resting heart rate and risk of type 2 diabetes: a prospective cohort study and meta-analysis. *Diabetes Metab Res Rev*. (2019) 35(2):e3095. doi: 10.1002/dmrr.3095

19. Carnethon MR, Yan L, Greenland P, Garside DB, Dyer AR, Metzger B, et al. Resting heart rate in middle age and diabetes development in older age. *Diabetes Care*. (2008) 31:335–9. doi: 10.2337/dc07-0874

20. Vranish JR, Holwerda SW, Kaur J, Fadel PJ. Augmented pressor and sympathoexcitatory responses to the onset of isometric handgrip in patients with type 2 diabetes. *Am J Physiol Regul Integr Comp Physiol*. (2020) 318 (2):R311–9. doi: 10.1152/ajpregu.00109.2019

21. Ishizawa R, Kim HK, Hotta N, Iwamoto GA, Mitchell JH, Smith SA, et al. TRPV1 (transient receptor potential vanilloid 1) sensitization of skeletal muscle afferents in type 2 diabetic rats with hyperglycemia. *Hypertension*. (2021) 77 (4):1360–71. doi: 10.1161/HYPERTENSIONAHA.120.15672

22. Kim HK, Hotta N, Ishizawa R, Iwamoto GA, Vongpatanasin W, Mitchell JH, et al. Exaggerated pressor and sympathetic responses to stimulation of the mesencephalic locomotor region and exercise pressor reflex in type 2 diabetic rats. *Am J Physiol Regul Integr Comp Physiol*. (2019) 317 (2):R270–9. doi: 10.1152/ajpregu.00061.2019

23. Sydó N, Sydó T, Merkely B, Carta KG, Murphy JG, Lopez-Jimenez F, et al. Impaired heart rate response to exercise in diabetes and its long-term significance. *Mayo Clin Proc*. (2016) 91:157–65. doi: 10.1016/j.mayocp.2015.10.028

24. Cernea S, Raz I. Management of diabetic neuropathy. *Metab Clin Exp*. (2021) 123:154867. doi: 10.1016/j.metabol.2021.154867

25. Freeman JV, Dewey FE, Hadley DM, Myers J, Froelicher VF. Autonomic nervous system interaction with the cardiovascular system during exercise. *Prog Cardiovasc Dis*. (2006) 48:342–62. doi: 10.1016/j.pcad.2005.11.003

Frontiers in
Cardiovascular Medicine

Innovations and improvements in cardiovascular treatment and practice

Focuses on research that challenges the status quo of cardiovascular care, or facilitates the translation of advances into new therapies and diagnostic tools.

Discover the latest Research Topics

See more →

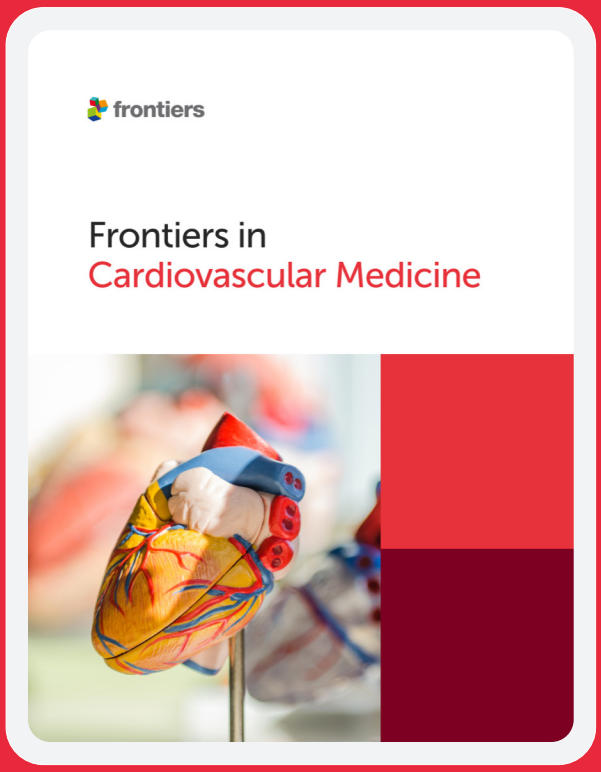

Frontiers

Avenue du Tribunal-Fédéral 34
1005 Lausanne, Switzerland
frontiersin.org

Contact us

+41 (0)21 510 17 00
frontiersin.org/about/contact